Department of Precision and Microsystems Engineering

Towards static balancing of compliant mechanical micro motion amplifiers

CLASSIFYING COMPLIANT AMPLIFIERS & DEVELOPING A PRELOADING MEMS MECHANISM

M.Y.Barel

Report no	:	2017.049
Coach	:	D. F. Machekposhti
Professor	:	Prof. dr. ir. J. L. Herder
Specialization	:	MSD
Type of report	:	Master Thesis
Date	:	18 October 2017

M. Y. Barel

Towards static balancing of compliant mechanical micro motion amplifiers

CLASSIFYING COMPLIANT AMPLIFIERS & DEVELOPING A PRELOADING MEMS MECHANISM

TU Delft

Towards static balancing of compliant mechanical micro motion amplifiers

CLASSIYING COMPLIANT AMPLIFIERS & DEVOLOPING A PRELOADING MEMS MECHANISM

By

Marije Yolinde Barel

in partial fulfilment of the requirements for the degree of

Master of Science
in Mechanical Engineering

at the Delft University of Technology,
to be defended publicly on Wednesday November 1, 2017 at 10:00.

Supervisor:	Prof. dr. ir. J. L. Herder	
Thesis committee:	Prof. dr. ir. J. L. Herder	TU Delft
	Dr. ir. J.F.L Goosen	TU Delft
	Dr. N. Tolou	TU Delft

This thesis is confidential and cannot be made public until November 1, 2024.

TU Delft

To my family

where the engineering is held high for the third generation.
To my father's father who was an electrical engineer, to my loving father who is a civil engineer. They both studied at the TuDelft. To my mother's father who worked in the wood industry and to my loving mom with whom I share a fantastic creativity. To my siblings with whom I can enjoyably debate until the dead of night.

Preface

At age 7 I lay awake at night, inventing a car which would run on two drums filled with water, reducing CO_2 emission. I questioned myself if it could generate enough energy. I put myself to sleep with the final thought: I do not have the knowledge to engineer this car… yet.

Here I am, 18 years later, making that dream come true as I heard of the challenge of static balancing compliant mechanical amplifiers. Besides an increased understanding in this amazing world of tiny movers, I got more confident in my personal skills as an engineer and the possibility for me to contribute to solving world problems, however small the solutions might be.

Support came from my daily mentor Davood Farhadi Machekposhti, who I have to thank for excellent guiding. My supervisor prof. dr. ir. Just L. Herder was a real inspiration for working with compliant mechanisms and the reason I chose this area of expertise. I also want to thank Metin Sitti and his department at the Max Planck Institute in Stuttgart, Germany, where I spent 3 months to do my research.

Naturally I want to thank my family and friends for their support. Especially my brother Marten Barel, Josko de Boer and Maarten Dogger who checked my writings. Boran Jia for trying to make the MEMS model on a smaller scale. Henry van der Deijl for helping with ANSYS modal analysis. And, Reinier Kuppens for helping with various small problems

A warm thanks to the entire department of Physical Intelligence at the Max Planck Institute at Stuttgart, Germany, where I have spent 3 months of my research. A special thanks to Dr, Ahmet Tabak for helping with the Comsol modelling struggle, Chantal Goettle without whom I would never had found the 3D printer at Max Planck which was vital to the rapid prototyping process, and Joshua Giltinan for his help on working with the laser cutters in the lab.

M. Y. Barel
Delft, October 2017

Contents

1 Simplified Dutch summary / Versimpelde Samenvatting 15

2 English Abstract 16

I INTRODUCTION 19

1 Introduction 21

2 List of abbreviations 22

3 Naming of parts 22

II LITERATURE REVIEW PAPER 25

III DESIGN PAPER 27

IV CHAPTERS 29

1 Approach towards the amplifier classification 31

2 Concept development for design challenge 33
2.1 Criteria for concepts 33
2.2 Force types analysis 33
2.3 Sub-concept design brainstorming 34
2.3.1 Actuation: Temperature 34
2.3.2 Actuation: Kinetics 34
2.3.3 Actuation: Electromagnetic 34
2.3.4 Actuation: Pressure 35
2.3.5 Actuation: Material 35
2.3.6 Guiding: Electromagnetic 35
2.3.7 Guiding: Material 35
2.3.8 Locking: Electromagnetic 35
2.3.9 Locking: Material 36
2.4 Weight tables and criteria for sub-concepts 40
2.4.1 Criteria 40
2.4.2 Tables 40
2.5 Total concept design generation 42
2.5.1 The ternary plot 42
2.5.2 Description of designs 42
2.5.3 Force displacements 47
2.6 Criteria and weight table for total concepts 47

3 Rapid prototyping method 49
3.1 General approach to rapid prototyping 49
3.2 Fabrication details 50
3.3 Bronze laser cutting 51

3.4 Vero Clear 3-point bending test 53
3.4.1 Test setup 53
3.4.2 Results 54
3.4.3 Conclusion, discussion and remarks 55
3.5 Changing the locking concept 55
3.6 Lever design 55
3.7 Symmetric design 56
3.7.1 Description 56
3.7.2 Modelled stiffness 56
3.7.3 Practical results 56
3.7.4 Discussion and other remarks 57
3.8 Asymmetric design 59
3.8.1 Description 59
3.8.2 Modelled stiffness 59
3.8.3 Practical results 59
3.8.4 Discussion and other remarks 60
3.9 Conclusion 60

4 Comsol and Ansys modelling 61
4.1 Comsol 61
4.2 Ansys 61

5 Concept optimization after prototyping 63
5.1 Configuration research 63
5.1.1 Results 65
5.1.2 Conclusions 65
5.2 Flexure lengths optimization 67
5.2.1 Optimization sequence 67
5.2.2 Optimization of hooks and other variables 68
5.2.3 Result of optimization 69
5.2.4 Discussion and other remarks 70
5.3 Buckling beam curvature calculation 70
5.4 Approach to scaling MEMS to Prototype 70

6 Final models and modelling 73
6.1 Static balancing and preloading force 73
6.1.1 Conclusion, discussion and other remarks 73
6.2 Stress analysis 73
6.2.1 Conclusion, discussion and other remarks 74
6.3 Modal analysis 76

7 Fabrication details 77
7.1 Intended fabrication for MEMS model 77
7.2 Fabrication methods for prototype 77

8 Additional Force displacement results 79
8.1 Force displacement of MS 79
8.2 Force displacement of the PB 79

9 Reflection / Personal development 81
9.1 Literature review approaches 81
9.2 Design approaches 81
9.3 Communication 81
9.4 Going abroad 82
9.5 Project/Time management: Delay caused by illness, dyslexia and machine breakdown 82

v APPENDIX....87

1 CMMA TIMELINE....88

2 Sub-concept weight tables....91

3 Force displacement sketches....94

4 Models....96
4.1 Lever models....97
4.2 Flexure > hooks....98
4.3 Symmetric model....99
4.4 Asymmetric model....100
4.5 MEMS model....101
4.6 Prototype fabrication Model....103

5 Calculation sheets....105

6 ANSYS Codes....107
6.1 Ansys during optimization sequence....107
6.2 MEMS code for stiffness calculations....110
6.3 MEMS model for Modal analysis....113
6.4 Prototype model for stiffness calculation....117
6.5 Prototype model for Modal analysis....120

7 Modelling stresses....124
7.1 MEMS, after preloading....124
7.2 MEMS, at extreme MS displacement....125
7.3 Prototype, after prelaoding....127
7.4 Prototype, at extreme MS displacment....128
7.5 Comsol modelling of hooks stresses....130
7.5.1 Tip displacement MEMS model....130
7.5.2 Tip load MEMS model....131
7.5.3 Tip load Prototype model....132

8 Eigenmodes....133
8.1 Models for MEMS....133
8.2 Modes for prototype....135

9 Bibliography....137

1 Simplified Dutch summary / Versimpelde Samenvatting

Het afstuderen beslaat het laatste jaar van de master Precision and Microsystems Engineering (Precisie en Mircosyteem Engineering), waarna de graad van ingenieur (ir.) kan worden behaald. Dat jaar is opgedeeld in een literatuuronderzoek naar de huidige staat van de wetenschap en ontwikkelen van een mechanisch ontwerp.

Flexibele mechanische beweging versterkers, afgekort met CMMA in het Engels, zijn mechanieken die, net als een heftboom of wipwap, een beweging versterken maar daarbij gebruik maken van elastische materialen. Voordelen van deze mechanieken zijn dat er geen gebruik meer wordt gemaakt van scharnieren en de meeste ontwerpen uit 1 stuk kunnen worden gefabriceerd. Toepassingsgebieden zijn o.a. sensoren en actuatoren, medische instrumenten en microscopen.

Gedurende mijn literatuuronderzoek heb ik 250 papers (wetenschappelijke verslagen) met daarin verschillende ontwerpen van CMMA gevonden. Hiervoor hebben we een classificatiesysteem ontworpen dat gebruik maakt van de eigenschapen: de type beweging die in de versterker kan worden gestopt, de type beweging die uit de versterker komt, en of de versterkingsfactor contant is of niet. Dit resulteert in 5 verschillende klassen met uiteindelijk 78 CMMA. Elke klas wordt gerepresenteerd door een niet-flexibelle versterker. De meeste CMMA vallen in de klasse van de “double slider”. Er zijn ook klassen waarvoor geen flexibele voorbeelden zijn gevonden.

Omdat CMMA elastische materialen gebruiken wordt er tijdens de beweging een deel van de energie opgeslagen in het mechaniek, er is een bepaalde actuatie-stijfheid. Om dit op te lossen kan een techniek worden toegepast die static balancing heet, statisch balanceren. Er wordt een energiebron aan het mechaniek toegevoegd, die energie vrijgeeft op hetzelfde moment als dat er energie wordt opgeslagen in het elastisch materiaal. De actuatie-stijfheid kan theoretisch worden gebracht naar 0 n/m. Het mechaniek kan nu in elke positie stil blijven staan, en is statisch gebalanceerd.

De toegevoegde energiebron bestaat uit een voor-geknikte balk. Het ontwikkelen van die energiebron in de vorm van een mechanisch ontwerp is het tweede deel in het afstudeer proces. Om de balk geknikt te krijgen is een mechaniek ontworpen, een voor-spanningssysteem met een vergrendeling (haken), een geleiding (double folded flexures), en een actuatie-methode (schok of schudden).

Gedurende mijn 3 maanden in Duitsland bij het Max Planck Institute heb ik meer dan 40 proefmodellen gemaakt met 2 eindconcepten als resultaat. Beide konden door schok of schudden worden voorgespannen. In Nederland zijn we met 1 van die concepten doorgegaan om een MEMS (Mechanisch Elektrisch Micro Systeem) te ontwikkelen. De totale diameter van het gehele ontwerp bedraagt ongeveer 30 mm, met balken van 0.024 mm dikte, gemaakt uit een silicium wafer plaat van 0.525 mm dik. Het ontwerp van het voorspanningssysteem is toegepast op een systeem wat alleen horizontaal beweegt zonder versterking en nog niet op een CMMA.

Vanwege machinepech kon het MEMS ontwerp nog niet worden gefabriceerd. Er is wel een prototype van schaal 6:1 gemaakt, waarvan twee modellen zijn gefabriceerd, waarbij een reductie van -126% en -123% is bereikt in de actuatie-stijfheid, waar 104.5% was voorspeld. De prototypes konden inderdaad met de hand door schok worden voorgespannen. De laagste theoretische eigenfrequentie van het prototype ligt op 3 Hz, en de laagste theoretisch eigenfrequentie van het MEMS model ligt op 22 Hz. De bijbehorende laagste eigenmodes actueren het voorspanningsmechaniek.

2 English Abstract

This document presents the result of a yearlong graduation project for the master Precision and Microsystems Engineering (PME) to become a mechanical engineer (Msc.) The project and this thesis have 2 major sections: a literature review and a design challenge.

Compliant mechanical motion amplifiers (CMMA) are mechanism that amplify motions using compliant/elastic structures. In contrast to gearing systems, compliant systems do not use hinges or pins to rotate around. Mechanisms with these properties can be miniaturised, for example using photolithography in silicon wafers, and can be monolithic in nature. These amplifiers can, among other applications, be used in sensor and actuation systems, medical instruments and microscope stages.

During my literature research I found 250 paper with CMMA design examples. A classification system is designed based on the geometrical advantage (GA) of the CMMA, either being constant or non-constant, based on the input port, either being translational or rotational, and based on the output port, either being translational or rotational. These properties result in 5 different classes, with a total of independent 68 CMMA designs. Each class is represented by a principle element. This is a rigid-body mechanism chosen for its simple / well-known status in mechanical engineering. The structure can be found in most of the CMMA of that class, even though not all samples of CMMA use that principle element. The class of the 'double slider' is represented the most by CMMAs. There are also classes without any CMMA samples.

The mechanical efficiency (ME) of CMMA or compliant mechanisms in general can be non-optimal because of the elastic energy storage during motion. To prevent the input energy from sinking in the elastic energy storage, and temporarily lowering the ME, a technique called 'static balancing', can be applied. In this technique an additional energy buffer can added to balance the total energy stored in the system, and ensuring most input energy is transformed into output energy, raising the ME.

For my design challenge we chose to apply a new way of static balancing, without manual preloading, onto a straight-line mechanism rather than a CMMA to simplify the problem. The source of elastic energy is applied in the structure of a buckled beam. The challenge is divided into an actuation problem, a guiding problem and a locking problem for preloading this buckling beam. After brainstorming and rapid-prototyping, executed in a 3 month period abroad at the Max Planck Institute at Stuttgart, Germany, the final concept existed of a double folded flexure guiding, locking hooks and shaking or applying shock to the main shuttle for actuation. There were two working concepts and prototypes after this period in Germany, one symmetric in shape and one with a reduced footprint. Both models can be preloaded using shock or shaking, either by hand or by a chemical shaker. Back at the TuDelft a topology study, on the concept with the reduced footprint, resulted in a theoretical model of silicon wafer material with a diameter of 30 mm, beam thicknesses of 0.024 mm and a wafer thickness of 0.525 mm.

Regrettably, the machine that was able to make this statically balanced MEMS design broke down and we were not able to fabricate this small model at this time of writing. We still hope to produce it in the future with an eye on publishing the paper about the design challenge. Meanwhile a 6:1 scale prototype has been fabricated of PMMA material with feather steel flexures. The theoretical eigenfrequency that can be used for preloading this prototype is 3 Hz, and can be actuated by shock that is applied by hand. Two prototypes were fabricated to evaluate the devices. The actuation stiffness, for the prototypes, after static balancing has been reduced by -123% and -126% compared to a theoretical -104.5% reduction was calculated using ANSYS. The final MEMS model has a theoretical preloading eigenfrequency of 22 Hz and a theoretical reduction of the actuation stiffness of 98.4 %.

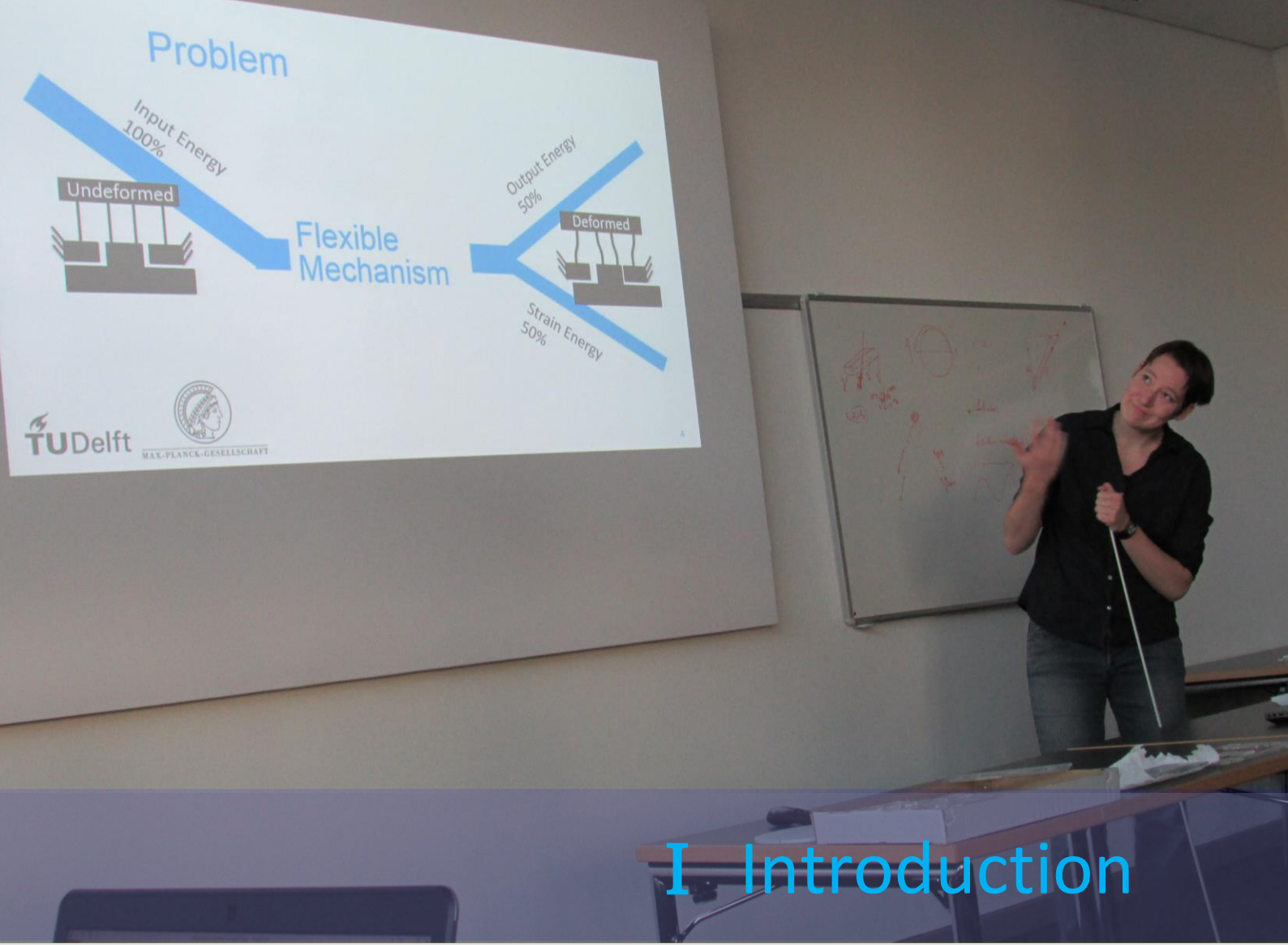

I Introduction

Cover: Introduction presentation at Max Planck Institute about design challenge

1 Introduction

In this thesis first, a classification system for compliant mechanical motion amplifiers is proposed as a result of the literature review. Secondly, a mechanical design for preloading a beam on MEMS scale is developed during the design challenge.

The literature review researches the current state of the art regarding compliant mechanical motion amplifiers. These are devices that amplify motion. For example, a 1 mm motion input is transformed into a 5 mm output. They do this by using material deflection properties. For example, instead of using a slider block joint, such devices can use a bending beam to amplify motion. There are many possible designs and there are no classification systems that successfully classify a large quantity of these devices. The literature review proposes a classification system for these devices.

The aim of making such a classification system is to enhance the accessibility of compliant mechanical motion amplifier designs. When a designer can search specifically for a type of design, the search for a suitable design concept will become more efficient.

The design challenge focuses on the development of a conceptual design for preloading a MEMS beam. In our device that is statically balanced, we can distinguish two major mechanisms. One with positive stiffness properties and another with negative stiffness properties. The main focus for the design challenge is the mechanism with negative stiffness, which contains a buckled beam that is preloaded using a so-called `preloading mechanism'.

The device can be preloaded without application of force on a specific location. Preloading can instead be performed by shaking the entire device at its first eigenfrequency. A case study is used to design the preloading mechanism. It uses a translational stage as the mechanism with positive stiffness properties. This mechanism is sometimes referred to as the case study itself. The case study is described in the design challenge paper.

The advantage of a statically balanced system is that elastic energy storage in the system is constant. Meaning that if one applies energy to the system to make a motion along a straight line, that energy directly goes into the motion and not in the elastic deformation of the compliant material. Therefore, the mechanical efficiency of the device is increased. Such an optimization in compliant systems aims at making the devices more suitable for transmission systems. For example, in sensors or actuators.

Vision

The static balancing of the translational stage is a first step in statically balancing compliant mechanical micro motion amplifiers. A statically balanced amplifier in combination with e.g. a piezo actuator might result in a range of motion that is wider than the range of the actuator itself. The concept of a preloaded / buckling beam that can be preloaded, by a generic force such as a change in pressure, temperature or shaking, enables fabrication with bath processing.

Readers guide

After the introduction, two papers are presented, one about the literature review and one about the design challenge. After this the thesis provides additional information on: approaches, concept development, rapid prototyping, concept optimization, theoretical modelling experimental evaluation and finally a reflection on the work of the past year.

2 List of abbreviations

MEMS	Micro Electro Mechanical System
CM	Compliant Mechanism
CMM	Compliant Micro Mechanism
CM(M)MA	Compliant Mechanical (Micro) Motion amplifier
SB-CMMMA	Statically Balanced CMMMA
(L)DFF	(Large) Double Folded Flexure
PB	Preload Block
MS	Main Shuttle

3 Naming of parts

Some components that frequently return are named. The concept drawing of the design challenge shows which parts are referred to by their names. There are 2 double folded flexures used in the final designs. The left one is indicated as the large double folded flexure, and the right one, next to the preload block is indicated as the small double folded flexures. Often a reference to a vertical or horizontal motion of a part is made. A vertical motion is the motion perpendicular to the main motion, a horizontal motion is a motion parallel to the main motion. The x-axis is considered to be parallel to the main motion, the y-axis perpendicular to the main motion and in plane of the drawing, and the z-axis is considered to come out of the paper.

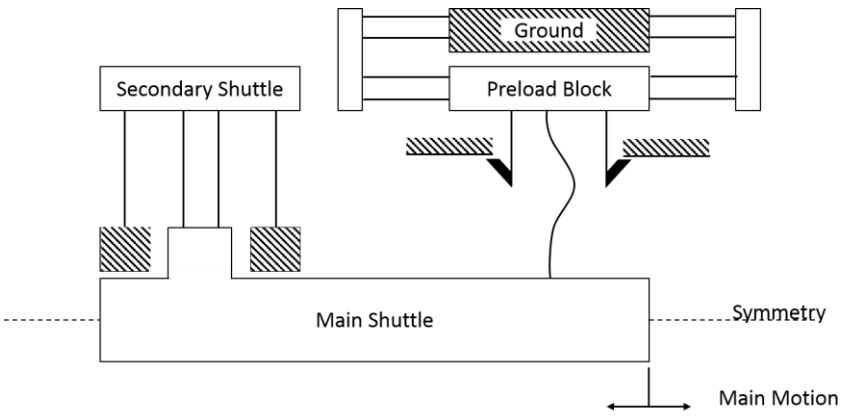

Figure 1 Concept drawing of design challenge

II Literature Review Paper

In this literature review paper, a large classification is made for compliant mechanical motion amplifiers. It classifies 68 independent CMMAs based on their type of input and output motion, which is either translational or rotational, and on their geometrical advantage, which is either constant or non-constant.

Cover: Hand sketching rigid-body mechanisms behind all CMMA found in literature review

Classifying Compliant Mechanical Motion Amplifiers by Geometrical Advantage.

M. Y. Barel, D. Farhadi Machekposhti, J. L. Herder, N. Tolou

Abstract— **Compliant mechanical amplifiers are mechanisms that reduce or increase motions and forces. Like levers and gears they can be used in actuation chains but compliant amplifiers use material bending properties instead of being rigid. There are more than 200 designs. This rising number has increased the need for a classification system which simplifies the designers quest for finding a suitable amplifier and indicates design opportunities.**

In this paper a classification system is created based on the properties of 'geometrical advantage' and input and output motion paths. This results in 6 classes depending on a constant or non-constant geometrical advantage, and on a combination of rotations and/or translations motion paths for the input and output ports. Each class is represented by a rigid body mechanism called a principle element.

It concludes that most of the 68 **compliant amplifier designs concepts classified are based on the principle elements. The classification reviews the current compliant amplifier designs and indicates new design options. The total number of concepts that is classified is less than the total designs found. Partially because some designs use the same design concepts, and partially because analyzation difficulties.**

Index Terms— **compliant mechanical, compliant transmission, mechanical amplifiers, geometrical advantage.**

I. INTRODUCTION

In the last decade compliant mechanical motion amplifiers (CMMAs) have been growing in numbers and reduced in size. A compliant mechanical motion amplifier is a device that amplifies motion, force and energy, using elastic deformation.

These devices are often 2D planar structures and are applied in the field of sensors and actuators, in for example: resonant accelerometers [1], electromagnetic devices [2], piezo actuators [3-5] or shape memory actuators [6]. Compliant amplifiers change the stroke that can be used for the input or output motions in actuation chains. They are also used in the field of micromanipulations as grippers [6-9] and in the field of visual observation in Fourier transform spectroscopy [10] and stage manipulation [11]. They are even used in the medical world for tissue cutting [12]. CMMAs can be fabricated using a wide range of techniques, such as: CNC milling machining[12], electro-discharge machining EDM [13], Bosch process in silicon [10] and photolithography [14]. The devices have many advantages over conventional assembled amplifiers. There is no need for lubrication, no wear and no backlash, they have fewer parts or monolithic structures so don't need assembly. Besides they are cost effective in batch fabrication. A nonlinear system of equations is needed to calculate elastic deformation which makes the compliant amplifiers complex. Compliant amplifiers can store strain energy while elastically deforming thereby reducing the performance of the device [15] . Designing and analyzing amplifiers can require the following techniques: Pseudo rigid body models [16], Topology optimizations/synthesis [14, 15, 17-24], Finite Element Method [3, 4, 10, 13, 18, 19, 25], Spring – Mass – Lever model analogy [26, 27], Instant center approach [28], Force method, Maxwell – Mohr [4], kinematic approach [29], and dynamic analysis [30].

The sheer number of CMMA designs existing today is extensive and therefor it is hard to oversee the current state of the field. It is acknowledged in literature that the analysis of compliant mechanical amplifiers is a non-standardized process and attempts have been made to normalize this process [30]. The fact that no classification of CMMA exist is partially due to the many different criteria used for analyzing CMMAs. As a result the biggest catalogue is small with only 9 different designs analyzed by means of 6 different specifications [23]. Classification of compliant mechanisms, without specialization in amplifiers, do exists [31]. There is also a literature review of micro motion devices wherein compliant mechanisms are discussed [32], but these readings do not have classes inside the group of CMMAs itself. Some designers use a heuristic approach [10] while others use design methods like instant center approach [16] or pseudo rigid body modeling [28]. All might benefit during this process from a classification of CMMAs. The classification of the CMMAs would not only be able to save time and induce qualitative novel design, by showing which designs already exist and can serve as a basic configuration for further design, but the classification can also indicate the design opportunities still available.

This paper presents a systematic approach to classifying CMMAs by using the input output displacement relations, also known as geometrical advantage (GA). Each emerging class is represented by a rigid-body mechanism, a principle element. The purpose is not only to aid the designer but also to raise awareness to the current state and the developmental opportunities in this relatively new field.

Categories	Keywords
Rigid body motion amplifiers	Stroke, Velocity, Amplifier, Amplification, Multiplier, Rigid body linkages
Compliant motion amplifiers	Displacement amplifying, Distributed, Elastic deformation, Deflection, Lumped, Flexure based, Monolithic, Overconstained, Single piece,
Syntheses and analysis methods for motion amplifiers	Kinematic, building block, FEM, Topology, instant center approach, design methodology, Grubler, pseudo rigid body model PRBM
Applications for motion amplifiers	Sensors, Grippers, Force amplifier, MEMS, Micro manipulation, Actuator, Stage

Table 1: Overview of sets of keywords

The classification is aimed at classifying:

1) By criterium or method that design engineers use at present time to analyse their designs.
2) By creating an unambiguous and systematic set of classification criteria by which new designs can be added.
3) A large quantity of the already known CMMAs.

Use should be made of the current criteria and analysis methods to ensure information from existing CMMAs can be processed into the classification. Building on existing information rather than making more analysis methods aims at not adding diversity in the field and thereby not complexifying the design process. New designs should be addable by designers as the classification grows. This requires that any designer classifies a design in the same way, hence the classes in the classification approach have to be unambiguous and systematic. The novelty of the classification in this paper is successfully classifying a large quantity of CMMAs.

This papers focuses on static amplification. There are two types of CMMAs, one that uses dynamic properties to amplify the stroke, like an oscillator, and one that uses static properties, like a lever system. CMMAs based on static properties don't rely on a moving mass and kinetic energy to transfer the input motion to a greater or smaller output motion. A dynamically based mechanical motion amplifier can use eigenfrequencies to transfer a motion [10]. Focusing on static amplification results in a base set of design classes that can also be used to design CMMAs that use dynamic properties, as dynamic designs can use static basic configurations [10].

II. METHOD

Several steps are taken to design a classification system for CMMAs. First a design library of CMMAs is created based on 250 papers. These papers are found using keywords from Table 1. Secondly design criteria used in design papers are collected. Thirdly the criteria for the classification approach are set based on the collected criteria.

There are many criteria found in the wide variety of papers. Most design criteria focus on the geometrical advantage (GA) [3, 18, 21, 33, 34], or another given input output displacement relationship [11, 18, 35]. Some do investigate the dynamics of the designs such as frequency [3, 34, 35], or use bode plots and force versus time and position versus time behavior [7]. Different analyses are done relating to stiffness: joint stiffness[7] , input stiffness [33, 35], out of plane stiffness [33], angular stiffness [35]. Other analysis are done relating to stress: Von misses stress [3, 13]. Some are interested in the kinematic behavior [21] and make computer analysis of the motion paths [35] or use rigid body representations [31]. Other topic are material properties, weight and buckling.

From this we conclude that the field has many different analysis criteria and many variations exist in the same class of criteria, which maybe can be considered classes of kinematic geometrical advantage, dynamic properties, fatigue /stress properties, and different kinds of stiffness properties (actuations, transmission and robustness/out of plane).

In the design of CMMAs two fields come together: mechanical and electronic, both have their own background. A great diversity of quantitative information is found in the mechanisms. For example a 6-bar (the ground is counted) mechanisms is called 5-bar, while in the same paper a four-bar (including the ground) is called a four-bar. [36]. This might also be why different versions of a input-output displacements relationships exist exist[3, 11, 18, 21, 33-35].

From the design criteria it can be concluded that GA is an important specification, no matter how it is defined by the designers. We define the GA as: *the change in position of output port divided by the change in position of the input port:*

$$GA = \frac{\delta_{out}}{\delta_{in}} \tag{1}$$

Where δ_{out} and δ_{in} represent the output and input displacement. This also strongly relates to the type of input and output ports. Is the displacement rotational or translational? This is why the GA dependency and the types of input output ports are used to build the classification system.

The 2 criteria of classification
The entire classification follows these 2 criteria of classification:

1) Does the GA of the mechanism depend on a variable, or is it constant?
2) Is the input port translation or rotational?
   Is the output port translation or rotational?

Criterium 1: The GA is constant if the it depends on variables that are constant such as the length of link. A lever is an example of a mechanisms with constant GA equation. No matter what position the lever is in, the GA is always the same. If not, the GA can be dependent on a variable like the input angle or output angle. A double slider mechanism is an example of a variable GA.

Criterium 2: By looking at the input and output port, it can determined if that port is translational or rotational. A double slider has a translational in and output port. A lever has a translational in- and output port because the GA is determined by only the x or y distance travelled by the in- and output points on a lever beam.

Using these properties we aim to classify as many CMMAs as we can. Nonetheless, not all designs from the design library can be classified. These designs where often lacking the essential information to be classified, such as the position of the input and/or output port or the GA equation, many of these where topology designed structures with unclear rigid body representations. Some designs simply do not have a rotational or translational motion of the input and/or output ports, but a combination of both. The ability to classify depends on the designer and how he/she set up the GA equation. Sometimes this was unclear and those designs are absent in the classification system. These designs are often evolutionary/ computer aided and/or topology optimized designs. Designs with more than one input or one output port are excluded too. Most amplifier designs found have one input and one output port.

After formulating different 'criteria of classification', different classes will emerge. Each class can be represented by a so called *principle element*. Its function is to aid designers to use the principle element as a first indication of how the compliant mechanism behaves. A CMMA can be represented by a pseudo rigid body model (PRBM). By looking at a compliant mechanism and its motion path one can make a rigid body model that closely describes the behavior of the compliant mechanism. Instead of completely calculating and drawing the full PRBM of every mechanism in the library, we have chosen a configuration that is the rigid body base of most compliant mechanism in its class, the principle element.

The GA of every principle element is given in the final classification overview. By using the principle elements' GA and combining it with other principle elements from a different class, more complicated structures can be modeled. Eventually the result of two principle elements might be simplified back to one principle element by only looking at its in- and output motion paths. Resulting back in the base classes that emerge from the classification criteria.

III. Results

A. Classes

The 2 criteria of classification for the classification system result in 5 different classes. For the 5 different classes rigid body mechanisms are chosen to represent the class. These are called the principle elements. They are: the four-bar, the arm and the crank-slider, the double-slider, the levers and the rotational-double-slider. These are presented in Figure 1.

The principle elements of each class are presented in Figure 2. These 5 classes will be discussed one by one. All the compliant amplifiers belonging to a class are referred to in Table 2. A short version of the class descriptions will be discussed here.

Class I: Four-bar
The principle element of this class is the four-bar. It has a rotational input and output. The kinematics of the four-bar have already been calculated [37]. On this we based the GA equation. The GA is dependent on the input angle and as such not constant. There is only one type of subgroup in this class, all the compliant designs directly correspond to the principle element configuration.

$$GA_{fourbar} = \frac{\phi_1 - \phi_0}{\theta_1 - \theta_0} = \frac{\tan^{-1}\left(\frac{A_1}{b - a\cos(\theta_1)}\right) + \cos^{-1}\left(\frac{D_1}{2d\sqrt{B_1}}\right) - \tan^{-1}\left(\frac{A_0}{b - a\cos(\theta_0)}\right) + \cos^{-1}\left(\frac{D_0}{2d\sqrt{B_0}}\right)}{\theta_1 - \theta_0} \quad (2)$$

$$A_n = a\sin(\theta_n)$$
$$\mathrm{B}_n = a^2 + b^2 - 2ab\cos(\theta_n)$$
$$D_n = K - 2ab\cos(\theta_n)$$
$$K = a^2 + b^2 - c^2 + d^2$$

n is either 0 or 1, where 0 indicates the original position and 1 the end position. The GA is based on the kinematics of a four-bar linkage described by G.L. Talbourdet [37]

Class II: Arm / Crank - Slider
The simplest principle element of this class is an arm. The input is the angle the link makes with the ground, the output is the translational motion or height of the other end of the links. The GA of this device is set as the change in angle of the link with the ground divided by the translational

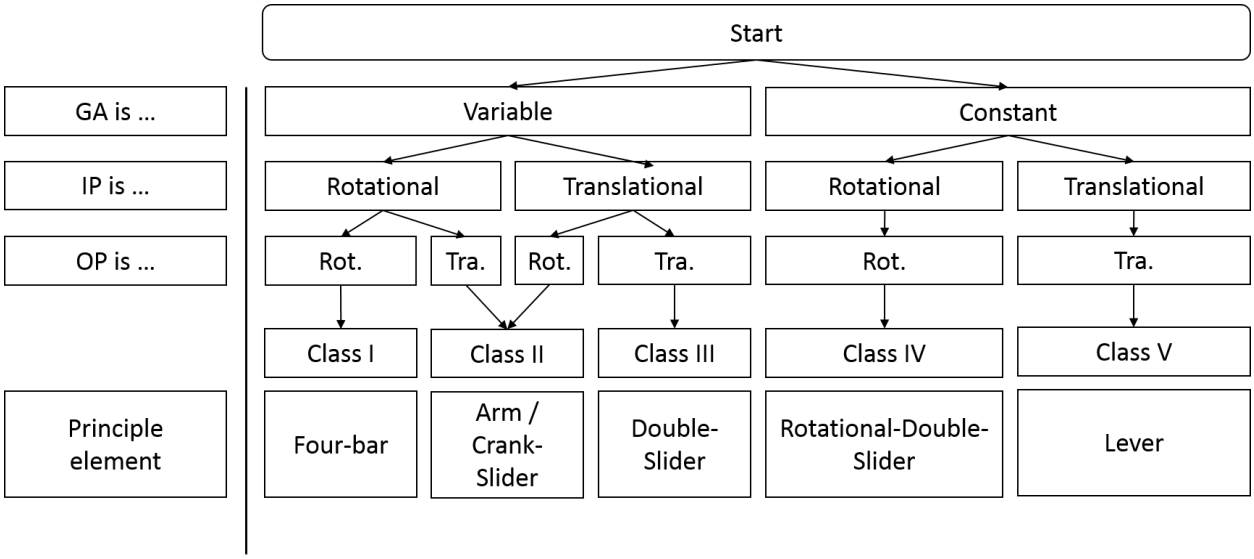

Figure 1: Classification Approach according to the 2 criteria of classification. Wherein: IP is Input Port, OP is Output Port, Rot. is Rotational, Tra. is Translational.

motion of the other end of the arm. The GA is variable. There are no compliant amplifiers in this class, however a cantilever would belong to this class. There were no examples found of a cantilever CMMA that were not part of a bigger mechanism. The arm element is included here as a principle element because it is used in combinations with other basic designs. Most designs with a rotational-translation input-output relation however can be represented with a crank-slider mechanism.

The second principle element in this class is a crank slider mechanism. The mechanism uses two links to transfer a rotational motion into a translational one. Input and output can be reversed, and then the GA needs to be inverted. The GA of this device is set as the change in translational displacement divided by the change in rotational displacement. It is non-constant and depends on the input rotational angle. There are three groups that can be distinguished: a solo crank-slider mechanism and two versions of symmetric implementation of the crank-slider design.

$$GA_{arm} = \frac{y_1 - y_0}{\theta_1 - \theta_0} = \frac{\mathrm{l}(\sin\theta_1 - \sin\theta_0)}{\theta_1 - \theta_0} \qquad (3)$$

$$GA_{crank-slider} = \frac{y_1 - y_0}{\theta_1 - \theta_0} = \frac{a(\sin\theta_1 - \sin\theta_0) + b(\cos\phi_0 - \cos\phi_1)}{\theta_1 - \theta_0} \qquad (4)$$

where 0 indicates the original position and 1 the end position.

Class III: Double-slider

The principle element of this class is a double slider (DS) mechanism. It consists of one link connected to two slider blocks. In this case the direction of travel of the slider blocks are not necessarily perpendicular to one another. The mechanism has a translational in- and output. The GA is set as the change in translational displacement of the output port divided by the change in translational displacement of the input port. The GA is non-constant and depends on the angle between the link and the axis of travel of the input block. There are 6 subgroups in this class. There is a number of DSs in series and circular designs.

$$GA_{ds} = \frac{y_1 - y_0}{x_1 - x_0} = \frac{S}{\mathrm{C}\sin(k) - S\cos(k)} \qquad (5)$$

$$S = \sin(\theta_1) - \sin(\theta_0)$$
$$C = \cos(\theta_1) - \cos(\theta_0)$$

where 0 indicates the original position and 1 the end position.

Class IV: Rotational-double-slider

The principle element of this class is a rotational double slider. A rotational DS (RDS) consists of 2 slider blocks and 2 links that are connected to the ground with a revolute joint. As the input link rotates, which is connected to the sliding blocks, it transfers momentum to the second link, shaped as a 'L'. The GA for this device is defined as the change in angle from the input link divided by the change in angle from the output link. The GA is constant. Other than this rigid mechanism there are no examples of compliant mechanisms in this class.

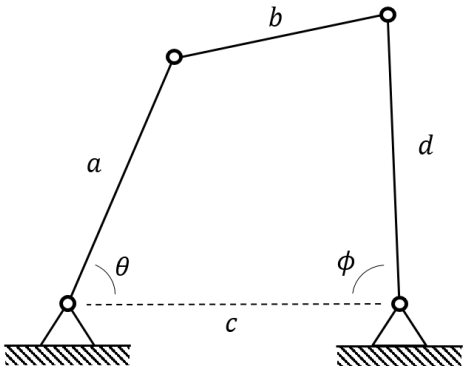

Class I: Four-Bar

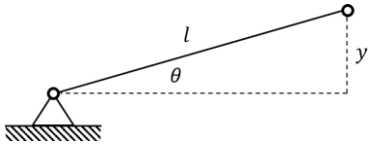

Class II-a: Arm

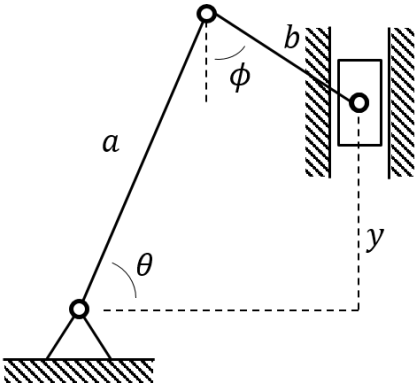

Class II-b: Crank-Slider

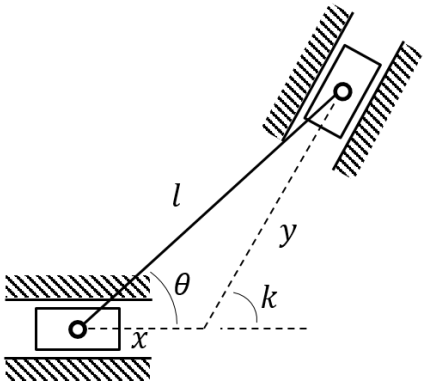

Class III: Double-Slider

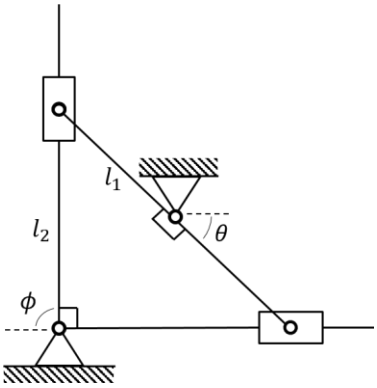

Class IV: Rotational-Double-Slider

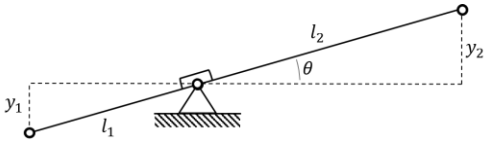

Class V: Lever

Figure 2: Principle Elements of the 5 different Classes

$$GA_{arm} = \frac{y_1 - y_0}{\theta_1 - \theta_0} = \frac{\mathrm{l}(\sin\theta_1 - \sin\theta_0)}{\theta_1 - \theta_0} \qquad (6)$$

where 0 indicates the original position and 1 the end position.

Class V: Lever

The principle element of this class is a lever mechanism. It has a translational input and output .

The GA is defined as the translational change of the output divided by the translational change of the input. The GA is constant and the height can be varied with the length of the two arms.

There are two subgroups in this class the single and the double lever designs. The double levers are levers in series. There are some similar designs in the single lever group.

$$GA_{lever} = \frac{y_{2(1)} - y_{2(0)}}{y_{1(1)} - y_{1(0)}} = \frac{l_2}{l_1} \qquad (7)$$

where 0 indicates the original position and 1 the end position.

B. Design opportunities

We designed a reference for designers to compare the designs presented in this paper. By presenting the design by following clear criteria of classification, we can see classes and subgroups emerging. Now that we have a better understanding of what is designed in the field we can better explore that what might come.

It might be explored if two non-constant GA mechanisms can be combined to make a mechanisms with a constant GA.

We have seen designs in series, like the DSs. By combining two principle elements new combinations can be found. DS40 is an example of this, this can be a combination of a crank-slider combined with a four-bar mechanism.

By expanding current developments in subgroups we can invent new subgroups. There are symmetric designs found in the crank-slider class. If we apply rotational symmetry on the crank-slider mechanisms we find a classic Watt-linkage. There are no examples of compliant versions of this mechanism in our classification. Knowing that there are DS mechanisms in series, it might be possible to have DS in parallel systems. This can result in designs that have multiple output ports or perhaps these two output ports in turn can be combined to make one final output motion.

By looking at linkages we can find new compliant configurations. For example the Jansen-linkage from the 'Strandbeesten'. Because the feet of this mechanism make a slider motion and the input is a rotational motion this mechanisms would be in the arm / cranks-slider class, class II.

By varying the principle element we can find new configurations. For example the configuration in Figure 3. The rotational-double-slider principle element has a constant GA of 0.5. Variation on this element might changes the GA and might widen the range of applications.

By looking at alternatives for the same application. A lot of development has taken place in the equal configurations of subgroup 3a of the DS class. But other designs in subgroup 3 might be a good alternative. They have the same amplification potential because they use the same GA.

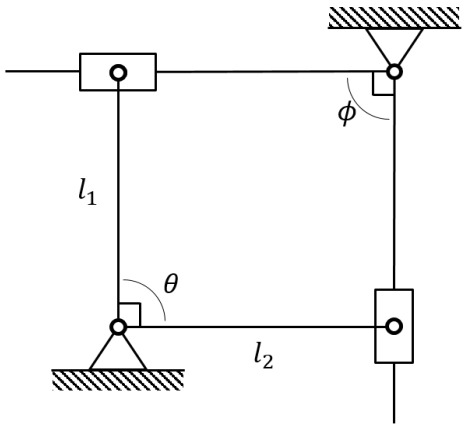

Figure 3: Variation on a Rotational-Double-Slider

Class + number	Notes	CMMA picture ref. number	Paper
FB1	1	Fig 6d	[32]*, [38]
FB2	1	Fig 3	([39]* [38])
FB3	1	Fig 7	[40]
CS1	1	Fig 1	[41]
CS2	2	Fig 2	[42]*, [36]
CS3	2	Fig 4	[43]*, [33]
CS4	2	Fig 6a	([32]* [22])
CS5	2	Fig 7	[44]
CS6	2	Fig 8	[45]
CS7	2	Fig 8	[46]
CS8	2	Fig 6a	([34]* [36]), [32], ([47] [3])
CS9	3	Fig 3	[48]

DS1	1	Fig 1	[35]
DS2	1	Fig 5	[38]
DS3	1	Fig 4	[35]
DS4	1	Fig 4	[28]
DS5	1	Fig 3	[39]
DS6	1b	Fig 2	[40]*, [41], [34], [42]
DS7	1b	Fig 1	[43]*, [44] , [45], [46], [47]
DS8	1b	Fig 1	[48]
DS9	1b	Fig 2	[49]
DS10	1b	Fig 2	[50]
DS11	1b	Fig 2	[16]*, [51]
DS12	1b	Fig 5	[52]*, [53], [54], [55], [33]
DS13	1b	Fig 2	[56]
DS14	1b	Fig 3a	[57]
DS15	2a	Fig 35	[28]*,[38]
DS16	2a	Fig 34	[28]
DS17	2a	Fig 5	[2]*,[33]
DS18	2	Fig 6	[38]
DS19	2	Fig 7	[58]
DS20	2	Fig 5	[59]*, [60]
DS21	2	Fig 1	[61]*, [25], [62]
DS22	3a	Fig 5(9)	[33]*, ([30] [22] [63] [15]), [17], ([64] [65] [66]), [26], [67], [67], ([68] [67]), [30]
DS23	3	Fig 5	[28]*, [69]
DS24	3	Fig 12	[70]
DS25	3	Fig 2	[70]*, [68]
DS26	3	Fig 5	[63]
DS27	4a	Fig 5	[71]*,[18], ([68] [70]), [17]
DS28	4a	Fig 5(1)	[33]*, [26]
DS29	4	Fig 1	[10]
DS30	4	Fig 12	[67]
DS31	5	Fig 2	([72]* [73])
DS32	5	Fig 2	[74]
DS33	6a	Fig 5(3)	[33]* [75]
DS34	6	Fig 5(8)	[33]*, [21]
DS35	6	Fig 1A	[76]
DS36	6	Fig 3	[70]
DS37	6	Fig 10A	[70]
DS38	6	Fig 1	[77]
DS39	6	Fig 15	[62]
DS40	6	Fig 3	[78]* ,[7], [32]

IV. Discussion

Building a classification that classifies a large number, 68, independent compliant designs concepts has never been done before. By doing so this classification is built on assumptions and classification criteria that can be discussed. At times it can be disputed if an additional limb in a compliant configuration can be considered a lever, an arm or if it is just an extension on the principle elements presented in this classification. Some examples of this are in FB1, that have an additional limb on the second link of the four-bar configuration. FB1's second reference gives a design for a bi-stable switching mechanism, but in the context of this classification it is also an example of a compliant four-bar which may be used as an amplifier design. In the latter the limb has no function for amplification, if compared with the principle element in- and output ports. More complex are examples in CS2, which have equal configurations. The input of these mechanisms are debatable. There are two lever-like structures attached to a symmetric crank-slider mechanism. The output is in the center of the design. Is the input a translational one on the lever-like structures? In their turn causing a rotational input for the crank slider part, or must it be considered the rotation of these lever-like structures that cause the same crank slider part to move? In the latter case the configuration is in the right class: a rotation to translation class. If we choose the input port to be translational, the mechanism it has to be in the double slider class. Even more interesting is that if this lumped design is drawn as a rigid body mechanism it should not be able to move at all. This design was chosen to be include this design in the library as it has a clear crank-slider element, and can be considered a rotational-translational design.

Many designs are not properly constrained, as the rigid body version of first referenced design in CS2 shows, it cannot move in the way that the designer intended. There are also designs that are under-constrained. DS2 is an example of a compliant double-slider mechanisms that becomes a four-bar mechanism if large motions are used. But perhaps it is these kinds of distributed compliance in four-bar mechanisms that make the four-bars fall into double-slider classes. There has been looked into the way the mechanism was designed to conclude into what categories this design would fall. There is a grey area where double-sliders and four-bar become the same compliant configurations. In the case of DS2 it is clear that the input and outputs of this compliant design fall into the DS class. In conclusion, designs may look the same, but depending on their input and output ports they can fall into different categories.

The GA of the principle element does not apply to all the compliant examples in the class. DS40 are examples of a slider input and, for small motion, and a slider output, but is not nearly a double slider configuration. It is up to the engineer to know when the principle element can be used and when not.

L1	1	Fig 3	[79]*, ([80, 81])
L2	1	Fig 2	[13]*, [80]
L3	1	Fig 3	[71]*, [82]
L4	1	Fig 1	[20]
L5	1	Fig 6c	[32]
L6	1	Fig 6b	[22]
L7	1	Fig 1	[83]
L8	1	Fig 5	[84]
L9	1	Fig 3	[9]
L10	1	Fig 5	([85]* [86] [87])
L11	1	Fig 6	[88]
L12	1	Fig 3	[89]
L13	1	Fig 2	[90]
L14	1	Fig 2	[91]
L15	2	Fig 3	([85]*, [86],[87]), [20]
L16	2	Fig 7	([85]*, [86],[87])

Table 2: Classified CMMA

Comments

Rows Every row shows one compliant amplifier design concept. That can be present in multiple papers.
* indicates the paper of which the figure reference is given.
() papers within have the exact same picture as each other

Notes

FB:
1 Single four-bar designs

CS:
1 Single Crank-Slider designs
2 Symmetric Designs. Crank-Slider configuration is applied twice as if a mirror is applied on the dashed y line. Lumped Compliance. Total GA is equal to the GA of the principle element.
3 other, here rotational-symmetric, using the rotational port as connection between both parts.

DS:
1 Single DS
1b Circular designs, 4 ds in a circle, can still be calculated using the GA of one DS, by looking at one quadrant of the circular designs.
2 2 DS in series
3 3 DS in series
4 4 DS in series
5 Circular designs in series
6 Other designs.

L:
1 Single lever designs
2 Double lever designs in series

V. Conclusion

We have built a classification system that is based on criterium or method that design engineers use at present time, the input and output motion types and GA. New designs can be added with ease as the definitions of each class are clear. The distribution of the classes is remarkable as the double slider contains by far the most designs. This is where subgroups will help to get a better understanding of the types of designs that are in the class.
The classification is aimed at classifying:

1) By criterium or method that design engineers use at present time to analyse their designs.
2) By creating an unambiguous and systematic set of criteria by which new designs can be added.
3) A large quantity of the already known CMMAs.

This resulted in successfully classifying 68 compliant designs concepts into 6 classes that are each represented by a principle element. It is remarkable how many compliant designs can be represented by the principle elements. Based on this it can be concluded that the variety, the number of principle elements that are used in CMMAs, is limited and that development of amplifiers is mainly focused on (geometrical) variations on the existing principle elements. The classification also indicates new design variations that might be explored and is a reference guide in CMMA design.

REFERENCES

1. Pedersen, C.B. and A.A. Seshia, On the optimization of compliant force amplifier mechanisms for surface micromachined resonant accelerometers. Journal of Micromechanics and Microengineering, 2004. 14(10): p. 1281.
2. Khan, S. and G.K. Ananthasuresh, A MICROMACHINED WIDE-BAND IN-PLANE SINGLE-AXIS CAPACITIVE ACCELEROMETER WITH A DISPLACEMENT-AMPLIFYING COMPLIANT MECHANISM. Mechanics Based Design of Structures and Machines, 2014. 42(3): p. 355-370.
3. Eskandari, A. and P.R. Ouyang, Design and optimization of a XY compliant mechanical displacement amplifier. Mechanical Sciences, 2013. 4(2): p. 303-310.
4. Ni, Y., et al., Modeling and analysis of an over-constrained flexure-based compliant mechanism. Measurement, 2014. 50: p. 270-278.
5. Huang, S.C. and G.J. Lan, Design and fabrication of a microcompliant amplifier with a topology optimal compliant mechanism integrated with a piezoelectric microactuator. Journal of Micromechanics and Microengineering, 2006. 16(3): p. 531-538.
6. Houston, K., et al. Polymer sensorised microgrippers using SMA actuation. in Robotics and Automation, 2007 IEEE International Conference on. 2007. IEEE.
7. Goldfarb, M. and N. Celanovic, A flexure-based gripper for small-scale manipulation. Robotica, 1999. 17: p. 181-187.
8. Grossard, M., et al., Mechanical and Control-Oriented Design of a Monolithic Piezoelectric Microgripper Using a New Topological Optimization Method. Ieee-Asme Transactions on Mechatronics, 2009. 14(1): p. 32-45.
9. Du, H., et al., A micromachined thermally-driven gripper: a numerical and experimental study. Smart materials and structures, 1999. 8(5): p. 616.
10. Sauceda-Carvajal, A., et al., Compliant MEMS Mechanism to extend resolution in Fourier Transform Spectroscopy. Micromachining and Microfabrication Process Technology Xix, 2014. 8973.
11. Brown, J.J., et al., Interchangeable Stage and Probe Mechanisms for Microscale Universal Mechanical Tester. Journal of Microelectromechanical Systems, 2012. 21(2): p. 458-466.
12. Bhargav, S.D.B., S. Chakravarthy, and G.K. Ananthasuresh, A Compliant End-Effector to Passively Limit the Force in Tele-Operated Tissue-Cutting. Journal of Medical Devices-Transactions of the Asme, 2012. 6(4).
13. Zubir, M.N.M. and B. Shirinzadeh, Development of a high precision flexure-based microgripper. Precision Engineering-Journal of the International Societies for Precision Engineering and Nanotechnology, 2009. 33(4): p. 362-370.
14. Larsen, U.D., O. Sigmund, and S. Bouwstra. Design and fabrication of compliant micromechanisms and structures with negative Poisson's ratio. in Micro Electro Mechanical Systems, 1996, MEMS '96, Proceedings. An Investigation of Micro Structures, Sensors, Actuators, Machines and Systems. IEEE, The Ninth Annual International Workshop on. 1996.
15. Kota, S., et al., Design of compliant mechanisms: Applications to MEMS. Analog Integrated Circuits and Signal Processing, 2001. 29(1-2): p. 7-15.
16. Nielson, A.J. and L.L. Howell, An investigation of compliant micro-half-pantographs using the pseudorigid body model. Mechanics of Structures and Machines, 2001. 29(3): p. 317-330.
17. Kota, S., et al., Tailoring unconventional actuators using compliant transmissions: Design methods and applications. Ieee-Asme Transactions on Mechatronics, 1999. 4(4): p. 396-408.
18. C. F. Lin, a.C.J.S., ed. A Post-Design of Topology Optimization for Mechanical Compliant Amplifier in MEMS. Tamkang Journal of Science and Engineering. Vol. 9. 2006. 215-222.
19. Canfield, S. and M. Frecker, Topology optimization of compliant mechanical amplifiers for piezoelectric actuators. Structural and Multidisciplinary Optimization, 2000. 20(4): p. 269-279.
20. Pedersen, C.B.W. and A.A. Seshia, On the optimization of compliant force amplifier mechanisms for surface micromachined resonant accelerometers. Journal of Micromechanics and Microengineering, 2004. 14(10): p. 1281-1293.
21. Hetrick, J. and S. Kota, An energy formulation for parametric size and shape optimization of compliant mechanisms. Journal of Mechanical Design, 1999. 121(2): p. 229-234.
22. Kota, S., et al. Synthesizing high-performance compliant stroke amplification systems for MEMS. in Micro Electro Mechanical Systems, 2000. MEMS 2000. The Thirteenth Annual International Conference on. 2000. IEEE.
23. Krishnan, G., Displacement-amplifying Compliant mechanisms for sensor applications. 2006, INDIAN INSTITUTE OF SCIENCE BANGALORE.
24. Shi, H., Modeling and analysis of compliant mechanisms for designing nanopositioners. 2013, The Ohio State University.

25. Liu, A.Q., et al., Self-latched micromachined mechanism with large displacement ratio. Journal of Microelectromechanical Systems, 2006. 15(6): p. 1576-1585.
26. Khan, S. and G.K. Ananthasuresh, Improving the Sensitivity and Bandwidth of In-Plane Capacitive Microaccelerometers Using Compliant Mechanical Amplifiers. Journal of Microelectromechanical Systems, 2014. 23(4): p. 871-887.
27. Hegde, S. and G. Ananthasuresh, A spring-mass-lever model, stiffness and inertia maps for single-input, single-output compliant mechanisms. Mechanism and Machine Theory, 2012. 58: p. 101-119.
28. Kim, C.J., S. Kota, and Y.M. Moon, An instant center approach toward the conceptual design of compliant mechanisms. Journal of Mechanical Design, 2006. 128(3): p. 542-550.
29. Tsai, Y.C., S.H. Lei, and H. Sudin, Design and analysis of planar compliant microgripper based on kinematic approach. Journal of Micromechanics and Microengineering, 2005. 15(1): p. 143-156.
30. Li, Z. and S. Kota. Dynamic analysis of compliant mechanisms. in ASME 2002 International Design Engineering Technical Conferences and Computers and Information in Engineering Conference. 2002. American Society of Mechanical Engineers.
31. Olsen, B.M., A design framework that employs a classification scheme and library for compliant mechanism design. 2010.
32. Ouyang, P.R., et al., Micro-motion devices technology: The state of arts review. International Journal of Advanced Manufacturing Technology, 2008. 38(5-6): p. 463-478.
33. Baichapur, G.S., et al., A Vision-Based Micro-Newton Static Force Sensor Using a Displacement-Amplifying Compliant Mechanism (DaCM). Mechanics Based Design of Structures and Machines, 2014. 42(2): p. 193-210.
34. Ouyang, P.R., et al., Design of a new compliant mechanical amplifier. Proceedings of the ASME International Design Engineering Technical Conferences and Computers and Information in Engineering Conference, Vol 7, Pts A and B. 2005, New York: Amer Soc Mechanical Engineers. 15-24.
35. Qin, Y.D., et al., Design and Kinematics Modeling of a Novel 3-DOF Monolithic Manipulator Featuring Improved Scott-Russell Mechanisms. Journal of Mechanical Design, 2013. 135(10).
36. Ouyang, P.R., W.J. Zhang, and M.M. Gupta, A new compliant mechanical amplifier based on a symmetric five-bar topology. Journal of Mechanical Design, 2008. 130(10).
37. Talbourdet, G., Mathematical solution of 4-bar linkage, Part I - Analysis of Single 4-bar linkage. Machine Design, 1941. 13(May 1941): p. 65-68.
38. Kim, C. and S. Kota. Design of a novel compliant transmission for secondary microactuators in disk drives. in ASME International Design Engineering Technical Conferences, Montreal, CA. 2002.
39. Henein, S., Short Communication: Flexure delicacies. Mechanical Sciences, 2012. 3(1): p. 1-4.
40. Conway, N.J., Z.J. Traina, and S.-G. Kim, A strain amplifying piezoelectric MEMS actuator. Journal of Micromechanics and Microengineering, 2007. 17(4): p. 781.
41. Xu, Q.S., Y.M. Li, and Ieee, Design of a New Decoupled XYZ Compliant Parallel Micropositioning Stage with Compact Structure. 2009 Ieee International Conference on Robotics and Biomimetics. 2009, New York: Ieee. 901-906.
42. Conway, N.J. and S.-G. Kim. Large-strain, piezoelectric, in-plane micro-actuator. in Micro Electro Mechanical Systems, 2004. 17th IEEE International Conference on.(MEMS). 2004. IEEE.
43. Xu, Q.S. and Y.M. Li, Analytical modeling, optimization and testing of a compound bridge-type compliant displacement amplifier. Mechanism and Machine Theory, 2011. 46(2): p. 183-200.
44. Pokines, B.J. and E. Garcia, A smart material microamplification mechanism fabricated using LIGA. Smart materials and structures, 1998. 7(1): p. 105.
45. Ni, Y., et al. Quasi-static and Modal Analysis of Bridge-Type Compliant Mechanism with Flexure Hinges. in 2013 Second International Conference on Robot, Vision and Signal Processing. 2013.
46. Lobontiu, N. and E. Garcia, Analytical model of displacement amplification and stiffness optimization for a class of flexure-based compliant mechanisms. Computers & structures, 2003. 81(32): p. 2797-2810.
47. Xiao, S., Y. Li, and X. Zhao. Design and analysis of a novel micro-gripper with completely parallel movement of gripping arms. in 2011 6th IEEE Conference on Industrial Electronics and Applications. 2011. IEEE.
48. Bolsman, C.T., J.F.L. Goosen, and F. van Keulen, Design Overview of a Resonant Wing Actuation Mechanism for Application in Flapping Wing MAVs. International Journal of Micro Air Vehicles, 2009. 1(4): p. 263-272.
49. Choi, K.-B., et al., A compliant parallel mechanism with flexure-based joint chains for two translations. International Journal of Precision Engineering and Manufacturing, 2012. 13(9): p. 1625-1632.

50. Choi, K.B., J.J. Lee, and S. Hata, A piezo-driven compliant stage with double mechanical amplification mechanisms arranged in parallel. Sensors and Actuators a-Physical, 2010. 161(1-2): p. 173-181.
51. Siu Wing Or, C.S.Y., Lai Wa Helen CHAN-WONG, Ping Kong Joseph Choy, Chou Kee Peter LIU, Piezoelectric device with amplifying mechanism. 2007, Asm Assembly Automation Ltd.: United State.
52. Schultz, J. and J. Ueda, Two-Port Network Models for Compliant Rhomboidal Strain Amplifiers. IEEE Transactions on Robotics, 2013. 29(1): p. 42-54.
53. Lau, G.K., et al., Lightweight mechanical amplifiers for rolled dielectric elastomer actuators and their integration with bio-inspired wing flappers. Smart Materials and Structures, 2014. 23(2).
54. Gary F. Hawkins, C.-Y.T., High stiffness vibration damping apparatus, methods and systems. 2014, The Aerospace Corporation: United State.
55. François Barillot, F.C., Ronan Le Letty, Piezoactive actuator with dampened amplified movement. 2005, Cedrat Technologies: United State.
56. McPherson, T. and J. Ueda, A Force and Displacement Self-Sensing Piezoelectric MRI-Compatible Tweezer End Effector With an On-Site Calibration Procedure. Ieee-Asme Transactions on Mechatronics, 2014. 19(2): p. 755-764.
57. Hao, G.B., X.W. Kong, and Asme, CONCEPTUAL DESIGN AND MODELLING OF A SELF-ADAPTIVE COMPLIANT PARALLEL GRIPPER FOR HIGH-PRECISION MANIPULATION. Proceedings of the Asme International Design Engineering Technical Conferences and Computers and Information in Engineering Conference 2012, Vol 4, Pts a and B. 2012, New York: Amer Soc Mechanical Engineers. 161-167.
58. Shyh-Chour, H. and C. Wei-Liang. Design of topologically optimal microgripper. in Systems, Man and Cybernetics, 2008. SMC 2008. IEEE International Conference on. 2008.
59. Turkseven, M., J. Ueda, and Ieee, Design of an MRI Compatible Haptic Interface. 2011 Ieee/Rsj International Conference on Intelligent Robots and Systems, 2011.
60. Turkseven, M. and J. Ueda, Analysis of an MRI Compatible Force Sensor for Sensitivity and Precision. Ieee Sensors Journal, 2013. 13(2): p. 476-486.
61. Li, J., et al. A self-limited large-displacement-ratio micromechanical amplifier. in The 13th International Conference on Solid-State Sensors, Actuators and Microsystems, 2005. Digest of Technical Papers. TRANSDUCERS '05. 2005.
62. Dinesh, M. and G. Ananthasuresh, Micro-mechanical stages with enhanced range. International Journal of Advances in Engineering Sciences and Applied Mathematics, 2010. 2(1-2): p. 35-43.
63. Kota, S., Compliant systems using monolithic mechanisms. Smart Materials Bulletin, 2001. 2001(3): p. 7-10.
64. Samuel Lee Miller, S.M.B., Murray Steven Rodgers, Microelectromechanical system and method for producing displacement multiplication. 2005, Memx, Inc.: United State.
65. Murray Steven Rodgers, S.L.M., Stephen Matthew Barnes, Jeffry Joseph Sniegowski, Paul Jackson McWhorter, Mirror positioning assembly with vertical force component compensation. 2003, Memx, Inc.: United State.
66. Samuel Lee Miller, S.M.B., Murray Steven Rodgers, Microelectromechanical system with stiff coupling. 2004, Memx, Inc.: United State.
67. Sridhar Kota, M.S.R., Joel A. Hetrick, Compliant displacement-multiplying apparatus for microelectromechanical systems. 2001, Sridhar Kota, M. Steven Rodgers, Joel A. Hetrick: United State.
68. Joel Hetrick, S.K., Displacement amplification structure and device. 2003, The Regents Of The University Of Michigan: United State.
69. Yogesh B. Gianchandani, J.A.H., Larry Li-Yang Chu, Micromechanical actuation apparatus. 2003, Wisconsin Alumni Research Foundation: United State.
70. James D. Ervin, D.M., Gregory F. Ervin, Sridhar Kota, Joel A. Hetrick, Surface Vibration Using compliant Mechanical Amplifier. 2010: United State.
71. Hetrick, J. and S. Kota. Size and Shape Optimization of Compliant Mechanisms: An Efficiency Formulation (DETC/MECH-5943). in ASME Design Engr. Technical Conf. 1998.
72. Samuel, B., A. Desai, and M. Haque, Design and modeling of a MEMS pico-Newton loading/sensing device. Sensors and Actuators A: Physical, 2006. 127(1): p. 155-162.
73. Schultz, J. and J. Ueda, Nested Piezoelectric Cellular Actuators for a Biologically Inspired Camera Positioning Mechanism. Ieee Transactions on Robotics, 2013. 29(5): p. 1125-1138.
74. Schultz, J. and J. Ueda, A Camera Positioner Driven by Muscle-Like Actuation. 2012 4th Ieee Ras & Embs International Conference on Biomedical Robotics and Biomechatronics (Biorob), 2012: p. 719-724.
75. Yin, L., G. Ananthasuresh, and J. Eder, Optimal design of a cam-flexure clamp. Finite elements in analysis and design, 2004. 40(9): p. 1157-1173.
76. Haruhiko Harry Asada, D.M.N., Phased array buckling actuator. 2013, Massachusetts Institute Of Technology: United State.

77. Kosa, E., L. Trabzon, and U. Sonmez, DYNAMIC BEHAVIOUR OF A NOVEL COMPLIANT MEMS FORCE AMPLIFIER BY MATLAB/SIMULINK, in Automation Equipment and Systems, Pts 1-4, W.Z. Chen, et al., Editors. 2012, Trans Tech Publications Ltd: Stafa-Zurich. p. 1541-1547.
78. Speich, J. and M. Goldfarb, A compliant-mechanism-based three degree-of-freedom manipulator for small-scale manipulation. Robotica, 2000. 18(01): p. 95-104.
79. Zubir, M.N.M., B. Shirinzadeh, and Y.L. Tian, A new design of piezoelectric driven compliant-based microgripper for micromanipulation. Mechanism and Machine Theory, 2009. 44(12): p. 2248-2264.
80. Zubir, M.N.M., B. Shirinzadeh, and Y.L. Tian, Development of novel hybrid flexure-based microgrippers for precision micro-object manipulation. Review of Scientific Instruments, 2009. 80(6): p. 14.
81. Zubir, M.N.M., B. Shirinzadeh, and Y. Tian, Development of a novel flexure-based microgripper for high precision micro-object manipulation. Sensors and Actuators A: Physical, 2009. 150(2): p. 257-266.
82. Jouaneh, M. and R. Yang, Modeling of flexure-hinge type lever mechanisms. Precision Engineering, 2003. 27(4): p. 407-418.
83. Nah, S.K. and Z.W. Zhong, A microgripper using piezoelectric actuation for micro-object manipulation. Sensors and Actuators a-Physical, 2007. 133(1): p. 218-224.
84. Zaidi, N.A. and S.A. Bazaz, ANALYTICAL MODELING OF DUAL ACTUATED COMPLIANT BEAM MICROGRIPPER SYSTEM. Journal of Theoretical and Applied Mechanics, 2014. 52(2): p. 459-468.
85. Su, X.-P.S. and H.S. Yang, Design of compliant microleverage mechanisms. Sensors and Actuators A: Physical, 2001. 87(3): p. 146-156.
86. Su, X.-P. and H. Yang, Single-stage microleverage mechanism optimization in a resonant accelerometer. Structural and multidisciplinary optimization, 2001. 21(3): p. 246-252.
87. Su, X.-P. and H. Yang, Two-stage compliant microleverage mechanism optimization in a resonant accelerometer. Structural and Multidisciplinary Optimization, 2001. 22(4): p. 328-334.
88. Zeimpekis, I., I. Sari, and M. Kraft, Characterization of a mechanical motion amplifier applied to a MEMS accelerometer. Journal of Microelectromechanical Systems, 2012. 21(5): p. 1032-1042.
89. Slocum, A., et al., Characterization of compliant structure force-displacement behavior. 2002, Google Patents.
90. Shi, H., H.-J. Su, and N. Dagalakis, A stiffness model for control and analysis of a MEMS hexapod nanopositioner. Mechanism and Machine Theory, 2014. 80: p. 246-264.
91. Cragun, R. and L.L. Howell. A constrained thermal expansion micro-actuator. in Micro-electro-mechanical Systems (MEMS). 1998.

Literature Review Paper Supplement

Containing:

Reference table
Picture library

Class + Number	Notes	CMMA picture number	individual names figures / designs	Paper
FB1	1	Fig 6d	FB1-1, FB1-2	[1]*, [2]
FB2	1	Fig 3	(FB1-3)	([3]* [2])
FB3	1	Fig 7	FB1-4	[4]
CS1	1	Fig 1	CS1-1	[5]
CS2	2	Fig 2	CS2-1*, CS2-2	[6]*, [7]
CS3	2	Fig 4	CS2-3*, CS2-4	[8]*, [9]
CS4	2	Fig 6a	(CS2-5)	([1]* [10])
CS5	2	Fig 7	CS2-6	[11]
CS6	2	Fig 8	CS2-7	[12]
CS7	2	Fig 8	CS2-8	[13]
CS8	2	Fig 6a	(CS2-9)*, CS2-10, (CS2-11)	([14]* [7]), [1], ([15] [16])
CS9	3	Fig 3	CS3-1	[17]
DS1	1	Fig 1	DS1-1	[18]
DS2	1	Fig 5	DS1-2	[19]
DS3	1	Fig 4	DS1-3	[18]
DS4	1	Fig 4	DS1-4	[20]
DS5	1	Fig 3	DS1-5	[21]
DS6	1b	Fig 2	DS1-6*, DS1-7, DS1-8, DS1-9	[22]*, [23], [14], [24]
DS7	1b	Fig 1	DS1-10*, DS1-11, DS1-12, DS1-13, DS1-14	[25]* +[26] , [27], [28], [29]
DS8	1b	Fig 1	DS1-15	[30]
DS9	1b	Fig 2	DS1-16	[31]
DS10	1b	Fig 2	DS1-17	[32]
DS11	1b	Fig 2	DS1-18*, DS1-19	[33]*, [34]
DS12	1b	Fig 5	DS1-20*, DS1-21, DS1-22, DS-1-23, DS1-24	[35]*, [36], [37], [38], [9]
DS13	1b	Fig 2	DS1-25	[39]
DS14	1b	Fig 3a	DS1-26	[40]
DS15	2a	Fig 35	DS2-1*, DS2-2	[20]*,[19]
DS16	2a	Fig 34	DS2-3	[20]
DS17	2a	Fig 5	DS2-4*, DS2-5	[41]*,[9]
DS18	2	Fig 6	DS2-6	[19]
DS19	2	Fig 7	DS2-7	[42]
DS20	2	Fig 5	DS2-8*,DS2-9	[43]*, [44]
DS21	2	Fig 1	DS2-10*, DS2-11, DS2-12	[45]*, [46], [47]
DS22	3a	Fig 5(9)	DS3-1*, (DS3-2), DS3-3, (DS3-4), DS3-5, DS3-6, DS3-7, (DS3-8), DS3-9	[9]*, ([48] [10] [49] [50]), [51], ([52] [53] [54]), [55], [56], [56], ([57] [56]), [48]
DS23	3	Fig 5	DS3-10*, DS3-11	[20]*, [58]
DS24	3	Fig 12	DS3-12	[59]
DS25	3	fig 2	DS3-13	([59]*)[57]
DS26	3	Fig 5	DS3-14	[49]

DS27	4a	Fig 5	DS4-1*, DS4-2, (DS4-3), DS4-4	[60]*,[61], ([57] [59]), [51]
DS28	4a	Fig 5(1)	DS4-5*, DS4-6	[9]*, [55]
DS29	4	Fig 1	DS4-7	[62]
DS30	4	Fig 12	DS4-8	[56]
DS31	5	Fig 2	(DS5-1)	([63]* [64])
DS32	5	Fig 2	DS5-2	[65]
DS33	6a	Fig 5(3)	DS6-1*, DS6-2	[9]* [66]
DS34	6	Fig 5(8)	DS6-3*, DS6-4	[9]*, [67]
DS35	6	Fig 1A	DS6-5	[68]
DS36	6	Fig 3	DS6-6	[59]
DS37	6	Fig 10A	DS6-7	[59]
DS38	6	Fig 1	DS6-8	[69]
DS39	6	Fig 15	DS6-9	[47]
DS40	6	Fig 3	DS6-10*, DS6-11, DS6-12	[70]* ,[71], [1]
L1	1	Fig 3	L1-1*, (L1-2)	[72]*, ([73, 74])
L2	1	Fig 2	L1-3*, L1-4	[75]*, [73]
L3	1	Fig 3	L1-5*, L1-6	[60]*, [76]
L4	1	Fig 1	L1-7*	[77]
L5	1	Fig 6c	L1-8	[1]
L6	1	Fig 6b	L1-9	[10]
L7	1	Fig 1	L1-10	[78]
L8	1	Fig 5	L1-11	[79]
L9	1	Fig 3	L1-12	[80]
L10	1	Fig 5	(L1-13)	([81]* [82] [83])
L11	1	Fig 6	L1-14	[84]
L12	1	Fig 3	L1-15	[85]
L13	1	Fig 2	(L1-16)	[86]
L14	1	Fig 2	L1-17	[15]
L15	2	Fig 3	(L2-1)*, L2-2	([81]*, [82],[83]), [77]
L16	2	Fig 7	(L2-3),	([81]*, [82],[83])

<table>
<tr><td colspan="4">Four-bar</td></tr>
<tr><td>FB1-1
  </td><td>FB1-2
 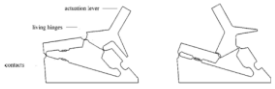
Fig. 7 Layout for a fully-compliant bistable switch as-fabricated (a) and closed (b)</td><td>FB1-3
 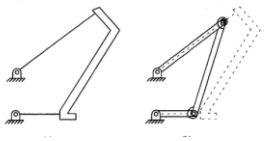 </td><td>FB1-4
 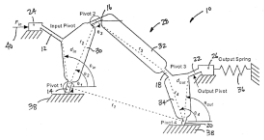 </td></tr>
<tr><td colspan="4">Crank-Slider</td></tr>
<tr><td>CS1-1
 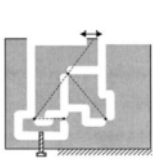 </td><td>CS2-1
 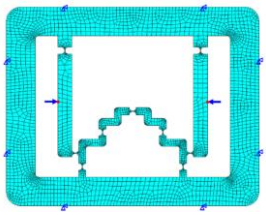 </td><td>CS2-2
 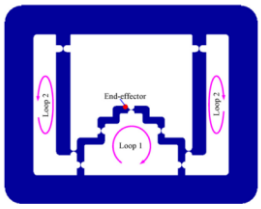
Fig. 1. 3D model of the five-bar micro-manipulator.</td><td>CS2-3
 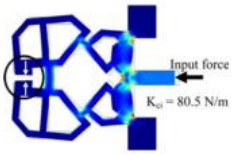 </td></tr>
<tr><td>CS2-4
 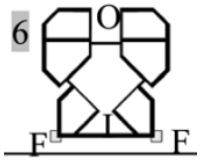 </td><td>CS2-5
 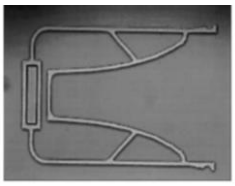 </td><td>CS2-6
 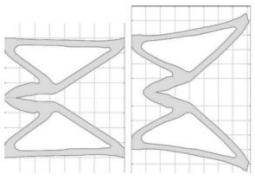 </td><td>CS2-7
 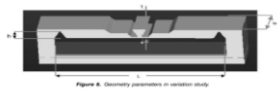 </td></tr>
<tr><td>CS2-8
 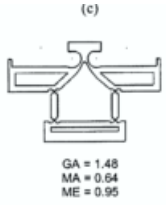 </td><td>CS2-9
  </td><td>CS2-10
 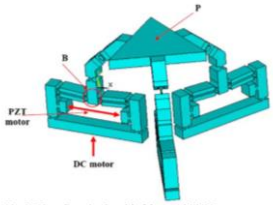
Fig. 5 Three-dimensional model of the spatial HMM</td><td>CS2-11
 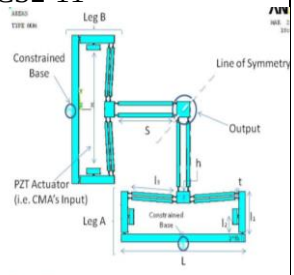
Figure 2. Planar motion generator CMDA based on symmetric bar topology.</td></tr>
</table>

CS3-1 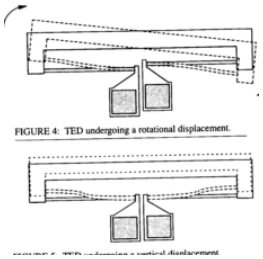 			
Double -Slider			
DS1-1 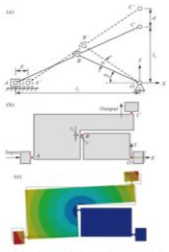	DS1-2 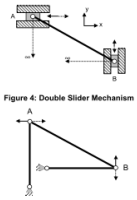 	DS1-3 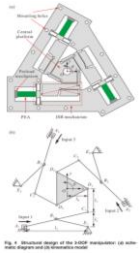	DS1-4 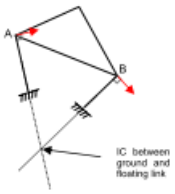
DS1-5 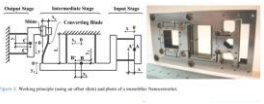	DS1-6 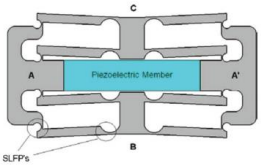 	DS1-7 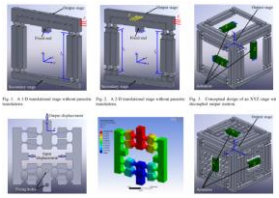	DS1-8 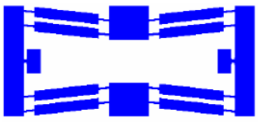
DS1-9 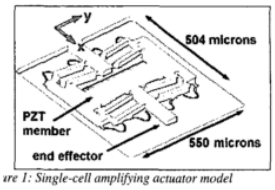 *ure 1: Single-cell amplifying actuator model*	DS1-10 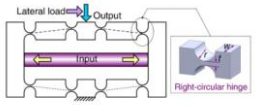 Fig. 1. A flexure-based bridge-type displacement amplifier with a backward output.	DS1-11 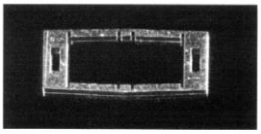 **Figure 2.** Nickel microamplification device.	DS1-12 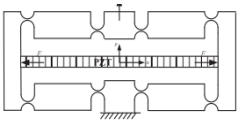 Fig. 1 Schematic of bridge-type amplifier with flexure hinge
DS1-13 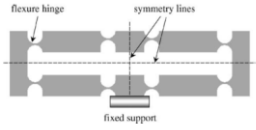 Fig. 3. Schematic of amplifier mechanism with circular flexure hinges at joints.	DS1-14 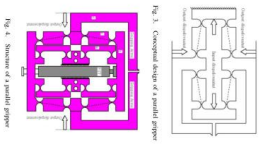	DS1-15 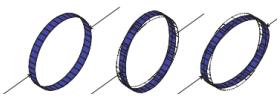	DS1-16 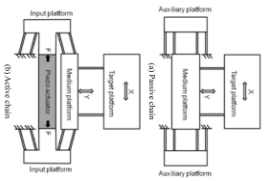

DS1-17 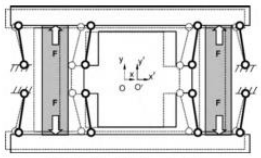 Fig. 2. Operational principle of actuating mechanism.	DS1-18 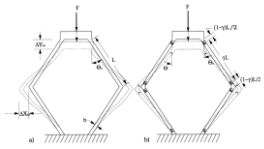	DS1-19 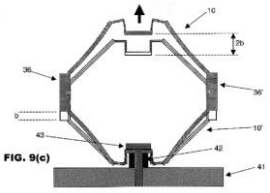 FIG. 9(c)	DS1-20 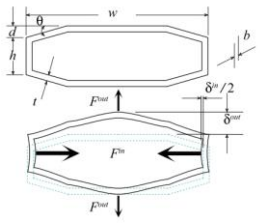 5. Example parameters for model verification.
DS1-21 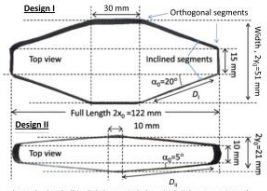 (Noted: the shell is slightly warped along its height. Its projected shadow in the top view does not represents the thickness)	DS1-22 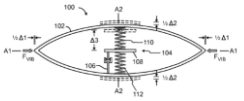	DS1-23 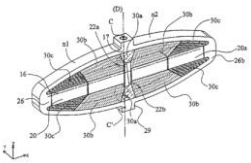	DS1-24 
DS1-25 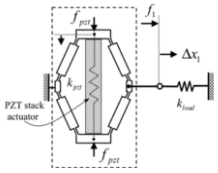 g. 2. Schematic diagram of a rhomboidal strain amplifier. A smal splacement $\Delta x_{1,ext}$ is amplified at the output, Δx_1.	DS1-26 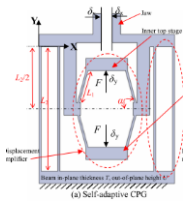 (a) Self-adaptive CPG	DS2-1 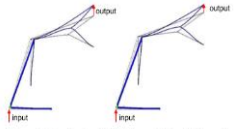 Figure 35: Design 2. ANSYS linear (GA = 8.54) and nonlinear deflection results.	DS2-2 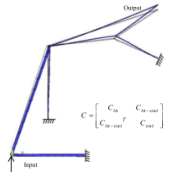
DS2-3 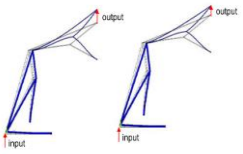 Figure 34: Design 1. ANSYS linear (GA = 8.65) and nonlinear deflection results	DS2-4 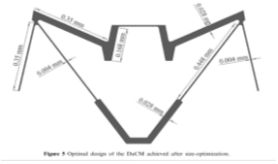	DS2-5 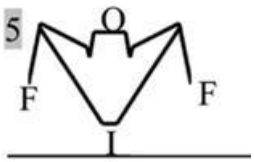	DS2-6 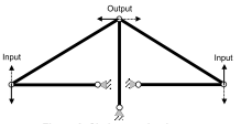 Figure 6: Six-bar mechanism
DS2-7 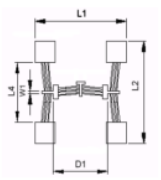 The V-shape beam microactuator dimension scheme	DS2-8 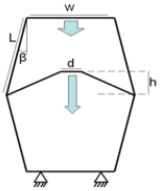 **Fig. 5.** 2D sketch of the mechanism. L, d, w, h represent size of relevant bars and β is the angle as shown.	DS2-9 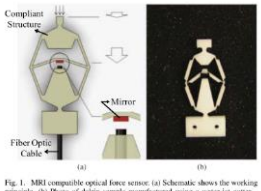 Fig. 1. MRI compatible optical force sensor. (a) Schematic shows the working principle. (b) Photo of delrin sample manufactured using a water-jet cutter.	DS2-10 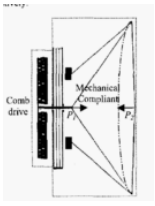

DS2-11 	DS2-12 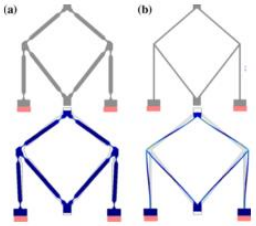	DS3-1 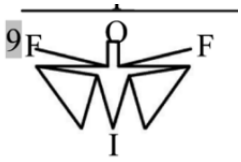	DS3-2 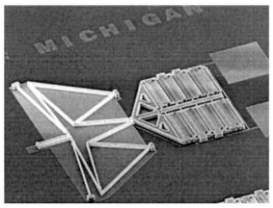
DS3-3 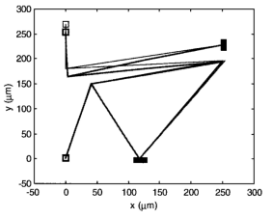	DS3-4 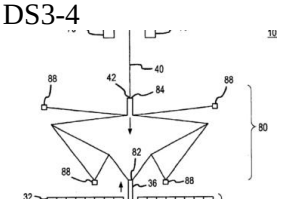	DS3-5 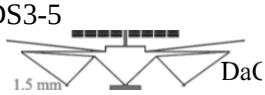	DS3-6 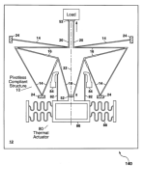
DS3-7 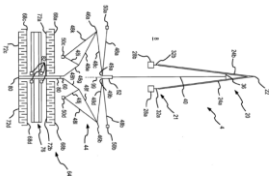	DS3-8 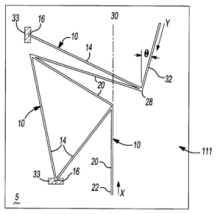	DS3-9 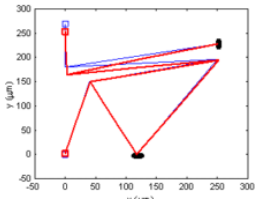	DS3-10 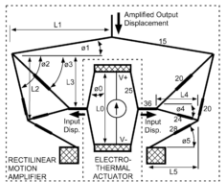
DS3-11 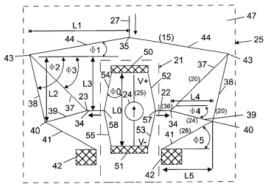	DS3-12 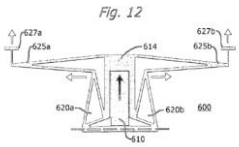	DS3-13 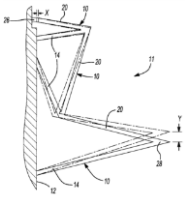	DS3-14 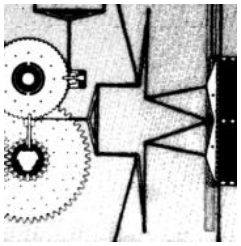
DS4-1 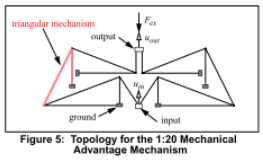 Figure 5: Topology for the 1:20 Mechanical Advantage Mechanism	DS4-2 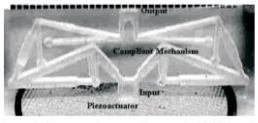 Figure 1. Piezoceramic actuator integrated with 20:1 stroke amplification mechanism [2].	DS4-3 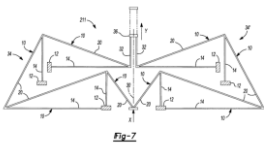 Fig-7	DS4-4 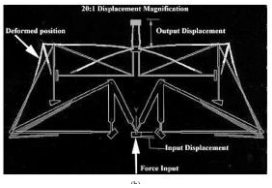

DS4-5 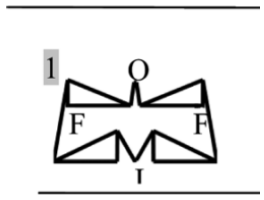	DS4-6 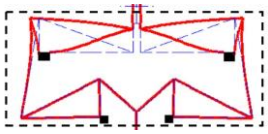	DS4-7 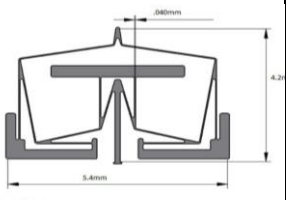 ıliant Structure.	DS4-8 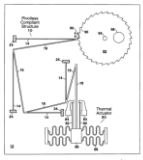
DS5-1 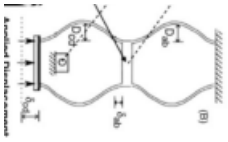	DS5-2 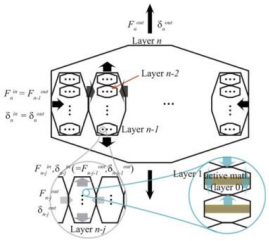	DS6-1 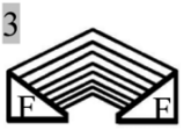	DS6-2 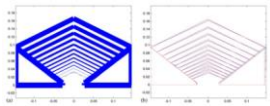
DS6-3 	DS6-4 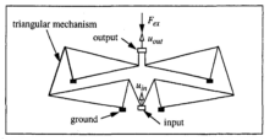	DS6-5 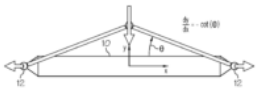	DS6-6 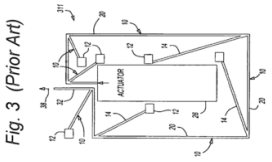
DS6-7 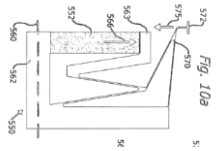	DS6-8 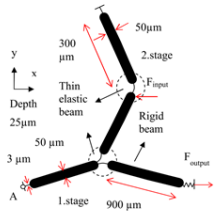 Fig.1:Dimensions of compliant micro force amplifier	DS6-9 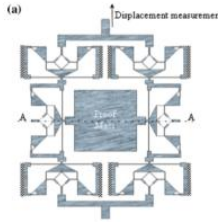	DS6-10 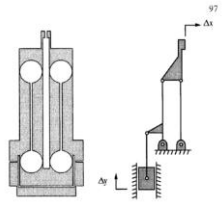 Fig. 3. Two-dimensional drawing of the gripper structure and the kinematically idealized schematic of (one half of) the flexure-based linkage.
DS6-11 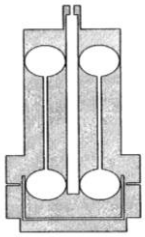	DS6-12 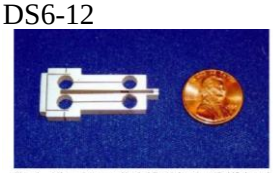 Fig. 9 Microgripper at Vanderbilt University (Goldfarb and Celanovic [16])		

Lever			
L1-1 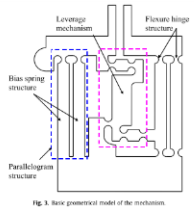 Fig. 3. Basic geometrical model of the mechanism.	L1-2 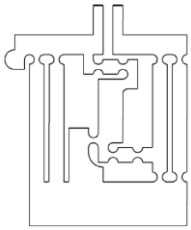 Basic geometrical model of the microgripper (second model).	L1-3 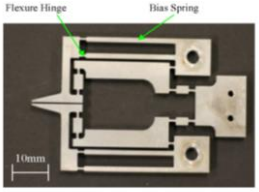 Fig. 2. Microgripper prototype.	L1-4 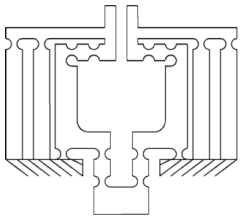 FIG. 2. Basic geometrical model of the microgripper (first model).
L1-5 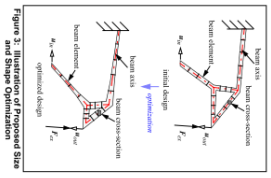 	L1-6 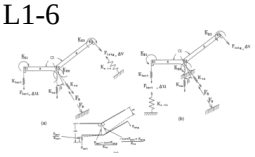	L1-7 	L1-8 
L1-9 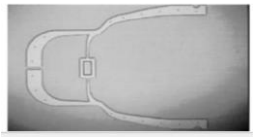	L1-10 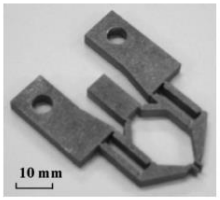 Fig. 1. The microgripper designed and fabricated.	L1-11 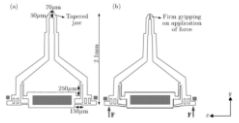 Fig. 5. Gripper arm and beam system design (a) with no force (b) under applied force	L1-12 
L1-13  	L1-14 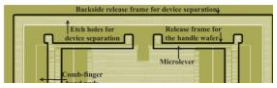 	L1-15 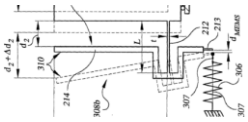	L1-16 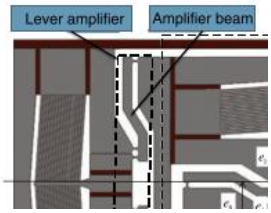
L1-17 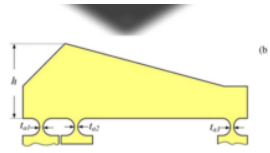	L2-1 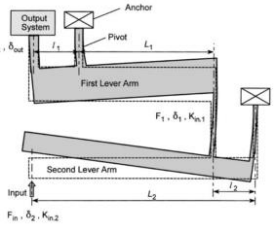 	L2-2 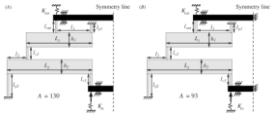	L2-3 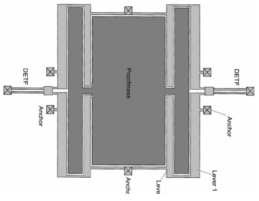

REFERENCES

1. Ouyang, P.R., et al., *Micro-motion devices technology: The state of arts review.* International Journal of Advanced Manufacturing Technology, 2008. **38**(5-6): p. 463-478.
2. Jensen, B.D. and L.L. Howell, *Identification of compliant pseudo-rigid-body four-link mechanism configurations resulting in bistable behavior.* Journal of Mechanical Design, 2003. **125**(4): p. 701-708.
3. Jensen, B., L. Howell, and L. Salmon, *Design of two-link, in-plane, bistable compliant micro-mechanisms.* Journal of Mechanical Design, 1999. **121**(3): p. 416-423.
4. Jensen, B.D., M. Farina, and K. Kurabayashi, *Compliant micro mechanism has base structure and link members which define four-bar linkage for providing amplified force or displacement output in response to input force*. 2002, UNIV MICHIGAN (UNMI-C) JENSEN B D (JENS-Individual) FARINA M (FARI-Individual) KURABAYASHI K (KURA-Individual) UNIV MICHIGAN (UNMI-C).
5. Yin, L. and G. Ananthasuresh, *Design of distributed compliant mechanisms.* Mechanics Based Design of Structures and Machines, 2003. **31**(2): p. 151-179.
6. Tian, Y., B. Shirinzadeh, and D. Zhang, *A flexure-based five-bar mechanism for micro/nano manipulation.* Sensors and Actuators a-Physical, 2009. **153**(1): p. 96-104.
7. Ouyang, P.R., W.J. Zhang, and M.M. Gupta, *A new compliant mechanical amplifier based on a symmetric five-bar topology.* Journal of Mechanical Design, 2008. **130**(10).
8. Reddy, A.N., et al., *Miniature Compliant Grippers With Vision-Based Force Sensing.* Ieee Transactions on Robotics, 2010. **26**(5): p. 867-877.
9. Baichapur, G.S., et al., *A Vision-Based Micro-Newton Static Force Sensor Using a Displacement-Amplifying Compliant Mechanism (DaCM).* Mechanics Based Design of Structures and Machines, 2014. **42**(2): p. 193-210.
10. Kota, S., et al. *Synthesizing high-performance compliant stroke amplification systems for MEMS*. in *Micro Electro Mechanical Systems, 2000. MEMS 2000. The Thirteenth Annual International Conference on*. 2000. IEEE.
11. Wang, M.Y. and S. Chen, *Compliant mechanism optimization: analysis and design with intrinsic characteristic stiffness.* Mechanics based design of structures and machines, 2009. **37**(2): p. 183-200.
12. Bharti, S. and M.I. Frecker, *Optimal design and experimental characterization of a compliant mechanism piezoelectric actuator for inertially stabilized rifle.* Journal of Intelligent Material Systems and Structures, 2004. **15**(2): p. 93-106.
13. Frecker, M. and S. Canfield, *Optimal design and experimental validation of compliant mechanical amplifiers for piezoceramic stack actuators.* Journal of Intelligent Material Systems and Structures, 2000. **11**(5): p. 360-369.
14. Ouyang, P.R., et al., *Design of a new compliant mechanical amplifier*. Proceedings of the ASME International Design Engineering Technical Conferences and Computers and Information in Engineering Conference, Vol 7, Pts A and B. 2005, New York: Amer Soc Mechanical Engineers. 15-24.
15. Cragun, R. and L.L. Howell. *A constrained thermal expansion micro-actuator*. in *Micro-electro-mechanical Systems (MEMS)*. 1998.
16. Eskandari, A. and P.R. Ouyang, *Design and optimization of a XY compliant mechanical displacement amplifier.* Mechanical Sciences, 2013. **4**(2): p. 303-310.
17. Tang, H. and Y. Li, *Development and Active Disturbance Rejection Control of a Compliant Micro-/Nanopositioning Piezostage With Dual Mode.* IEEE Transactions on Industrial Electronics, 2014. **61**(3): p. 1475-1492.
18. Qin, Y.D., et al., *Design and Kinematics Modeling of a Novel 3-DOF Monolithic Manipulator Featuring Improved Scott-Russell Mechanisms.* Journal of Mechanical Design, 2013. **135**(10).

19. Kim, C. and S. Kota. *Design of a novel compliant transmission for secondary microactuators in disk drives*. in *ASME International Design Engineering Technical Conferences, Montreal, CA*. 2002.
20. Kim, C.J., S. Kota, and Y.M. Moon, *An instant center approach toward the conceptual design of compliant mechanisms.* Journal of Mechanical Design, 2006. **128**(3): p. 542-550.
21. Henein, S., *Short Communication: Flexure delicacies.* Mechanical Sciences, 2012. **3**(1): p. 1-4.
22. Conway, N.J., Z.J. Traina, and S.-G. Kim, *A strain amplifying piezoelectric MEMS actuator.* Journal of Micromechanics and Microengineering, 2007. **17**(4): p. 781.
23. Xu, Q.S., Y.M. Li, and Ieee, *Design of a New Decoupled XYZ Compliant Parallel Micropositioning Stage with Compact Structure*. 2009 Ieee International Conference on Robotics and Biomimetics. 2009, New York: Ieee. 901-906.
24. Conway, N.J. and S.-G. Kim. *Large-strain, piezoelectric, in-plane micro-actuator*. in *Micro Electro Mechanical Systems, 2004. 17th IEEE International Conference on.(MEMS)*. 2004. IEEE.
25. Xu, Q.S. and Y.M. Li, *Analytical modeling, optimization and testing of a compound bridge-type compliant displacement amplifier.* Mechanism and Machine Theory, 2011. **46**(2): p. 183-200.
26. Pokines, B.J. and E. Garcia, *A smart material microamplification mechanism fabricated using LIGA.* Smart materials and structures, 1998. **7**(1): p. 105.
27. Ni, Y., et al. *Quasi-static and Modal Analysis of Bridge-Type Compliant Mechanism with Flexure Hinges*. in *2013 Second International Conference on Robot, Vision and Signal Processing*. 2013.
28. Lobontiu, N. and E. Garcia, *Analytical model of displacement amplification and stiffness optimization for a class of flexure-based compliant mechanisms.* Computers & structures, 2003. **81**(32): p. 2797-2810.
29. Xiao, S., Y. Li, and X. Zhao. *Design and analysis of a novel micro-gripper with completely parallel movement of gripping arms*. in *2011 6th IEEE Conference on Industrial Electronics and Applications*. 2011. IEEE.
30. Bolsman, C.T., J.F.L. Goosen, and F. van Keulen, *Design Overview of a Resonant Wing Actuation Mechanism for Application in Flapping Wing MAVs.* International Journal of Micro Air Vehicles, 2009. **1**(4): p. 263-272.
31. Choi, K.-B., et al., *A compliant parallel mechanism with flexure-based joint chains for two translations.* International Journal of Precision Engineering and Manufacturing, 2012. **13**(9): p. 1625-1632.
32. Choi, K.B., J.J. Lee, and S. Hata, *A piezo-driven compliant stage with double mechanical amplification mechanisms arranged in parallel.* Sensors and Actuators a-Physical, 2010. **161**(1-2): p. 173-181.
33. Nielson, A.J. and L.L. Howell, *An investigation of compliant micro-half-pantographs using the pseudorigid body model.* Mechanics of Structures and Machines, 2001. **29**(3): p. 317-330.
34. Siu Wing Or, C.S.Y., Lai Wa Helen CHAN-WONG, Ping Kong Joseph Choy, Chou Kee Peter LIU, *Piezoelectric device with amplifying mechanism*. 2007, Asm Assembly Automation Ltd.: United State.
35. Schultz, J. and J. Ueda, *Two-Port Network Models for Compliant Rhomboidal Strain Amplifiers.* IEEE Transactions on Robotics, 2013. **29**(1): p. 42-54.
36. Lau, G.K., et al., *Lightweight mechanical amplifiers for rolled dielectric elastomer actuators and their integration with bio-inspired wing flappers.* Smart Materials and Structures, 2014. **23**(2).
37. Gary F. Hawkins, C.-Y.T., *High stiffness vibration damping apparatus, methods and systems*. 2014, The Aerospace Corporation: United State.
38. François Barillot, F.C., Ronan Le Letty, *Piezoactive actuator with dampened amplified movement*. 2005, Cedrat Technologies: United State.

39. McPherson, T. and J. Ueda, *A Force and Displacement Self-Sensing Piezoelectric MRI-Compatible Tweezer End Effector With an On-Site Calibration Procedure.* Ieee-Asme Transactions on Mechatronics, 2014. **19**(2): p. 755-764.
40. Hao, G.B., X.W. Kong, and Asme, *CONCEPTUAL DESIGN AND MODELLING OF A SELF-ADAPTIVE COMPLIANT PARALLEL GRIPPER FOR HIGH-PRECISION MANIPULATION*. Proceedings of the Asme International Design Engineering Technical Conferences and Computers and Information in Engineering Conference 2012, Vol 4, Pts a and B. 2012, New York: Amer Soc Mechanical Engineers. 161-167.
41. Khan, S. and G.K. Ananthasuresh, *A MICROMACHINED WIDE-BAND IN-PLANE SINGLE-AXIS CAPACITIVE ACCELEROMETER WITH A DISPLACEMENT-AMPLIFYING COMPLIANT MECHANISM.* Mechanics Based Design of Structures and Machines, 2014. **42**(3): p. 355-370.
42. Shyh-Chour, H. and C. Wei-Liang. *Design of topologically optimal micrograpper*. in *Systems, Man and Cybernetics, 2008. SMC 2008. IEEE International Conference on*. 2008.
43. Turkseven, M., J. Ueda, and Ieee, *Design of an MRI Compatible Haptic Interface.* 2011 Ieee/Rsj International Conference on Intelligent Robots and Systems, 2011.
44. Turkseven, M. and J. Ueda, *Analysis of an MRI Compatible Force Sensor for Sensitivity and Precision.* Ieee Sensors Journal, 2013. **13**(2): p. 476-486.
45. Li, J., et al. *A self-limited large-displacement-ratio micromechanical amplifier*. in *The 13th International Conference on Solid-State Sensors, Actuators and Microsystems, 2005. Digest of Technical Papers. TRANSDUCERS '05.* 2005.
46. Liu, A.Q., et al., *Self-latched micromachined mechanism with large displacement ratio.* Journal of Microelectromechanical Systems, 2006. **15**(6): p. 1576-1585.
47. Dinesh, M. and G. Ananthasuresh, *Micro-mechanical stages with enhanced range.* International Journal of Advances in Engineering Sciences and Applied Mathematics, 2010. **2**(1-2): p. 35-43.
48. Li, Z. and S. Kota. *Dynamic analysis of compliant mechanisms*. in *ASME 2002 International Design Engineering Technical Conferences and Computers and Information in Engineering Conference*. 2002. American Society of Mechanical Engineers.
49. Kota, S., *Compliant systems using monolithic mechanisms.* Smart Materials Bulletin, 2001. **2001**(3): p. 7-10.
50. Kota, S., et al., *Design of compliant mechanisms: Applications to MEMS.* Analog Integrated Circuits and Signal Processing, 2001. **29**(1-2): p. 7-15.
51. Kota, S., et al., *Tailoring unconventional actuators using compliant transmissions: Design methods and applications.* Ieee-Asme Transactions on Mechatronics, 1999. **4**(4): p. 396-408.
52. Samuel Lee Miller, S.M.B., Murray Steven Rodgers, *Microelectromechanical system and method for producing displacement multiplication*. 2005, Memx, Inc.: United State.
53. Murray Steven Rodgers, S.L.M., Stephen Matthew Barnes, Jeffry Joseph Sniegowski, Paul Jackson McWhorter, *Mirror positioning assembly with vertical force component compensation*. 2003, Memx, Inc.: United State.
54. Samuel Lee Miller, S.M.B., Murray Steven Rodgers, *Microelectromechanical system with stiff coupling*. 2004, Memx, Inc.: United State.
55. Khan, S. and G.K. Ananthasuresh, *Improving the Sensitivity and Bandwidth of In-Plane Capacitive Microaccelerometers Using Compliant Mechanical Amplifiers.* Journal of Microelectromechanical Systems, 2014. **23**(4): p. 871-887.
56. Sridhar Kota, M.S.R., Joel A. Hetrick, *Compliant displacement-multiplying apparatus for microelectromechanical systems*. 2001, Sridhar Kota, M. Steven Rodgers, Joel A. Hetrick: United State.
57. Joel Hetrick, S.K., *Displacement amplification structure and device*. 2003, The Regents Of The University Of Michigan: United State.
58. Yogesh B. Gianchandani, J.A.H., Larry Li-Yang Chu, *Micromechanical actuation apparatus*. 2003, Wisconsin Alumni Research Foundation: United State.

59. James D. Ervin, D.M., Gregory F. Ervin, Sridhar Kota, Joel A. Hetrick, *Surface Vibration Using compliant Mechanical Amplifier*. 2010: United State.
60. Hetrick, J. and S. Kota. *Size and Shape Optimization of Compliant Mechanisms: An Efficiency Formulation (DETC/MECH-5943)*. in *ASME Design Engr. Technical Conf*. 1998.
61. C. F. Lin, a.C.J.S., ed. *A Post-Design of Topology Optimization for Mechanical Compliant Amplifier in MEMS*. Tamkang Journal of Science and Engineering. Vol. 9. 2006. 215-222.
62. Sauceda-Carvajal, A., et al., *Compliant MEMS Mechanism to extend resolution in Fourier Transform Spectroscopy.* Micromachining and Microfabrication Process Technology Xix, 2014. **8973**.
63. Samuel, B., A. Desai, and M. Haque, *Design and modeling of a MEMS pico-Newton loading/sensing device.* Sensors and Actuators A: Physical, 2006. **127**(1): p. 155-162.
64. Schultz, J. and J. Ueda, *Nested Piezoelectric Cellular Actuators for a Biologically Inspired Camera Positioning Mechanism.* Ieee Transactions on Robotics, 2013. **29**(5): p. 1125-1138.
65. Schultz, J. and J. Ueda, *A Camera Positioner Driven by Muscle-Like Actuation.* 2012 4th Ieee Ras & Embs International Conference on Biomedical Robotics and Biomechatronics (Biorob), 2012: p. 719-724.
66. Yin, L., G. Ananthasuresh, and J. Eder, *Optimal design of a cam-flexure clamp.* Finite elements in analysis and design, 2004. **40**(9): p. 1157-1173.
67. Hetrick, J. and S. Kota, *An energy formulation for parametric size and shape optimization of compliant mechanisms.* Journal of Mechanical Design, 1999. **121**(2): p. 229-234.
68. Haruhiko Harry Asada, D.M.N., *Phased array buckling actuator*. 2013, Massachusetts Institute Of Technology: United State.
69. Kosa, E., L. Trabzon, and U. Sonmez, *DYNAMIC BEHAVIOUR OF A NOVEL COMPLIANT MEMS FORCE AMPLIFIER BY MATLAB/SIMULINK*, in *Automation Equipment and Systems, Pts 1-4*, W.Z. Chen, et al., Editors. 2012, Trans Tech Publications Ltd: Stafa-Zurich. p. 1541-1547.
70. Speich, J. and M. Goldfarb, *A compliant-mechanism-based three degree-of-freedom manipulator for small-scale manipulation.* Robotica, 2000. **18**(01): p. 95-104.
71. Goldfarb, M. and N. Celanovic, *A flexure-based gripper for small-scale manipulation.* Robotica, 1999. **17**: p. 181-187.
72. Zubir, M.N.M., B. Shirinzadeh, and Y.L. Tian, *A new design of piezoelectric driven compliant-based microgripper for micromanipulation.* Mechanism and Machine Theory, 2009. **44**(12): p. 2248-2264.
73. Zubir, M.N.M., B. Shirinzadeh, and Y.L. Tian, *Development of novel hybrid flexure-based microgrippers for precision micro-object manipulation.* Review of Scientific Instruments, 2009. **80**(6): p. 14.
74. Zubir, M.N.M., B. Shirinzadeh, and Y. Tian, *Development of a novel flexure-based microgripper for high precision micro-object manipulation.* Sensors and Actuators A: Physical, 2009. **150**(2): p. 257-266.
75. Zubir, M.N.M. and B. Shirinzadeh, *Development of a high precision flexure-based microgripper.* Precision Engineering-Journal of the International Societies for Precision Engineering and Nanotechnology, 2009. **33**(4): p. 362-370.
76. Jouaneh, M. and R. Yang, *Modeling of flexure-hinge type lever mechanisms.* Precision Engineering, 2003. **27**(4): p. 407-418.
77. Pedersen, C.B.W. and A.A. Seshia, *On the optimization of compliant force amplifier mechanisms for surface micromachined resonant accelerometers.* Journal of Micromechanics and Microengineering, 2004. **14**(10): p. 1281-1293.
78. Nah, S.K. and Z.W. Zhong, *A microgripper using piezoelectric actuation for micro-object manipulation.* Sensors and Actuators a-Physical, 2007. **133**(1): p. 218-224.
79. Zaidi, N.A. and S.A. Bazaz, *ANALYTICAL MODELING OF DUAL ACTUATED COMPLIANT BEAM MICROGRIPPER SYSTEM.* Journal of Theoretical and Applied Mechanics, 2014. **52**(2): p. 459-468.

80. Du, H., et al., *A micromachined thermally-driven gripper: a numerical and experimental study.* Smart materials and structures, 1999. **8**(5): p. 616.
81. Su, X.-P.S. and H.S. Yang, *Design of compliant microleverage mechanisms.* Sensors and Actuators A: Physical, 2001. **87**(3): p. 146-156.
82. Su, X.-P. and H. Yang, *Single-stage microleverage mechanism optimization in a resonant accelerometer.* Structural and multidisciplinary optimization, 2001. **21**(3): p. 246-252.
83. Su, X.-P. and H. Yang, *Two-stage compliant microleverage mechanism optimization in a resonant accelerometer.* Structural and Multidisciplinary Optimization, 2001. **22**(4): p. 328-334.
84. Zeimpekis, I., I. Sari, and M. Kraft, *Characterization of a mechanical motion amplifier applied to a MEMS accelerometer.* Journal of Microelectromechanical Systems, 2012. **21**(5): p. 1032-1042.
85. Slocum, A., et al., *Characterization of compliant structure force-displacement behavior*. 2002, Google Patents.
86. Shi, H., H.-J. Su, and N. Dagalakis, *A stiffness model for control and analysis of a MEMS hexapod nanopositioner.* Mechanism and Machine Theory, 2014. **80**: p. 246-264.

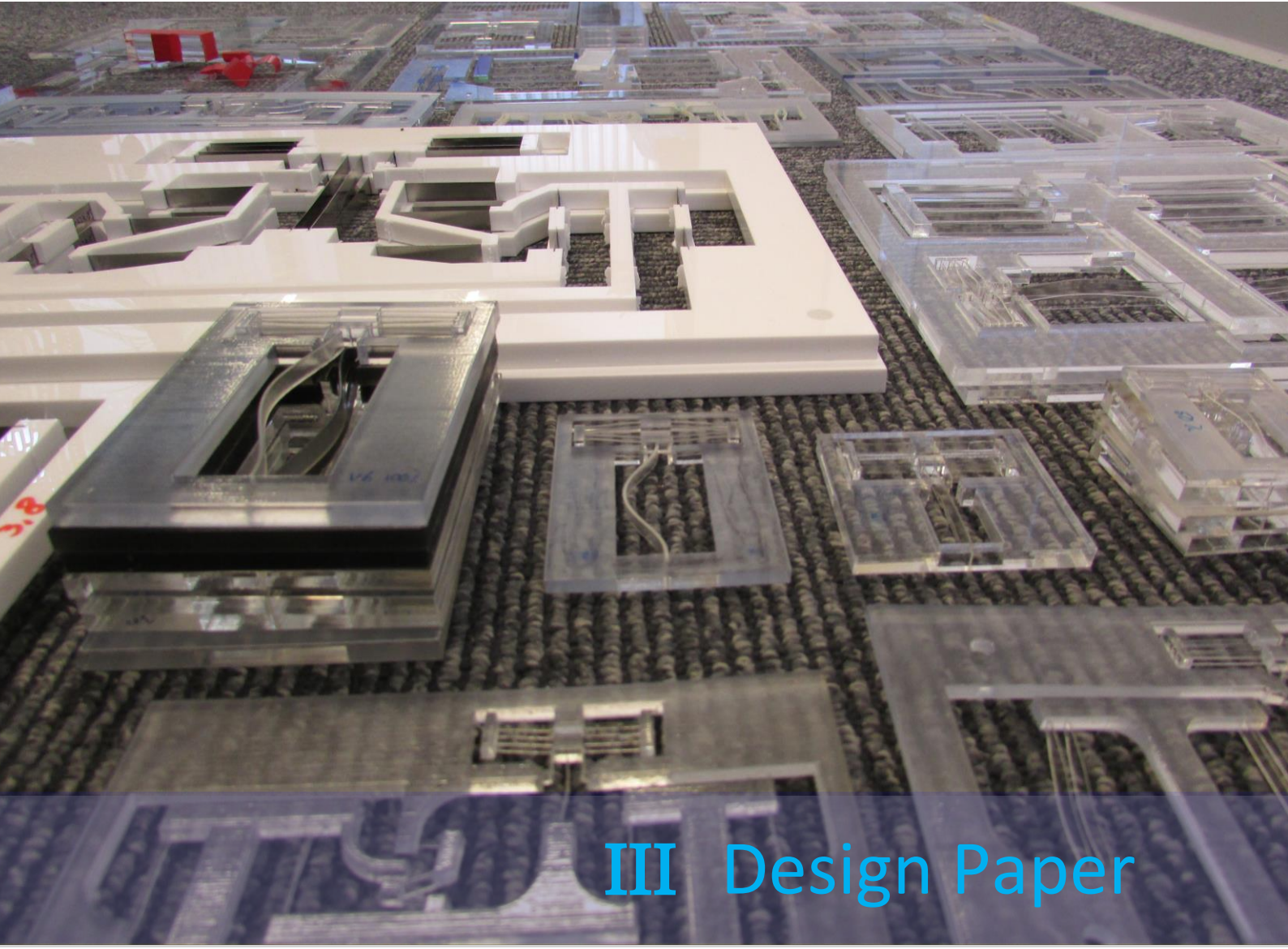

III Design Paper

In this design paper a mechanism is developed for preloading a buckling beam in a straight line guiding system in order to make the system statically balanced. The preloading mechanism consists of 3 combined sub-designs for latching (hooks), guiding (a double folded flexure) and actuation (shaking). The total model, including the straight line mechanism is analysed, fabricated and tested.

Cover: Models made in Germany (rapid prototyping) and the Netherlands (white models)

Permanent Preloading by Acceleration for Statically Balancing MEMS Devices

M. Y. Barel, D. Farhadi Machekposhti, J. L. Herder, M. Sitti, N. Tolou

***Abstract*— Static balancing is used to reduce the actuation stiffness in a translational stage compliant mechanism. The planar and monolithic compliant mechanism is preloaded using a buckling beam of which the top part is guided by a double folded flexure. Hooks lock the top part of the beam in place ensure a permanent static balancing of the entire device. The preloading action is caused by an external shaking or shock to the device. A theoretical MEMS model with a radius of 18.6 mm is develop and a 6:1 prototype is fabricated and tested on static balancing and first eigenfrequency and mode. Finite element modelling is used to on both models to predict static balancing and eigenmode behaviour. Experiments on two equally fabricated prototypes show a reduction of -123% and -126% actuation stiffness where -104.5% was predicted for both of them. The expected reduction for the designed MEMS device is 98.4%. The experimental first eigenfrequency of the prototype is 3.10+-0.25 Hz against a theoretical 3.09 Hz. The theoretical first eigenfrequency of the MEMS model is 21.8 HZ. The prototype is successfully preloaded by applying shaking or shock by hand. The predicted minimal energy requirement for this is 4.9e-3, where 6.4e-3 J and 5.9e-3 J where calculated based on experimental results. The expected minimal energy required for preloading the designed MEMS device is 1.0e-5 J**

***Index Terms*—MEMS, static balancing, zero stiffness, compliant mechanisms, negative stiffness, buckling beam, latching hooks, preloading by acceleration**

I. INTRODUCTION

A. State of the art

As mechanisms become smaller the use of compliant mechanism (CM) becomes more evident. CM use elastic deformation rather than rigid joints to move. Such that there is no need for lubrication, no wear and no backlash, they have fewer part or monolithic structures so do not need assembly. They are also cost effective in batch fabrication. CM are however often non-linear and complex. They are sensitive to high stress concentrations and material fatigue. CM can store strain energy while elastically deforming thereby reducing the mechanical efficiency of the device as the stored energy is not available at the output port.

This problem of elastic energy storage is most present in distributed types of CM. With lumped compliance the deformation is located in a small location. In distributed compliance the deformation is located over a large range of the moving part. Both systems store energy and as such have a reduced efficiently in transferring force and displacement to another location.

CMs can have applications in for example sensors and actuators [1-6], stages [7, 8] and microgrippers [6, 9-12].

CMs can also be classified in another two types using dynamic and/or static properties. Cm based on static properties do not rely on a moving mass to transfer motion. A dynamically based CM can use eigenfrequencies to transfer motion or motions. Static balancing focusses on static designs where mass does not play a role. As friction and damping are absent or nearly zero in the design, static balancing focusses on the stiffness properties of the design only. Our design uses some dynamic properties for preloading, but focuses on a mechanism that is analysed quasi-statically after preloading.

The drawback of temporarily storing elastic energy while deflecting the CM can be solved with the technique of static balancing. 5 equivalent criteria for static balancing of cm are described by [13]. These criteria are: Constant potential energy, continuous equilibrium, natural stability or zero stiffness, zero virtual work and zero natural frequency and constant speed. The paper states that when the potential energy is constant the device is statically balanced.

The temporary storage of strain energy in CM can be stabilized by implementing another sink/source that counteracts the storage of the original storage as can be seen in *Figure 1*. For example, to a positive stiffness device a negative stiffness can be introduced to balance the system.

There are various methods to add a potential energy source. Springs like zero-length springs can be used to balance the mechanism. [14-17]. These balancing springs can be turned into compliant versions of springs [18, 19]. Weights can also be implemented to function as potential energy sources [20, 21]. Other designs even use magnetics for balancing a stick and release system [22] and to cancel table vibrations [23]. Introducing negative stiffness into the system can also be used to counteract the positive stiffness in the mechanisms [9, 24-27]. Negative stiffness can be introduced by using buckling beams [28-30].

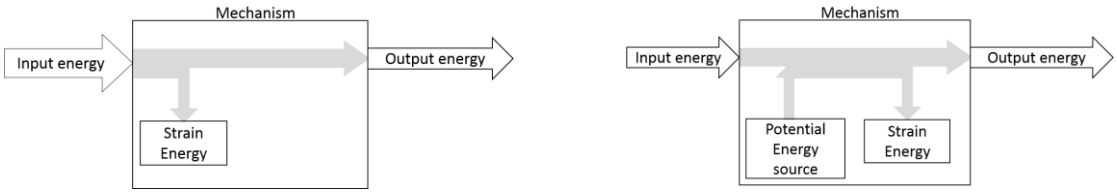

a) Non-balanced system *b) Statically balanced system*

Figure 1: Concept of static balancing based on energy diagrams in [13]

These are concepts that might be applied in MEMS such that they can be balanced. A collinear-type statically balance compliant micro mechanism [31] is an example of a SBCM where a curved fixed-fixed double layer beam is compressed by a load from the top and meets a cantilever beam in the middle. As the curved fixed-fixed beam is bi-stable, this will act as a negative stiffness when it meets the positive stiffness from the cantilever. [32] Presents two concepts, one where the preload force is perpendicular to the travel path, and one where force and path are parallel to each other. The second concept has an equal configuration as in the collinear-type statically balance compliant micro mechanism. The first concept used buckling beams as implemented negative stiffness.

The thesis of N. Tolou [33] from 2012 was aimed at introducing the first statically balance compliant mechanisms (SB-CMs) for MEMS and precision engineering. A linear combination of two bi-stable behaviours in a compliant mechanism were used to create a near zero actuation force, where 91% reduction was expected and 80% reduction was achieved after fabrication. A bi-stable CM combined with a linear stiffness CM was also designed and resulted in a reduction of actuation force by a range of 90% to 98% and a stiffness reduction by a range of 85% to 99,5 %. Two constant force mechanisms were also used to create static balancing, actuation force saw a maximum om 99,5% reduction, stiffness 98%. The thesis states that the two constant force mechanism design is negatively influenced by hysteresis of material, which results in a 10% error of the balancing force during measurement. The cover shows two constant force structures made out of carbon nanotube forest that are connected with two hooks creating a statically balanced CM. Alternatives for using hooks for static balancing CMs are other latching structures. Latching structures that are known to MEMS are a rack-and-tooth mechanism [34], and two teeth back-to-back structure to lock flexures into place [35].

B. Problem/vision

There are limited designs that implement static balancing in micro mechanisms. Implementations of buckling beam and flexures are found. How the preloading motion itself is actualized is also an important aspect of static balancing design. So far, all the SBCMM use a force on a specific location for applying the preloading force. Not only the preloading element itself but how the preloading is applied (actuation), how the preloading motion is guaranteed (guiding) and how the preloaded element keeps preloaded (locking) are part of the total design of SBCM. By exploring new possibilities in this preloading field, new applications and more design options may be found. The employability of these SBCMM is enhanced as the ineffective mechanical efficiency are counteracted by preloading.

C. Research objective

In this paper a method and preloading concept for preloading a micro beam is developed and applied in a translational stage compliant micro mechanism. Preloading is no longer applied by directly moving a component, but by shaking or applying shock.

The *method* section is broken up in two parts, a part before and a part during and after the process of rapid prototyping. The part before rapid prototyping discusses the conceptual preloading concept. Then these concepts are further refined using rapid prototyping after which the methods used for fine detailed design are presented. In the *results* section the final detailed designs, and the theoretical and experimental result of the final designed MEMS device and 6:1 prototypes are presented. These will be discussed in *discussion* section followed by the *conclusion* section. Drawings of the models can be found in the *Design section.*

II. METHOD

A. The basic setup

As springs and weights, they require assembly, used for preloading are not applicable in monolithic MEMS, compliant structures that provided a negative stiffness element need to be found. A wider range of implementation is reached by development of a negative stiffness mechanism that can be matched with different positive stiffness devices. Therefor use is made of a positive stiffness mechanism to provide a backdrop for designing a preload mechanism. For this a double folded flexure is used, that has 1 degree of freedom. A buckling beam is chosen as negative stiffness element. This is a compact way of implementing a compliant version of a zero-length spring that is used for SB. The basic concept of this setup can be found in Figure 2. The figure is showing a possible

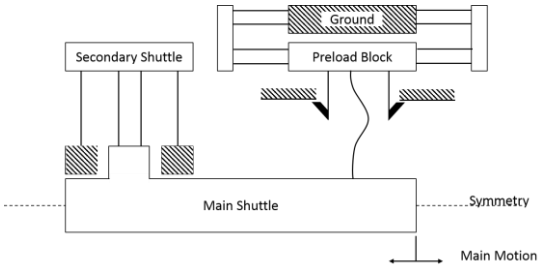

Figure 2: Conceptual impression of design challenge

configuration solution to the design challenge. It shows the double folded flexure in the left whereto the main shuttle is attached that moves horizontally. A buckling beam is attached on the right side of the main shuttle. The preload block needs to move downwards to preload the buckling beam.

B. Criteria for the design

To make the conceptual approaches to preloading the design space is determined.

1) The eventual design has to be planar. This is to ensure applications in flat designs. Use can be made of 3D or 2,5D solution that are temporary to apply the preloading.
2) The approaches need to be applicable in a MEMS materials, silicon wafer material. The design has to be monolithic and without manual assembly, as most MEMS devices are.
3) The preload has to be permanent without external intervention. E.g. not temperature dependent. It might be reversible but only with outside intervention
4) Criteria classes for the design are:
    a. Fabrication, less complex is better
    b. Robustness to outside influences, less is better
    c. Footprint, smaller is better
    d. Complexity, less steps in design process is better.
    e. Range of motion, larger is better
    f. Accuracy, more accurate is better.

C. Sub-solutions for Actuating, Guiding and Locking

Using different force types: Temperature, audio, electromagnetic, pressure and material, a morphological table is developed. Sub-designs are generated to find a wide range of design options, these sub-designs fulfil the function of actuation, guiding or locking.

1) Guiding: Provide a straight line motion for the preload block. In line with the preload beam, vertical.
2) Locking: Maintaining the preload block position after actuation.
3) Actuation: Providing force on the preload block such that it moves to its desired end position.

A new brainstorming tool was used to find the best potential design combination of guiding, locking and actuation. First, concepts were made for each sub-designs, they were ranked using weight tables. Then the four best scoring designs are used in a 'ternary plot'. This plot has 3 axes: guiding, locking and actuation. It is shown in Figure 11. This ternary plot is a variation on a morphological table. In a morphological table, 4 sub-designs in each design section would result in 4^3 results. The ternary plot generates 16 designs.

Its advantages are a reduced generation of designs without eliminating one of the sub-design solutions. Because the results are used in rapid prototyping, variation on the concepts can still be made so only an indication /orientation of the possible design is needed in our case. This is what the ternary plot generates.

Its disadvantage is that one should be cautious to only look at the generated concept in the cell. Variations can be made in the cell itself and also with different combinations of sub-designs. It best not used to rule out other concepts, but as an orientation tool.

The best potential design that came forth of brainstorming and selection is a design where big mass motion is used for actuation, double folded flexures for guidance and flexures for locking. Using this combination of sub-concepts designs where made in the rapid-prototyping development stage.

D. Calculations

Stiffness of components

The calculation used for estimating stiffnesses in rapid prototyped designs:

Positive stiffness of unbuckled flexures:

$$K_{pos} = 12\frac{EI}{L^3} \tag{1}$$

Negative stiffness of buckled flexures:

$$K_{neg} = -\frac{8\pi^2 EI}{L^3} \tag{2}$$

With L length, E young modulus, I the second moment of inertia. In all cased the beams are fixed cannot rotate at both ends and.

Due to the effect of load stiffening the calculations are less accurate. Therefor FEM analysis is used later to optimize

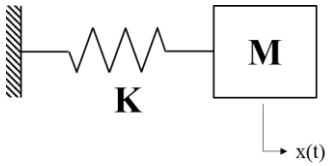

Figure 3: Dynamic model representation

the design with more accurate stiffnesses. The calculations are used in the rapid prototyping face.

The preloading force is not influencing the negative stiffness of the buckling beam. It does however influence the yield strength and the max displacement (stroke). These equations originate from [27].

$$u_{\max} = \alpha\left(2L\sqrt{\frac{dL}{3L}}\right) \tag{3}$$

$$\sigma_y = 2\pi E\frac{h}{L}\sqrt{\frac{dL}{L}} \tag{4}$$

With, α as deflection factor, L as length, dL as the preload displacement, E as young modulus, u the displacement, h the height of the flexure, (in our case the in-plane thickness, the smallest value of the flexure dimensions) and σ as stress.

Preloading by acceleration

The device will be preloaded by shaking the main shuttle. The device can be modelled and analysed as a one spring and mass system as long as the second or higher eigenmodes of the original system are not excited in any way. This is because all moving parts displacements can then be described by the main shuttle displacement. When the first mode is excited the mode should equal to the intended quasi-static motion. Friction forces of any kind are ignored as they are expected to only have a small contribution. Damping forces are also disregarded. The model representation is given in Figure 3.

Where M is the simplified mass, and K is the simplified stiffness, and x (t) is de displacement of the main shuttle. They can be calculated by adding up the individual masses/stiffnesses with respect to their individual displacements and rewriting them to one mass / stiffness with respect to the main shuttles displacement.

The total energy described in the system is given in equation 5. The minimal amount of energy needed for preloading is can be described by equation 6. The first eigenfrequency can be described with equation 7.

$$E(x,t) = \tfrac{1}{2}Kx(t)^2 + \tfrac{1}{2}M\dot{x}(t)^2 \tag{5}$$

$$E_{\min}(x_d) = \tfrac{1}{2}Kx_d{}^2 \tag{6}$$

Where x_d is the displacement needed for preloading.

$$\omega_n = \frac{1}{2\pi}\sqrt{\frac{K}{M}} \tag{7}$$

With ω_n in Hz. This can be used to calculate the simplified mass in during ANSYS modelling, with which we will calculated the natural frequency and the simplified stiffness.

Preloading by external shaking

When the device is shaken by an external force we can model this with equation 8.

$$F_0\cos(\omega t) = M\ddot{x}(t) + Kx(t) \tag{8}$$

Where

$$\begin{aligned} x(t) &= \left(x_0 - \frac{F_0}{K - M\omega^2}\right)\cos(\omega_n t) \\ &+ \left(\frac{\dot{x}_0}{\omega_n}\right)\sin(\omega_n t) + \left(\frac{F_0}{K - M\omega^2}\right)\cos(\omega t) \end{aligned} \tag{9}$$

Assuming x_0 and $\dot{x}_0$ are 0 at the start the equation can be simplified towards:

$$x(t) = \left(\frac{F_0}{K - M\omega^2}\right)\left(\cos(\omega_n t) + \cos(\omega t)\right) \tag{10}$$

If $x(t) \geq x_d$ the preload will occur.

III. Concept

A. *From flexure locking to hook latching*

Prototypes are made from the preload concepts using rapid prototyping. From this it is experienced that flexure locking is not working properly. The flexures become undone easily and cannot withstand the force caused by the buckled preload beam. Because hooks carry the load along the length of the flexure, they are better suited for withstanding the preload forces. It was experienced that the double folded flexure construction, where the outer flexures are connected to the ground, requires the ground structure to be expended inward and underneath the preload block. This undermines a good stiffness for the ground structures. Based on this we can enforce two optimizations:

1) Use hooks for locking
2) Use a double folded flexure where the beams connected to the ground are all on one side (in this

case two beams at the top connect to the ground and two beams at the lower end connect to the preload block.

A series of more porotypes are made where hooks are used. They do exhibit the wanted locking behaviour.

B. Symmetric design and a symmetric design (rapid prototyping)

From rapid prototyping two design where develop that use two different configurations of double folded flexure, hooks and shaking for preloading. There designs can be found in the design drawing section. The first design is a symmetric design, shown in Figure 12, where the two preloaded beams are used. The second design is an asymmetric design, shown in Figure 13, where there is only one preloaded beam. The advantage of the second design is the reduced footprint. However, this design needs a lever mechanism to ensure a straight line motion of the shuttle. (due to load stiffening the flexures of the double folded flexure construction suspending the main shuttle, no longer displace equally) Both design can be preloaded using shock. The symmetric design had enough mass to preload using a frequency shaking table. The asymmetric design is used as a starting point for the MEMS static balancing mechanism as it has a smaller footprint.

IV. DIMENSIONAL DESIGN

A. Design component: lever configuration

The asymmetric design has an extra design feature, a lever. The lever ensures that the intermediate shuttle of the double folded flexure moves half the distance of the main shuttle. A study is done to determine what type of lever design and if one or two need to be applied. The goal is to have a straight line motion and minimize the rotations of the shuttle. 6 cases where under study where each had an equal preload displacement of -0.22 e-3 mm applied to buckle the preload beam. The buckling beam is 16 mm long. After the preload step the shuttle is moved 1 mm to the positive x direction and then 1 mm to the negative x direction. The 6 configuration can be found in figure 16.

From this study it is concluded that the minimal vertical displacement of the shuttle is found in the configuration with two inverted levers with -0.0511 um in and +0.0210 um in extreme outer position. This is 23.2% and 9.54% respectively of the preload displacement. The rotations of the shuttle are dramatically reduced after adding rigid parts in the double folded flexures. If 50% of the 8 mm beams are compiled rigidly, in the centre of the beam, the rotations of the main shuttle are reduced from $1.3 \times 10^{-4}\ Rad$ to $0.5 \times 10^{-4}\ Rad$.

B. Design component: hook design

The hook design plays an important role in locking the mechanism in the preloaded position. In the hook design the flexures longest dimension is parallel to the tension load. In the design it is important to consider:

1) The preload displacement needed for preloading.
2) The max stress on the locking area and direction of total force needed for locking
3) The force needed during preloading.

1) The preload displacement after preloading determines the statically balanced range of motion. The main shuttle can is only balanced as long as the buckling beam is buckled. The preload displacement needed for preloading is determined by the height of the hook / the distance that the hook needs to overcome before it can latch into the right position.

2) The contact area between the hook and the ground for locking determines the determines the pressure on the area / max stress on that area and direction of total force needed for locking. If the contact area directs the force into the direction of the flexure movement, the hook can unlock.

3) The force needed during preload is determined by the contact area between the hook and the ground during preloading. If the force is high the main shuttle has to provide that extra force during the preloading. Less force is better.

Based on these tree considerations variations of hooks are drawn that can be seen in Table 1: the position of the flexure has influence on the direction of the total force during locking (2), the contact surface during preload influences the preload displacement (1) and the force needed during preload (3), the contact surface for locking influences the max stress on the locking area and the direction of total force needed for locking (2), and also the preload displacement needed for preloading (1).

In Table 1**,** three versions of flexure positions are drawn. The first, back, position was used during the fast prototyping face, it can lock, however when the hook is latched the force of the contact surface between the hook and the ground after latching can push the hook off the ground structure. This effect is reduced in the ‘middle’ case where the locking force is in line with the flexure instead of to the right. The best solution is found in the case of the ‘front’ configuration where the locking force is on the left of the flexure, resulting in a bending moment of the flexure toward the ground ensuring locking.

The contact surface during preload has different versions, either a straight line under a certain angle or a non-straight line surface contact profile. The friction can be influence by using a certain line profile. However, as can be seen between the round and the straight line profile examples, the contact area for locking is reduced with a round shape. This is not acceptable as the stress limits in the hook are set to a solid limit. The contact area for locking is more important than the friction and displacement needed for preloading. A non-round shape is preferred. An irregular shape would not be a logical option as it has an irregular contact surface and friction force. A strait line will result in

a point contact with the ground surface as the hook bends for preloading, a desired effect as the friction forces will thereby reduce. A shallow slope will cause more friction as the horizontal displacement that has to take place will be enlarged and the bending moment will increase. A steep slope will minimize the contact area for locking. How these two effects will interact with each other is unknown. As a result, it has been chosen to use an angle of $\frac{1}{8}\pi$ rad for the contact. The contact surface for locking needs to consist of two interlocking shaped surfaced for maximum surface contact and minimum stress in the materials. Both flat and angled designs have been used in the prototypes and both work. The angled design has the advantage of directing the reaction forces such that the bending of the flexure is towards the ground structure ensuring the lock. It needs however a larger preload displacement. The sharper edges are harder to fabricate and induce local stresses. As the locking is already ensured by the flexure position in the front of the hook, the angled contact surface is redundant. So, the choice is made for a flat contact surface for locking. Now the concept shape of the hooks is determined, there are two more considerations. The number of hooks used in the final design and the orientation of the hooks. The first one will be determined by a final optimization of the total configuration and the second one partially depend on the number of hooks. If all hooks used point to the same direction the configuration will be more prone to shaking influences from the outside. The hooks have to be counter-configurated. Back to back or tip to tip. The Back to back configuration is more preferred because the ground structures can be directly attached to the rest of the ground structures. A tip to tip configuration would mean the ground structures have to be s-shaped to point into the right direction. If there are more than two hooks, a tip to tip configuration is preferred on each side of the buckling preload beam for the same reason of reducing the compliance and footprint of the ground structures. Stop-blocks are added below the hooks to prevent overshooting.

Also, the structure that leads to the ground contact of the hooks is made thinner so that it can bend a little and spread the force load more evenly over the number of hooks.

C. Design component: buckling beam curvature

A curvature is used for the buckling beam prevent them from moving into each other. This curvature is calculated to be such that if one would make a straight line between the top end bottom of the flexure, the midpoint would outlay with more than the fabrication error plus the flexure thickness. The fabrication error of the silicon material is 1-10% of the beam thickness. This results in a curvature centre that is 1 m away in x direction in the vertical middle of the beams for the final MEMS device. If two beams are used they can either both bend in the same direction, or bend opposite ways. Theoretical this should not have any effects on the design. It was chosen to let both bend the same way.

Position of flexure	Contact surface preload	Contact surface locking
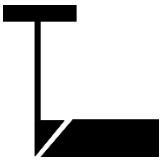 Back	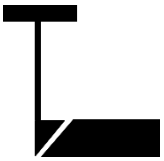 Straight	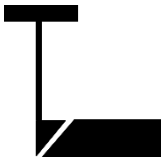 Flat
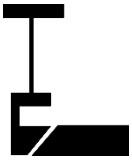 Middle	 Round / Other	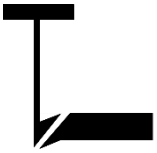 Angled / Other
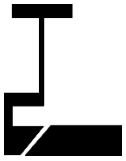 Front		

Table 1: hook designs

V. Experimental evaluation

A. Fabrication

There is a small difference between the preload displacement and the width of the hook sin the drawing, this is to compensate for material removal by the laser.
The MEMS designs intended fabrication is silicon wafer material with in plane young modulus of 169 GPa and out of plane young modulus of 130 GPa. The prototypes are made out of PMMA acrylic material with flexure steel flexures of 183 GPa.

B. Measurement setup

Three experiments are executed to evaluate the prototype of the statically balanced MEMS design. The force-displacement relationship of the main shuttle in x-direction and the force-displacement relationship of the preload block in the y-direction are measured using the same setup, wherein the model is mounted in two different orientations according to the measurement. The third measurement is a video capture of the first eigenmode in a supported horizontal, a non-supported horizontal and a vertical orientation. Such that the first eigenmode can be determined. 2 models of the same prototype are used for these measurements.

Force-displacement
The force-displacement is measured in one direction, the x-axis of the prototype. A force sensor (FUTEX Model FLLSB200 S_BEAM junior loadcell, FSH000102) with a resolution of 0.0021 N, and a range of +-2.1 N. A stage (PI M-505.4DG S/N 107054253) with a resolution of 16 nm, and an additional laser (με MICRO-EPSILON optoNCDT 1401, ILD1401-200) with a resolution of 0.1 mm (due to a 1kΩ resistor). A camera (CANON PowerShot SX500 IS) is used for the recordings.

Table 2 shows the measurements sets.

The displacement describes the path of the shuttle. The path goes from the central position (A) to de described displacement (B), to the negative described displacement (-B) and back to the central position (A). The number of steps is the steps the stage takes to reach from A to B. The wait time is the time the between the current and the next step-command. The stage needs that time to actually move from the current to the next step.

Set 1 measures the stiffness without preloading. Set 2 and 3 measures the stiffness starting without preloading, and preloading during the described path. Set 4 measures the stiffness starting with preloading. Set 5 measures the stiffness starting with without preloading, such that deviations of the measurement devices are visible.
From sets 1-4 at least one repetition is recorded with the camera.

Eigenfrequency
The eigenfrequency is measured using the camera. For each model the recordings are made as seen in Table 3. In each recording the main shuttle is started by hand from the side (location A), and ones by preloading and unpreloading the preload block (location B). In the horizontal position the main shuttle deflects due to gravity in the z direction. To reduces its effect on stiffnesses a support, a long cord, is connected to the x-axis centre of the main shuttle. The camera does never touch this cord.

The recordings are analysed noting down the time at which the shaking starts and at every 20th multiple of the back-and-forth motions, so at cycle 0,20,40,60 etc. This was counted twice, to prevent mistakes.

set	Displace-ment (um) model 1	Displace-ment (um) model 2	Steps (#)	Wait time (us)	Repeti-tions
1	12000	14000	120	500	3x
2	20000	20000	200	500	3x
3	-20000	-20000	200	500	3x
4	20000	20000	200	500	3x
5	20000	20000	20000	5	1x

Table 2: Model 1 and 2, measurement sets

REC	Position	Support
1	Horizontal	Yes
2	Horizontal	No
3	Vertical	No

Table 3: Recording measurement sets

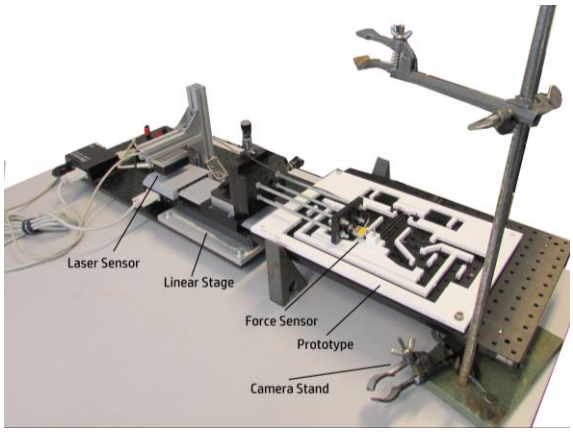

Figure 4: Measurement setup

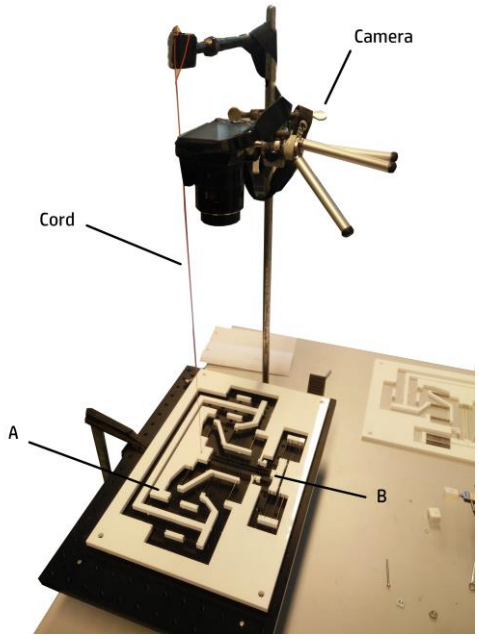

Figure 5: Recording setup

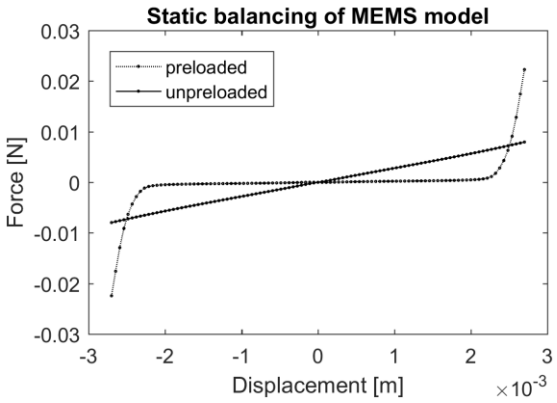

Figure 6: Theoretical Static balancing of MEMS model

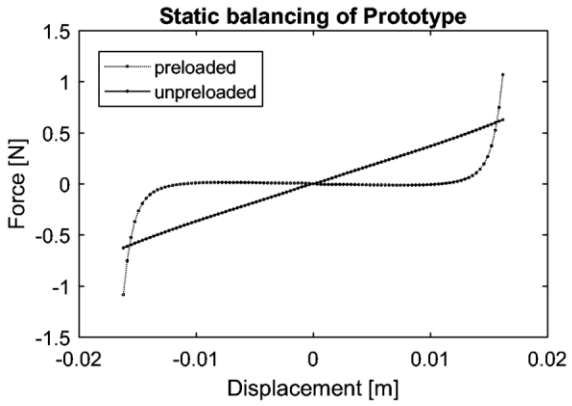

Figure 7: Theoretical Static balancing of prototype model

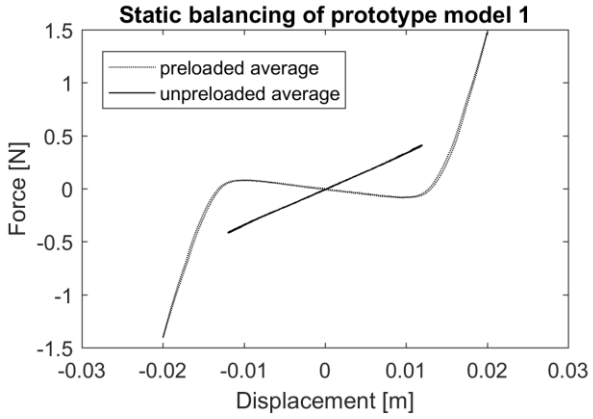

Figure 8: Experimental static balancing of prototype model 1

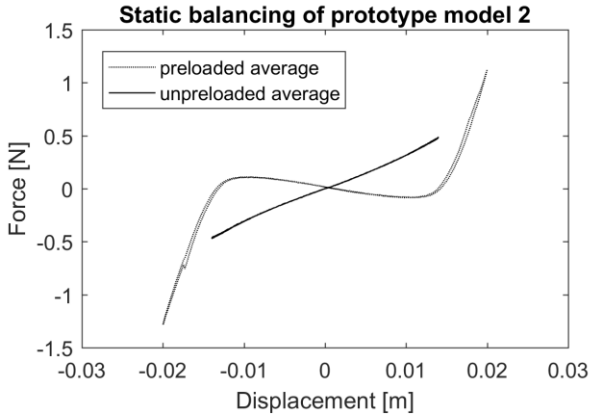

Figure 9: Experimental static balancing of prototype model 2

Mode	Eigenfrequency (HZ)
1	21.8
2	98.3
3	98.3
4	139.7
5	139.9
6	180.6
7	287.5
8	288.4
9	298.5
10	301.8

Table 4: Theoretical eigenfrequencies of MEMS model

Modes	Frequency (Hz)
1	3.09
2	36.7
3	36.8
4	49.6
5	49.7
6	73.5
7	75.1
8	82.7
9	82.9
10	125.4

Table 5: Theoretical eigenfrequencies of Prototype model

MEMS	Theory
ω_n [Hz]	21.8
K [N/ m] @ 1mm	2.8
M [kg]	1.49e-4
x_d [m]	2.7e-3
$E_{\min}$ [J]	1.0e-5

Prototype	Theory	Practice	
		Prototype 1	Prototype 2
ω_n [Hz]	3.09	3.1±0.25	3.1±0.25
K [N/ m] @ 6 mm	37.3	32.2	29.3
M [kg]	0.099	0.085	0.077
x_d [m]	16.2e-3	20e-3	20e-3
$E_{\min}$ [J]	4.9e-3	6.4e-3	5.8e-3

Table 6: Dynamic preloading results

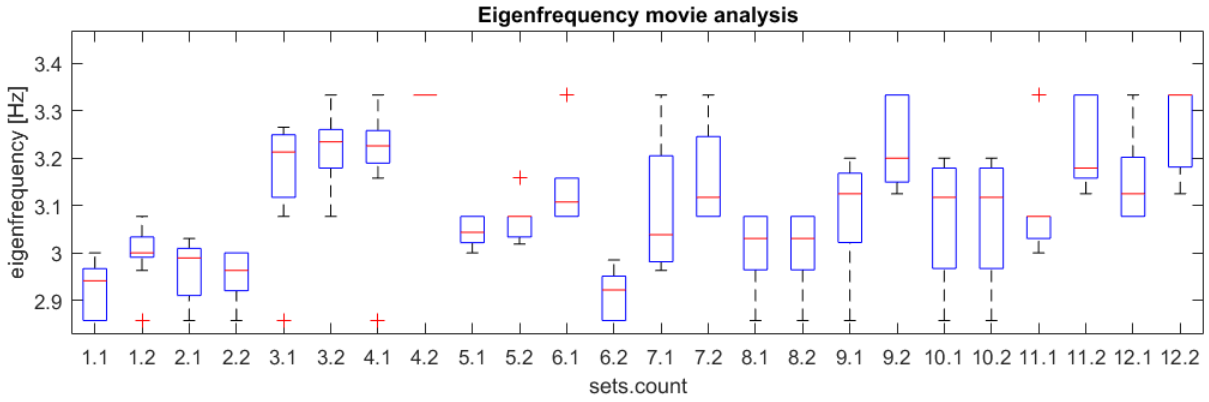

Figure 10: Eigenfrequency movie analysis

VI. Results

The design drawings section shows the final models for the MEMS design, Figure 15 and the fabrication drawing for the prototype, Figure 14.

A. MEMS device, theoretical results

Figure 6 gives the theoretical static balancing for the MEMS device. In the statically balanced area starting at 2.11 sec till at 2.89 sec, the preloaded force is between + 8.72e-5 N and -8.70e-5, the unpreloaded +0.00513 N and -0.00513 N, the displacement ranges from 0.00211 m till -0.00211 m. At these extremes the actuation stiffness is reduces from 2.43 N/m till 0.041 N/m, which is a reduction of 98.4%.

The force at the start of preloading begins with -0.0236 N. The max force, the hooks need to carry is -0.024 N at the max displacement of 0.0027 m. At 2.11 s this force is -0.0303 N.

Table 4 gives the first 10 eigenfrequencies calculated with ANYSY. To be able to preload the mechanism the first eigenmode can be used at 21.8 Hz. As long as the second mode is not excited the preloading can be executed. At the 2nd 3rd 4th and 5th eigenmode the midpieces of the large double flexures are excited, a rotation around y-axis. The levers are excited at the 6th and 7th mode and the horizontal motion of the main shuttle is then no longer secured.

The rotations around x or y axis of the parts, midpieces of large double folded flexure, levers and preload secondary shuttles are approximations for both the MEMS as the prototype ANSYS calculation of the eigenfrequencies, as the off diagonal terms for the second moment of inertia of these parts are ignored. The off diagonal terms for rotation around z axis are all zero and not approximations. The first mode where the hooks are affected is at mode 12, 365.4 Hz.

B. Prototype model, theoretical results

After optimization a prototype is fabricated on a 6:1 scale. The 6:1 scale is a result of the fabrication method used. The measurements fabrication drawing are slightly off to a 6:1 scale as they compensate for the laser burning away some of the material.

Figure 7 shows the theoretical static balancing for the prototype. At 2.14 sec till at 2.86 sec, the preloaded force is between + 0.00951 N and -0.00959 N, the unpreloaded +0.432 N and –0.432 N, the displacement ranges from 0.0117 m till -0.0117 m. At these extremes the actuation stiffness is reduces from 37.0 N/m till 0.815 N/m, which is a reduction of 97.8%. However, this line is slightly bi-stable. With max value in the statically balanced curvature of -0.0135 N @ 2.25 s, and unpreloaded value of 0.296 N, displacement 0.0081 m. Here the actuation stiffness is reduced from 36.5 N/m to -1.67 N/m, which is a reduction of -104.5%.

The force at the start of preloading begins with -0.670 N. The max force, the hooks need to carry is -2.27 N at the max displacement of 1.07 m. At 2.11 s this force is -2.72 N.

Table 5 gives the first 10 eigenfrequencies calculated with ANSYS for the prototype. To be able to preload the mechanism the first eigenmode can be used at 21.8 Hz. As long as the second mode is not shaken the preloading can be executed. At the 2nd 3rd the levers are excited and the horizontal motion of the main shuttle is then no longer secured. The first mode where the hooks are affected is at mode 8, 82.7 Hz.

C. *Prototype model, experimental results*

Figure 8 shows the static balancing of prototype model 1. Of all data combined, difference between the average line and the individual runs is given by a median of -1.00x10^-3N with a 25th percentile of -2.3x10^-3N and a 75th percentile of 0.66x10^-3 N. Number of runs on preload average is 3, number of runs on unpreloaded average is 3. The data point interval is 100 um in all cases.

At -0.01 m till at 0.01, the preloaded force is between + +0.08 N and -0.08 N, the unpreloaded -0.34N and +0.33 N. At these extremes the average actuation stiffness is reduces from 33.5 N/m till -8 N/m, which is a reduction of -1.23%

Figure 9 shows the static balancing of prototype model 1. Of all data combined, difference between the average line and the individual runs is given by a median of 0.00x10^-3N with a 25th percentile of 25th percentile = -1.33x10^-3N and a 75th percentile of 1.33x10^-3 N. Number of runs on preload average is 3, number of runs on unpreload average is 3. The data point interval is 100 um in all cases.

At -0.01 m till at 0.01 (is max force values), the preloaded force is between + -0.11 N and +0.08N, the unpreloaded -0.31N and +0.32 N. At these extremes the actuation stiffness is reduces from an average of 31.5 N/m till -8.5 N/m, which is a reduction of -1.26%

Figure 10 shows the analysis of the eigenfrequency recording that show the eigenfrequencies. Set 1 to 6 are from prototype 1, sets 6 to 12 are from prototype 2. Sets 1 and 2,7 and 8 are taken horizontal without main shuttle support in the form of a rope. Sets 3, 4, 9, 10 are horizontal with rope support. The other sets are taken in a vertical position. In all uneven set numbers, the models are excited at location A. All even set numbers after the model has been preloaded and unpreloaded again, excited at location B. From this analysis the eigenfrequency is determined to be 3.1±0.25 Hz.

It is possible to preload the models by applying shock or shaking by hand. Table 6 shows the results for dynamic preloading the stiffnesses are determined at 0.006 m displacement from the centre for the prototype and 1 x10^-3, for mems. The stiffness for the prototype models is an average of the two data point in the hysteresis loop of the averaged data). The displacement needed for preloading given are for full preload, preload can partially happen at lower displacements. The simplified mass is calculated with equation 7. The minimal needed energy is calculated with equation 6. The devices can also be preloaded by moving the shuttle to the extreme position instead of shaking the device.

VII. Discussion.

The effect of gravity where not considered during ANSYS calculations. During the stiffness measurements the main shuttle was suspended by the linear stage. This suspending was not picked up by the force sensor as it was in a different direction. However, in the eigenfrequency recording the main shuttle deflected in z direction. Therefore, it was chosen to suspend the main shuttle with a long cord. The influence of gravity will be smaller in the MEMS device as the masses are reduced.

The prototype is a 6:1 scale model regarding the flexure length. The placement of flexures is slightly different due to fabrication but flexure lengths are scaled 6:1.

Large deviations were found between the hand calculated stiffness and the stiffnesses after fabrication. Most model where bi-stable where the calculations predicted a positive stiffness. The fabrication of these devices also was very rough. With variation of some beams of +- 0.1 mm with beams there were supposed to be 0.8 mm thick. Even so the concepts work in both models.

The first eigenfrequency excites the main shuttle. If the hooks are not excited the latching by hooks should be very robust.

One of the difficulties of static balancing is getting the zero stiffness. There is often a difference between the calculated and the fabricated model stiffnesses, what makes it hard to make the system balanced. An adjustable stiffness would overcome this problem.

The prototype had to be 6:1 because of the smallest dimensions in the design, that where the hooks. The laser was not able to make smaller gabs between the hook and the ground structure. This problem does not exist in the MEMS device. However, some kind of lever system that reduces the displacement needed by the main shuttle to pull the hooks down might be used to reduce range of motion needed for preloading, perhaps making the footprint even smaller. In the prototype this solution might have enabled us to make a smaller prototype.

The fabrication of the tips of the hooks will become more difficult in smaller designs. A lever solution might also solve that problem as the hook-shape can be enlarged.

The eigenfrequency for the MEMS device for preloading is higher than that of the prototype. This is also caused by a change in material. In an even smaller model the stiffness of the flexures will scale with a power of 1 while the mass will scale by the power of 3 when the x, y, z dimensions scale. The max allowable stress in the material will determine the max stiffness that can be used. A max footprint can determine the max masses. The eigenfrequency will go up faster than the factor by which the footprint is reduced. However, the max eigenfrequencies that can be used for preloading that can be applied is not reached yet. So, it should be possible to make smaller MEMS devices using this preloading technique.

In the experiments it became apparent that the hooks do not latch at the same time. This means the structure can be half preloaded before the given minimal preload

displacement given for the prototypes. It also means the hooks do not carry an equal amount of force. In fact, a gab was still visible between one of the hooks and the ground in both prototype models. Even so the hooks in the MEMS device are calculated such that one can carry the full preload force, but it is expected that MEMS device fabrication is more precise and both hooks might have contact. Also, the ground structure wherein the hooks lock is made such that is can slightly bend and spread the forces over the two hooks.

VIII. Conclusion

A new approach for preloading a compliant MEMS device is proposed in this paper. Shaking the mechanism in the first eigenmode is expected to result in preloading a beam in the design. That beam acts as a negative stiffens mechanism which creates a state of static balancing in the device.

This proposed approach is validated by implementing static balancing into a translational stage design. A large scale prototype was made and the design validated by theoretical, experimental and fem models. It was shown that the two fabricated and tested prototype models have a stiffness reduction of -123% and -126% where -104.5 was predicted. Their eigenfrequencies are estimated at 3.1 +- 0.25 Hz where 3.09 was predicted. Static balancing was successfully implemented with shaking the device (by hand) instead of manually latching the hook by applying force to a specific location. The devices can also be preloaded by moving the shuttle to the extreme position instead of shaking the device. The predicted minimal energy requirement for both fabricated porotype models is 4.898e-3 J, where 6.433e-3 J and 5.866e-3 J where calculated based on experimental results. The expected minimal energy required for preloading the designed MEMS device is 1.0206e-5 J.

Future work will include the fabrication and measurement of the of the MEMS device.

TERNARY PLOT

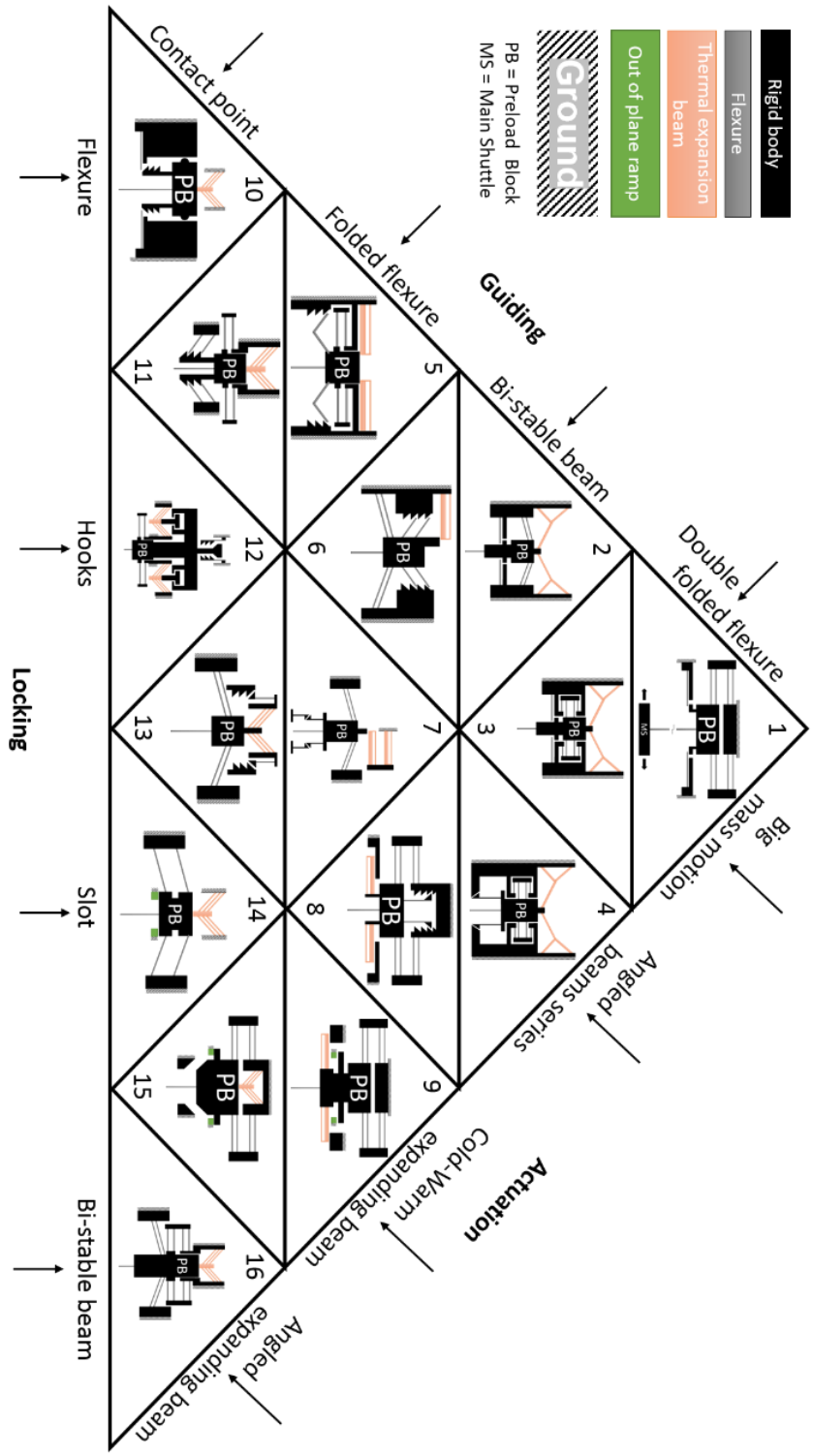

Figure 11 Ternary plot used for brainstorming

DESIGN DRAWINGS

Figure 12: Symmetric design

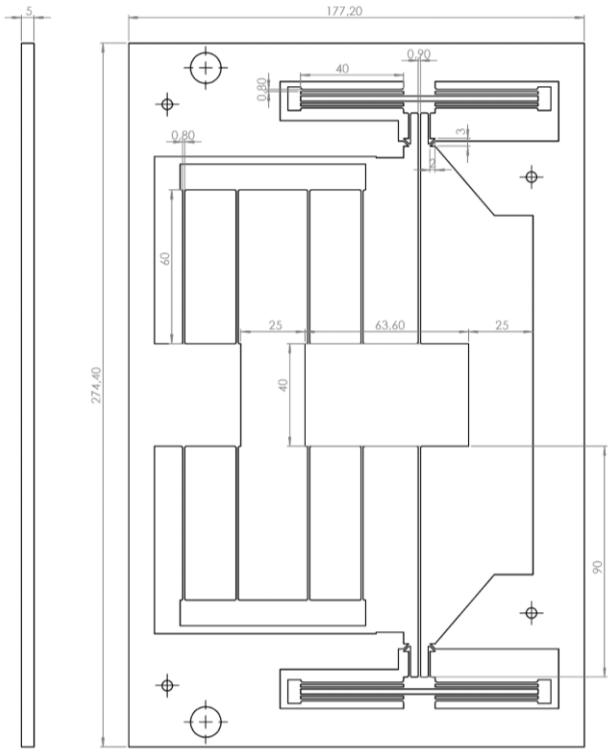

Figure 13: Asymmetric design

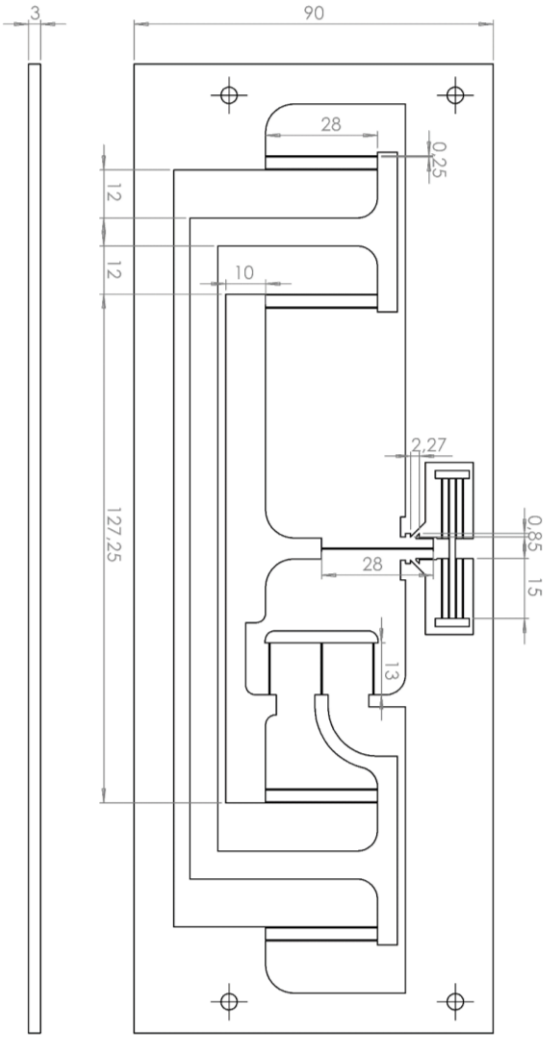

Figure 14: Prototype fabrication model

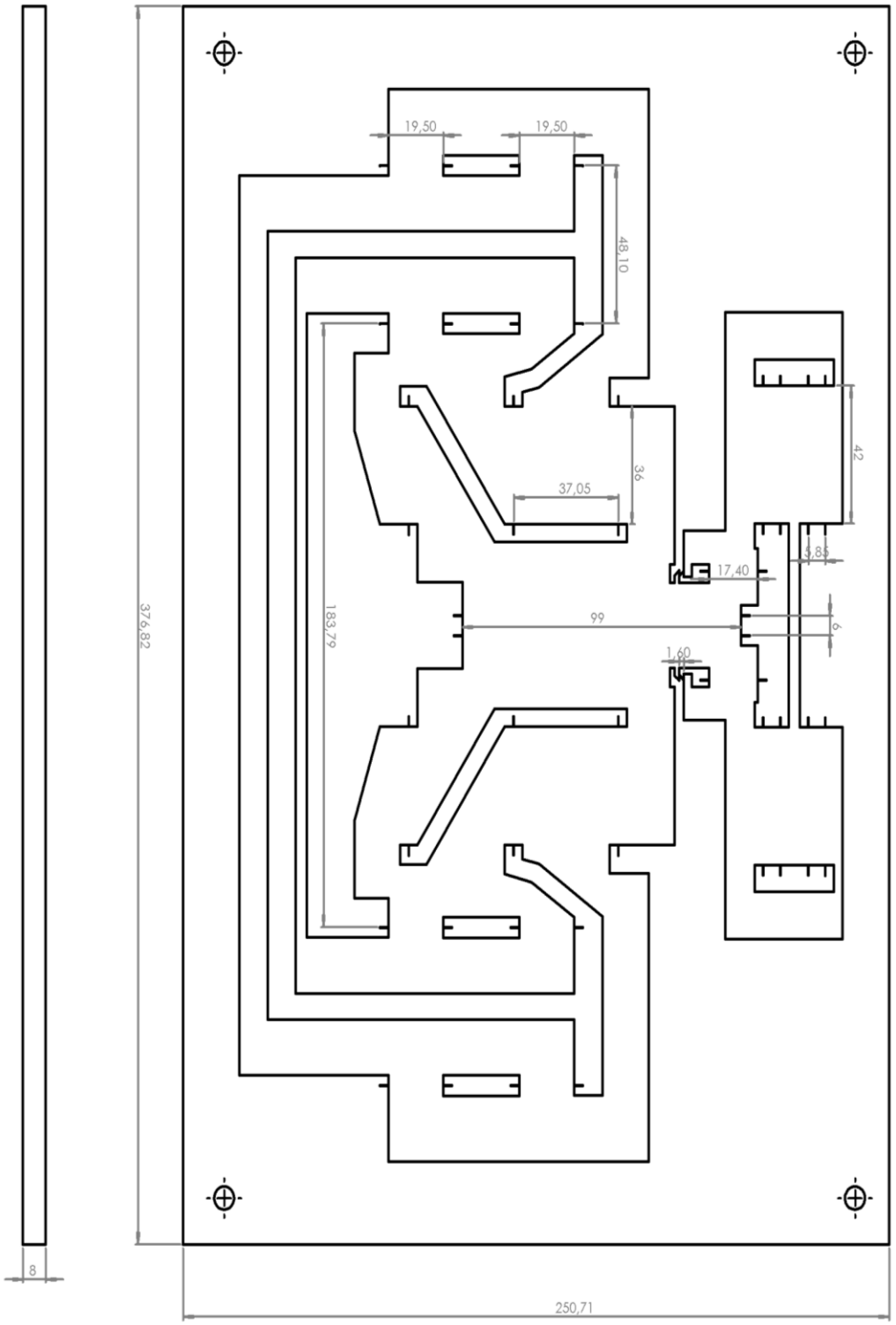

Figure 15: MEMS model

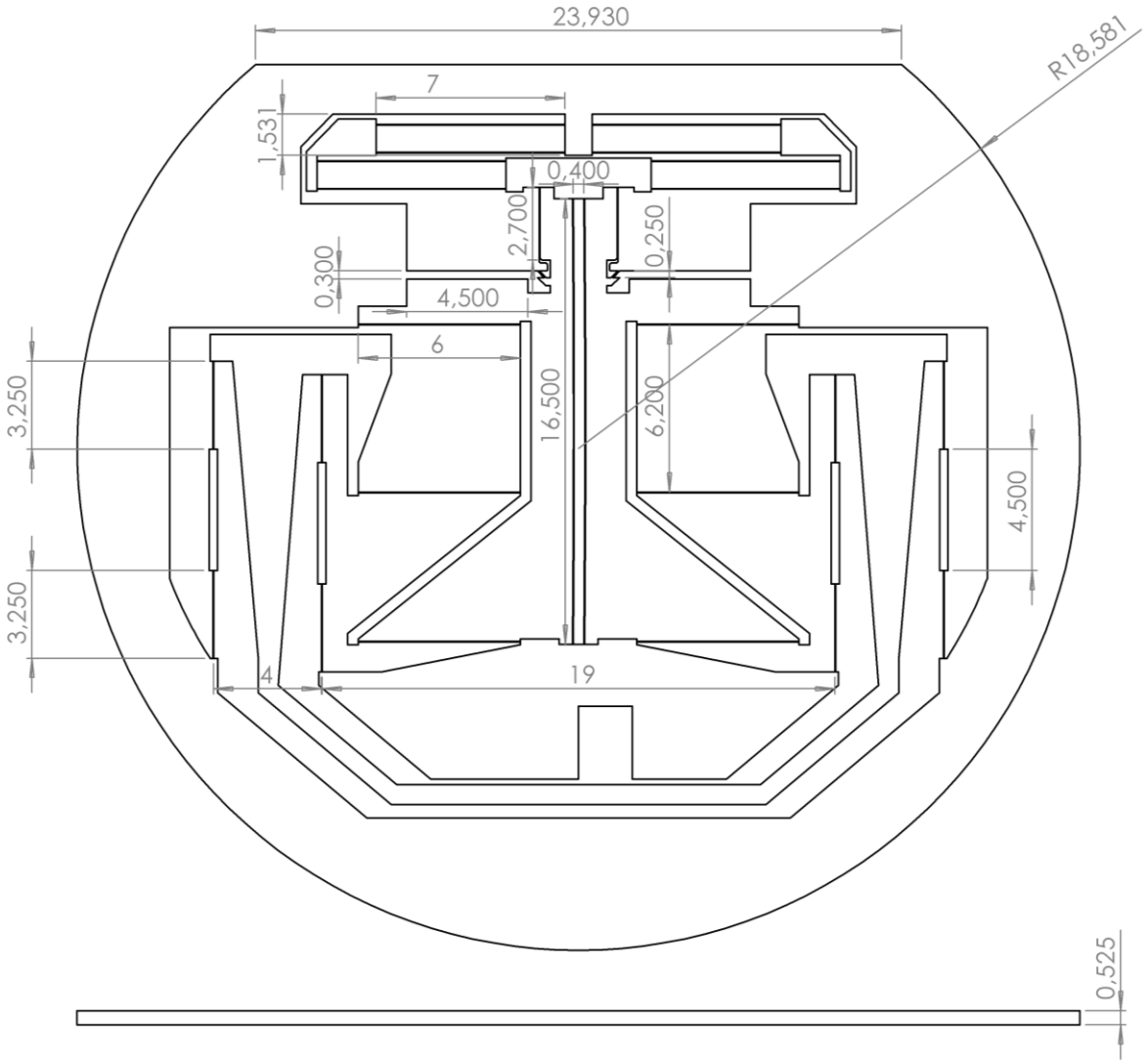

Figure 16: Concept Configurations

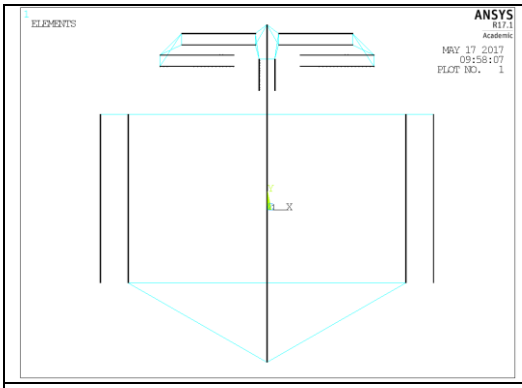

Figure 2STR

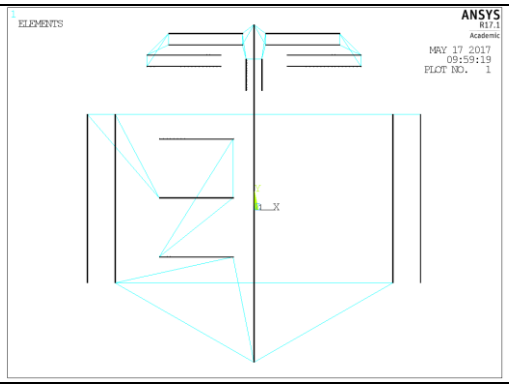

Figure 3StrInvL

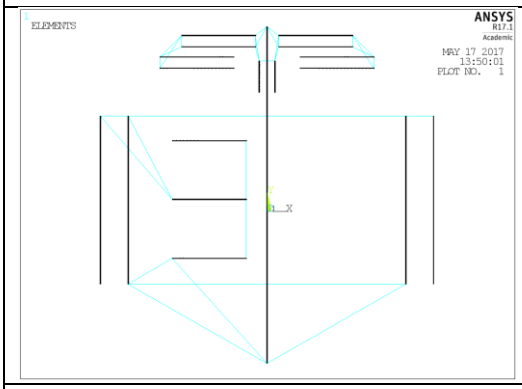

Figure 4 StrL

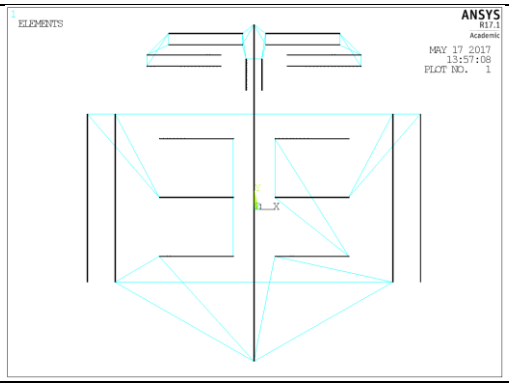

Figure 5 StrMix

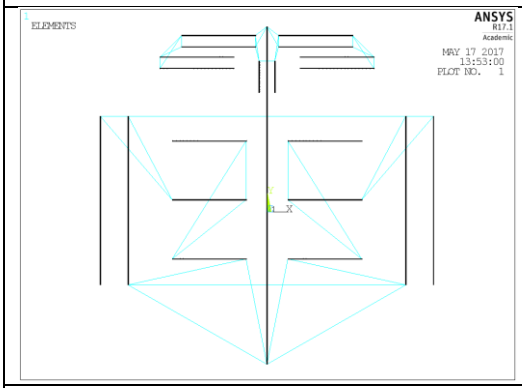

Figure 6 StrTInvL

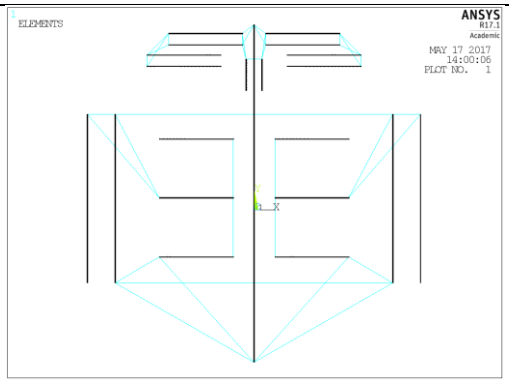

Figure 7 StrTL

Str – Strait double folded flexure, no levers
StrInvL – Straight double folded flexure, one inverted lever
StrL – Strait double folded flexure, one normal lever
StrTInvL – Strait double folded flexure, two inverted levers
StrMix – SDDF, one normal and one inverted lever
StrTL - SDDF, two normal levers

References

1. Pedersen, C.B. and A.A. Seshia, *On the optimization of compliant force amplifier mechanisms for surface micromachined resonant accelerometers.* Journal of Micromechanics and Microengineering, 2004. **14**(10): p. 1281.
2. Khan, S. and G.K. Ananthasuresh, *A MICROMACHINED WIDE-BAND IN-PLANE SINGLE-AXIS CAPACITIVE ACCELEROMETER WITH A DISPLACEMENT-AMPLIFYING COMPLIANT MECHANISM.* Mechanics Based Design of Structures and Machines, 2014. **42**(3): p. 355-370.
3. Eskandari, A. and P.R. Ouyang, *Design and optimization of a XY compliant mechanical displacement amplifier.* Mechanical Sciences, 2013. **4**(2): p. 303-310.
4. Ni, Y., et al., *Modeling and analysis of an over-constrained flexure-based compliant mechanism.* Measurement, 2014. **50**: p. 270-278.
5. Huang, S.C. and G.J. Lan, *Design and fabrication of a microcompliant amplifier with a topology optimal compliant mechanism integrated with a piezoelectric microactuator.* Journal of Micromechanics and Microengineering, 2006. **16**(3): p. 531-538.
6. Houston, K., et al. *Polymer sensorised microgrippers using SMA actuation*. in *Robotics and Automation, 2007 IEEE International Conference on*. 2007. IEEE.
7. Awtar, S., *Synthesis and analysis of parallel kinematic XY flexure mechanisms*. 2003, Massachusetts Institute of Technology.
8. Sauceda-Carvajal, A., et al., *Compliant MEMS Mechanism to extend resolution in Fourier Transform Spectroscopy.* Micromachining and Microfabrication Process Technology Xix, 2014. **8973**.
9. Tolou, N. and J.L. Herder, *Concept and modeling of a statically balanced compliant laparoscopic grasper.* ASME Paper No. DETC2009-86694, 2009.
10. Goldfarb, M. and N. Celanovic, *A flexure-based gripper for small-scale manipulation.* Robotica, 1999. **17**: p. 181-187.
11. Grossard, M., et al., *Mechanical and Control-Oriented Design of a Monolithic Piezoelectric Microgripper Using a New Topological Optimization Method.* Ieee-Asme Transactions on Mechatronics, 2009. **14**(1): p. 32-45.
12. Du, H., et al., *A micromachined thermally-driven gripper: a numerical and experimental study.* Smart materials and structures, 1999. **8**(5): p. 616.
13. Gallego, J.A. and J.L. Herder. *Criteria for the static balancing of compliant mechanisms*. in *ASME Conf. Proc*. 2010.
14. Deepak, S.R. and G. Ananthasuresh, *Static balancing of a four-bar linkage and its cognates.* Mechanism and Machine Theory, 2012. **48**: p. 62-80.
15. Leblond, M. and C.M. Gosselin. *Static balancing of spatial and planar parallel manipulators with prismatic actuators*. in *ASME Design Engineering Technical Conferences*. 1998.
16. R, S.D., *Static balancing of rigid-body linkages and compliant mechanisms.* phd work, 2012. -(-): p. 244.
17. Herder, J.L., *Energy-free Systems. Theory, conception and design of statically*. Vol. 2. 2001.
18. Leishman, L.C., D.J. Ricks, and M.B. Colton. *Design and evaluation of statically balanced compliant mechanisms for haptic interfaces*. in *ASME 2010 Dynamic Systems and Control Conference*. 2010. American Society of Mechanical Engineers.
19. Morsch, F.M. and J.L. Herder, *Design of a generic zero stiffness compliant joint.* Proceedings of IDETC/CIE ASME, 2010.
20. Gosselin, C.M. and J. Wang, *Static balancing of spatial six-degree-of-freedom parallel mechanisms with revolute actuators.* Journal of Field Robotics, 2000. **17**(3): p. 159-170.
21. Trease, B. and E. Dede, *Statically-balanced compliant four-bar mechanism for gravity compensation.* Ann Arbor, 2004. **1001**: p. 48109.

22. Hirose, S., et al., *Internally-balanced magnet unit.* Advanced robotics, 1986. **1**(3): p. 225-242.
23. James D. Ervin, D.M., Gregory F. Ervin, Sridhar Kota, Joel A. Hetrick, *Surface Vibration Using compliant Mechanical Amplifier*. 2010: United State.
24. de Lange, D.J., M. Langelaar, and J.L. Herder. *Towards the design of a statically balanced compliant laparoscopic grasper using topology optimization*. in *ASME 2008 International Design Engineering Technical Conferences and Computers and Information in Engineering Conference*. 2008. American Society of Mechanical Engineers.
25. Lassooij, J., et al., *A statically balanced and bi-stable compliant end effector combined with a laparoscopic 2DoF robotic arm.* None (EN), 2012.
26. Stapel, A. and J.L. Herder, *Feasibility study of a fully compliant statically balanced laparoscopic grasper.* ASME Paper No. DETC2004-57242, 2004.
27. Hoetmer, K., et al., *Negative stiffness building blocks for statically balanced compliant mechanisms: design and testing.* Journal of Mechanisms and Robotics, 2010. **2**(4): p. 041007.
28. Eijk, J.v., *On the design of plate-spring mechanisms.* 1985.
29. Chen, G. and S. Zhang, *Fully-compliant statically-balanced mechanisms without prestressing assembly: concepts and case studies.* Mechanical Sciences, 2011. **2**(2): p. 169-174.
30. Pluimers, P.J., et al., *A compliant on/off connection mechanism for preloading statically balanced compliant mechanisms.* Proceedings of the ASME IDETC, Chicago, IL, 2012.
31. Tolou, M., P. Estevez, and J.L. Herder. *Collinear-type statically balanced compliant micro mechanism (SB-CMM): experimental comparison between pre-curved and straight beams*. in *Proceedings of the ASME Design Engineering Technical Conferences and Computers and Information in Engineering Conference, Aug*. 2011.
32. Tolou, N., V.A. Henneken, and J.L. Herder. *Statically balanced compliant micro mechanisms (sb-mems): Concepts and simulation*. in *Proceedings of the ASME Design Engineering Technical Conferences & Computers and Information in Engineering Conference, Montreal, Canada, Aug*. 2010.
33. Tolou, N., *Statically Balanced Compliant Mechanisms for MEMS and Precision Engineering*. 2012, PhD Thesis, Delft University of Technology, Delft, the Netherlands.
34. Syms, R.R.A., H. Zou, and J. Stagg, *Robust latching MEMS translation stages for micro-optical systems.* Journal of Micromechanics and Microengineering, 2004. **14**(5): p. 667.
35. Liu, H.-B. and F. Chollet, *Moving Polymer Waveguides and Latching Actuator for 2$\times $2 MEMS Optical Switch.* Journal of Microelectromechanical Systems, 2009. **18**(3): p. 715-724.

IV Chapters

This section will discuss several chapters regarding the approaches to the work presented in the papers, concept development, rapid prototyping method, Comsol and ANSYS modelling, concept optimization after rapid prototyping, final models and modelling, fabrication details, additional experimental results, and a reflection on the past year.

Cover: Max Planck Institute taken from the guest house (white building) at sunset

1 Approach towards the amplifier classification

The following steps were taken to develop a database:

1. Collecting papers
2. Creating sub-selection of papers based e.g. on CMMA designs, rigid body designs, design methods and possible existing classifications.
3. Collecting what criteria are used in design papers as analysing criteria (the designer's needs).
4. Creating a database in Microsoft Excel, Figure 2 Design library. Organizing a label to every design, a label to every paper, a description for some of the designs, and a rigid body sketch for all the collected designs. The total number of designs is 235 if one counts the rows.
5. Making a time map, shown in appendix 1, of all designs found to get an idea of the evolution of the designs.
6. Lying all figures of the designs on the floor, certain similarities where found. This created the classes based on structure, called principle elements: lever, double slider, four-bar, rotational double slider, piston, pantograph, five-bar, watt linkage, 'spiderleg' (a lot of double sliders in series).
7. The classification was improved by the current rules described in the literature review paper using the Geometrical Advantages of the designs.

The flowchart, Figure 3 Flowchart of approach steps, is a visual representation of the steps taken. There are no arrows because the lines can go back and forth, but generally the flow is from left to right and from top to bottom.

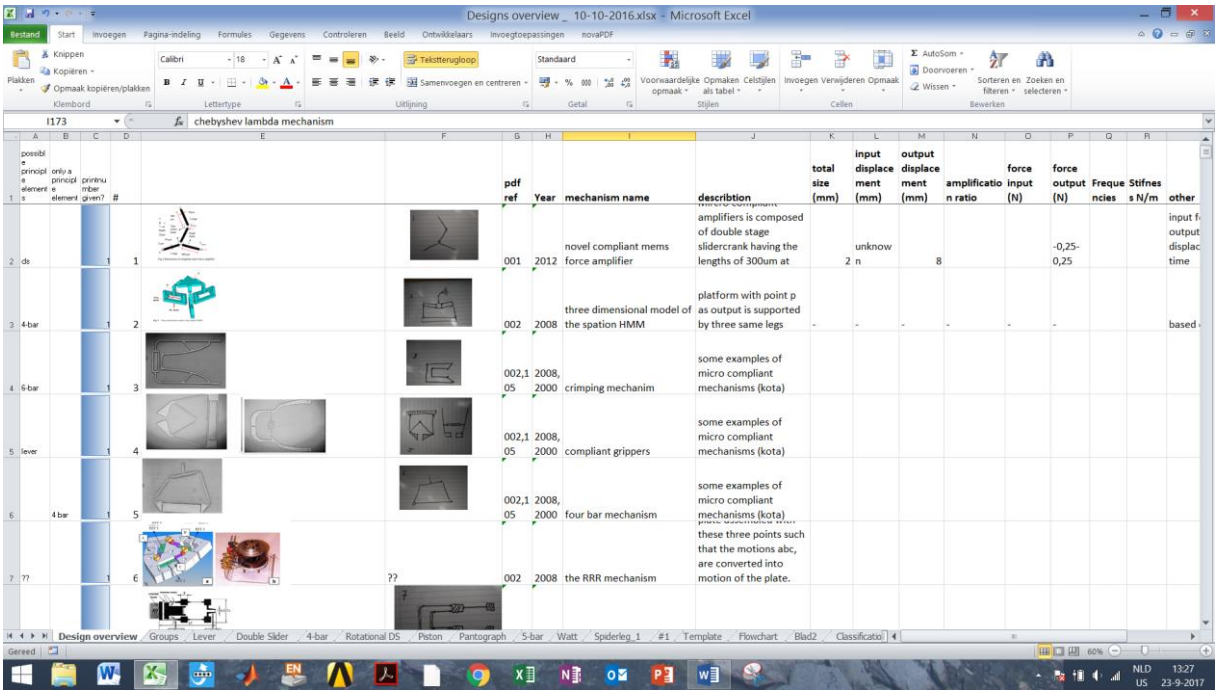

Figure 2 Design library

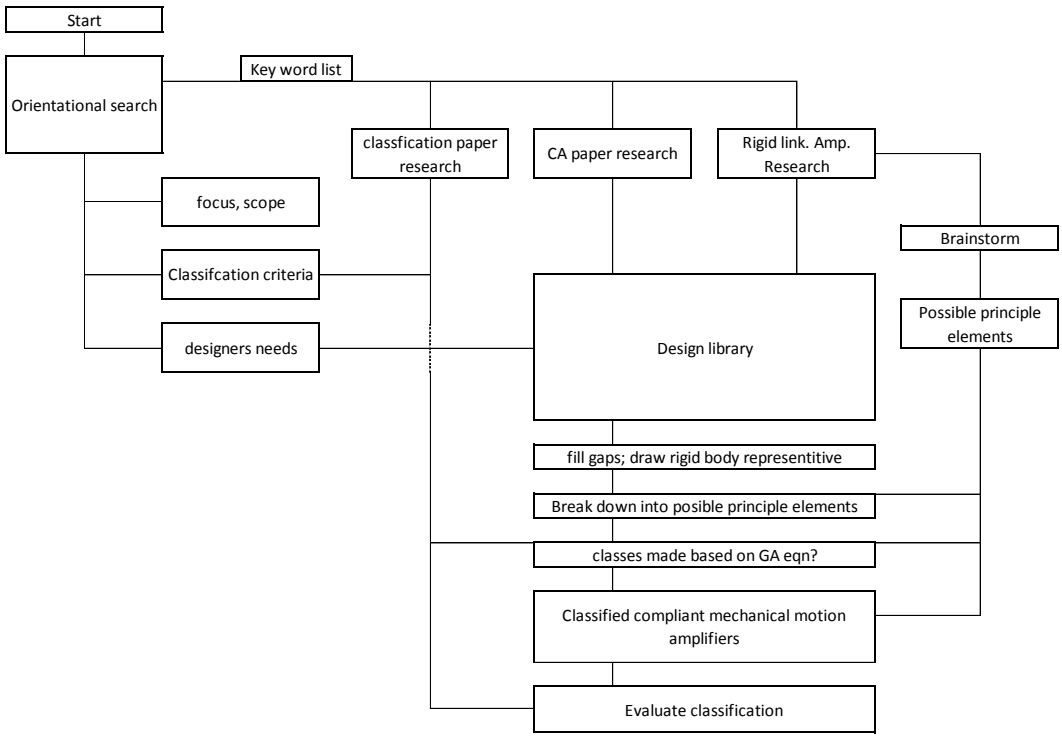

Figure 3 Flowchart of approach steps

2 Concept development for design challenge

The following steps are taken in the concept development of the preloading mechanism for a straight-line compliant mechanism, such that it can be statically balanced:

1 Criteria for concepts are set.
2 First force types are collected and analysed.
3 The force types are used in the sub-concept brainstorming.
4 The subplots are analysed by criteria using weigh tables.
5 Total concepts are generated by using a new combining of sub-concepts approach, a ternary plot.
6 The total designs are then analysed by criteria using weight tables.

2.1 Criteria for concepts

To make the conceptual approaches to preloading, the design space is determined. The following criteria are interpreted after each step and used for ranking concepts.

1 The eventual design has to be planar. This is to ensure applications in flat designs. Use can be made of 3d or 2,5D solution that are temporary to apply the preloading.
2 The approaches need to be applicable in a MEMS materials: specifically, silicon wafer material. The design has to be monolithic and without manual assembly, as most MEMS devices are.
3 The preload has to be permanent without external intervention. E.g. not temperature dependent. It may be reversible, but only with outside intervention.
4 Criteria for the design are:
    a. Fabrication, less complex is better
    b. Robustness to outside influences, less is better
    c. Footprint, smaller is better
    d. Complexity, less steps in design process is better.
    e. Range of motion, larger is better
    f. Accuracy, more accurate is better.

2.2 Force types analysis

As a first indication, the forces needed are in the range of mN and the range of motion is in mm. Multiple force-types are investigated as possible options. They are used to brainstorm for design solutions. Some forces can already be eliminated based on their range of effect.

1 Temperature
2 Audio / Kinetic force
3 Electromagnetic
4 Pressure
5 Material
6 Optics
7 Van der Waals

Optics
A possible way of applying force is by using light. However, the force caused by photon absorption and reflection is in the range of nanonewtons. Optics are there for excluded from our analysis.

Van der Waals
Van der Waals forces needs close surface contact. This makes it unsuitable for activation and guiding. A large surface area is needed to generate appropriate force and does not suit a small footprint design wish. Van der Waals forces are there for excluded.

2.3 Sub-concept design brainstorming

The design development of the preloading mechanism is divided into 3 components. A preload block (PB) is attached to the top of the beam to be able to handle the beams top motion. The sub-concept divisions are locking this PB, guiding the PB and actuation of the PB so that is move to the intended position. For each section concepts are developed by force type.

A description of each solution is given. Sketches can be found in Figure 4 Sub-concept sketches for actuation, Figure 5 Sub-concept sketches for guiding and Figure 6 Sub-concepts sketches for locking.

2.3.1 Actuation: Temperature

Angled Shape Beam, and Angled Beams in Serie.
When heating beams, they can expand. By constructing two beams in a v shape and fixing the outer ends a downwards motion is created when the beams expend. This gives two results. Angled beams can be used in series to create larger range of displacement.

Dual Material Beam
By using materials with two different heat expansion coefficients and adding heat, one material will expand faster than the other, hence a bending motion will occur.

Cold-Warm Beam
A larger mass will need more time to heat up under the same conditions than a smaller mass. By shaping a beam into a thin and a thick member, one side will expend quicker than the other side and a bending motion will occur.

2.3.2 Actuation: Kinetics

Small and Big mass motion
Two masses can be distinguished; a shuttle that is connecting the negative stiffness building blocks to the positive stiffness building blocks, and a smaller mass that is the outer end of the buckling beam that needs to be moved for preloading only.

By shaking in the frequency of the larger shuttle mass (M) or the smaller preload block mass (m), motions can be created for preloading. In the case of the smaller mass, only the preload block itself will displace and thereby be actuated. In case of the shuttle motion the shuttle (a) moves sideways, creating tension in the buckling flexure (b) and pull the preload block into a preloaded position (c). If it is locked at this down position, the shuttle can move back to the centre position and the buckling flexure will be preloaded.

2.3.3 Actuation: Electromagnetic

External and Internal Magnets, Comb-drive and Piezo Actuators
Electromagnetics can be used in various way: by adding a magnetic material locally and applying external field, motion can be created; by adding two local sources of magnetic material and influencing ones strength, a motion can be created; by using a well-known concept in MEMS, a comb-drive, design, a motion can be created; or a piezo material can be used to create the wanted actuation.

2.3.4 Actuation: Pressure

Local and Global Pressure
Pressure can be applied either in a local or global manner.
Figure a) In a local manner a bellow (b) or air chamber can be filled with a fluid expending the chamber and pushing the preload block (c) away from the ground which fixes the other end of the local chamber. The fluid material can be supplied by a tube (a).

Figure b) In the global version a chamber (a) is completely sealed and the environmental pressure is changed. The chamber expands or collapses like the local chamber moving the preload block (b).

2.3.5 Actuation: Material

Water evaporation
Water can be adhered between two surfaces (b), the surface of the preload block (c), and a ground surface (a). By evaporation the amount of water is reduced and the two surfaces where to the water is adhered, will come closer.

Water attraction
By using a water attracting material (b) between the ground and the preload block (a), compression can be created by adding water to the system. The ground and the preload block will be pushed apart.

2.3.6 Guiding: Electromagnetic

Magnets
Magnets can be used to make a guiding system, for example some kind of rail or wall can be made that keeps the preload block in a straight line. It is unknown how this can be applied in MEMS but as a concept this can be discovered.

2.3.7 Guiding: Material

Hydrophobic
Hydrophobic materials can be used to let the preload block move in the middle of, for example a half pipe design. The material repels the wet environment and it will stay in the middle of a trench.

Double folded flexure, Bi-stable beam, Folded flexure
A double folded flexure is a well-known design in MEMS to force straight line motion. Another method for positioning is a bi-stable beam that suspends the preload block and moves it from the not preloaded to the preloaded position. A single folded flexure can act like a double folded flexure guide in a straight line for small motions, but for larger motion the guiding will be more difficult.

Rolling contact, Slid, Boxed, point Contact
A rolling contact can prevent the preload block from moving in an unwanted position and reduces friction. A slid can guide the preload block in a straight motion and prevent rotation. A boxed design also prevents out of plane motions. A point contact does only prevent rotation if there are enough contacts. It has reduced friction compared to a boxed or slid design.

2.3.8 Locking: Electromagnetic

Comb-Drive/ Magnets
A failing comb-drive, where the fins are touching can be used as locking. So, can magnets, which do the same.

2.3.9 Locking: Material

Adhesion, Solidify, Hydrophilic

Two surfaces that touch can be used for locking, like post-its, a sticking material can be used. Freezing water also locks a mechanisms into place. A big surface can stick to water using surface tension; hence a hydrophilic solution can be used.

Friction, Flexure beam, Hooks, Slot, Bi-stable Beam

By inducing friction, locking can be created. Flexure beams that fall into small slots can create a lock where the flexure beams are perpendicular to the locking wall or at an upwards facing angle. Form closed shapes can lock the preload block, hooks use parts with high stiffness and a parallel flexure to the wall to lock the design into place. A shape falling into a slot can lock the design too. A buckled beam that suspends the preload block can be bi-stable and moves from the not preloaded to the preloaded position. High stiffness prevents it from becoming undone after preload actuation.

Actuation

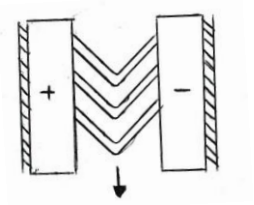

(a) Angled Shape Beam

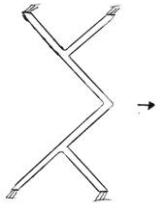

(b) Angled Beams in Serie

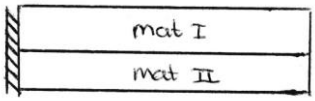

(c) Dual Material Beam

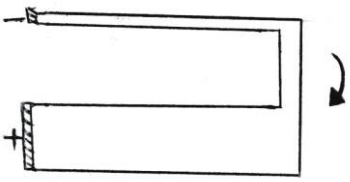

(d) Cold-Warm Beam

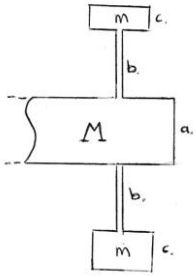

(e) Small and Big Mass Motion

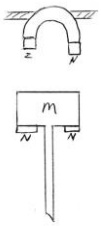

(f) External Magnets

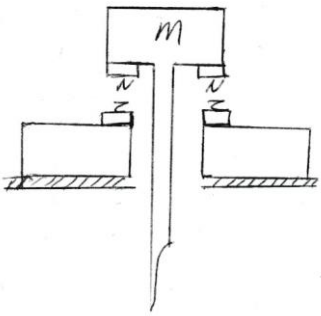

(g) Internal Magnets

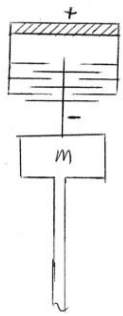

(h) Comb-Drive

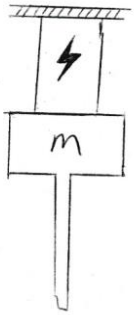

(i) Piezo-Actuators

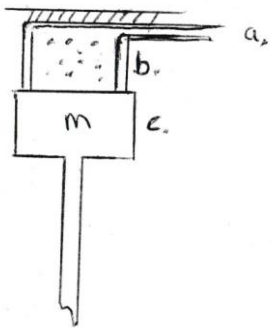

(j) Local Pressure

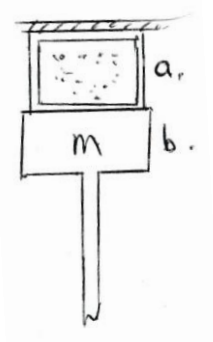

(k) Global Pressure

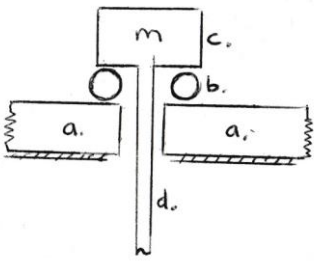

(l) Water Evaporation

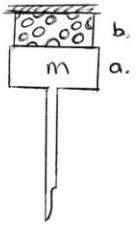

(m) Water Attraction

Figure 4 Sub-concept sketches for actuation

Guiding

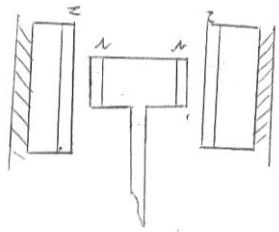

(a) Magnets

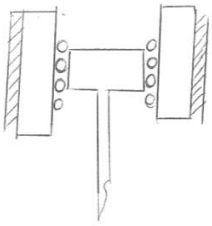

(b) Hydrophobic

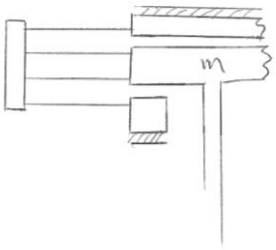

(c) Double Folded Flexure

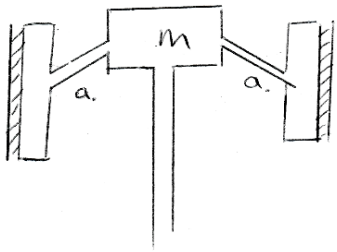

(d) Bi-stable Beam

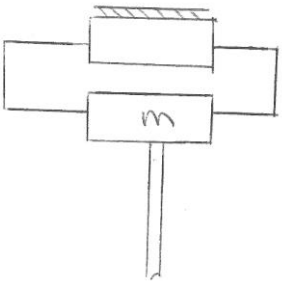

(e) Folded Flexure

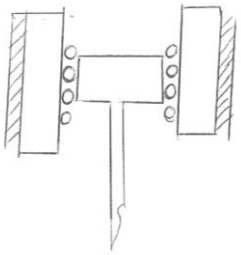

(f) Rolling Contact

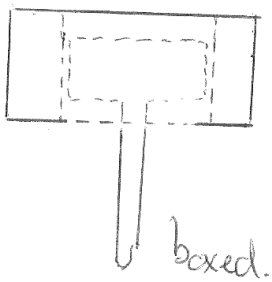

(g) Slid / Boxed

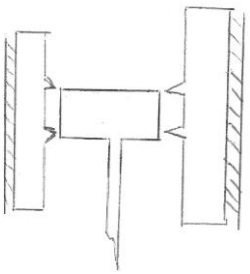

(h) Point Contact

Figure 5 Sub-concept sketches for guiding

Locking

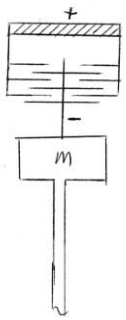

(a) Comb-Drive / Magnets

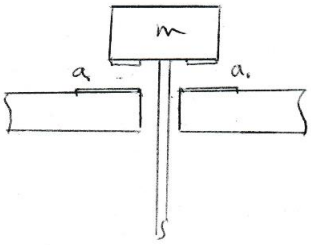

(b) Adhesion

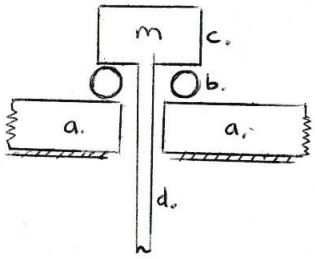

(c) Solidify / Hydrophilic

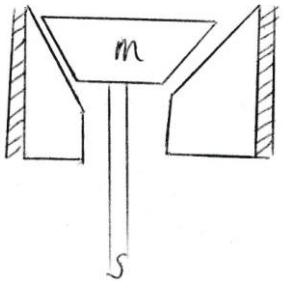

(d) Friction

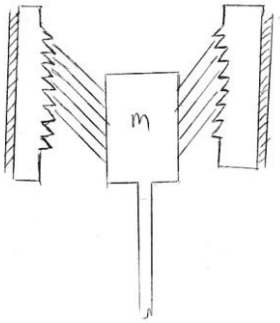

(e) Flexure Beam

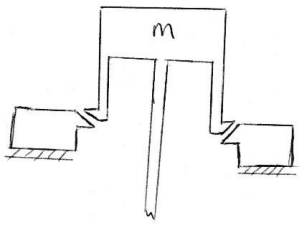

(f) Hooks

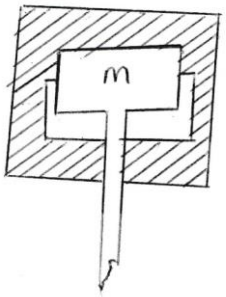

(g) Slot

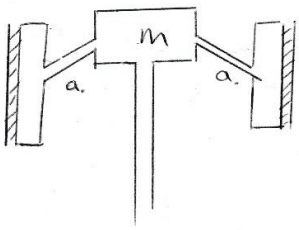

(h) Bi-stable Beam

Figure 6 Sub-concepts sketches for locking

2.4 Weight tables and criteria for sub-concepts

2.4.1 Criteria

The designs are ranked on fabrication, design and range. The first criterium in fabrication is the number of material present in the end product. If there are more materials in the end product the fabrication is more difficult. The second criterium is whether the design is a planar or 3D design. When the concepts are applied in MEMS, that use lithography, planar designs are preferred. 3D designs are designs that use some out of plane construction for preloading. The third criterium is the number of layers needed during fabrication. This is counting masks and deposition layers. This is an estimation. More layers means a more complex and time-consuming fabrication.

For design there are two criteria. First, if there is any background information available. This is not important in developing new techniques for SB-CMM but is a consideration for the ease with which a novel approach can be implemented. Therefore, this is used as a criterium for ranking here, as the implementation of a design where more properties are known from, for example techniques used in CM. This directly introduces the second criteria, the presence of the design in MEMS applications. If the design solution is well documented but unknown in MEMS application in SB-CMM can be more difficult as well.

'Range' is an indication of the force and displacement that can be generated by the solution. These are estimations and are classified as 'small' or 'good'. Indicating whether it is on the small side or it is appropriate for our design challenge.

Compared with the overall criteria for the final design, the criteria for the sub-solutions are considering criteria 1,2,4a,4d,4e. Missing criteria 3, permanent preload without external intervention e.g. it is robust to environmental influences, will be considered in the next phase of the design. The robustness can be improved without changing the concepts and as such this criterium is not applicable here. Missing criteria 4b, robustness to outside influences, can also be influenced in later design choices and is not an important indication in this stage. Missing criteria 4c, footprint, is influenced by the concepts here but ranked as less important because elimination bases on footprint alone is considered less important that the complexity of fabrication. Missing criterium 4f, accuracy, is influenced by the later optimization of the concepts and therefore not applied on this phase.

2.4.2 Tables

The weight tables of the sub-concepts can be found in appendix 0.

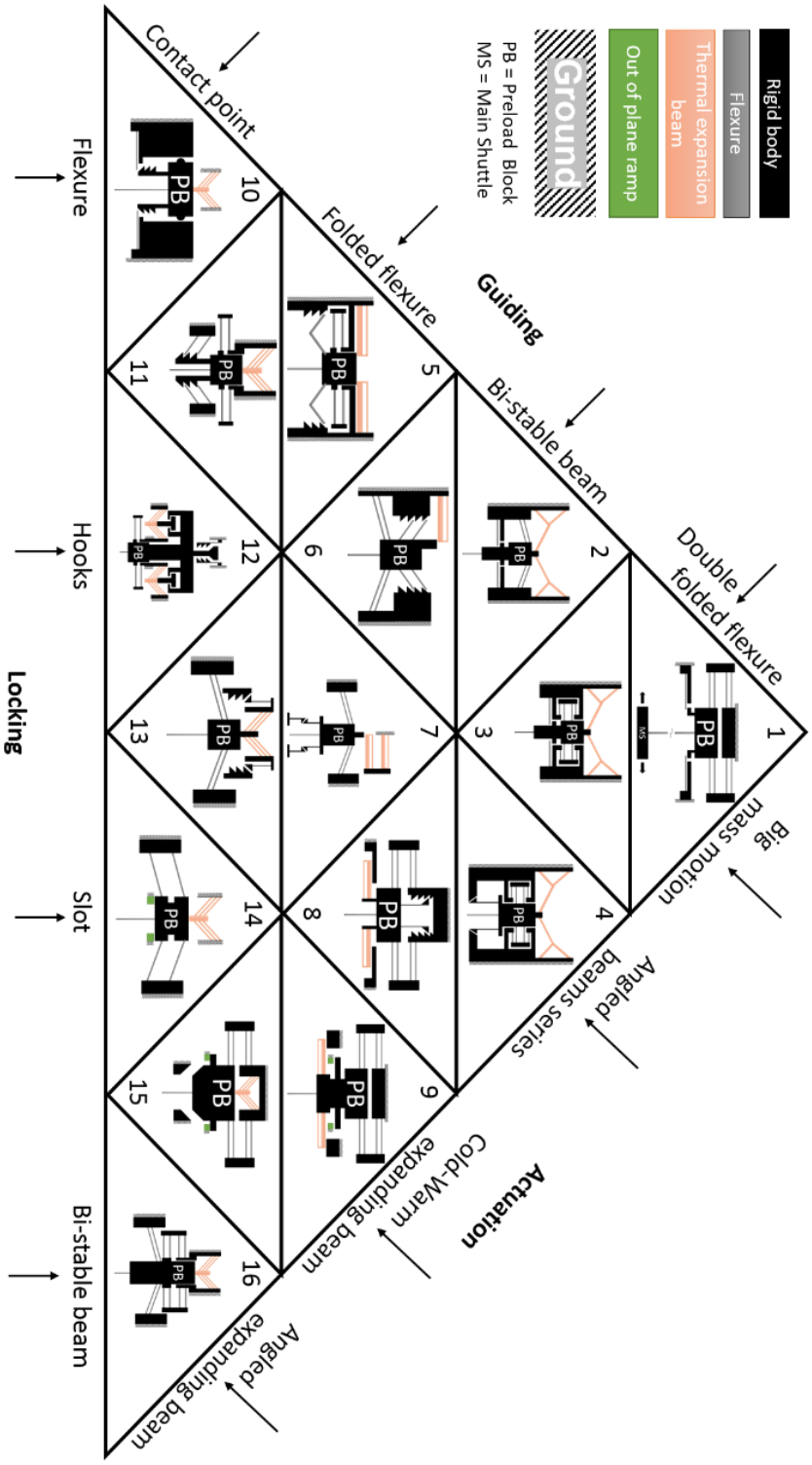

Figure 7 Ternary plot

2.5 Total concept design generation

The total design concept for the preloading mechanisms is generated using a ternary plot. This new method enables quicker design generation without fully losing design concept options. First the ternary plot is explained, then the design concepts are described, next force sketches of the designs are made and finally the concepts are ranked using weight tables.

2.5.1 The ternary plot

To generate total design solutions from the 3 sub concepts areas, I used a 'ternary plot', Figure 7 Ternary plot. In this plot the highest scoring concept solutions are represented 7 times. The second highest scoring concept 5 times. The third 3 times and the fourth 1 time.

The motivation for this plot assumes that the highest scoring sub-concepts have the highest success potential but the lower scoring concepts do not need to be fully excluded because of that. By not combining all 4 solutions of the 3 sub-concepts components, but by generating design concept combinations based on the concepts, total design solutions have been reduced from $4^3 = 64$ to $7+5+3+1=16$ solutions. While using this plotting technique one should keep in mind that this brainstorm is not a 100% coverage of design solutions, nor is the cell a 100% coverage of all the sub-concept variations. More variation can be made using the following considerations:

1) Compression or tension in solids /flexures
2) The footprint of the design combination
3) Placing a concept in a single or a double arrangement and the double arrangement in a parallel and/or series arrangement.
4) Internal or external placing of the ground contact with respect to the design concepts centre.
5) Adaptability of the range of motion: Example: make one hook for one position or use a range of positions a hook can be clicking into.

Other configurations and combinations are possible, but for now this first brainstorm is assumed to be a good starting point. I consider different options without fully excluding concepts, but I do have some semi-random solutions for the different variables for a cell, even so, in solutions 7, 5, or 3 I try to give an impression of the varieties I can come up with. In the analysis section it may come forward why one variety is better than the other one. From this I might decide to choose another variety for a cell. In this way the ternary plot is a method somewhere between variation and combinations of concepts. Reducing time spend on the brainstorm without fully losing design options.

2.5.2 Description of designs

1 Double folded flexure, big mass motion, Flexure

Big mass moves, preload flexure is under tension, preload block moves down, locking flexures bend down and slide on the sidewall of the preload block, there is a gap, the flexures lock into the gap, big mass motion is stopped. Locking flexures cannot bend upwards due to a stop block. Preload block is preloaded. Double folded flexures guide the preload block in a translational motion downwards during the preloading.

2 Bi-stable beams, angled beams series thermal actuator, flexure

Heat is applied, thermal beams expand, preload block moves down, locking flexures bend down and slide on the sidewall of the preload block, there is a gap, the flexures lock into the gap, locking flexures cannot bend upwards due to a stop block. On the halfway point of the preloading displacement guiding bi-stable beam will no longer resist the displacement and from now on apply a force downwards together with the thermal expanding beams. Preload block is

preloaded, heat disappears, thermal actuator is not attached to preload block and moves back to original position.

3 Double folded flexure, angled beams series thermal actuator, flexure
Heat is applied, thermal beams expand, preload block moves down, locking flexures bend down and slide on the sidewall of the preload block, there is a gap, the flexures lock into the gap, locking flexures cannot bend upwards due to a stop block. Motion is guided by double folded flexures. Preload block is preloaded, heat disappears, thermal actuator is not attached to preload block and moves back to original position.

4 Double folded flexure, angled beams series thermal actuator, hooks
Heat is applied, thermal beams expand, preload block moves down, motion is guided by double folded flexures. The preload block moves down, hooks flexure inwards until they surpass two ground blocks. Block is preloaded, heat disappears, thermal actuator is not attached to preload block and moves back to original position.

5 Folded flexure, cold warm beam, flexure
Heat is applied, cold warm beam bends and pushes down on preloading block, folded flexures guide the motion. Two locking flexures slide over a sawtooth structure. This way the preload block can only move down and not up. The block is preloaded, heat disappears, thermal actuator is not attached and retracts.

6 Bi-stable beam, cold warm beam, flexure
Heat is applied, cold warm beam bends and pushes down on preloading block. Two locking flexures slide over a sawtooth structure. This way the preload block can only move down and not up. The block is preloaded, heat disappears, thermal actuator is not attached and retracts. On the halfway point of the preloading displacement the guiding bi-stable beam will no longer resist the displacement and from now on only apply a force downwards together with the thermal expanding beams.

7 Bi-stable beam, cold warm beam, hooks
Heat is applied, cold warm beam bends and pushes down on preloading block. Hooks slide over each other until they surpass each other. The block cannot go up again. The block is preloaded, heat disappears, thermal actuator is not attached and retracts. On the halfway point of the preloading displacement guiding bi-stable beam will no longer resist the displacement and from now on only apply a force downwards together with the thermal expanding beams.

8 Double folded flexure, cold warm beam, hooks
Heat is applied, cold warm beam bends and pushes up on grounded blocks, thermal actuator is attached to the preload block. Hooks slides over a sawtooth structure. The block cannot go up again. The block is preloaded, heat disappears, thermal actuator is not attached and retracts. A double folded flexure guides the block downwards.

9 Double folded flexure, cold warm beam, slots
Heat is applied, cold warm beam bends and pushes down on preloading block. A double folded flexure guides the block downwards. The green blocks in the drawing are two ramps. The top part in the drawing is ramped, the lower part in the drawing is a 90° wall sticking straight out of the drawing paper. This way the preload block moves out of the paper over the blocks and because of the double folded flexure, after surpassing the ramp, goes back into the paper again. The block cannot go back up because of the 90° wall.

10 contact point, angled thermal beam actuator, flexure
Heat is applied, thermal actuator expends beams and moves the block down. Two locking flexures slide over a sawtooth structure. This way the preload block can only move down and not up. The block is preloaded, heat disappears, thermal actuator is not attached and retracts. Point contacts guide the block down.

11 folded flexure, angled thermal beam actuator, flexure
Heat is applied, thermal actuator expends beams and moves the block down. Two locking flexures slide over a sawtooth structure. This way the preload block can only move down and not up. The block is preloaded, heat disappears, thermal actuator is not attached and retracts. A folded flexure guides the block down.

12 folded flexure, angled thermal beam actuator, hooks
Heat is applied, thermal actuator expends beams and moves the block down. A folded flexure guides the block down. Backlash in the actuators prevent the preload block from going up after preloading and cooling down. An out of plane ramp block is pressed in between two hook structures to lock the preload block.

13 Bi-stable beam, angled thermal beam actuator, hooks
Heat is drained, thermal actuator retracts. It has a bit of flexing so the hooks go down and lock into the sawtooth profile. The heat is restored. The hooks are locked the thermal actuator pushes the preload block down. The bi-stable beams snap and pull the hooks lower into the sawtooth profile.

14 Bi-stable beam, angled thermal beam actuator, slot
Heat is applied, thermal actuator expends beams and moves the block down. The green block are ramps (as in concept 9) the preload block moves out of plane. Half way during the motion the snap though beams snap. The preload block falls into the slot. Heat is removed, actuator retracts.

15 Double folded flexure, angled thermal beam actuator, slot
Heat is applied, thermal actuator expends beams and moves the block down. Double folded flexure guides the block down over two ramps into the slot. Heat is removed, the actuator retracts.

16 Double folded flexure, angled thermal beam actuator, Bi-stable beam
Heat is applied, thermal actuator expends beams and moves the block down. Double folded flexure guides the block down. The snap trough beams snap and prevent the block from coming back up again. The heat is removed.

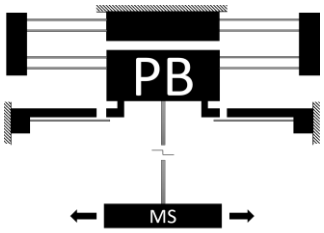

(a) Concept

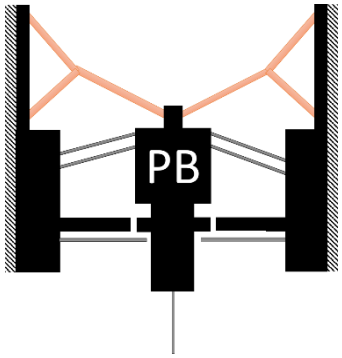

(b) Concept 2

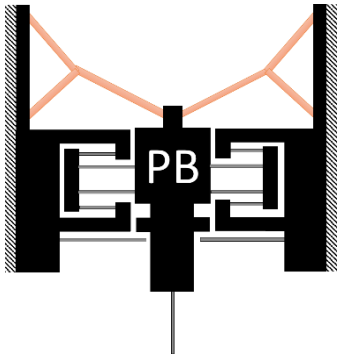

(c) Concept 3

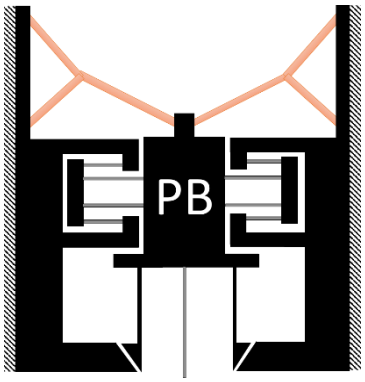

(d) Concept 4

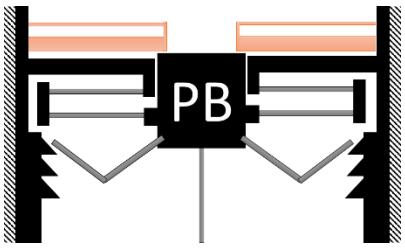

(e) Concept 5

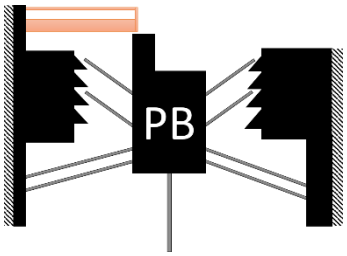

(f) Concept 6

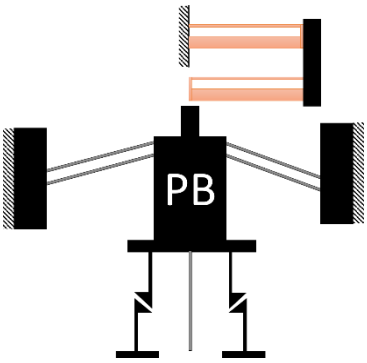

(g) Concept 7

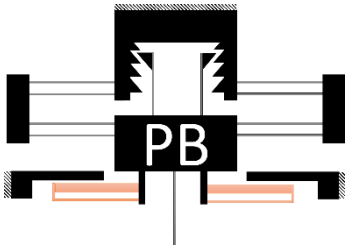

(h) Concept 8

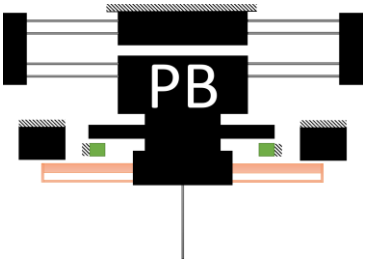

(i) Concept 9

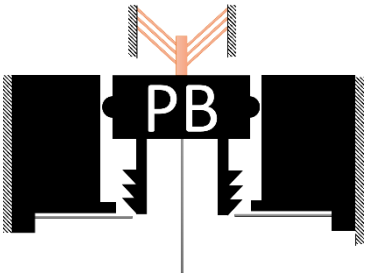

(j) Concept 10

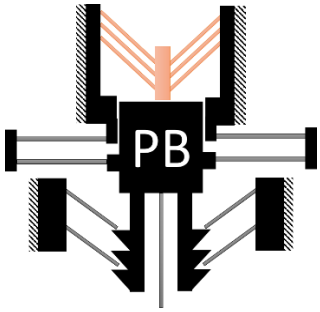

(k) Concept 11

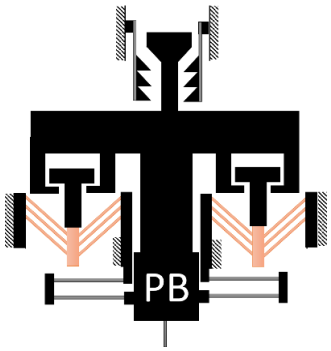

(l) Concept 12

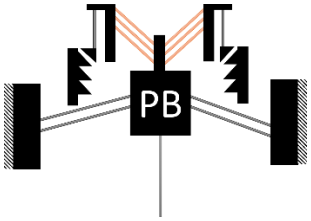

(m) Concept 13

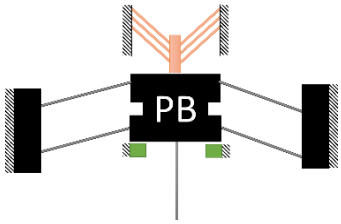

(n) Concept 14

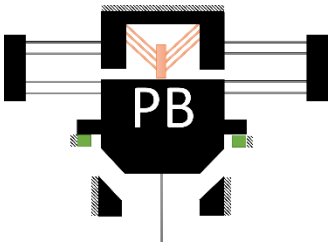

(o) Concept 15

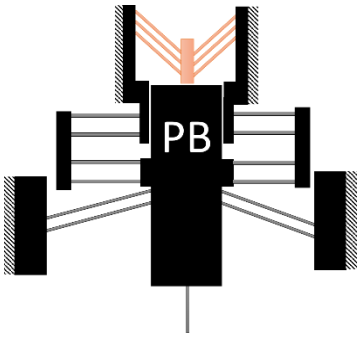

(p) Concept 16

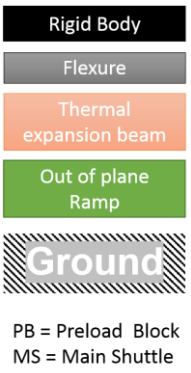

Legend

Figure 8 Concept sketches for total preloading mechanism

2.5.3 Force displacements

First, the separate force displacement diagrams for sub concepts are drawn. Next, the force displacement diagrams for concepts are drawn. In these drawings the reaction force of the preloading beam is neglected. L indicated a Locked position, when a return motion is attempted the force will go up straight as indicated by the arrows. In two cases there is double locking, meaning the preload block cannot go up and cannot go down anymore. The drawings are in appendix 3.

2.6 Criteria and weight table for total concepts

All criteria are applied to the concepts. Each concept is individually scored for each criteria. The lower the score, the better the concept. Not all criteria are equally important. A weight ranging from 1 to 3, where 3 is most important, are chosen per class, meaning a - e. The weight is then spread over each criterium in that class. The following weights are given a (3), b (2), c (1), d (3), e (1). The score is then rounded to one decimal point. Comments are given to some scores in the table. The criteria used are:

1 All designs meet this criterium.
2 All designs meet this criterium.
3 Flexure locking solutions and bi-stable beams may be sensitive to outside shock.
4 Criteria for the design are:
    a. Fabrication, less complex is better
        i. Number of Materials
        ii. 2d vs 3D (3d=1, 2d = 0)
    b. Robustness to outside influences, less is better ((3 is bad, 2 is okay, 1 is none)
        i. Gravity
        ii. Shaking
        iii. Temperature change
    c. Footprint, smaller is better
        i. It is hard to make a good assessment on the final footprint. For the actuation, the big mass motion actuation (concept 1) has the smallest footprint of all, the others might be around the same size and depend on final details of the concept and the needed range of motion for the actuators. Contact points (concept 15) for guiding might be the smallest guiding design. The others might be around the same size. Slots (concept 9, 14, 15) are probably the smallest for locking as they can use a gab in the structure of the preload block to lock, where the other designs need an extra flexure beam. The concepts mentioned will receive a -1 score for their smaller footprint.
    d. Complexity
        i. Is the actuation motion translational (1 is no, 0 is translational)?
        ii. Are there unwanted motions possible of the preload block (1 = yes, 0 = no)?
    e. Range of motion, larger is better
        i. Is the position of the preload block changeable? (1 = no, 0 = yes). if the position is controllable design can be tuned after fabrication.
    f. None of the designs are tune-able for stiffness.

Criteria →	a.i	a.ii	b.i	b.ii	b.iii	d.i	d.ii	e.i	c.i	Total score
Weight → Concepts ↓	1.5	1.5	0.66	0.66	0.66	1.5	1.5	1	1	
1	1	0	2*	3	1	0	0*	1	-1	5,5
2	2	0	1	1	2	0	0	1	0	6,6
3	2	0	1	1	2	0	0*	1	0	6,6
4	2	0	1	1	2	0	0*	1	0	6,6
5	2	0	1	2*	3*	1	1*	0	0	10,0
6	2	0	1	1	3*	1	0*	0	0	7,8
7	2	0	1	1	2	1*	0	1	0	8,1
8	2	0	1	2*	3*	1	0*	0	0	8,5
9	2	1	2*	1	2	1	0*	1	-1	9,3
10	2	0	3*	3*	3*	0	1*	0	0	10,4
11	2	0	1	2*	3*	0	1*	0	0	8,5
12	2	0	2*	1	2	0	1*	1	0	8,8
13	2	0	1	1	3*	0	0	0	0	6,3
14	2	1	2*	1	2	0	0	1	-1	7,8
15	2	1	2*	1	2	0	0*	1	-2	6,8
16	2	0	1	2*	2	0	0	1	0	7,3

Table 1 Weight table for total design concepts

Comments

b.i 1) gravity might influence shaking. 9) out of plane motion might be sensitive to gravity. 10) need out of plane cover/contact point. 12) top is not suspended. 14,15) out of plane motion wanted and therefore probably more sensitive to gravity. **b.ii** 5,8) Might enable further than intended preloading. 10) no so much stiffness to prevent further preloading. 16) no solid preloading, with bad shaking the locking might become undone. **b.iii** 5,6,10,11) temperature change might cause overshoot in positioning. 13) thermal actuator does not get decoupled after preloading. **d.ii** 1,3,4,8,9, 15) double folded flexure is over-constraining the concept. 5,11,12) out of plane rotation, in plane rotation. 6) over-constraining by locking flexures. 10) rotations are not blocked.

3 Rapid prototyping method

3.1 General approach to rapid prototyping

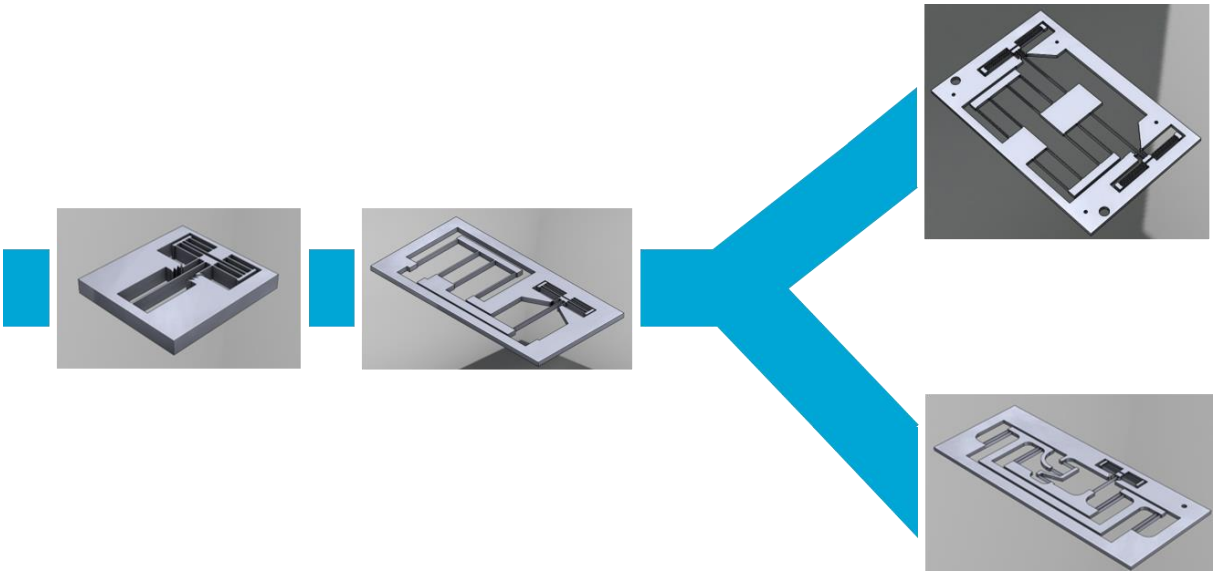

Figure 9 Design evolution during rapid prototyping

The following steps were taken during the rapid prototyping phase:

1. Find the right equipment for the job. The institute has 2 laser cutters and 1 UV light 3D printer. One of the laser cutters can cut bronze or metal material but one cantilever sized 8 mm already takes more than an hour to make. Therefore this more precise machine could not be used. A full model would take days to make. The 3d printer is also relatively slow compared to laser 2. Machine details can be found in chapter 3.2
2. The first models start by modelling a buckling beam and the preloading mechanism (first picture). The smallest achievable beam thickness that the machine can produce from 5 mm PMMA material is determined. Hand calculations of stiffnesses are used to calculate a needed flexure length. The first models work with horizontal flexures for locking but are quickly replaced with hook designs. The hooks are optimized by calculating the needed hook displacement (determines hook height) by hand and playing around with the other dimensions until a design is found that lock and does not break.
3. A main shuttle and LDDF are added to the preload mechanism to find if we can induce static balancing. The thickness of the flexures varies a lot and so many models do break due to high stresses and thin structures. Also, the heat of the laser has some influence on the flexure stiffnesses. It is tried to make a modular structure with a stationary LDDF and shuttle to which distinctive designs of the preloading part can be added. This approach saves PMMA material and space as the stationary part only has to be fabricated once. Without much success this modular design was created and worked but the connection between the parts had backlash, and so it was decided to continue with full/total designs.
4. From the challenge to save material and space a one-sided asymmetric design was made. (second picture in the evolution). It soon became apparent that main shuttle could rotate under the forces of the buckling beam. So, to overcome this the designs had to be changed.
5. That resulted in 2 final concepts, one symmetric, and one asymmetric and supported by lever structures of which the concept design is explained in the chapter 3.6.

6 It was tried to fabricate the asymmetric design using the 3D printer, as this fabrication might give better beam thicknesses. The thicknesses are more constant. But the material properties used in this machine (Vero Clear) where difficult to predict. It also changes under the abortion of water and light. A small 3-point bending test was performed with all combinations of material, in chapter 3.4. After production and testing the asymmetric model, it became clear that the material has 'memory' and only slowly returns to the original position. It was not possible to preload the device using a shaking table, but it could be preloaded by hand using shock and shaking. The model size is 250 x 90 x 3 mm.

7 A symmetric design was made using PMMA and tested on a shaker. It could preload at 380 rpm. The model size is 270 x 170 x 5 mm.

3.2 Fabrication details

There were 3 different machines used during the rapid prototyping stage.

1. Lpkf laser & electronics: protolaser us (laser cutting):
    a. Materials: metal/ bronze laser cutting
    b. Maximum footprint: much bigger than required
    c. Time estimation for an object*: 10 hours
    d. Smallest beam thickness: 150 microns

2. Epilog: laser mini (laser cutting):
    a. Maximum footprint: 24x12 inch
    b. Material: Acrylics/wood laser cutting
    c. Time estimation for an object*: 10 min
    d. Smallest beam thickness: 800 ± 200 microns

3. Stratasys: objet 260 Connex (UV light 3d printing):
    a. Maximum footprint: much bigger than required
    b. Material: Vero Clear or Tango Black material.
    c. Time estimation for an object*: 1,5 h
    d. Smallest beam thickness: 100 microns

*object: a total model with straight line guiding and preload mechanism

3.3 Bronze laser cutting

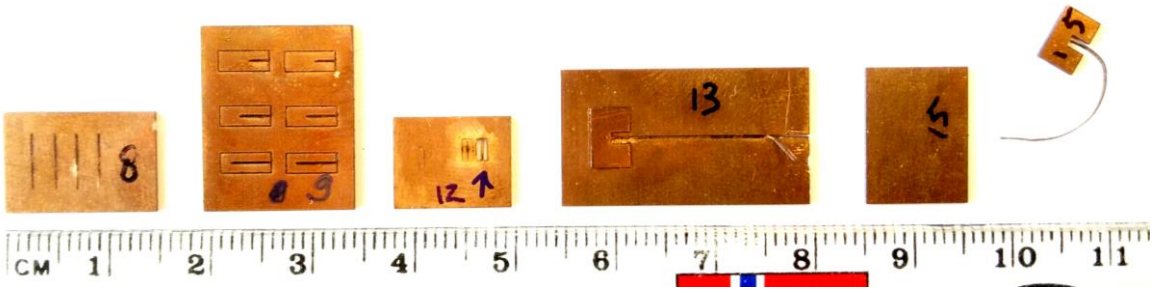

Figure 10 Bronze models

Attempts have been made on the LPKF laser to cut cantilever beams out of bronze. This was done as an orientation on what equipment was best suited for rapid prototyping. Fabrication with the LPKF laser cutter was very time consuming and therefore not chosen for RP.

It was investigated what the smallest beam thickness might be on this machine out of 0,5 mm bronze plating. In
Figure 10 Bronze models, models 8 are used to investigate the gab thickness. Models 9 are first attempt cantilevers, they all did break. The smallest beam I could make and safely make free of the cut surrounding material was 122 um, shown, model 12. Measurement where taken with a microscope with laser measurement features, the results can be seen in Figure 11 Cantilever tip thickness measurement and Figure 12 Cantilever tip laser measurement.

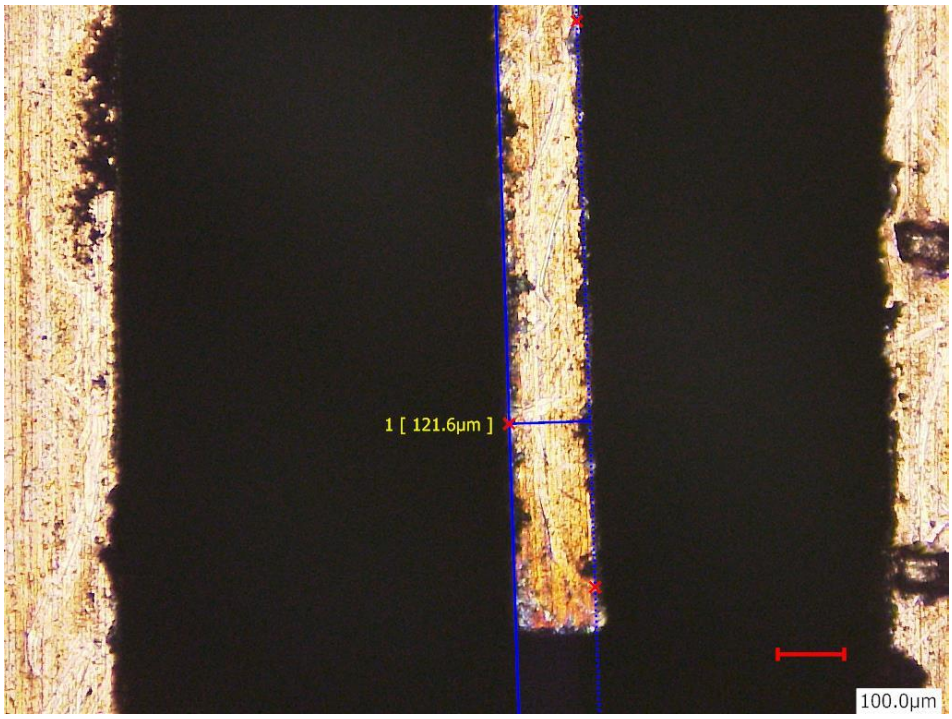

Figure 11 Cantilever tip thickness measurement

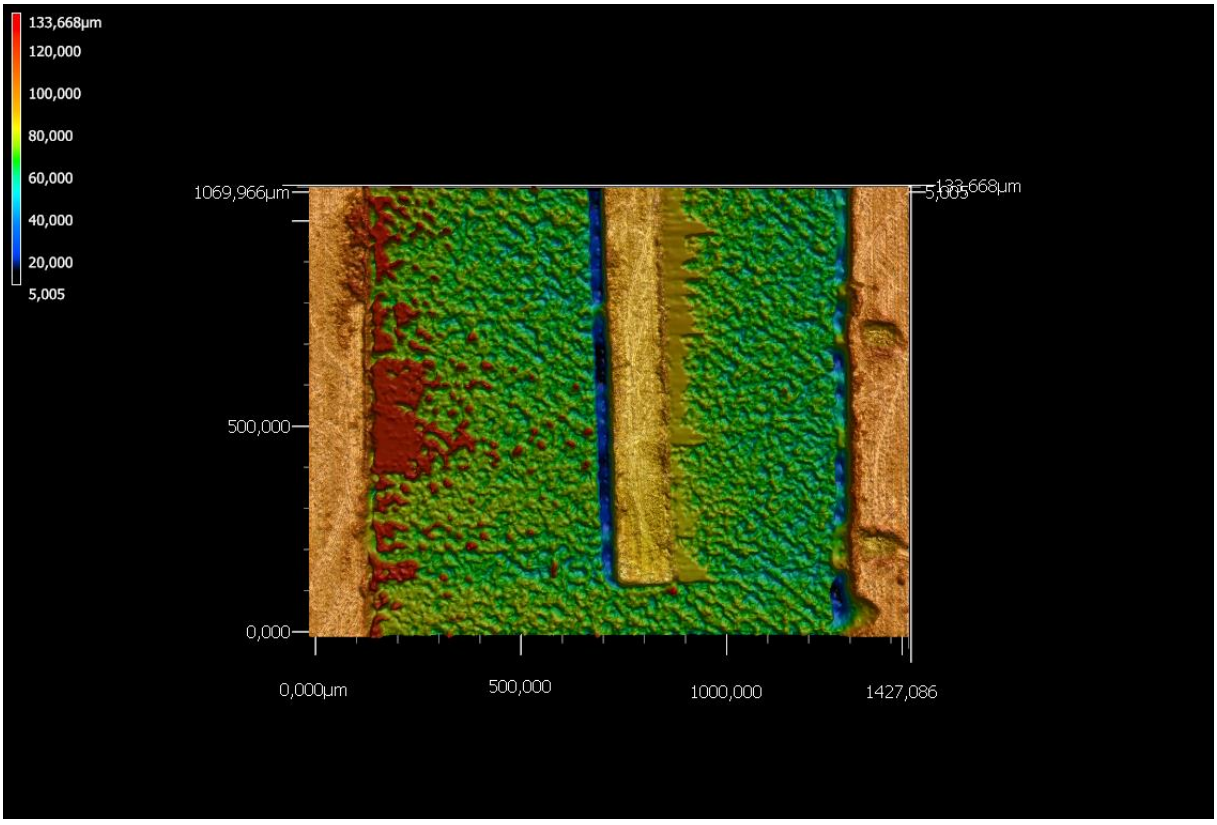

Figure 12 Cantilever tip laser measurement

3.4 Vero Clear 3-point bending test

A 3-point bending test was conducted to get estimates for the material properties used for the 3D UV printer. Chantal Goettle and I tested a combination of material printed in a beam of 30 mm long x 5 mm wide. With a thickness variation from 0.1 to 0.5 mm. We devised a code for every sample being #.00 where # indicates the thickness. For example 1.10 = 1. = 0.1 mm thickness. 2.10 = 0.2 mm thickness. The second digit indicates the type of material. 0.#0= type of material: 0.10 = RGD8710-DM, 0.20 = RGD8720-DM, 0.30 = RGD8730-DM, 0.70 = FLX9070, 0.95 = FLX9095, 0.VC = Vero Clear. Due to copyright I cannot show the material property sheet from Stratasys for the used materials, but it was found online (6-3-2017) at:

http://usglobalimages.stratasys.com/Main/Files/Material_Spec_Sheets/MSS_PJ_PJMaterialsDataSheet.pdf?v=635785205440671440

From their data sheet we collected:

	Young modulus (MPa)	Tensile strength (MPa)
RGD8710-DM	Not in datasheet	Not in datasheet
RGD8720-DM	2000-3000	50-65
RGD8730-DM	Not in datasheet	Not in datasheet
FLX9070	Not in datasheet	Not in datasheet
FLX9095	Not in datasheet	Not in datasheet
Vero Clear RGD810	2000-3000	50-65

Table 2 Material properties 3D printing

3.4.1 Test setup

Figure 13 3-point bending test measurement setup

The setup consists of a BOSE, Electroforce Testinstrument 3220-AT, with a stepping displacement of 0.0065 um, with the thereto belonging force sensor 1516 DMW. The support

mounts are printed with Vero Clear material. The distance between the two lower supports is 20 mm.

3.4.2 Results

The stiffness of every sample was calculated from the force and displacement data. The data is plotted and the maximum found stiffness in the plot for every sample is used to determine the young modulus with equation 1. The results can be found in Table 3 Measurement results of 3-point bending test. Some sample do not have any results as they were too thin to measure the reaction force. If a sample is not in the list it is because we were unable to fabricate it.

$$k = \frac{48EI}{L^3} \tag{1}$$

Sample	k(N/m)	E (GPa)
1.10	-	-
2.10	30	5,06
3.10	147	7,35
4.10	320	6,75
5.10	590	6,37
3.20	136	6,80
4.20	315	6,64
5.20	565	6,10
2.30	-	-
5.30	440	4,75
4.70	-	-
5.70	-	-
5.95	-	-
1.vc	-	-
2.vc	28	4,73
3.vc	140	7,00
4.vc	318	6,71
5.vc	630	6,80

Table 3 Measurement results of 3-point bending test

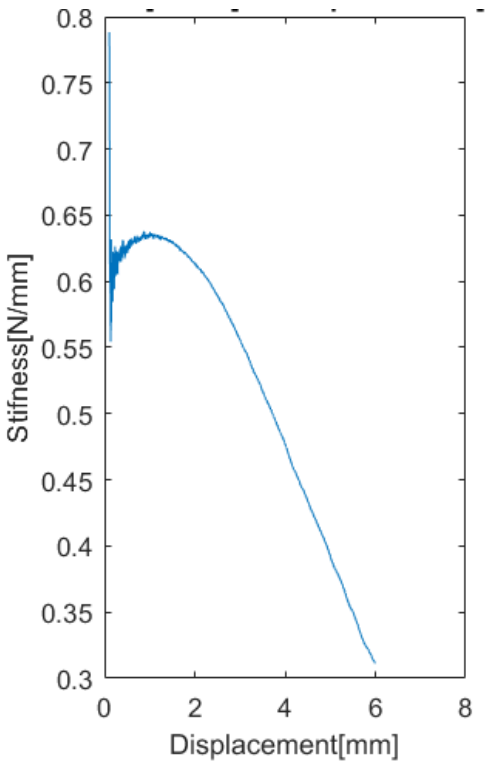

Figure 14 Stiffness plot for sample 5,VC

3.4.3 Conclusion, discussion and remarks

As the Vero Clear material is the material of interest in this research, because it will be used to fabricate the models from, we will only consider its results. The extra samples where made because it might be contributory to others in the Max Planck department.

From the Vero Clear results we can assume that the Young modulus for 2, VC is an outlier as we were not able to measure the thinner sample 1.VC due to low forces. The remaining Vero Clear samples indicate a much higher Young modulus than predicted in the material properties sheet. The stiffness plots made were not constant at all, and the maximum stiffness was taken. An example of such a plot is given in Figure 14 Stiffness plot for sample 5,VC. One can only speculate that that might have cause a higher Young modulus estimation.

Experience from handling the models in RP though indicate a much lower Young modulus than predicted by the material properties sheet. All in all it does not give us a clearer picture of what the real material properties are.

3.5 Changing the locking concept

As can be read in the design paper, the concept of using flexures for locking was quickly replaced by using hooks. Both concept models made by rapid prototyping can be found in appendix 4.2 . A simple hook model that is also used in plastic model casings was the first concept. It was later optimized after RP as is discussed in detail in the paper.

3.6 Lever design

A lever design solution is needed to overcome the problem of the changing stiffness in the flexures of the LDFF due to load stiffening as the buckling beam presses down on the main shuttle. For this a short comparison is done between two lever designs. The two design model's drawings can be found in appendix 4.1. Both are 3d printed with the Stratasys UV light 3D printer out of Vero Clear material.
Model V2.3 is based on a design found in literature [1]. Model V3 is based on a concept found in literature [2].

Soon after fabrication and testing the motion of the models by hand model V3 broke down. It became apparent that the required range of motion could not be met by this design. At closer inspection, the two flexures making up the centre of rotation connect to a 'lever block' which is in turn connected to the secondary and the main shuttle of the DFF. This lever block does not only rotate but also moves in y-axis, putting too much stress on the lever flexures and resulting in breaking. The whole construction also had a higher stiffness than model V2.3

Model V2.3 works, did not break and is therefore used in further rapid prototyping.
Two video captures can be seen in Figure 15 Model V2.3 testing by hand and Figure 16 Model V3 testing by hand

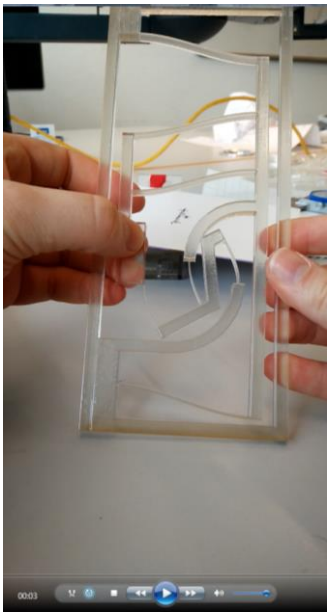

Figure 15 Model V2.3 testing by hand

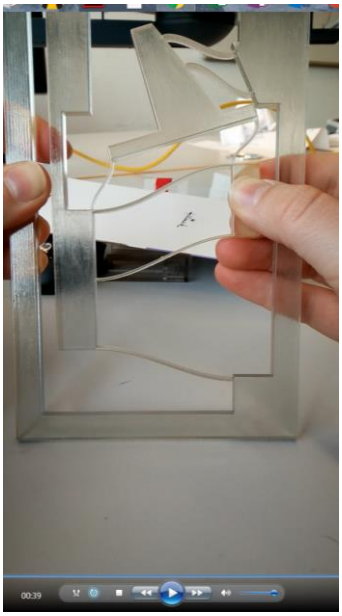

Figure 16 Model V3 testing by hand

3.7 Symmetric design

3.7.1 Description

The full drawing of the symmetric design can be found in appendix 4, measuring 270 x 170 x 5 mm. The symmetric design uses symmetry to prevent the effect of load stiffening on the main shuttle. By applying the LDDF on both sides of the MS and applying the preloaded beam on both sides as well the MS shuttle can move over one axis. The model was made from PMMA material plate with the Epilog: laser mini.

3.7.2 Modelled stiffness

The laser cutter makes beams of variating stiffness. The beam thicknesses in the drawing are reduced by 0.1 mm because of the laser. Based on this assumption the stiffness calculation sheet, shown in appendix 5 , was used to calculate the stiffnesses.

Positive stiffness	127 N/m
Negative stiffness	-131 N/m
Difference	4 N/m

3.7.3 Practical results

The measurements I could perform at the Max Planck Institute were of inadequate quality. I only had a simple string and set of weights to measure the stiffnesses. For that reason, only have measurements of the asymmetric design where taken.

This model is larger than the asymmetric design and because of it I could test it successfully for preloading on a platform shaker. The chemical shaker is a New Brunswick™ Innova® 2300. It has an rpm from 25 to 500. And an orbit diameter of 1 inch (2.5 cm). A high-speed camera was mounted on top of the shaking platform to register motion of the model. During the preloading test the model was slightly suspended from the platform by small spacer rings.
The test starts with 0 rpm and up to the value where preloading will occur, if it does at all.

Extra weight was added in the form of PMMA slats to the models MS to be able to preload the structure. Preloading was successfully implemented at 380 rpm. Just after preloading one of the flexures of the LDFF breaks. I was also able to preload the structure by shaking/shock by hand as well before doing the shaking test.

3.7.4 Discussion and other remarks

The shaking test was used as an indication for when preloading would occur, it was not used as a measurement to be able to determine exactly when preloading would occur and under which conditions.

I tried repeating this test and taking better data but therefore I needed more models. In my last week at Stuttgart, delays and mistakes at ordering services had depleted the resource of PMMA plates I needed. All the models I tried making with the leftover material broke due to the laser fabrication deviations.

PMMA was experienced as a very brittle material. Earlier during RP Delrin material was considered. I tried to order it weeks before I would leave Stuttgart. It never arrived in time for me to use it due to the failing orders.

It can also be seen in the model V2.5 that the flexures in the DFF for the PB are very close together. During the rapid prototyping I failed to keep an eye I on this as I was trying to fit the model into the maximum plate size that was accepted by the laser cutter. Therefore, the PB could rotate a little bit. This might even have worked in advantage as the rotation of the block would mean less stress on the buckling beam and the forces on each hook were able to level off.

The fact that the model broke just after preloading, might have been caused by the sudden drop in stiffness, deflecting the flexures further. There were no stop-blocks integrated in the design to prevent the model from moving a certain MS displacement. We might also have to consider fatigue as the model was put through a lot of shaking before it was preloaded.

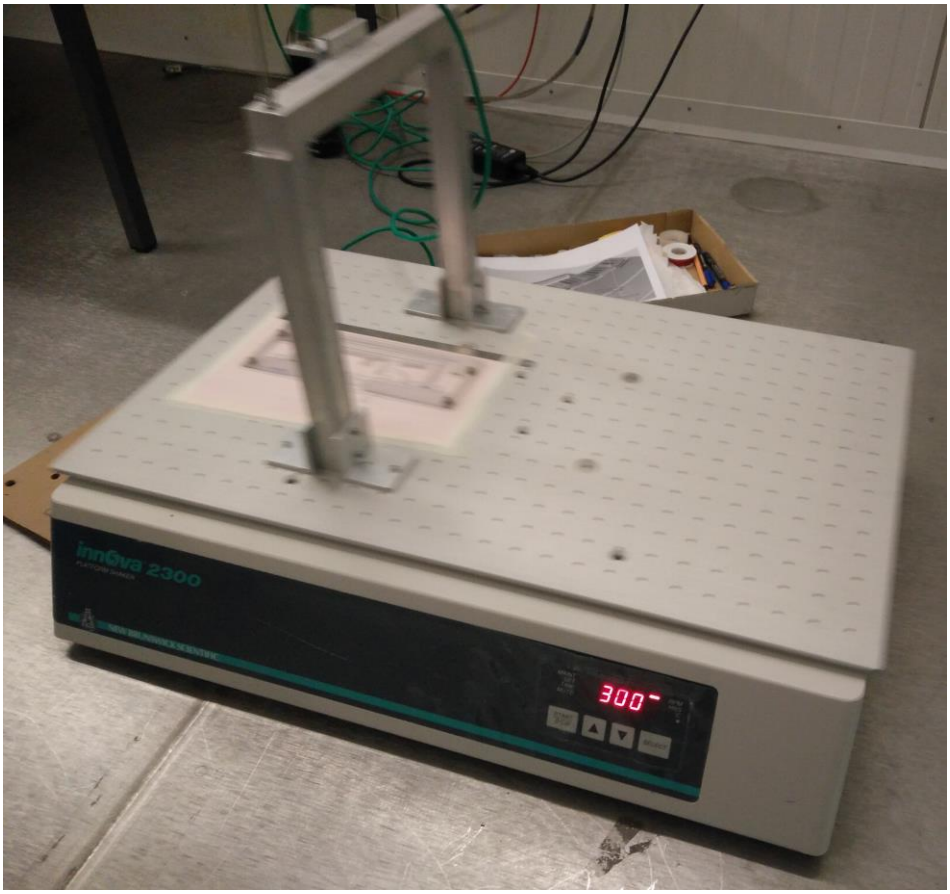

Figure 17 Platform shaker measurement setup

Figure 18 Video capture of high speed camera just after preloading

3.8 Asymmetric design

3.8.1 Description

The full drawing of the symmetric design can be found in appendix 4.4, measuring 250 x 90 x 3 mm. This model consists of one LDFF structure, one lever and the preload mechanism concept that was also used in the symmetric design. The lever ensures the secondary shuttle and the MS move in a 1:2 displacement relationship to each other preventing the effects of load stiffening caused by a one-sided force applied by the buckling beam on the MS. The lever prevents the MS from moving in a vertical direction. The model has stop block to prevent the hooks from displacing further than intended. The LDFF has double flexures in place to have enough positive stiffness, without adding to the stress in the flexures. The model was made from Vero Clear material on the Stratasys: objet 260 Connex 3D printer.

3.8.2 Modelled stiffness

The effects of 3D printing on the Vero Clear material is unknown. Chantal Goettle and I performed a 3-point bending test without getting very usable and accurate material Young modulus result. From handling the 3D printed Vero Clear material, performing a 3-point bending test and using a material properties sheet the material properties of Vero Clear material are hard to predict, and so it was chosen to use the same Young modulus as for PMMA material. From handling the earlier 3D models, it feels like the yield stress of this material is higher than that of PMMA. It does however seem to have 'memory' properties, meaning that it looks like it permanently deforms but with time the material returns to the original position. Therefore, the choice was made to use the same limit to yield stress is used as for PMMA material. It is also, obviously, sensitive to light changing the material properties as the object is made with a UV-light 3D printer. The 3D printer is producing slightly trapezoidal flexures. It is assumed that the flexures have the same thickness as the intended thicknesses drawn in the full drawing. In it are the thinnest beams the machine could make at the height of the model. When reducing this thickness even more the 3d printer stops making a beam in z-axis, so the beam is not as high as it should be.

Based on experience with other models, the negative stiffness is much higher in relation to the positive stiffness, or the positive stiffness lower in relation with the negative stiffness. Other models made where strongly bi-stable. For this reason, the model is intentionally made with a positive stiffness to compensate for this effect. A calculation sheet, shown in appendix 5, was used to calculate the stiffnesses after preloading.

Positive stiffness	50 N/m
Negative stiffness	-28 N/m
Difference	22 N/m

Table 4 Static balancing values asymmetric model

3.8.3 Practical results

Preload the asymmetric design in the same way as the symmetric design was without success. It is possible to preload the model by shock and shaking by hand.

Stiffness measurements where done with a mass and a weight on this model. Due to friction and a poor setup the results are not accurate or practical meaning anything other than to give an indication of the stiffnesses. Figure 19 Stiffness measurement setup, give an impression of this setup. The weights were put in the plastic cup which is attached with a string to the MS of the design.

It was found that the un-preloaded stiffness was 4 ±0.5 mm @10gr, 24 N/m, and the preloaded stiffness was 8 ± 0.5 mm @10gr, 12 N/m.

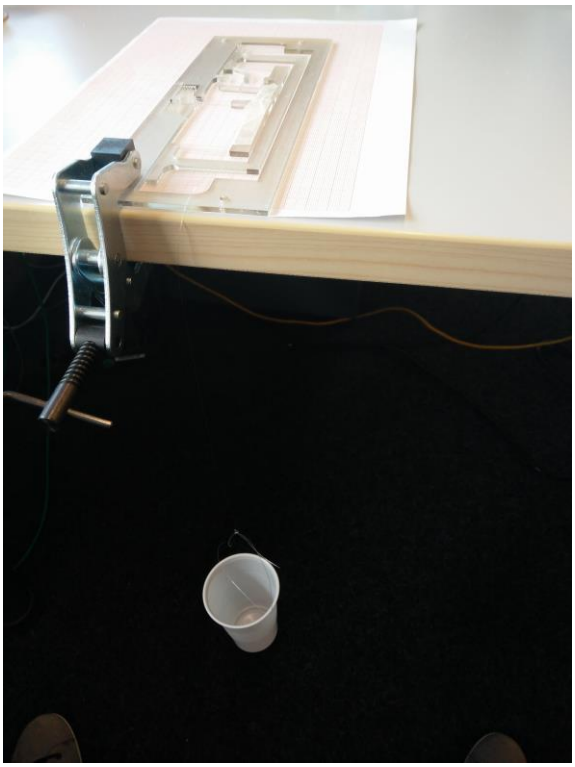

Figure 19 Stiffness measurement setup

3.8.4 Discussion and other remarks

Using the Vero Clear material, it was extremely difficult to make a good estimation of the material properties. Only by making multiple prints one could get a feel for how the material behaved. The advantages however, were to have a less brittle material and a smaller footprint due to finer printing details. Though the department had many great machines, a setup with a linear stage and force sensor to measure the stiffnesses for these models where not one of them. I was allowed to invest in this but due to delivery times and relative short stay in Germany this was not something I could follow up with. As the designs where to be used as a proof of concept the current results would had to do.
The modelled stiffness of 22 N/m and the measured stiffness of 12 N/m are very far apart, and the modelling and measuring of the models should be improved. In my opinion, it were fine mid-term results though for developing a statically balanced MEMS device. The fact that the model could preload by shaking and shock by hand is proof of the concept working, which was the goal for the RP.

3.9 Conclusion

Preloading by shaking with a platform shaker was implemented successfully on a symmetric model measuring 270 x 170 x 5 mm, at 380 r.p.m (0.8 mm beam thickness). The model was laser cut from PMMA material. A reduction in footprint was established by reducing symmetry in the mechanism, resulting is a 250 x 90 x 3 mm model (0.25 mm beam thickness). The design can be preloaded by shock and by shaking by hand. The model was 3D printed out of Vero Clear material.

4 Comsol and Ansys modelling

Software versions used:

ANSYS mechanical APDL 17.1	FEM analysis program
Comsol Multiphysics 5.2a	FEM analysis program
MATLAB R2016a	Data analysis program
Solidworks 2016	Drawings program

4.1 Comsol

For some reason still unknown, we were not able to model the solidworks models correctly in COMSOL. The idea was to import the models, add a displacement on the MS and have a non-linear analysis for the reaction forces at the MS. I struggled with this for 2 months trying to find a solution to our unknown problem. Even at the finest settings for meshing COMSOL was not always able to calculate a result. If it found one it was still off by a factor of 100 (!) with our predicted stiffnesses. Dr. Ahmet Tabak spend much time on this helping to find the problem, even with his experience we resourced to a COMSOL help desk service but even they could not help us find the problem. We never found a solution to this problem and I had to use ANSYS for modelling which I had not expected.

My experience with ANSYS was extremely limited. I only used it once and only by user interface. I had no experience using command code. As I struggled to understand the programming of ANSYS, because I found the help resources very confusing, I decided to wait with this modelling till I was back in the Netherlands and Davood Farhadi Machekposhti could give me an introduction based on files that he used for his modelling.

4.2 Ansys

There will be several studies executed in ANSYS. The following give the main introduction to all ANSYS code used.

Figure 20 ANSYS key point numbering, shows the basic setup of keypoints in ANSYS. The dashed lines indicate the flexures. The thick lines indicate the rigid parts added to the flexures of the LDFF. They are added during the configuration optimization. (Key point 1 and 2 are hidden in the numbing of key point 201 and 202.) Rigid lines connect the keypoints (not shown in figure) such that the resemble the rigid parts in the model. Table 5 keypoints and part connection shows which key point belong to which rigid parts. Every flexure from a design part has a codename to indicate the line which stands for L(length)(from)keypoint1(to)keypoint2. They are given in Table 6 Important lengths in modeling, Curve_Rad 1 determines a key point which is the centre of the radius for the curved beams between key point 1 and 2 and between key point 201 and 202. The reason for this is explained in chapter 5.3. The other flexures that are not named in the table have equal lengths of the flexure from a part that is named in the table. Meaning the 8 flexures of the DFF of the PB, the 8 flexures of the LDFF, the 6 flexures of the Levers and the 2 flexures for the hooks are of equal length.

For the beam elements Beam188 is used. For the rigid lines MPC184 is used. For the beam cross-section a cross-section is imported that is a rectangle with the flexure thickness, in the end result this is 24 um, and a height of 525 um, the thickness of a silicon wafer or the height needed for other modelling. The problem is solved non-linearly and in de case of modal analysis the non-linear solutions are also used as starting point for the modal analysis.

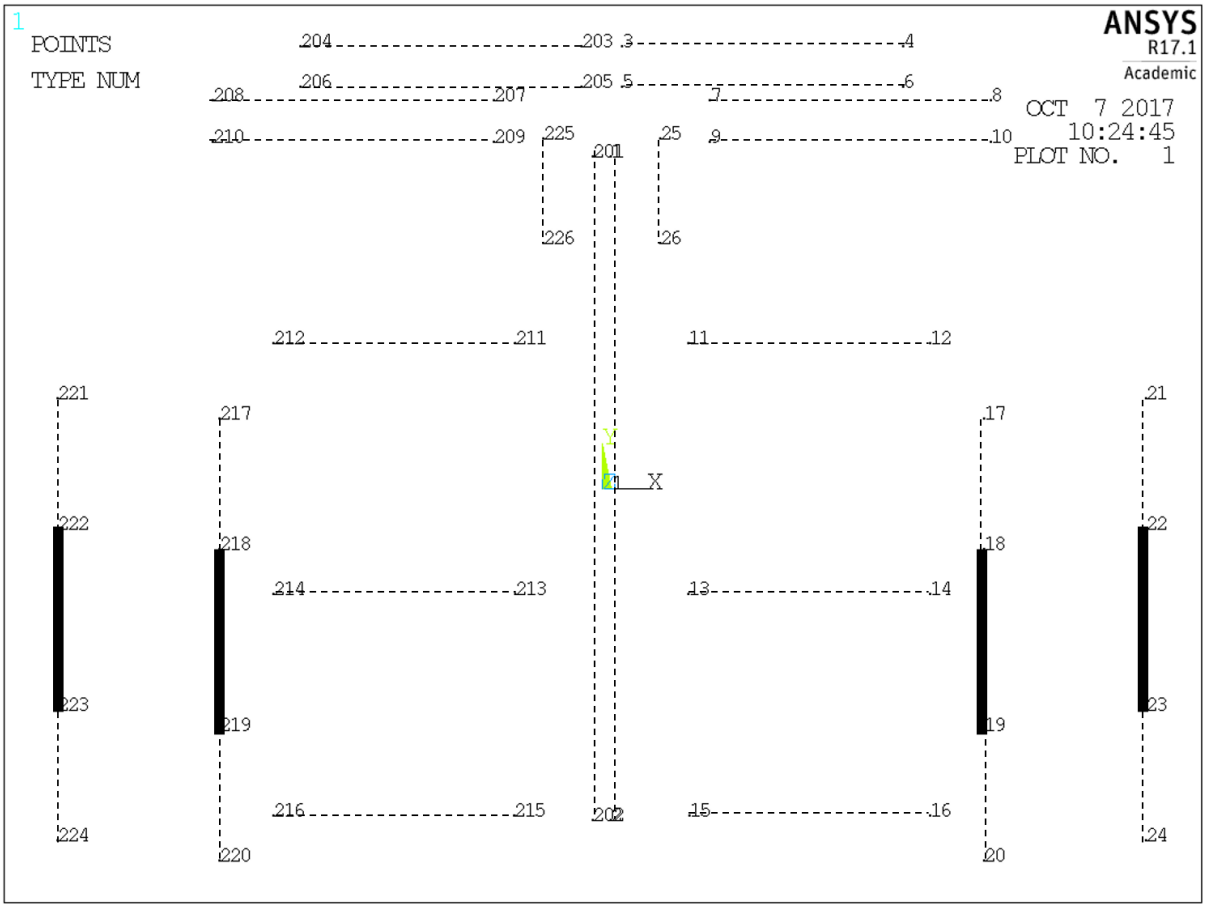

Figure 20 ANSYS key point numbering

Part	**Key point**	
Preload Block (PB)	1,7,9,25,203,201,207,209,225	
Secondary shuttle of PB	4,6,8,10	204,206,208,210
Hooks	26	226
Lever*	11,13,15	211,213,216
Main shuttle (MS)	2,15,20,202,215,220	
Secondary shuttle of MS	14,17,21,214,217,221	
Ground	3,5,12,24,203,205,212,224,203,205	

Table 5 keypoints and part connection

*the lever had several configuration in the lever configuration research

Flexures	**Other important lengths**
L12*	L1113
L34	L2024
L1112	L220
L1720	L35
L2526	
	Curve_Rad1

Table 6 Important lengths in modeling

*this is the y-axis length between the keypoints

5 Concept optimization after prototyping

It was chosen to optimize the asymmetric model develop during RP. Though the model is more complex because of its extra lever part it is smaller than the symmetric model, and meets the wish for a small footprint.
Several steps are taken to optimize the concept:

1 A configuration research is executed to determine the best lever placement.
2 The flexure lengths are optimized using an optimization protocol.
3 A beam curvature needed for the MEMS design is calculated.
4 A prototype 6:1 scale is developed for testing

5.1 Configuration research

During the configuration research an answer is sought to the question: What is the best placement for a lever regarding the vertical motion and rotation of the MS? To reduce the rotation of the MS even more rigid parts are added mid-flexure of the flexure in the LDFF of the best scoring configuration regarding vertical displacement.

During this research the levers orientation is varied and the number of levers is varied between 0,1 and 2. The 6 configurations studied are shown in Figure 21 Str till Figure 26 StrTL. More information on how the figures and the code work please read chapter 4. Earlier orientation on the configuration was done and experimented on while using an 'angled LDFF' configuration (the flexures where tilted and caused the MS not to move horizontal anymore), this resulted in the names Straight DFF for the configuration of the LDFF used from the beginning.

All the cases are preloaded with -0,22 e-3 mm on key point 1 in the y-direction. After preloading in time step 1, the shuttle is moved 1 mm to the positive x direction on key point 2 and in time step 3, -1 mm to the positive x direction.

Short hands are used for every configuration.

Str	Straight double folded flexure (SDDF), no levers
StrInvL	SDDF, one inverted lever
StrL	SDDF, one normal lever
StrTInvL	SDDF, two inverted levers
StrMix	SDDF, one normal and one inverted lever
StrTL	SDDF, two normal levers

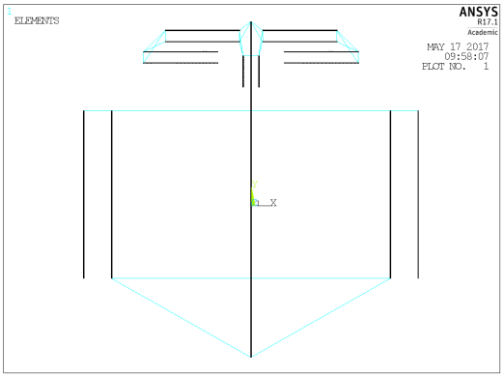

Figure 21 Str

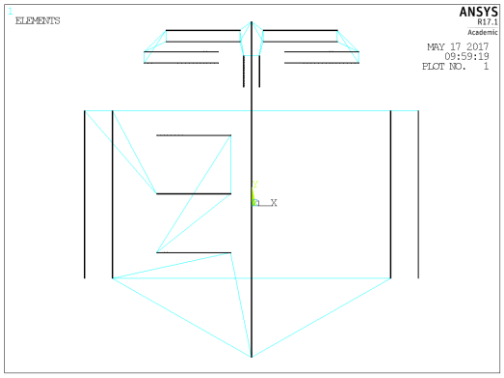

Figure 22 StrInvL

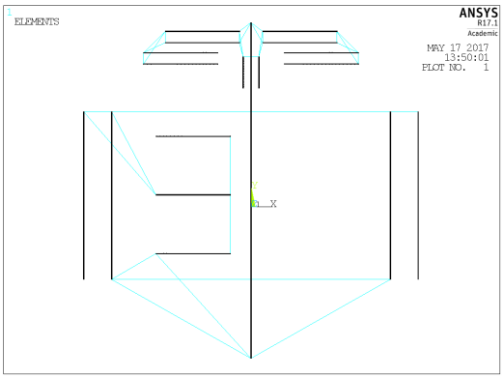

Figure 23 StrL

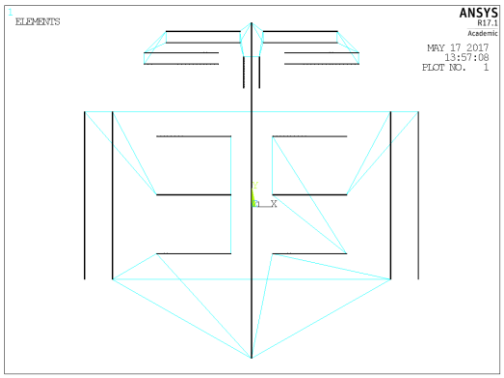

Figure 24 StrMix

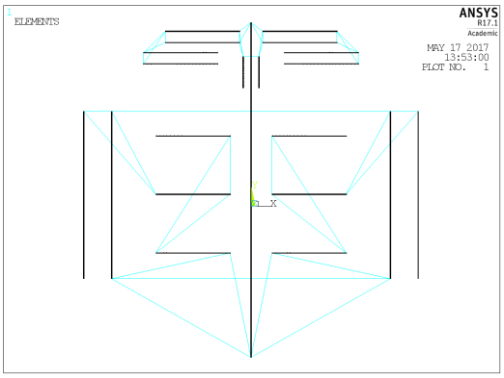

Figure 25 StrTInvL

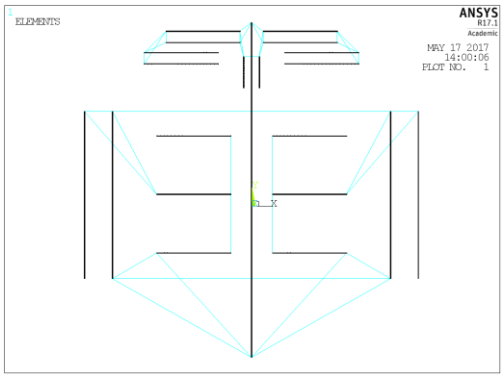

Figure 26 StrTL

5.1.1 Results

The displacement data from ANSYS is plotted in MATLAB for keypoints: 1;2;18;218. Resulting in a vertical displacement plot and a MS rotation plot.

5.1.2 Conclusions

Not all lines are clearly visible in the plot because they are very close to one another. The yellow line is near the light blue in the left, and near the red in the right picture.

The inverted lever compensates the preload displacement in vertical direction. One inverted lever overcompensates, and two compensate each other and the preload very well, resulting in the flattest line in the vertical displacement graph. However, the two inverted levers create the biggest rotation on the shuttle of all configurations. Here, the design without levers, Str, has the best results. The vertical displacement is however much more critical for static balancing than the rotation of the MS. The displacement results for the StrTInvlever is between -0.0511 um and 0.0210 um, which is 23.2 and 9.54% of the preload displacement.

If rigid parts are added mid-flexure to the LDFF flexures for the StrTInvL the reaction forces change. In 50% 4 mm from the 8 mm long beams are rigid. The difference in vertical displacement is minor for 50 % of the flexures being a riding parts, compared to 87.5 % of the flexures being a rigid part. Stresses are not crossing 200 MPa in the case of 50 % rigid parts, they do in the case of 87.5% rigid parts. Rotations of the MS do decrease with the rigid part added to the LDFF, the results are better for 50% rigid parts than for 87.5%.

So, therefore it was to continue optimization of the conceptual structure of a StrTInvL with 50 % rigid DFF.

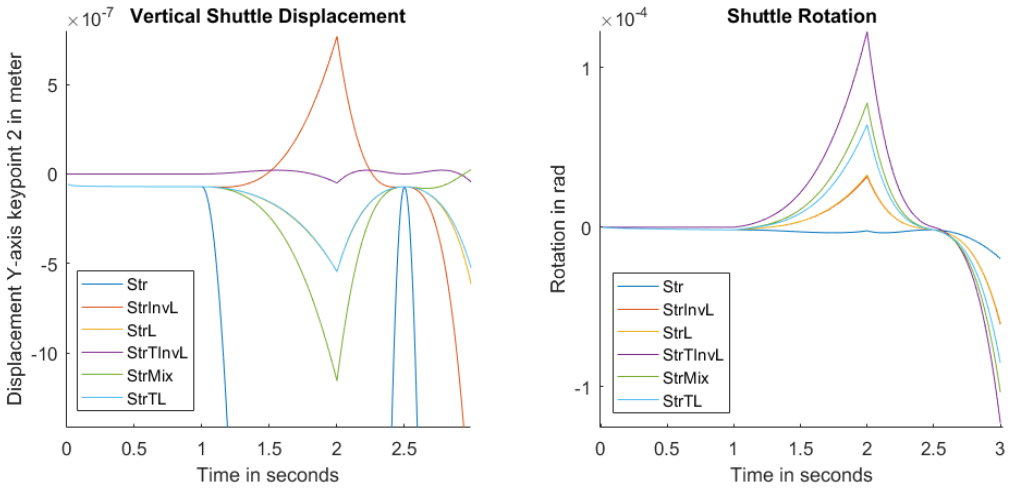

Figure 27 Results for all 6 configurations with no rigid parts added

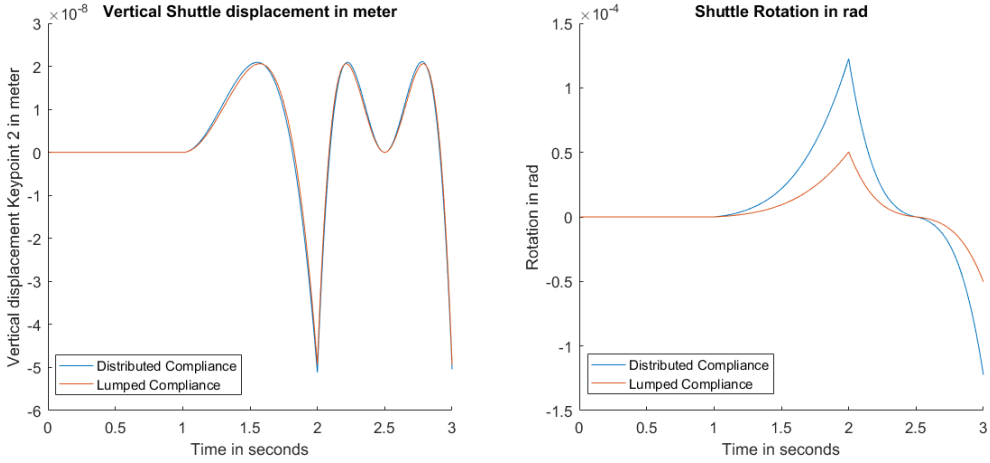

Figure 28 Results for StrTInvL with 50% and 87,5% rigid parts added to LDFF

5.2 Flexure lengths optimization

The optimization of the stiffnesses in the final configuration of the MEMS design was done by hand in ANSYS. First the constraints and wishes are stated. Then the optimization process starts with a hand drawing of the configuration with possible sizes. The optimization sequence optimized certain parts of the design one by one, being: the preload beam, the levers, the LDDF. The smaller double folded flexures and the hooks not in optimization in this sequence because their influence is very small. They are optimized later. An example of the code used during this optimization can be found in appendix 6.1

Constraints:

1 Maximum footprint for entire design is 24 mm diameter
2 Maximum. Von Misses stress in the design is 200 MPa
3 Min gaps in separate design features for fabrication is 50 um. If the hooks are in 45 degrees angle this results more or less in min preload of 250 um.
4 Min allowed beam thickness is 24 um.
5 Preload by shuttle displacement, means there should be enough shuttle displacement possible to preload the preload beams.

Wishes:

1 Design footprint as small as possible
2 Y displacement of the shuttle as small as possible
3 Rotation of shuttle as small as possible
4 A large range of motion must be statically balanced
    a. Larger range of motion is better
    b. Less reaction force is better after preloading (static balancing force is better)

The start configuration is the hand drawing of configuration in the diameter of the footprint. This should have a minimal influence on the final optimization as there are no configuration changes of the design, only beam length changes. From this start configuration the estimates for maximum lengths of the beams, to stay within the footprint, are made.
In the optimization sequence a short hand is used: (constr. 1+,2+,4+, 5-) mean that the choice made has a positive effect on constraints 1 2 4 and a negative effect on 5.

5.2.1 Optimization sequence

1 Starting configuration: hand drawing
2 Estimation of maximum beam lengths for optimization constraints

3 Optimize preload beam:

We start with the preload beam because it is the largest design feature in the design. It is assumed it has the biggest influence on the footprint and the other design features, for example the double folded flexures of the main shuttle. It influences the reaction forces on the hooks, the force needed for preloading and the static balancing of the design.

a. Thickness of the beams is as small as possible
   Reason: C: 1+,2+,4 W: 1+

b. Preload displacement is as small as possible
Reason: C: 1+, 2+, 3, 5 W: 4- (even at the smallest value there is enough MS displacement possible)

c. Length of the beam (L12) is as small as possible
Reason: C: 1+, 2 (sets the length) W: 1+

d. Number of beams is left open
Reason: Is optimized later in step 6 to create a balanced system.

4 Optimization of levers

The levers are chosen second because the levers dimensions are set by the maximum stresses allowed and have considerable influence on the footprint and a bit on the stiffness in the design.

a. Lever beam thickness as small as possible
Reason: C: 1+, 2+, 4 W: 1

b. Lever beam length (L1112) as small as possible
Reason: C: 1+, 2+ W: 1

c. Lever arm length (L1113) as small as possible
Reason: C: 1+ W: 1, 2

5 Optimizing the large double folded flexure

This section is chosen third, as it determines largely the stiffness of the shuttle. Thirst the optimization towards stress is done. Then the preload beam number is set, and after slight changes in de large double folded flexure are made. To get to the static balancing.

a. Beam thickness as small as possible
Reason: C: 1+ 2+ 4+ W: 1+ 2- 3- 4

b. Beam length of flexure part (L1720 – L1819) as short as possible
Reason: C: 1+, 2- W: 1+ 2+ 3+ 4a+ 4b-

6 Filling the open options

a. the number of preload beams is determined, using the stiffness of the LDDF, to slightly make the system bi-stable.

7 Balancing the system

a. By enlarging the rigid part in the LDFF (L1819) the system is balanced.

After changing the variable, the ANSYS code is run and the maximum stress in the system is measured. Accordingly, the variable is changed again until all constraints are met. The maximum stress is measured during a ANSYS run in which the displacement of the MS is determined by the displacement needed to get to the min displacement for the preloading block.

5.2.2 Optimization of hooks and other variables

The hook flexures are optimized after determination of the hook shape. The hook shape chosen is already explained in the design paper. After this shape, it is known what the deflection of the

flexure needs to be and what an estimate for the force after preloading it needs to withstand. It was chosen that each hook needs to be able to carry the full after preload estimated force load.

To make the hooks as small as possible the flexure thickness is chosen to be 24 um. Based on this and the min allowed stiffness, and the preload displacement the flexure length of the hooks (L2526) was calculated.

The estimated force on all hooks after preloading was 0.062N. It was chosen that all hooks on one side of the buckling beam withstand a total load of 0.07 N. This way it was ensured the hooks would always be overengineered regarding stresses. A total amount of 2 hooks are enough to withstand the force after preloading.

The remaining variables are determined by the total footprint available. It was discovered that constraint of a maximum footprint of a diameter of 24 mm was impossible to meet while staying below the maximum stress of 200 MPa. There for the maximum footprint constraint was diminished to the wish to have the footprint as small as possible.

The distance between the flexures of the LDFF (L220 and L224) is determined by the space the levers and other components need and by the displacement between the secondary shuttle of the MS and the MS needed for preloading. The distances are later checked on rotation and vertical movement of the MS and are all acceptable. This also sets the diameter of the footprint needed for the entire model.

The length of the flexure of the preload(L34) block are set based on the preload displacement needed. The longer the flexures can be within the diameter of the smallest footprint we can achieve the better this is for reducing the forces needed for preloading. So, the flexures are made long while fitting in the diameter and check for crossing the maximum stiffness requirement.

The distance between the flexures (L35) are set according to a min of 1 mm separation distance, this is chosen to prevent rotation but still keep the total footprint down. If the separation distance is enlarged the flexure length will become shorter. As the flexure length is more important to the preloading, the separation distance is set to be as small as possible without sacrificing rotation of the preload block.

5.2.3 Result of optimization

All beam thicknesses: 24 um
Preload displacement: 0.25 um
Number of preload beams: 2

	mm
L12	16,5
L34	7
L1112	6
L1819	4,5
L1720	11
L2526	2,6
L1113	6,2
L2024	4
L220	9,5
L35	1

Table 7 Dimensional results

5.2.4 Discussion and other remarks

Optimizing the design is a complex process which was very time consuming. The number of variables is large and determining a logical order for optimization is not easy. The choice between an automatic optimization or an optimization executed by hand was not easy to make either. The time needed to program an automatic optimization was estimated to be extensive and the understanding of the problem would have been harder. With the hand optimization the problem-solving process was better understood and mistakes in the process easier to solve. Both would cost a lot of time, so it was chosen to use an optimization process by hand.

Changing step 6 and 7 the other way around is also possible. Choose the number of beams to be slightly under-preloaded (not bi-stable) and weaken the stiffness in the LDDF. I tried this but these results scores less good on y-displacement and rotation of the MS and the balancing itself.

After calculation with the ANSYS modelling the results for the variables are drawn in an solidworks file. After the final modelling the keypoints positions of the solidworks file are read out and fed back into the ANSYS model to create an equal model as of the drawing. This creates the final file that is check on stresses, static balancing, forces and other aspects.

5.3 Buckling beam curvature calculation

To prevent a non-buckling situation for the buckling beam the beams are given a slight curvature. This is also explained in the design paper.

From the intended fabrication, that will be discussed in chapter 7, the deviation in fabrication for a beam is around 1 till 10% of the beam thickness. To ensure the beam always buckles one way the midpoint of the beam must be off-centre with 10% of the beam thickness + the beam thickness itself. The beam thickness is 24 um, so the off-centre displacement is 26.4 um. With a y-axis length of the beam of 16.5 mm (L12). This results in a curvature for the beams centre of 1.2891 m or less needed to ensure one sided buckling.

The curvature radius used during optimization was 1 m. It was chosen to leave the radius at 1 m as this reduced the number of steps needed to verify the model once more on maximum stresses and static balancing. Not changing the curvature radius to up to 1.2891 mm was expected to have no major contribution to reducing the footprint, as this radius compared to the length of the flexure is large in both cases.

5.4 Approach to scaling MEMS to Prototype

To be able to scale the design a scaling factor needs to be determined. The scaling factor depends on the smallest minimal detail possible the make regarding the hooks. They are the critical element in scaling the design.

The minimal laser width is 0.1 mm. The constraint for the hooks is set as follows: The minimal contact surface after preloading needs to be more than 80% of the hook surface. This is used as a save guard. The hooks are tested on the maximum force after preloading on the hook tips. The stresses need to be below yield stress. The minimal gab between two object for laser cutting is 0.1 mm.

The minimal gab between the hook and the ground is under an angle of 45°, the horizonal (and vertical) minimal gab between the hook and the ground therefore becomes 0,141 mm. The laser cutting process will add another 0.1 mm to that. The final gab horizonal gab between the hook and the ground will be set at 0.25 to ensure deviations.

The preload displacement is 0.25 mm times the scale factor. As the hook has a 45° tip, the total height and length of the hook tip will be the same.

The contact surface (CS) between the hook and the ground is given in equation 2, and the results for different scaling factors are given in Table 8 Contact surface after scaling. This results in a scale factor choice of 6 to ensure enough contact surface between the hook and the ground.

$$CS = 0.25 * scale - 0.25 \quad (2)$$

scale	contact surface (mm)	% of hook surface
1	0	0
2	0,25	50
3	0,5	67
4	0,75	75
5	1	80
6	1,25	83
7	1,5	86

Table 8 Contact surface after scaling

The flexures thickness after scaling would be 1,44 mm. As PMMA material is very brittle it is chosen to use steel flexures instead with a Young modulus of 183 GPa. The thicknesses for flexures available for fabrication are given in Table 9 Available flexures and their property indications. They are model in ANSYS in an orientation of what flexures might be used. The maximum yield stresses are calculated and an assessment of the ability for static balancing is made.

To improve static balancing results a combination of flexures can be made. Stiffer flexures are preferred to use in fabrication because they improve out of plane stiffens. As the prototype is 6 times bigger, gravity forces will have a bigger influence on the out of plane behaviour. How large this effect will be, is not calculated as that will be experienced when handling the prototype. Stiffer flexures will also result in forces that are easier to measure as the change of having this force sensor at TuDelft will be enlarged.

So, a combination of 0.1 mm for the flexures of the LDFF and 0.15 mm flexures for all other flexures is tried. A maximum stress of 148 MPa in the design is found with a slightly bi-stable static balancing. With a maximum value of 0.16 N at the extreme displacement of the MS of 2.7 mm (that is when PB has a preload displacement of 1.5 mm). And a maximum force of -0.02 N (with positive MS displacement) in the bi-stable regime. Full final results will be given in chapter 6.

After calculation with the ANSYS modelling the results for the variables are drawn in an solidworks file. After the final modelling the keypoints positions of the solidworks file are read out and fed back into the ANSYS model to create an equal model as of the drawing. This will change the results slightly and therefore full results are not given here.

0,3 mm	Above 200 MPa	-
0,25 mm	Above 200 MPa	-
0,20 mm	Above 200 MPa	-
0,15 mm	Below 200 MPa	No static balancing
0,10 mm	Below 200 MPa	A little static balancing
0,05 mm	Below 200 MPa	A little static balancing

Table 9 Available flexures and their property indications

6 Final models and modelling

The final mems model can be found in appendix 4.5. The ANSYS modelling consists of three parts, one for stiffness-displacement analysis, one for stress analysis and one for modal analysis before preloading. The final prototype model drawing for laser cutting can be found in appendix 4.6. The ANSYS modelling also consists of three parts. In the ANSYS modelling code the keypoints from the drawings are used and the initial coding using flexure length (for example L1112 =…) is not used anymore. They are still in the code, that can be found in appendix 6, to be able to compare the difference between the models after optimization and the models after drawing.

6.1 Static balancing and preloading force

The results for static balancing can also be found in the design paper. However, we will have a closer look at the stiffness around the origin. Near the origin, shown in Figure 31 Zoom in on MEMS model and Figure 32 Zoom in on Prototype model, we can see a small fluctuation in the force. It is very small compared to the forces in the plots of the whole static balancing range. It is not investigated where this is coming from as its influence is considered to be negligible. However, it might be caused by the fact that the model is not symmetric, causing minor vertical displacements of the MS and extra force influences on the MS by the levers.

Another point of interested is the forces that might be expected to be on the hooks, the results are shown in Figure 33 PB preloading MEMS model and Figure 34. The following situation is modelled in ANSYS: Displacement on PB is applied while horizontal displacement on MS is set to zero. After preloading the displacement on the PB is zero and the MS is moved from +2.7 mm to -2.7 mm times the scale used for the prototype device. This simulates the forces on the hooks after preloading. The contact of the hooks during preloading in not modelled.

6.1.1 Conclusion, discussion and other remarks

The PB forces in the plot for the prototype show a slight asymmetric shape. This might be caused by the small number of data point at the outer sides of the slope.

6.2 Stress analysis

Both the MEMS model and its prototype are checked for maximum stresses in the design. Two situations are modelled in ANSYS to simulate the most extreme stress situations. One where MS is moved from +2.7*scale mm to -2.7*scale m, without preloading (MS displacement). And one where the MS is held at 0 horizontal displacement and the buckling beam is preloaded with 0.25*scale mm preload displacement (PB displacement).

The hooks undergo a separate modelling in COMSOL. The MEMS hook is checked for maximum load after preloading on the tip of one hook of -0.08 N in y-axis, and it is checked for a maximum displacement of the hook tip of -0.25 mm in x-axis to simulate preloading. The hook used in the prototype is only checked for the stress in the PMMA with a hook tip load of -3 N in y-axis, while the top of the hook is constrained.

The maximum stresses found in each situation are given in Table 10 Modeling maximum stress results. The stress plots of the design from ANSYS are found in appendix 7. The maximum allowable stress we use for the MEMS model made from silicon is 200 MPa, for the prototype made with steel flexures is also set at 200 MPa and the maximum stress for PMMA is 72 MPa. The MEMS hook with -0.08N load on the tip shows a displacement of the tip hook (in all directions) of 47 um.

Situation	Maximum stress (MPa)
MEMS model, MS displacement	170
MEMS model, PB displacement	189
Prototype model, MS displacement	182
Prototype model, PB displacement	201
MEMS hook, -0.25 mm x-axis displacement	150
MEMS hook, -0.08 N y-axis tip load	40
Prototype hook, -3 N y-axis tip load	0.085

Table 10 Modeling maximum stress results

6.2.1 Conclusion, discussion and other remarks

All stresses are below the allowable yield stress except for the prototype mode, PB displacement with is crossing it with 1 MPa. This is so small that the stress is considered acceptable. Reducing this stress would mean re-optimizing of the model and having a lower stiffness for the flexures, decreasing out of plane stiffness.
Overall the stresses are slightly underestimated as the hook contacts are not modelled. They are considered to be of very small influence and thus the current results for the models are considered acceptable.

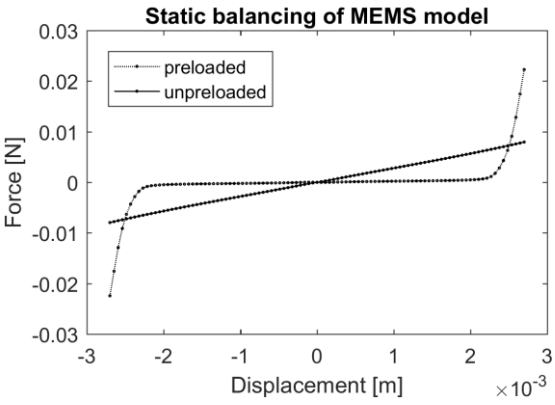

Figure 29 Theoretical Static balancing of MEMS model

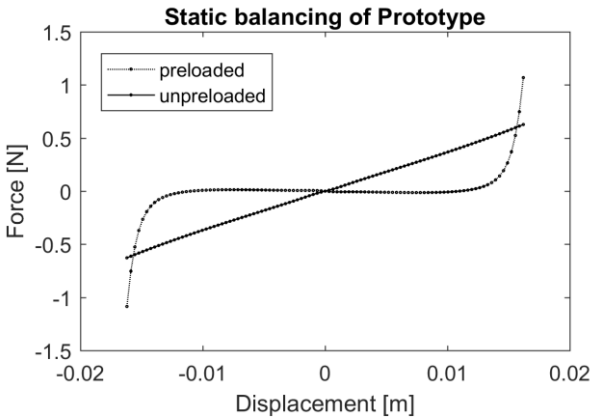

Figure 30 Theoretical Static balancing of prototype model

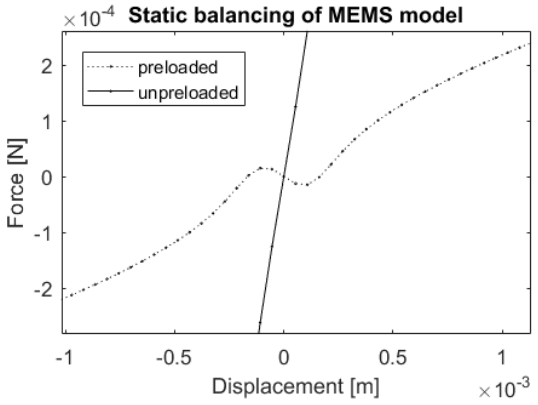

Figure 31 Zoom in on MEMS model

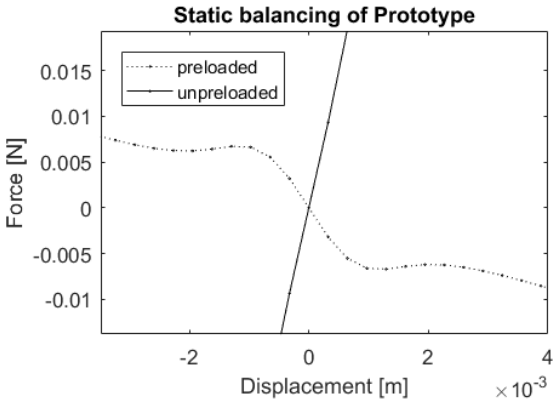

Figure 32 Zoom in on Prototype model

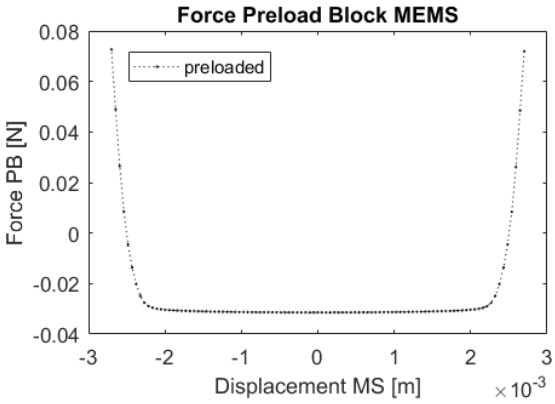

Figure 33 PB preloading MEMS model

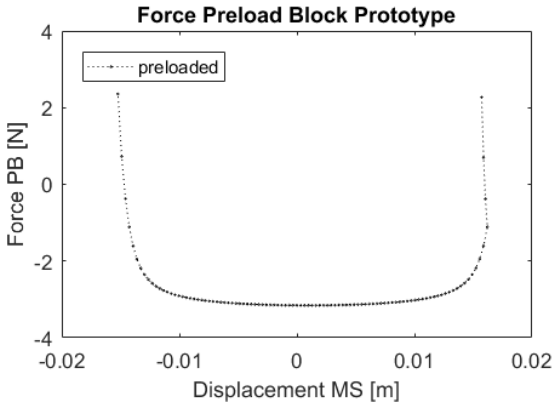

Figure 34 PB preloading prototype model

6.3 Modal analysis

A modal analysis is performed in ANSYS for both the prototype and the MEMS model. The solidworks drawings where used to collect data on inertia of every 'solid' (being not a flexure) part. The parts are model in Ansys by adding point masses to the existing modelling. The location of these point masses where also gathered by evaluation in solidworks.

The flexure masses are modelled by adding a density to their elements. The modelling for the 'solid' parts has some specific errors. The moments of inertia in solidworks used are 'taken at the output coordinate system', as described by solidworks. Meaning that there are 9 inertia moments given: Ixx, Ixy, Iyz, Iyx… ect. Ansys would only take 3, the principle moments of inertia given at the local coordinate system given for a mass, mass21. The coordinate systems for every mass are parallel to the global coordinate system but placed in the centre of mass. The coordinate system used in solidworks is a global one in the middle of the design. It is in the same direction as the global coordinates in ANSYS. Luckily for most parts their local coordinate system is equal to the global coordinate system in both solidworks and ANSYS and can correctly be model. The parts that are models slightly wrong are: the levers, the secondary shuttle of the PB, the hooks, and the midpieces of the LDFF. They have non-zero values for Ixy and Iyx. That are ignored in ANSYS.

This has an influence on the higher frequencies: the parts that are slightly wrongly modelled have low masses compared to the other parts in the models. Rotation in around the z-axis are modelled correctly as only of diagonal terms Ixy and Iyx are non-zero for these parts.
These errors are considered allowable as the first mode is of interested for the preloading by shaking and that is modelled correctly. Mode with rotations around Z-axis are of most interest and they are modelled correctly. The other errors are considered to be minor compared to the large masses.

The first 10 eigenfrequencies can be found in the design paper. The 10 modes belonging to that can be found in the appendix **Fout! Verwijzingsbron niet gevonden.**. The plots of the MEMS model show grey lines, they are coming from the symbol for the mass21, the point masses. As the MEMS model is very small the symbols are relatively very large.

7 Fabrication details

7.1 Intended fabrication for MEMS model

After optimization and modelling the final MEMS design the model is ready for the fabrication phase. It is intended to be fabricated at DIMES a company which will used deep reactive ion etching for a 525 um thick wafer. The MEMS model will be combined with other models designed for this process for other research projects such that one mask can be made for multiple designs. More than one MEMS and other models can then be created by re-using the mask. The company has an instruction document on how to prepare the model drawing for the mask.

Regrettable we were never able to execute this intended fabrication. At the time the MEMS model was ready the machine that DIMES uses for this fabrication was under maintenance and after that I had to wait for other to finish their design to fit them all onto one mask. That moment never arrived.

My hope is that the model will still be fabricated and the results added to the design paper to make finally finish the design process.

As a last attempt to create a small model we try to use a laser cutter at our department. From earlier tests we knew the laser creates tapered beam with a centre width of around 50 um. Boran Jia has working experience with this machine and will try to fabricate a model for show. The last update on this process is that if we make a 2:1 model such that the beam thicknesses can become around 50 um, to diameter of the model is too large for the machine. So, the idea was to increase the beams of the 1:1 model such that we have a model for show, but that is not fully functional, and perhaps a model 1:1 with the 24 um beam thicknesses to experiment what the end result would be like. This turned out to be a lot of work for a model that we would only use as a show model. The decision was made not to make the models on the laser cutter at the department as we were not able to make a functional model.

7.2 Fabrication methods for prototype

After determining the scale and the design of the prototype it is laser cut with a Baby laser BL25-1411-1 from Lion Lasers. Steel flexures are cut to size and glued, with super glue, into the PMMA model. The model has slots where the flexures fall into. The final laser cut drawing has added bridges added between parts to keep distance relations after fabrication and before flexure gluing. The bridges are later removed by using breaking and a melting device.

This type of fabrication is sensitive to fabrication errors made by a deviation of the laser beam width, which is critical for the hooks, and cutting errors for the flexures. To minimize the cutting errors on the flexures, flexures of equal dimensions are cut in the same batch such that the error is equal in all flexures with these equal dimensions. So first the flexures are cut to strips with a height of 8 mm and then cut to length. Two models are fabricated to compare the results and with it their deviation regarding fabrication.

8 Additional Force displacement results

Results given here are extra of what is in the paper

8.1 Force displacement of MS

The results for static balancing can also be found in the design paper. Minor differences can be seen in the static balancing of the two models. This might be due to fabrication differences.

We will have a closer look at the stiffness around the origin. Other than in the modelling we cannot find a fluctuation of the force near the origin. We can only speculate why that may be. The forces are not too small for the force sensor to pick up. Differences between the model after fabrication and the modelled model might be the cause. It might even be the that the modelling around the origin is off, due to fact that we are making almost zero-stiffness calculations.

8.2 Force displacement of the PB

The force displacement relationship for the PB is also measured. For the preload block measurement, the same setup is used as is described in the design paper for the MS displacement measurement, but the force sensor is recalibrated to +-3.7 N with a new resolution of 0.0037 N. The measurement would start when the force on the PB was around -0,02 N such that the results could be calibrated afterwards. A laser on the stage can coarsely measure the absolute position of the force sensor, where the stage itself gives us a relative displacement. Combining this data, I plotted some of only the results where the MS is supported by a cord. One of measurement runs of prototype model 1 turned out to be wrongly measured and is therefore ignored. Three repetitions of preloading the PB are executed.

It is hoped that we can see the latching action of the hooks then they surpass the ground structure. In that way we can determine the preload displacement. First the hooks will be free, then the hooks will touch the ground structure, thirdly they will displace to surface the ground structure and then will return to a non-displaced position and be latched.

From looking at the model while executing the measurement we can see that the hooks do not preload at the same time. When the slope of the force suddenly increases at the end the hooks hit the stop blocks. There are no appended force differences that indicate hook preloading. Apparently, the force change of the hooks latching is so small that we cannot distinguish it from force generated by the DFF of the PB.

The forces are comparable with the forces on the hooks modelled for the PB in the chapter 6. Both plots show a force of 2,5 N before the hooks hit the stop block. Due to the reduced steps in the modelling plot the maximum force can only be estimated to be between 2 and 3 N.

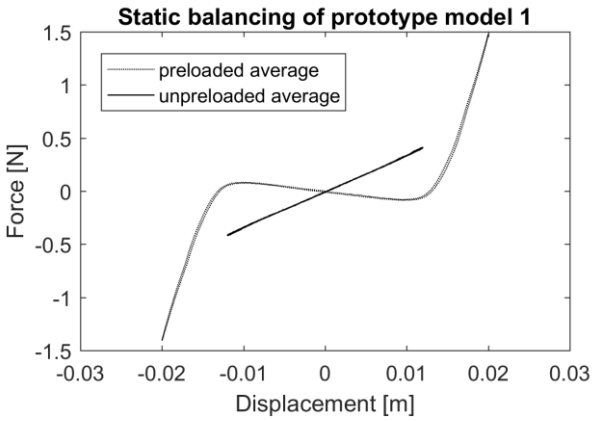

Figure 35 Experimental static balancing of prototype model 1

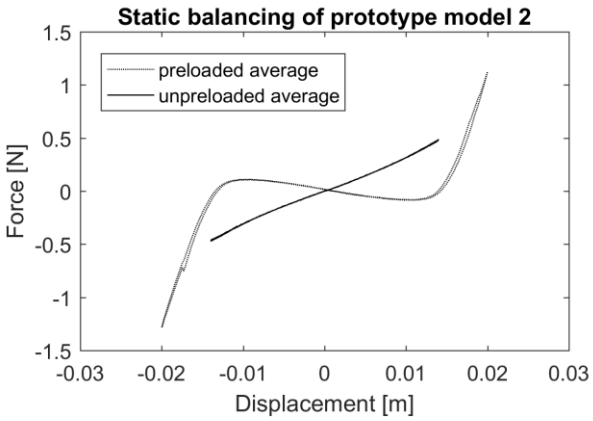

Figure 36 Experimental static balancing of prototype model 2

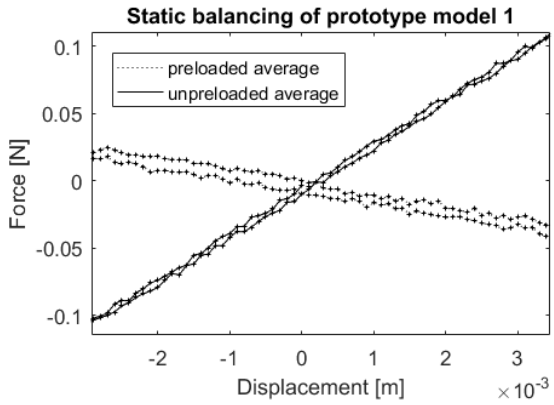

Figure 37 Zoom in on model 1

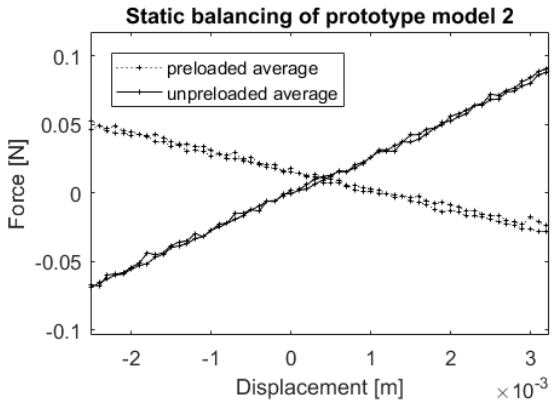

Figure 38 zoom in on model 2

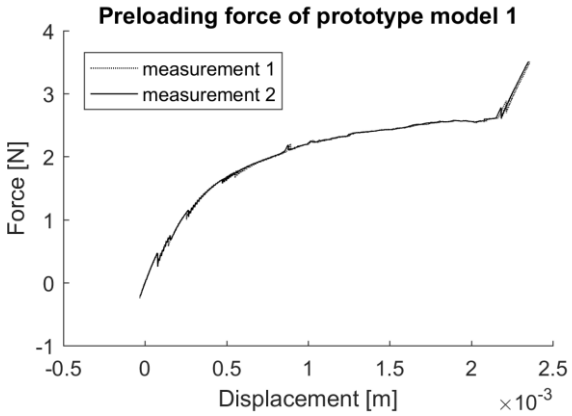

Figure 39 hook latching model 1

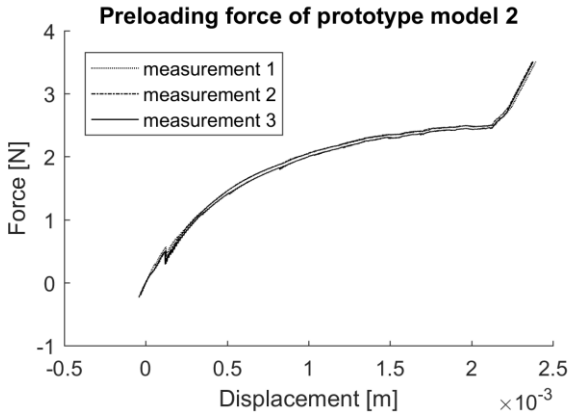

Figure 40 Hook latching model 2

9 Reflection / Personal development

9.1 Literature review approaches

I worked very precisely to formulate the correct classes for the 250 papers and their designs. I had some trouble with applying the classification rules to all designs as can become clear from the discussion in the design paper. (The intended motion of the amplifiers compared with their small displacements or larger displacement could cause designs to fall into different classes.) This took a large amount of time due to the large number of designs. A lot of re-checking steps where involved. Even so, this is still my preferred approach compared to designing a classification for a smaller number of designs. The large number of design distinguished this paper from some other attempts to classify CMMA. I would recommend in-dept. feedback on the designs classified at this moment and if others do indeed make the same conclusions as I did, as intended.

9.2 Design approaches

The design steps taken where efficient and effective. I did go of the beaten path with a ternary plot version to improve on the brainstorming and concept generation. This did speed-up the design process without losing important quality. During my stay in Germany we discovered that we were not able to let COMSOL deal with the level of detail in my design. (I did go to another COMSOL course back in NL but even that did not solve my problems.) This caused me to divert to ANSYS, which with I had only very limited experience. I needed Davoods help on setting that up properly, which I chose to do when I was back from Germany, for better communication facilities. Until that time I used hand calculations and this was fine for work at the Physical Intelligence department, which really lent itself for the approach of rapid prototyping. Rapid prototyping was a new process for me which I would not have been able to execute at the TuDelft. I chose a more pragmatic route to develop not one but two working (on larger scale) concepts for preloading using two different fabrication techniques. From this I learned to work on various machines, two different laser cutters and one 3D UV-light printer. Back in the Netherlands I learned to use ANSYS to optimize one of the two designs for the final MEMS design, added another new skill to my engineering life. I think I chose the right approaches though a ANSYS course of some kind would have been effective too, in Germany those options were limited.

9.3 Communication

Maintaining proper communication with mentors, supervisors and directors, is crucial in working efficient and effectively. I my regard, I learned how to deal with people with busy agendas and bringing priority subjects under people's attention when it had to. As I also demonstrated by my ability to go abroad. My mentor Davood and supervisor Just Herder where regularly updated on my actions and I could get useful advice and guidance when needed. Even in the face of disagreements, communications where still good.

9.4 Going abroad

I wanted to go abroad to gain more experience outside my comfort zone and the culture of the TuDelft. In many aspects I did reach those goals.

My first learning goal was in organizing a stay abroad. Before I began my graduation project I had already spoken out for the wish to go abroad. At that time new connections with TAG HEUER were made. Considering this perspective my graduation subject was chosen to be on the static balancing of amplifiers. Regrettably TAG HEUER had no experience with graduation students and they rejected my proposal to study abroad in Switzerland at their company. After this I learnt there was an opportunity to go to Imperial College, London, but they charged money for supervision, so this was not an option for me. At this time my graduation project was already underway. Using a contact of Just Herder, I met the department of Metin Sitti.
It was arranged did I could work at the Max Planck Institute in Stuttgart, Germany, in the department of physical intelligence of which Metin Sitti is the science director (more info on the department: www.is.mpg.de/sitt). We organized a position of guest researcher, and I stayed at the local guest house. I was also able to arrange several funds, my stay at the guest house was sponsored and I was able to get financial support from the Erasmusbeurs.

As guest researcher I was able to do my own work which involved rapid prototyping. In a short amount of time I had to communicate with a lot of people to find out what kind of equipment I could use, how the machines worked, and who had what kind of experience to help me out. This gave me a new perspective on intercultural competence and communication skills. I learnt about different work ethics and organisation styles regarding people and property.

The department of Metin Sitti has a lot of International researchers. In this way I was challenged by people with different assumptions and cultural values. I was able to learn from this host environment. I already had some international experience but not in a formal working environment. I also made some good friends in Stuttgart which with whom I still have contact.

On a more personal note, I wanted to go abroad to overcome my fear of moving home and becoming homesick. And I did. I am confident I can find a job in a new unknown place without much trouble. I can even see myself working abroad. For me this was the most important lesson of life which going abroad could give me.

9.5 Project/Time management: Delay caused by illness, dyslexia and machine breakdown

I started my graduation project in September 2016. Going abroad did take away some time to work on the project as housing and moving take time too. After coming back from Stuttgart, I became ill, causing me to work only half of the days from may till august. I have had an excellent work ethic and discipline from high school on, and I experienced no problem managing my tasks and planning.

One of the major setbacks was the fabrication of the MEMS design. It was to be fabricated by DIMES but the machine used for this fabrication broke down and had to be readjusted before it could be used again. As for this moment I am still waiting, for others to finish their design so I we can produce the MEMS model using one wafer mask. For this there were no good alternatives. I have asked Boran Jia to create a 2:1 scale prototype on the new laser cutter owned by the PME department. We were not successful. For this reason, I had to divert to using 6:1 scale prototypes that were created on the laser cutters in the main workshop.

Once we finished the MEMS model, these results will be added to the design paper which we aim to get published.

Writing the thesis report and papers have been a major undertaking as I am dyslectic. (Normally the workload a dyslectic student can carry for their studies is set at 80%, this means a 2,5 months delay based on the dyslexia alone.) I needed more guidance than I could get regarding this problem of writing. Especially in developing a writing method that worked for me. The steps in writing that were explained to me where not enough. I asked for help by supervisor, friends and the universities platform for studying with a disability, where I was a member of. The last one informed me there had been a workshop on writing a thesis with dyslexia but it was not given anymore. So, I had to find out by myself.

I felt very misunderstood when people commented that writing is hard for everyone. It is like saying that I had to toughen up and it feels very disrespectful, even when it was intended to ease the problem. It blocked the type of guidance I needed and I felt more frustrated than ever. My advice to everyone: never ever judge someone else's problem (aloud) by your own experiences. It is their problem and as important to them as they find it to be. I was able to address this problem and share it with my supervisors, even though they were not always able to help, they did have that intention.

In the end I develop more steps in the writing process which I am gladly sharing as it can help others.

- Acknowledge the problem, try to find a good way to communicate and explain what you are experiencing to others. Take time to experiment and discover what might cause the problem.
- Motivation. I am a very dedicated and disciplined person. I know very well where my limits are and what frustrates me. I kept being motivated by one main though I developed. "Writing is like the growing of a flower, from the mud it rises. The more I feed it, the more beautiful it becomes. Nothing of what I give it, will go to waste." Even so, I had to share my pure frustrations with friends to give it some relief and every time I finished something little I would appreciate it intensely, even if it was just 20 minutes of writing 3 sentences I would congratulate myself for my dedication.
- Process the information you want to write. I am a highly visual oriented person. I can see the block of information like colour. Making the thesis can feel like filling in a colouring book. Sharing and processing the information in many ways helps to give the information a 'location', a 'weight' and a 'shape', setting out the lines of what to draw. For me information is best understood in their 'virtual essence' in thought, where they have a location: how it is connected to other bits of information and how they are located in time (if at all). A weight: is it complex information, how much energy is needed to understand it and to remember it, is it important? And a shape: is it a large amount, has it sub-amounts, is it like a spiderweb or a round ball of independent information?
- Develop a structure in chapters. Make the information linear. Meaning that the colouring book does not have a start or finish. Written language does not allow for that. So, the 'virtual essence' must be flattened.
- Write keys. Choose them wisely! Divide information and conquer! This is where I got the most confused. I can write key words and sentences, but the next step of processing that into a logical story without losing eye on the timeline and importance of information, and especially what information would link to what other kind of information, seemed impossible. As I call it, it caused a state of dis-orientation with writing, causing lots of frustration. Every colour of information that was clear so far suddenly becomes vague, the 'essence' is ripped apart. It is like a computer processor that cannot comprehend the large amount of information and try to write at the same time. The writing process itself cost so much energy that there is none left to transform the keyword into a logical story. To make the transition from keys to text better something has to give, either the writing or storing/organizing the information. I realized, visual keys are very important. (This is also the reason that working in LATEX is not an option for me.

It creates even more confusion.) They should contain independent information and be very, very short to be functional and not a burden. Every key sentence I have to read before writing will flood the computer processor. Keys can be:

  - One word
  - One fact
  - A picture
  - A timeline
  - A mind map
  - A video
  - An audio recording.

- Writing a hand-written draft of independent information. I found out that translating the keys to a story works best when I write a draft by hand. No spelling, no grammar, nothing except for focussing on the message to tell. This hand writing became a crucial step that I had not foreseen. They had to be blocks of information that are independent to read in order to organize the information later.
- Digitalizing writing. Now it is time for grammar and spelling and re-writing to improve the story.
- Ordering information. I leave the keys in the text as long as possible. They link the information. Now it is time to make the information dependent, adding that one line that links one piece of information to the other.
- Feedback from others on the general story. This is an important step for me to get feedback about if the structure is as logical to another as it is to me. I did not get others to see the importance of this for me for a long time. It gives me confidence I am on the right way and makes the writing process a heck of a lot more efficient for me as I do the reordering of the information now instead of after the re-writing. This does not mean other have to read the story. If I would just go through the story with them telling what is in the text, that is good enough too.
- Let it rest. Forget about what you wrote, so you can re-read it better later.
- Re-writing and reading again. Now from a stranger's perspective. The good thing is that I can rewrite text just fine. The dis-orientation is then gone, and I can just focus on making the text like a flower.
- Ask other to re-read. Luckily, I have some amazing friends that would do the painstaking job of spelling and grammar checking. I am poor at this myself and depend on their input to recognize my mistakes.
- Take lots of time. The draft writing process is so intense I can only do it effectively for 2 hours a day. I started both my literature paper and design paper in Germany. I still sometimes misjudge the time I need for it because how much I can do on a day is not well predictable.

I have done everything I could to make this work a shining flower and reflecting on this all I manage my time efficient and effectively even in adversity. I hope you agree!

V APPENDIX

1 CMMA TIMELINE

These pictures are all taken from papers. Each picture has a label number, with that label number the paper reference can be found where the picture is taken from.

108	[3]	120	[4]	131	[5]	141	[6]	151	[7]
109	[8]	121	[9]	132	[10]	142	[11]	152	[12]
112	[13]	122	[14]	133	[15]	143	[16]	153	[17]
113	[18]	123	[19]	134	[20]	144	[21]	154	[22]
114	[23]	124	[24]	135	[25]	145	[26]	155	[27]
115	[28]	126	[19]	136	[29]	146	[30]	158	[31]
116	[32]	127	[33]	137	[34]	147	[35]		
117	[36]	128	[37]	138	[38]	148	[39]		
118	[40]	129	[41]	139	[42]	149	[43]		
119	[36]	130	[44]	140	[45]	150	[46]		

Table 11 Label number to reference for timeline

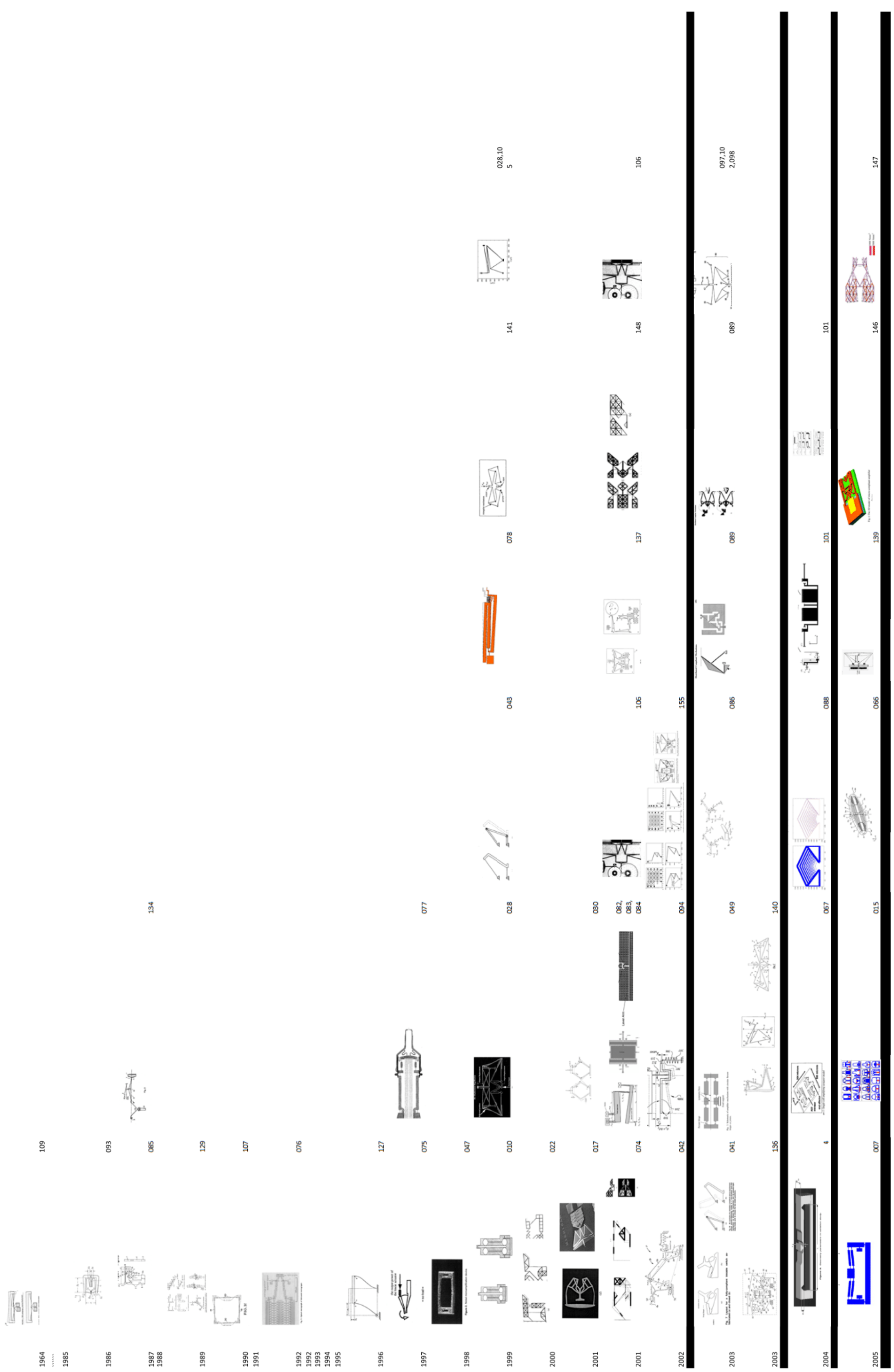

1964 109
1985
1986 093
1987 1988 085 134
1989 129
1990 1991 107
1992 1992 1993 1994 1995 076
1996 127
1997 075 077
1998 047
1999 010 028 043 078 141 028,10 5
2000 022
2001 017 030
2001 074 082, 083, 084 106 137 148 106
2002 042 094 155
2003 041 049 086 089 089 097,10 2,098
2003 136 140
2004 4 067 088 101 101
2005 007 015 066 139 146 147

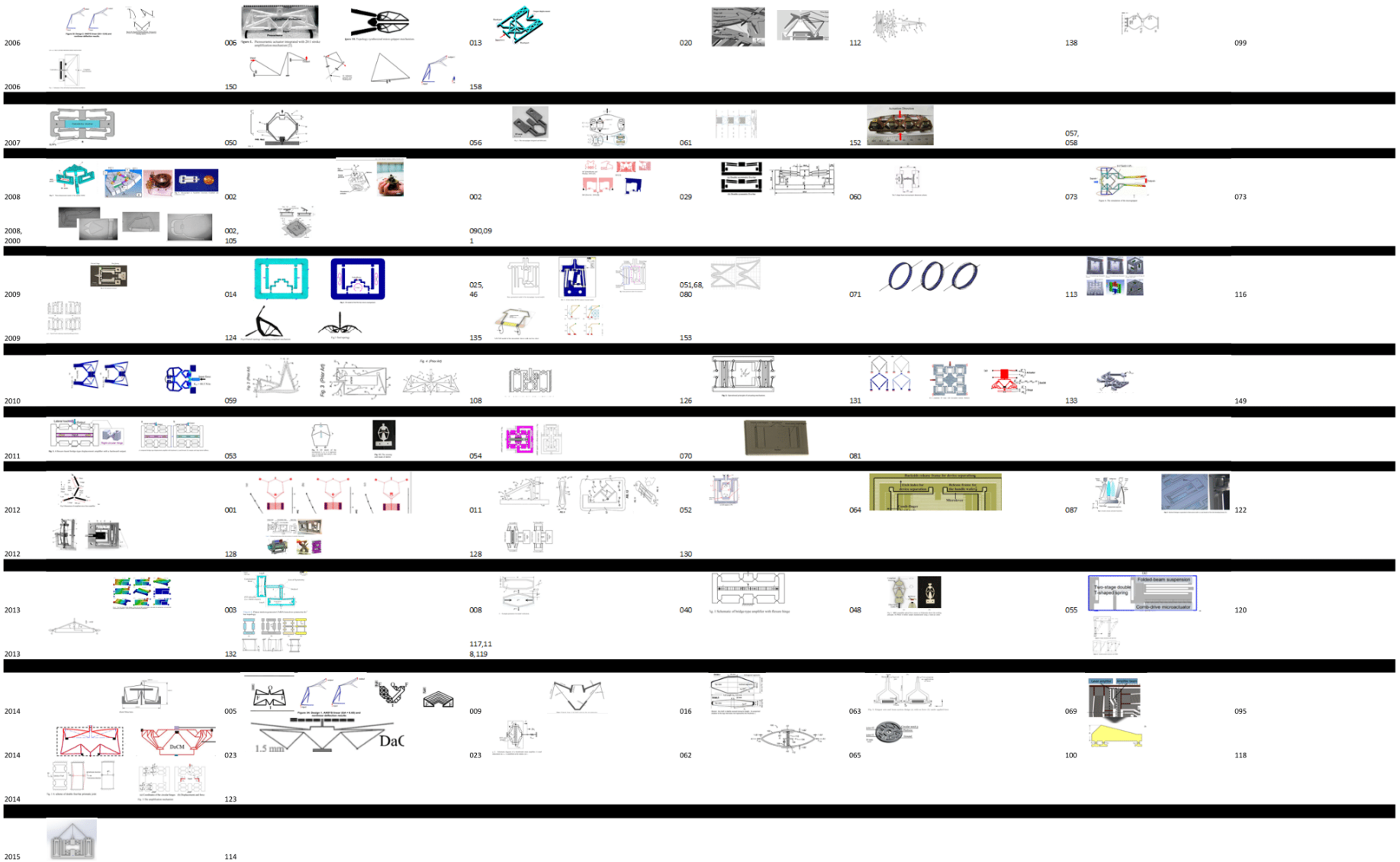

Figure 41 Timeline

2 Sub-concept weight tables

Locking	Total Score	Criteria number							
Design name		1	2	3	4	5	6	7	Other considerations
Comb-drive		1	Planar	2	Short	Yes	Yes	Unk	
	11	++	++	++	++	++	++	-	
Magnets		3	3D	7	Long	A little	No	Unk	
	-10	+-	--	--	--	-	--	-	
Adhesion		2	Planar	5	Medium	Yes	Yes	Unk	
	5	+	++	-	+-	++	++	-	
Solidify		2	Planar	2	Short	Yes	Yes	Unk	
	10	+	++	++	++	++	++	-	
Hydrophilic		2	Planar	2	Short	Yes	Yes	Unk	
	10	+	++	++	++	++	++	-	
Friction		1	Planar	2	Short	Some	Unk	Unk	More actuation force needed
	5	++	++	++	++	+-	-	-	-
Flexure Beam		1	Planar	2	Short	Yes	Yes	Good	More actuation force needed
	13	++	++	++	++	++	++	++	-
Hooks		1	Planar	2	Short	Yes	Yes	Good	More actuation force needed
	13	++	++	++	++	++	++	++	-
slot		1	Planar	4	Medium	Yes	Yes	Good	Solid construction
	12	++	++	+-	+-	++	++	++	++
Bi-stable Beam		2	Planar	2	Short	Yes	Yes	Unk	Might also be guiding
	12	++	++	++	++	++	++	-	+

Table 12 Weight table for locking

Actuation	total score	Criteria number								
Design name		1	2	3	4	5	6	7	8	Other considerations
Angled beam expansion		1	Planar	2	Short	Yes	Yes	Unk	1 mm #2	Beam has a translational motion.
	11	++	++	++	++	+	+	-	+	+
Angled beam series		1	Planar	2	Medium	Some	Not well	Unk	larger than 1 mm #2	Beam has a translational motion. Construction has larger footprint.
	7	++	++	++	+-	+-	+-	-	++	+-
Dual material beam		2	3D	4	Medium	Yes	Unk	Unk	Unk	Beam has a rotation motion.
	-4	+	--	+-	+-	+	-	-	-	-
Cold-warm beam		1	Planar	2	Short	Yes	Yes	Unk	Unk	Beam has a rotation motion.
	7	++	++	++	++	+	+	-	-	-
Small mass motion		1	Planar	2	Short	No	No	#1	#1	Needs external actuator, higher frequency than the big mass.
	2	++	++	++	++	--	--	+-	+-	--
Big mass motion		1	Planar	2	Short	No	No	#1	#1	Preload beam is pulled. Needs external actuator.
	4	++	++	++	++	--	--	+-	+-	-+
External magnets		3	3D	7	Long	Little	No	Unk	Unk	
	-11	+-	--	--	--	-	--	-	-	
Internal magnets		3	3D	7	Long	Little	No	Unk	Unk	
	-11	+-	--	--	--	-	--	-	-	
Comb drive		1	Planar	2	Short	Yes	Yes	Unk	Small	The range of motion is too small
	x	++	++	++	++	++	++	-	--	Disqualified
Piezo		2	Planar	3	Short #3	Yes	Unk	Unk	Unk	Requires assembly
	x	+	++	+	+-	++	-	-	-	Disqualified
Local chamber		2	3D	5	Long	No	No	Unk	Unk	External material water add. Might clock the device.
	-11	+	--	-	--	--	--	-	-	-
Global chamber		2	3D	5	Long	No	No	Unk	Unk	
	-10	+	--	-	--	--	--	-	-	
Water attraction material		3	Planar	3	Short	No	No	Unk	Unk	External material water add. Might clock the device.
	-2	+-	++	+	++	--	--	-	-	-
Water evaporation		2	Planar	3	Short	No	No	Unk	Unk	External material water add. Might clock the device.
	-1	+	++	+	++	--	--	-	-	-

#1 Depends on mass motion actuator

#2 For aluminum

#3 Need assembly

Table 13 Weight table for actuation

Guiding	Total Score		Criteria number								
Design name			1	2	3	4	5	6	7	8	Other Concisterations
Push pull magnets			3	3d	7	Long	Yes	No	Unk	Good	Unstable withoug feedback loop
	9		+-	--	--	--	++	--	-	++	--
Hydrophobic			2	Planar	3	Medium	Little	No	Unk	Unk	Small footprint
	2		+	++	+	+-	+-	--	-	-	++
Double Folded Flexure			2	Planar	2	Short	Yes	Yes	Good	Good	Pure translation
	17		++	++	++	++	++	++	++	++	+
Bi-stable Beam			2	Planar	2	Short	Yes	Yes	Good	Good	Migth also be locking
	17		++	++	++	++	++	++	++	++	+
Folded Flexure			2	Planar	2	Short	Yes	Yes	Good	Good	Not pure translation
	15		++	++	++	++	++	++	++	++	-
Rolling Contact			1	Planar	2	Short	Yes	Unk	Good	Good	
	8		++	++	++	++	--	--	++	++	
Slid			1	Planar	2	Short	Yes	Unk	Good	Good	Friction
	12		++	++	++	++	++	-	++	++	-
Boxed			1	3D	5	Medium	No	No	Good	Good	Out of plane motion is prevented, fritction present
	-1		++	--	-	+-	--	--	++	++	+-
Contact Point			1	Planar	2	Short	Yes	Unk	Good	Good	
	13		++	++	++	++	++	-	++	++	

Table 14 Weight table for guiding

3 Force displacement sketches

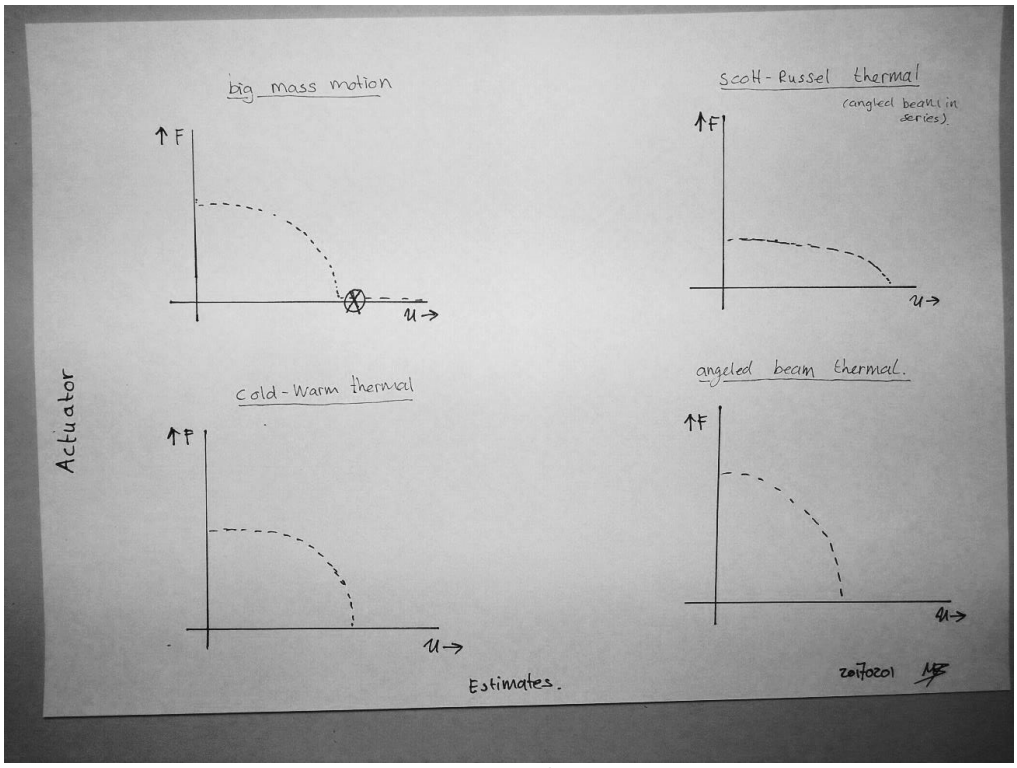

Table 15 Sketches for actuator

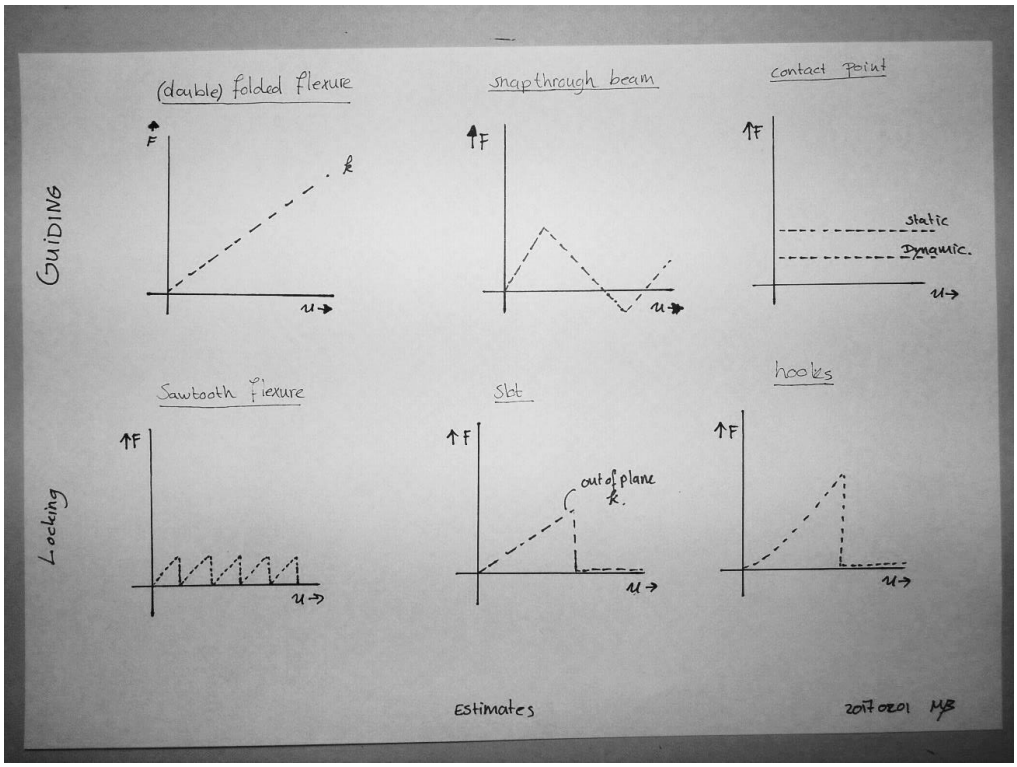

Table 16 Sketches for guiding and locking

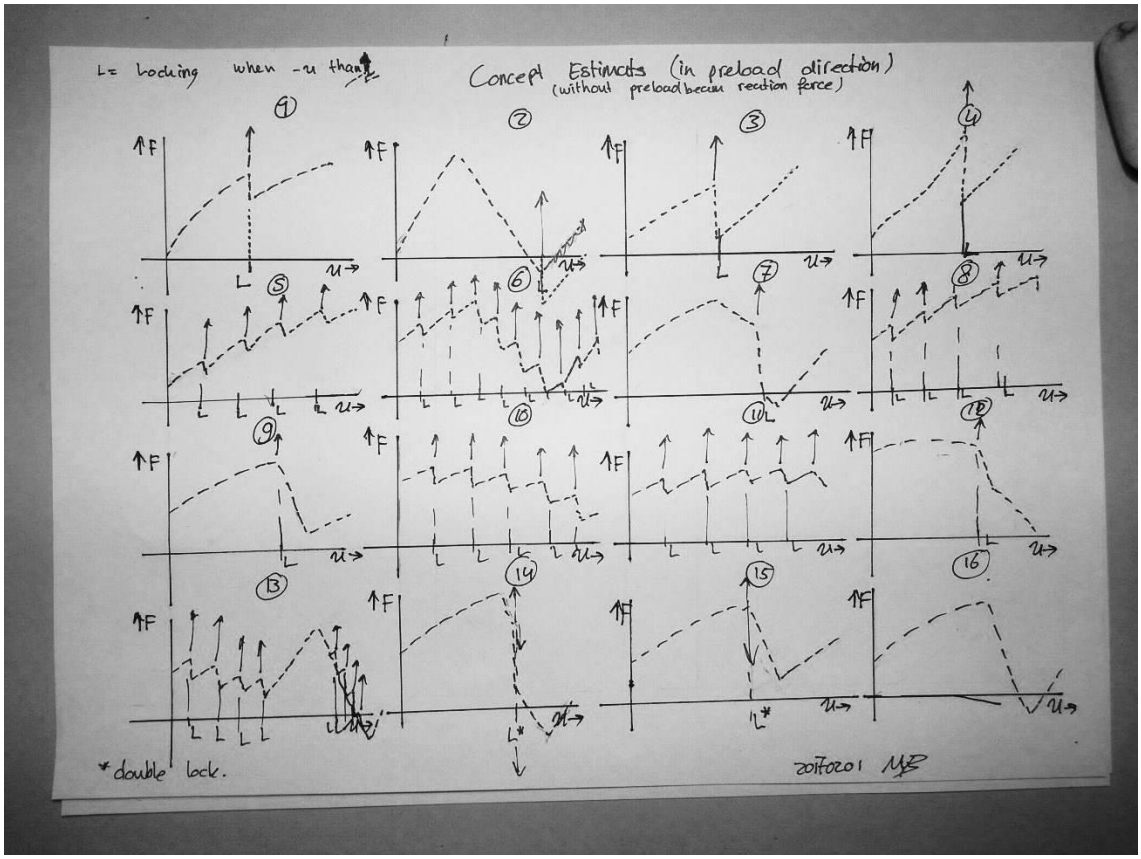

Table 17 Sketches for total solutions

4 Models

4.1 Lever models

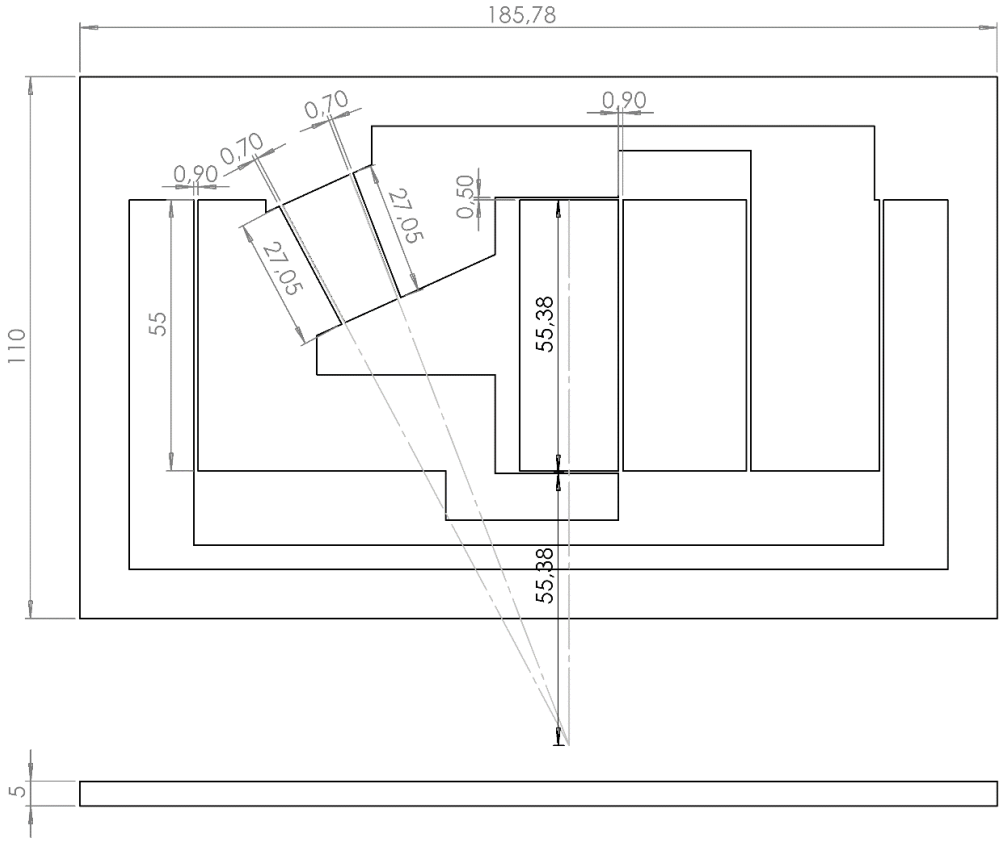

Figure 42 20170312 Lever model V3

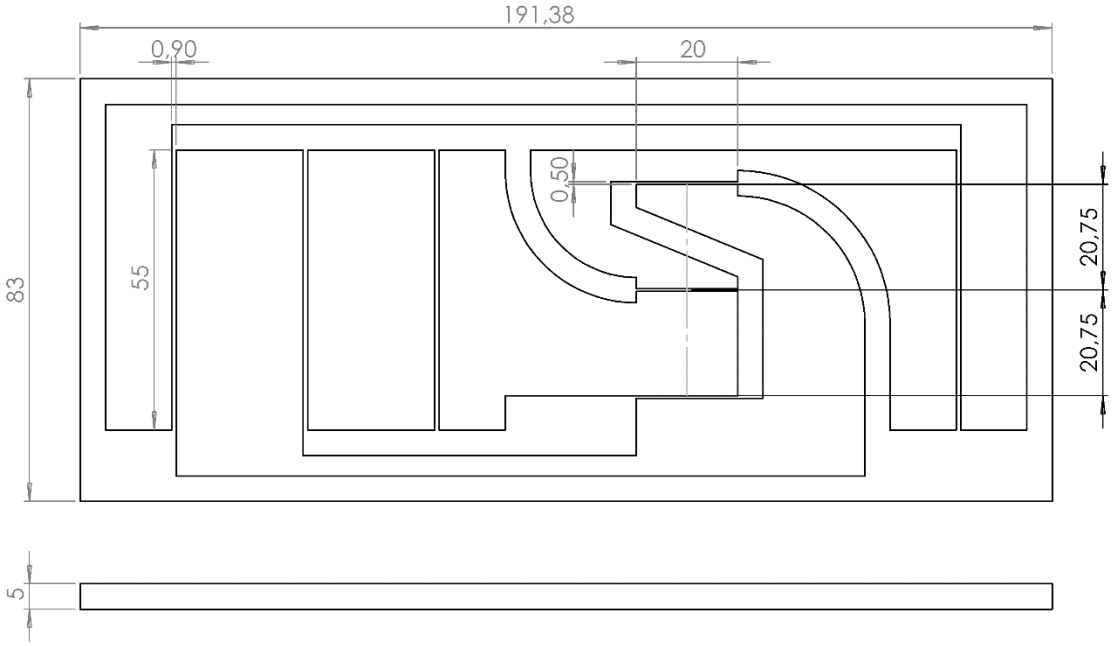

Figure 43 201703013 lever model V2.3

4.2 Flexure > hooks

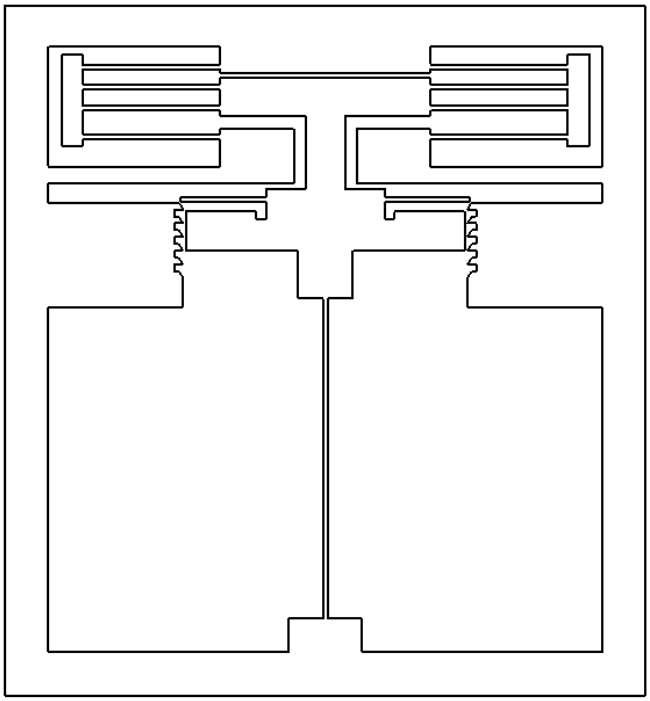

Figure 44 Total concept with flexure locking

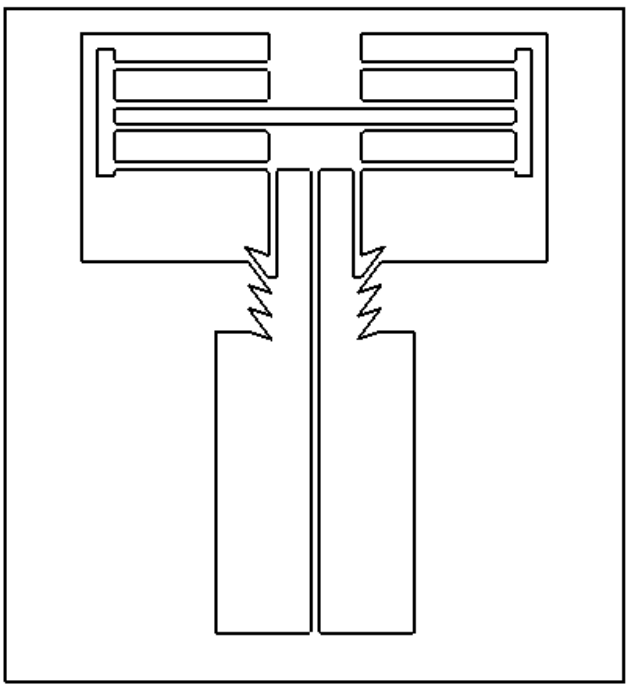

Figure 45 Total concept with hooks locking

4.3 Symmetric model

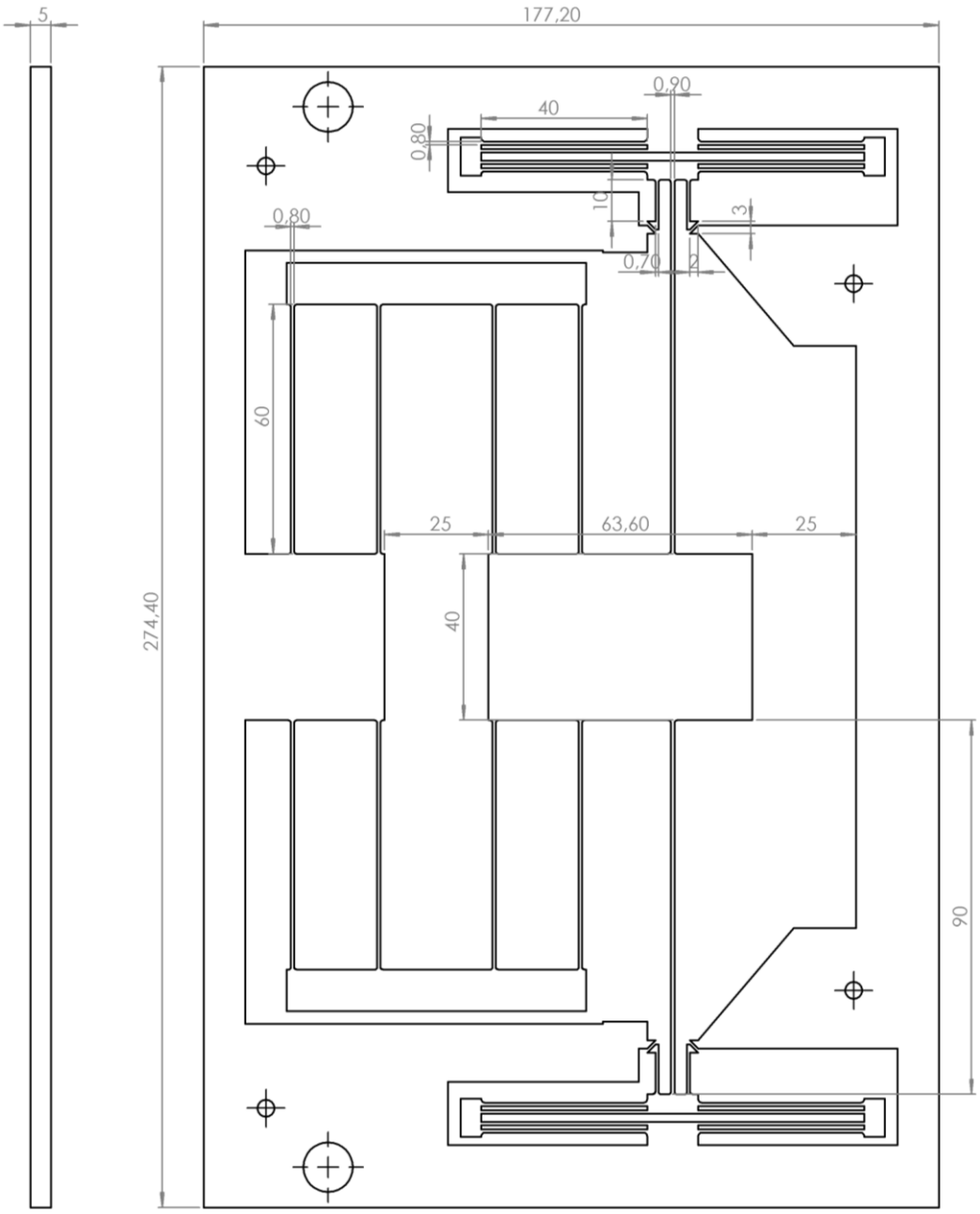

Figure 46 Symmetric model

4.4 Asymmetric model

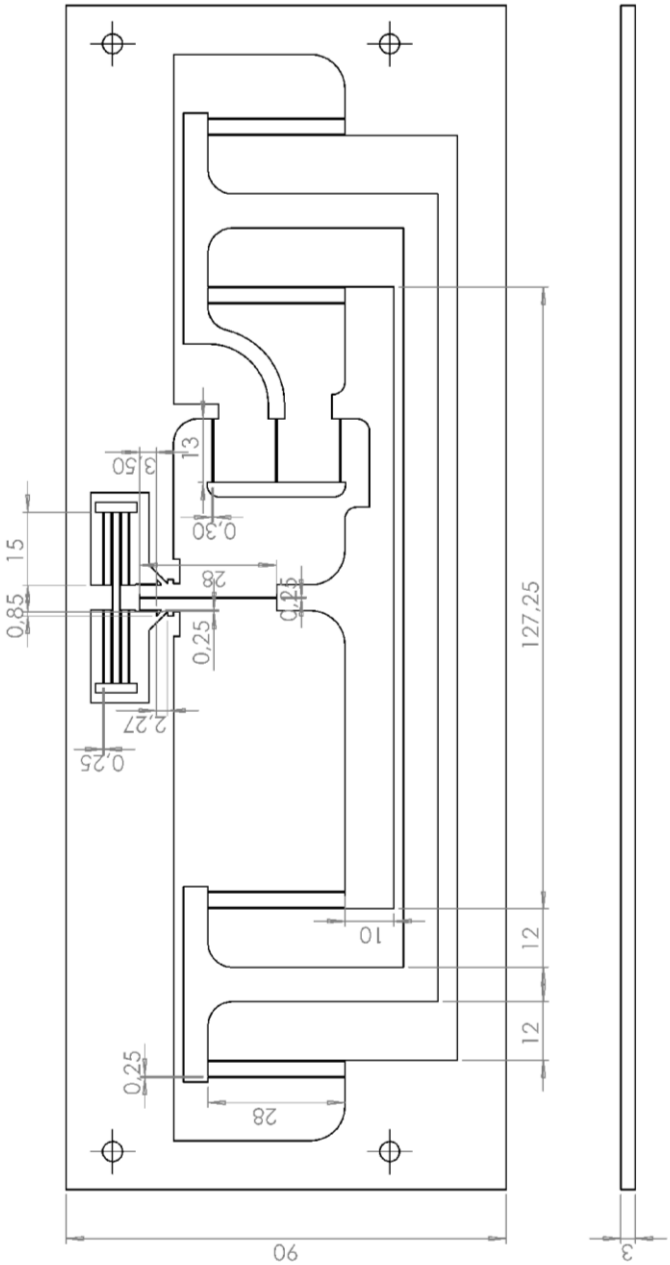

Figure 47 Asymmetric model

4.5 MEMS model

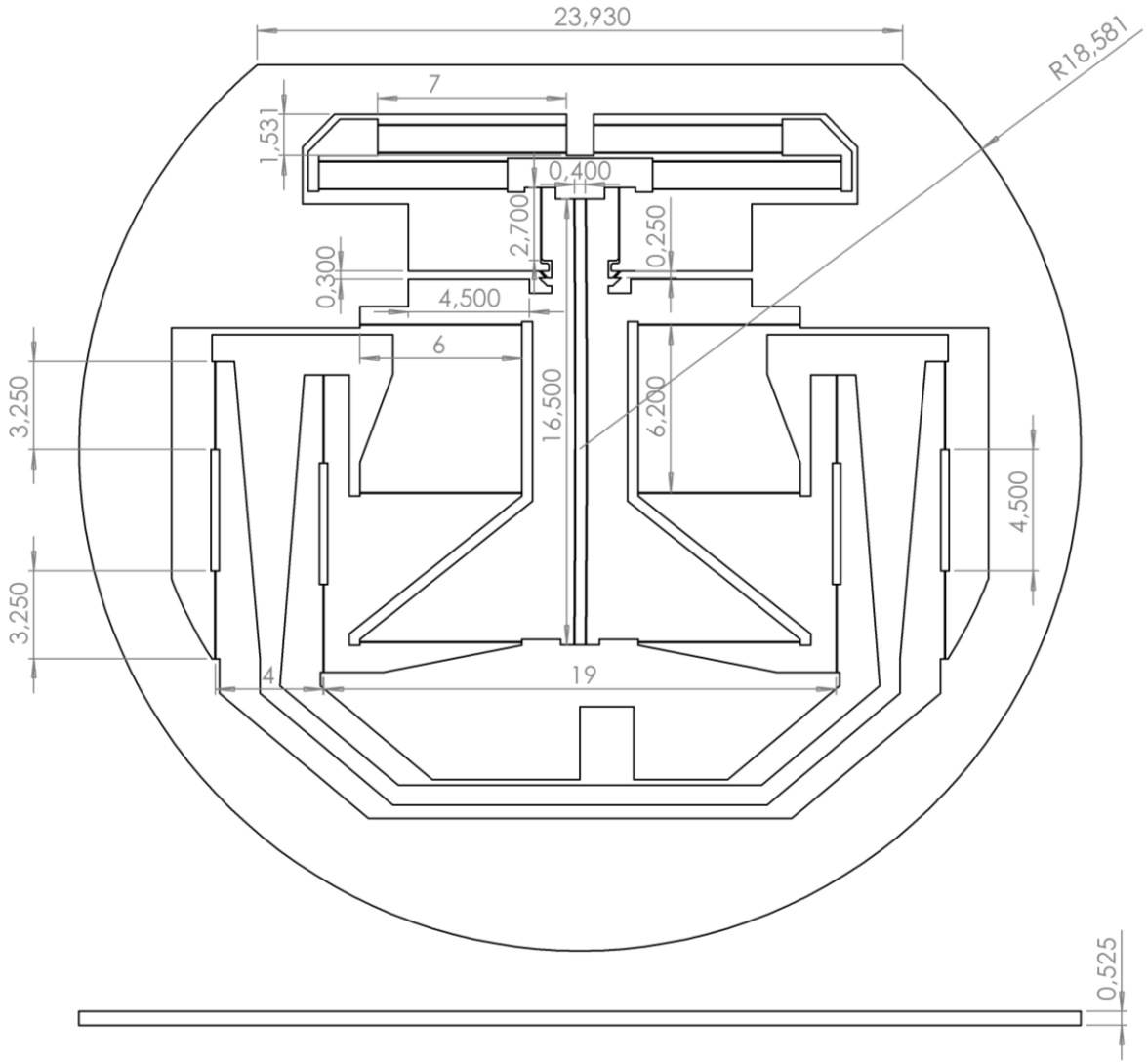

Figure 48 MEMS model

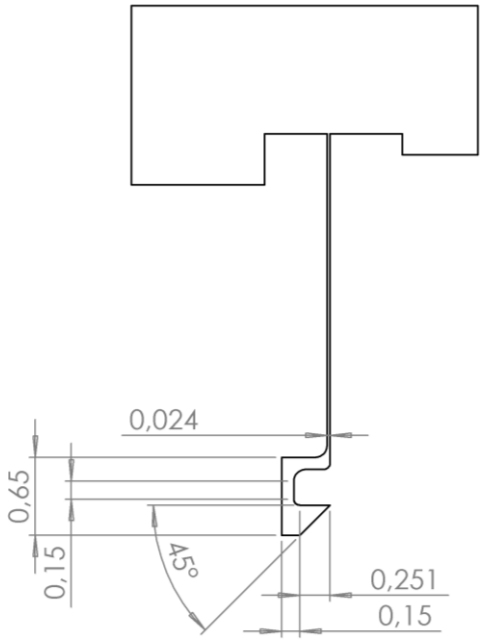

Figure 49 Close up hooks

4.6 Prototype fabrication Model

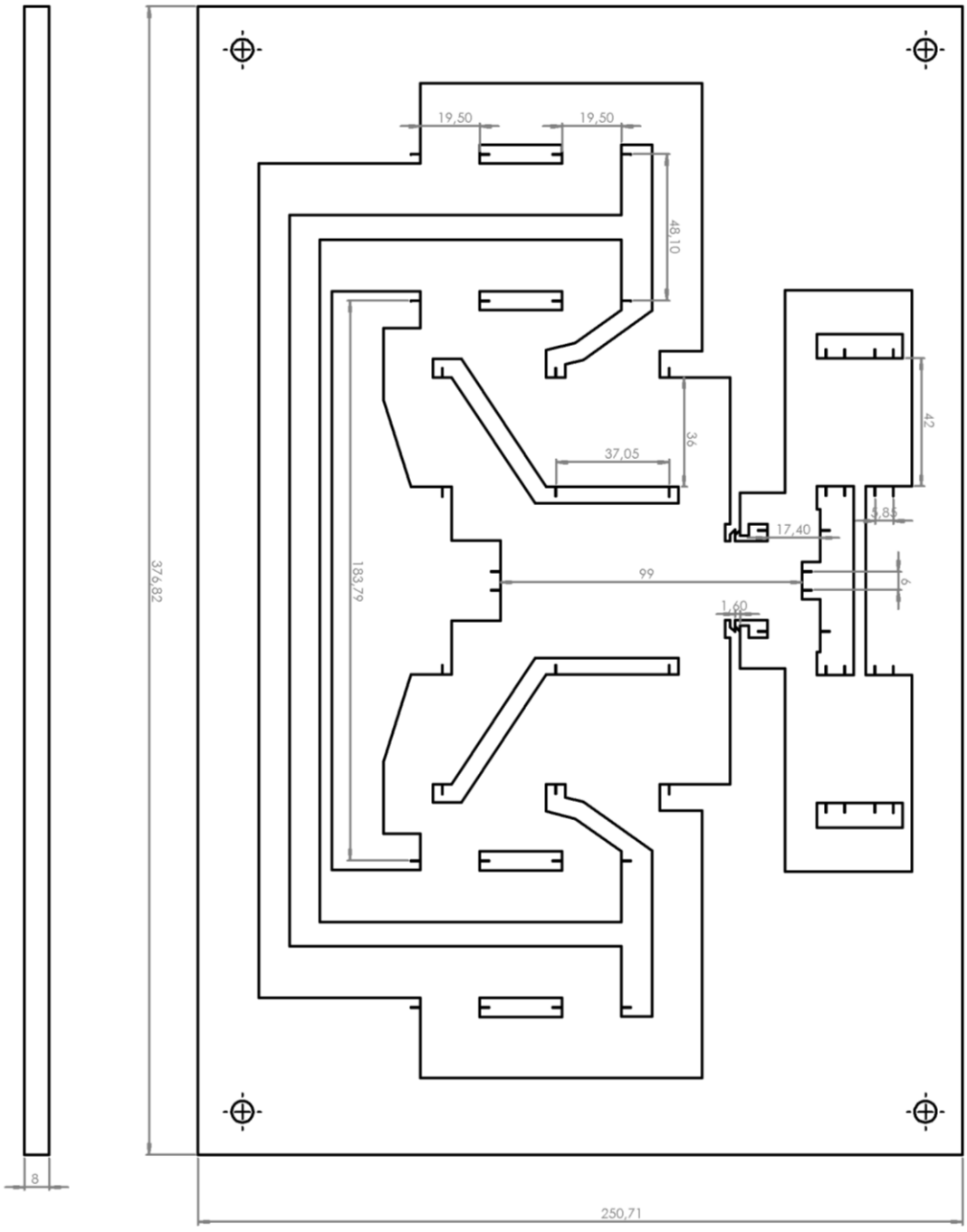

Figure 50 Prototype model

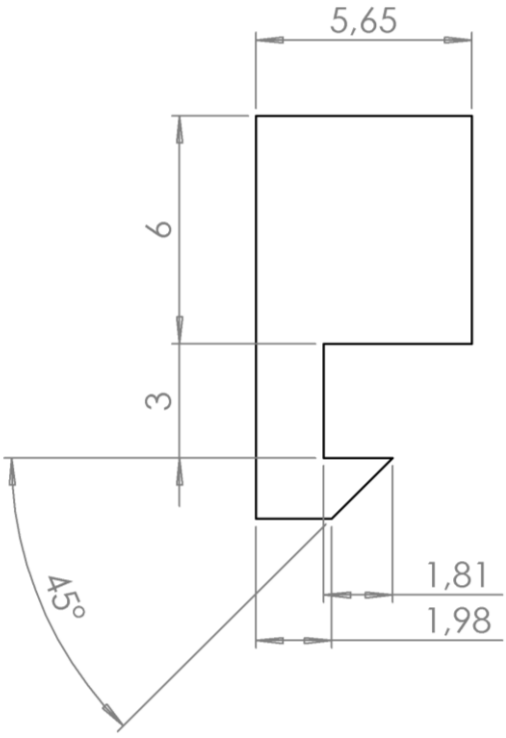

Figure 51 Close up hooks

5 Calculation sheets

Calculation sheet for total design

There are tree parts involved. The negative, to be preloaded, beam that buckels, the possitive guiding for the shuttle and the possitive guiding for the preload block and the hooks that deflect

General properties				**Subcalculations**			**End results**			
Material	E	Pa	2,00E+09							
	Yield	Pa	5,00E+07							
Pi			3,14E+00							
Material thickness		mm	5,00E+00							
alpha			1,00E+00							
double folded flexures										
material E	E	Pa	2,00E+09	inertia	m^4	1,43E-13	Total stiffness	N/m	127,037	
Length beam	l	mm	60							
Number of beams	n	#	8				Force required for Max Stroke	N	2,27E+00	**
Thickness	h	mm	0,7				Max Yield str	Pa	4,17E+07	needs to be below yield stress
Matrial plate thickness	b	mm	5,00E+00							
buckling beam										
material E	E	Pa	2,00E+09	inertia	m^4	2,13333E-13	Total stiffness	N/m	-131,595	
Length beam	l	mm	80	Max stroke from center	mm	17,88854382				
Number of beams	n	#	2				Force required for Preloading, one beam	N	2,63E+00	
Thickness	h	mm	0,8				Max Yield str.	Pa	2,43E+07	needs to be below yield stress
Matrial plate thickness	b	mm	5,00E+00							
preload displacement	pr.d	mm	3,00E+00				Difference between neg and pos part in stiffness		-4,55769	needs to be close to 0
double folded flexures for preloading										
material E	E	Pa	2,00E+09	inertia	m^4	1,42917E-13	Total stiffness	N/m	428,75	
Length beam	l	mm	40	Stroke = pr.d	m	3,00E+00	Force required for Stroke	N	1,29E+00	
Number of beams	n	#	8							
Thickness	h	mm	0,7				Max Yield str	Pa	1,58E+07	needs to be below yield stress
Matrial plate thickness	b	mm	5,00E+00							
hooks										
material E	E	Pa	2,00E+09	inertia	m^4	9,00E-14	Total stiffness	N/m	2160	*note
Length beam	l	mm	10							
Number of beams	n	#	4							
Thickness	h	mm	0,6							
Matrial plate thickness	b	mm	5,00E+00							

Figure 52 calculation sheet for symmetric model V2.5

Calculation sheet for total design

There are tree parts involved. The negative, to be preloaded, beam that buckels, the possitive guiding for the shuttle and the possitive guiding for the preload block and the hooks that deflect

General properties				**Subcalculations**			**End results**			
Material VeroClear	E	Pa	2,00E+09							
	Yield	Pa	5,00E+07	? Gok						
Pi			3,14E+00							
Material thickness		mm	3,00E+00							
alph			1,00E+00							
double folded flexures										
material E	E	Pa	2,00E+09	inertia	m^4	3,91E-15	Total stiffness	N/m	34,16545	
Length beam	l	mm	28							
Number of beams	n	#	8				Force required for Max Stroke	N	7,55E-01	**
Thickness	h	mm	0,25				Max Yield str	Pa	4,23E+07	needs to be below yield stress
Matrial plate thickness	b	mm	3,00E+00							
buckling beam										
material E	E	Pa	2,00E+09	inertia	m^4	3,90625E-15	Total stiffness	N/m	-28,09996	
Length beam	l	mm	28	Shuttle displacement mx fro	mm	9,205795276				
Number of beams	n	#	1				Force required for Preloading, one beam	N	3,93E-01	
Thickness	h	mm	0,25	desired shuttle displacemen	mm	22,08774321	Max Yield str.	Pa	3,19E+07	needs to be below yield stress
Matrial plate thickness	b	mm	3,00E+00	>from triangle		11,0438716				
preload displacement	pr.d	mm	2,27E+00				Difference between neg and pos part			
							in stiffness		22,04015	needs to be close to 0
double folded flexures for preloading										
material E	E	Pa	2,00E+09	inertia	m^4	3,90625E-15	Total stiffness	N/m	222,2222	
Length beam	l	mm	15	Stroke = pr.d	m	2,27E+00	Force required for Stroke	N	5,04E-01	
Number of beams	n	#	8							
Thickness	h	mm	0,25				Max Yield str	Pa	3,03E+07	needs to be below yield stress
Matrial plate thickness	b	mm	3,00E+00							
hooks										
material E	E	Pa	2,00E+09	inertia	m^4	3,91E-15	Total stiffness	N/m	1093,294	*note
Length beam	l	mm	3,5							
Number of beams	n	#	2							
Thickness	h	mm	0,25							
Matrial plate thickness	b	mm	3,00E+00							

Lever										
shutle displacement		mm	22,08774	inertia	m^4	6,75E-15	Normal force on beam	N	1,38E-01	
arm length lever		mm	13	deflection angle	rad	0,866576007	Horizontal force	N	0,117615	
beam thickness		mm	0,3							
beam length		mm	13				horizontal stifness one beam	N/m	5,324887	
yought modulus	E		2,00E+09				stifness 3 beams combined	N/m	15,97466	
							max stress	Pa	0,00E+00	39995816 (original calculation for V2

Figure 53 Calculation sheet for asymmetric model V9

6 ANSYS Codes

6.1 Ansys during optimization sequence

```
FINISH
/CLEAR
/OUTPUT


pi = 3.14159265359

!!!!!!!!!!!!!!!!!!!!!!!!!!!!!!!!!!!!!!!!!!!!!!!!!!!!!!!!!!!!!!!!!!!!!!!!!!!!
x1 = 0
y1 = 0
LOCAL, 11, 0, x1, y1, 0, 0, 0, 0

!!!!!!!!!!!!!!!!!!!!!!!!!!!!!!!!!!!!!!!!!!!!!!!!!!!!!!!!!!!!!!!!!!!!!!!!!!!!


L12 = 16.5e-3          !length preload beam
L34 = 3.5e-3           !length small dff
L1112 = 4.5e-3         !length lever
L1720 = 10e-3          !length total beam big dff
L1819 = 6e-3           !length ridig part big dff
L2526 = 0.1e-3         !length hooks
L1113 = 5.5e-3         !length arms lever
L2024 = 2e-3           !length between big dff arms one side
L220 = 6e-3            !length between center en inner big dff
L35 =  0.5e-3          ! length between beams small dff
Loff = 1e-6            !offset for big dff
Curve_Rad1 = 1000e-3

LBuck=2
!!!!!! Calculation for arce center1 !!!!!!!
CX1 = -Curve_Rad1




!!!!!!!!!!!!!!!!!!!!!!!!!!!!!!!!!!!!!!!!!!!!!!!!!!!!!!!!!!!!!!!!!!!!!!!!!!!!


n_elements = 20
substeps = 100

/PREP7
ET,1,BEAM188
ET,2,MPC184
ET,3,BEAM188
KEYOPT,2,1,1


/ESHAPE,1

SECTYPE,1,BEAM,MESH,MEMS
SECOFFSET,CENT,,,
SECREAD,'MEMS_BeamCross_Marije_25um','SECT','C:\Users
\Marije\Dropbox\02                    Universiteit\Graduation
Project\Thesis - Small beam preload\4 Modeling',MESH


MPTEMP,,,,,,,,
MPTEMP,1,0
MPDATA,EX,1,,169e9
MPDATA,EY,1,,169e9
MPDATA,EZ,1,,130e9
MPDATA,PRXY,1,,0.064
MPDATA,PRYZ,1,,0.36
MPDATA,PRXZ,1,,0.28
MPDATA,GXY,1,,50.9e9
MPDATA,GYZ,1,,79.6e9
MPDATA,GXZ,1,,79.6e9
MP,DENS,1,2330
MP,Mu,1,0.14



!!!!!!!!!!!!!!!!!!!!!!!!!!!! Keypoints  !!!!!!!!!!!!!!!!!!!!!!!!!!!!

CSYS,11


k , 1 , 0.2e-3        , L12-2e-3                    , 0
k , 2 , 0.2e-3      , 0-2e-3                        , 0

k , 30 , 0.1e-3     , L12-2e-3                      , 0
k , 31 , 0.1e-3     , 0-2e-3                        , 0


k , 3 , 2e-3          , L12-4e-3                    , 0
k , 4 , 2e-3+L34   , L12-4e-3                       , 0
k , 5 , 2e-3          , L12-4e-3-L35*1              , 0
k , 6 , 2e-3+L34   , L12-4e-3-L35*1                 , 0
k , 7 , 2e-3*2        , L12-4e-3-L35*2 , 0
k , 8 , 2e-3*2+L34            , L12-4e-3-L35*2 , 0
k , 9 , 2e-3*2                , L12-4e-3-L35*3 , 0
k , 10 , 2e-3*2+L34           , L12-4e-3-L35*3 , 0
k , 11 , 1e-3                 , L1720/2+L1113 , 0
k , 12 , 1e-3+L1112           , L1720/2+L1113 , 0
k , 13 , 1e-3                 , L1720/2             , 0
k , 14 , 1e-3+L1112           , L1720/2             , 0
k , 15 , 1e-3                 , L1720/2-L1113    , 0
k , 16 , 1e-3+L1112           , L1720/2-L1113    , 0
k , 17 , L220         , L1720                       , 0
k , 18 , L220+Loff            , L1720/2+L1819/2, 0
k , 19 , L220+Loff            , L1720/2-L1819/2 , 0
k , 20 , L220         , 0         , 0
k , 21 , L220+L2024           , L1720               , 0
k , 22 , L220+L2024+Loff , L1720/2+L1819/2, 0
k , 23 , L220+L2024+Loff , L1720/2-L1819/2 , 0
k , 24 , L220+L2024           , 0                   , 0
k , 25 , 2e-3         , L12-4e-3-L35*3    , 0
k , 26 , 2e-3       , L12-4e-3-L35*3-L2526          , 0


k , 201 , -0.2e-3       , L12-2e-3      , 0
k , 202 , -0.2e-3       , 0-2e-3        , 0
k , 230 , -0.1e-3       , L12-2e-3      , 0
k , 231 , -0.1e-3       , 0-2e-3        , 0
k , 203 , -(2e-3)               , L12-4e-3      , 0
k , 204 , -(2e-3+L34)           , L12-4e-3      , 0
k , 205 , -(2e-3)               , L12-4e-3-L35*1    , 0
k , 206 , -(2e-3+L34)           , L12-4e-3-L35*1    , 0
k , 207 , -(2e-3*2) , L12-4e-3-L35*2    , 0
k , 208 , -(2e-3*2+L34)         , L12-4e-3-L35*2    , 0
k , 209 , -(2e-3*2) , L12-4e-3-L35*3    , 0
k , 210 , -(2e-3*2+L34)         , L12-4e-3-L35*3    , 0
k , 211 , -(1e-3)               , L1720/2+L1113   , 0
k , 212 , -(1e-3+L1112)         , L1720/2+L1113   , 0
k , 213 , -(1e-3)               , L1720/2             , 0
k , 214 , -(1e-3+L1112)         , L1720/2             , 0
k , 215 , -(1e-3)               , L1720/2-L1113    , 0
```

```
k , 216 , -(1e-3+L1112)         , L1720/2-L1113    , 0
k , 217 , -(L220)               , L1720                  , 0
k , 218 , -(L220+Loff)          , L1720/2+L1819/2 , 0
k , 219 , -(L220+Loff)          , L1720/2-L1819/2 , 0
k , 220 , -(L220)               , 0          , 0
k , 221 , -(L220+L2024)         , L1720        , 0
k , 222 , -(L220+L2024+Loff), L1720/2+L1819/2, 0
k , 223 , -(L220+L2024+Loff), L1720/2-L1819/2, 0
k , 224 , -(L220+L2024)         , 0          , 0
k , 225 , -(2e-3)               , L12-4e-3-L35*3    , 0
k , 226 , -(2e-3)               , L12-4e-3-L35*3-L2526, 0

k , 300 , -(Curve_Rad1), L12/2, 0

!!!!!!!!!!!!!!!!!!!!!!!!!!!!!!!!!! Lines !!!!!!!!!!!!!!!!!!!!!!!!!!!!!!

!!!!!!!!!Flexible lines!!!!!!!
*GET,Line_ID1,LINE,0,NUM,MAXD
CSYS,11

LARC,1,2,300,Curve_Rad1
LARC,30,31,300,Curve_Rad1
L , 3 , 4
L , 5 , 6
L , 7 , 8
L , 9 , 10
L , 11 , 12
L , 13 , 14
L , 15 , 16
L , 17 , 18
L , 19 , 20
L , 21 , 22
L , 23 , 24
L  ,  25,  26

LARC,201,202,300,Curve_Rad1
LARC,230,231,300,Curve_Rad1
L , 203 , 204
L , 205 , 206
L , 207 , 208
L , 209 , 210
L , 211 , 212
L , 213 , 214
L , 215 , 216
L , 217 , 218
L , 219 , 220
L , 221 , 222
L , 223 , 224
L  ,  225 ,  226

*GET,Line_ID2,LINE,0,NUM,MAXD


!!!!!!!!!Rigid lines!!!!!!!!!!
CSYS,11

L , 1 , 3
L , 1 , 5
L , 3 , 5

L , 4 , 6
L , 8 , 10
L , 6 , 8
L , 4 , 10
L , 4 , 8

L , 11 , 13
L , 16 , 13
L , 16 , 11

L , 14 , 17
L , 17 , 21
L , 14 , 21
L  , 18, 19
L  , 22,  23

L , 15 , 20
L , 20 , 2
L , 2 , 15

L , 5 , 25
L , 3 , 25

!mirror

L , 201 , 203
L , 201 , 205
L , 203 , 205

L , 204 , 206
L , 208 , 210
L , 206 , 208
L , 204 , 210
L , 204 , 208

L , 211 , 213
L , 216 , 213
L , 216 , 211

L , 214 , 217
L , 217 , 221
L , 214 , 221

L  , 218, 219
L  , 222,  223

L , 215 , 220
L , 220 , 202
L , 202 , 215

L , 205 , 225
L , 203 , 225

!cross links
L , 20 , 220
L , 21 , 221
L , 17 , 217
L , 21 , 217
L , 17 , 221
L , 25 , 225
L  , 15,  215

L  , 1,  201
L  , 2,  202
L  , 1,  203
L  , 3,  201
L  , 20,  202
L  , 2,  220

L  , 202,  231
L  , 31,  2
L  , 231,  31
L  , 202,  31
L  , 231,  2

L  , 201,  230
L  , 30,  1
L  , 230,  30
L  , 201,  30
L  , 230,  1


*GET,Line_ID3,LINE,0,NUM,MAXD
CSYS,11


!!!!!!!!!!!!!!!!!!!!!!!!!!!!!!!!!!!!!!!!!!!!!!!!!!!!!!!!!!!!!!!!!!!!!!!!!!!!!!!!!!!
```

```
TYPE,1
SECNUM,1
REAL,1
LSEL,S,LINE,,Line_ID1+1 ,Line_ID2
LESIZE,ALL, , ,n_elements

LMESH,ALL

TYPE,2
SECNUM,1
REAL,1
LSEL,S,LINE,,Line_ID2+1 ,Line_ID3
LESIZE,ALL, , ,1
LMESH,ALL


/SOL
/ESHAPE,1
NLGEOM,1
OUTRES,ALL,ALL
SOLCONTROL,ON,ON
AUTOTS,ON
NEQIT,10
NSUBST,substeps ,,substeps

!!!!!!!!!!!!!!!!!!!!!!!!!!!!!!!!!!!!!!!!!!!!!!!!!!!!!!!!!!!!!!!!!!!!!!!!!!!!!!!

TIME,1

dk , 7 , all
dk , 9 , all
dk , 12 , all
dk , 24 , all

dk , 207 , all
dk , 209 , all
dk , 212 , all
dk , 224 , all

dk,1,uy, -0.25e-3
dk,2,ux,0
SOLVE

TIME,2
DK,2,ux, 3e-3
SOLVE

Time,3
DK,2,ux,-3e-3
solve
!!!!!!!!!!!!!!!!!!!!!!!!!!!!!!!!!!!!!!!!!!!!!!!!!!!!!!!!!!!!!!!!!!!!!!!!!!!!!!!

/POST1
/RGB,INDEX, 100, 100, 100, 0
/RGB,INDEX, 80, 80, 80, 13
/RGB,INDEX, 60, 60, 60, 14
/RGB,INDEX, 0, 0, 0,15
/ESHAPE,1
PLDISP,0
```

6.2 MEMS code for stiffness calculations

```
FINISH
/CLEAR
/OUTPUT


pi = 3.14159265359

!!!!!!!!!!!!!!!!!!!!!!!!!!!!!!!!!!!!!!!!!!!!!!!!!!!!!!!!!!!!!!!!!!!!!!!!!!!
x1 = 0
y1 = 0
LOCAL, 11, 0, x1, y1, 0, 0, 0, 0

scale = 1
!!!!!!!!!!!!!!!!!!!!!!!!!!!!!!!!!!!!!!!!!!!!!!!!!!!!!!!!!!!!!!!!!!!!!!!!!!!



L12 = 16.5e-3  !length preload beam
L34 = 7e-3   !length smalldff
L1112 = 6e-3  !length lever
!L1720 = 12.5e-3   !length total beam big dff
L1819 = 4.5e-3   !length ridig part big dff
L1720 = 6.5e-3+L1819
L2526 = 2.6e-3   !length hooks
L2690 = 0.25e-3 !hook width
L1113 = 6.2e-3   !length arms lever
L2024 = 4e-3  !length between Ldff arms one side
L220 = 9.5e-3   !length between center en inner ldff
L35 =  1e-3  ! length between beams small dff
Loff = 1e-6   !offset for ldff
Curve_Rad1 =  1
LBuck=2

!!!!!! Calculation for arce center1 !!!!!!!
CX1 = -Curve_Rad1

!!!!!!!!!!!!!!!! Material properties !!!!!!!!!!!!!!!!!!!!!!!!!!!!!!!

n_elements = 20
substeps = 100

/PREP7
ET,1,BEAM188
ET,2,MPC184
ET,3,BEAM188
KEYOPT,2,1,1



/ESHAPE,1
SECTYPE,1,BEAM,MESH,MEMS
SECOFFSET,CENT,,,
SECREAD,'MEMS_BeamCross_Marije_24um','SECT','C:\Users
\Marije\Dropbox\02                    Universiteit\Graduation
Project\Thesis - Small beam preload\4 Modeling',MESH


MPTEMP,,,,,,,,
MPTEMP,1,0
MPDATA,EX,1,,169e9
MPDATA,EY,1,,169e9
MPDATA,EZ,1,,130e9
MPDATA,PRXY,1,,0.064
MPDATA,PRYZ,1,,0.36
MPDATA,PRXZ,1,,0.28
MPDATA,GXY,1,,50.9e9
MPDATA,GYZ,1,,79.6e9
MPDATA,GXZ,1,,79.6e9
MP,DENS,1,2330
MP,Mu,1,0.14
```

```
!!!!!!!!!!!!!!!!!!!!!!!!!!!!!!!!!!!!!!!!!!!!!!!!!!!!!!!!!!!!!!!!!!!!!!!!!!!
!!!!!!!!!!!!!!!!!!!!!!!!!!!!!!!!!!!!!!!!!!!!!!!!!!!!!!!!!!!!!!!!!!!!!!!!!!!! Keypoints   !!!!!!!!!!!!!!!!!!!!!!!!!!!!!!!!!!!!!!!!!!!!!!!!!!!!!!!!!!!!!!!!!!!!!!!!!!!

CSYS,11

k ,  1 ,  0.000212      ,     0.00825   ,  0
k ,  2 ,  0.000212      ,     -0.00825    ,        0
k ,  3 ,  0.0005        ,     0.010986    ,        0
k ,  4 ,  0.0075        ,     0.010986    ,        0
k ,  5 ,  0.0005        ,     0.009962    ,        0
k ,  6 ,  0.0075        ,     0.009962    ,        0
k ,  7 ,  0.002687      ,     0.009638    ,        0
k ,  8 ,  0.009687      ,     0.009638    ,        0
k ,  9 ,  0.002687      ,     0.008614    ,        0
k ,  10  ,  0.009687        ,  0.008615          ,  0
k ,  11  ,  0.002162        ,  0.003589          ,  0
k ,  12  ,  0.008162        ,  0.003589          ,  0
k ,  13  ,  0.002162        ,  -0.002634         ,  0
k ,  14  ,  0.008162        ,  -0.002634         ,  0
k ,  15  ,  0.002186        ,  -0.008158         ,  0
k ,  16  ,  0.008162        ,  -0.008158         ,  0
k ,  17  ,  0.009512        ,  0.001729          ,  0
k ,  18  ,  0.009512        ,  -0.00152          ,  0
k ,  19  ,  0.009512        ,  -0.00602          ,  0
k ,  20  ,  0.009512        ,  -0.00927          ,  0
k ,  21  ,  0.013536        ,  0.002227          ,  0
k ,  22  ,  0.013536        ,  -0.001022         ,  0
k ,  23  ,  0.013536        ,  -0.005522         ,  0
k ,  24  ,  0.013536        ,  -0.008772         ,  0
k ,  25  ,  0.001442        ,  0.008677          ,  0
k ,  26  ,  0.001442        ,  0.006077          ,  0

!mirror
k ,  201,  -0.000212,          0.00825   ,        0
k ,  202,  -0.000212,          -0.00825          ,  0
k ,  203,  -0.0005 ,        0.010986    ,        0
k ,  204,  -0.0075 ,        0.010986    ,        0
k ,  205,  -0.0005 ,        0.009962    ,        0
k ,  206,  -0.0075 ,        0.009962    ,        0
k ,  207,  -0.002687,          0.009638          ,  0
k ,  208,  -0.009687,          0.009638          ,  0
k ,  209,  -0.002687,          0.008614          ,  0
k ,  210,  -0.009687,          0.008615          ,  0
k ,  211,  -0.002162,          0.003589          ,  0
k ,  212,  -0.008162,          0.003589          ,  0
k ,  213,  -0.002162,          -0.002634         ,  0
k ,  214,  -0.008162,          -0.002634         ,  0
k ,  215,  -0.002186,          -0.008158         ,  0
k ,  216,  -0.008162,          -0.008158         ,  0
k ,  217,  -0.009512,          0.001729          ,  0
k ,  218,  -0.009512,          -0.00152          ,  0
k ,  219,  -0.009512,          -0.00602          ,  0
k ,  220,  -0.009512,          -0.00927          ,  0
k ,  221,  -0.013536,          0.002227          ,  0
k ,  222,  -0.013536,          -0.001022         ,  0
k ,  223,  -0.013536,          -0.005522         ,  0
k ,  224,  -0.013536,          -0.008772         ,  0
k ,  225,  -0.001442,          0.008677          ,  0
k ,  226,  -0.001442,          0.006077          ,  0



k ,  90 , (0.9e-3 + L2690)*scale        , (L12/2-0.67e-3-
L2526   )*scale,  0
k ,  290   ,  -(0.9e-3 + L2690   )*scale  ,        (L12/2-
0.67e-3-L2526   )*scale,     0
```

```
k ,  300,  -(Curve_Rad1)*scale,     L12/2*scale,   0


!!!!!!!!! Lines !!!!!!!!!!!!!!!!!!!!!!!!!!!!!!

!!!!!!!!!Flexiblelines!!!!!!!
*GET,Line_ID1,LINE,0,NUM,MAXD
CSYS,11


LARC,1,2,300,Curve_Rad1
!LARC,30,31,300,Curve_Rad1
L   ,     3 ,  4
L   ,     5 ,  6
L   ,     7 ,  8
L   ,     9 ,  10
L   ,     11  ,  12
L   ,     13  ,  14
L   ,     15  ,  16
L   ,     17  ,  18
L   ,     19  ,  20
L   ,     21  ,  22
L   ,     23  ,  24
L   ,     25,  26

LARC,201,202,300,Curve_Rad1
!LARC,230,231,300,Curve_Rad1
L   ,     203,  204
L   ,     205,  206
L   ,     207,  208
L   ,     209,  210
L   ,     211,  212
L   ,     213,  214
L   ,     215,  216
L   ,     217,  218
L   ,     219,  220
L   ,     221,  222
L   ,     223,  224
L   ,     225,  226



*GET,Line_ID2,LINE,0,NUM,MAXD


!!!!!!!!!Rigidlines!!!!!!!!!!
CSYS,11

L   ,     1 ,  7
L   ,     1 ,  9
L   ,     7 ,  9

L   ,     4 ,  6
L   ,     8 ,  10
L   ,     6 ,  8
L   ,     4 ,  10
L   ,     4 ,  8

L   ,     11  ,  13
L   ,     16  ,  13
L   ,     16  ,  11

L   ,     14  ,  17
L   ,     17  ,  21
L   ,     14  ,  21
L   ,     18,  19
L   ,     22,  23

L   ,     15  ,  20
L   ,     20  ,  2
L   ,     2 ,  15

L   ,     9 ,  25
L   ,     7 ,  25

L , 226 , 290
!mirror

L   ,     201,  207
L   ,     201,  209
L   ,     207,  209

L   ,     204,  206
L   ,     208,  210
L   ,     206,  208
L   ,     204,  210
L   ,     204,  208

L   ,     211,  213
L   ,     216,  213
L   ,     216,  211

L   ,     214,  217
L   ,     217,  221
L   ,     214,  221

L   ,     218,  219
L   ,     222,  223

L   ,     215,  220
L   ,     220,  202
L   ,     202,  215

L   ,     209,  225
L   ,     207,  225

L , 26 , 90
!cross links
L   ,     20  ,  220
L   ,     21  ,  221
L   ,     17  ,  217
L   ,     21  ,  217
L   ,     17  ,  221
L   ,     25  ,  225
L   ,     15,  215

L   ,     1,   201      !outer preload beams
L   ,     2,   202
L   ,     1,   207
L   ,     7,   201
L   ,     20,  202
L   ,     2,   220

!L   ,     202,   231          !inner preload beams connection
(down and top part)
!L   ,     31,  2
!L   ,     231,   31
!L   ,     202,   31
!L   ,     231,   2

!L   ,     201,   230
!L   ,     30,  1
!L   ,     230,   30
!L   ,     201,   30
!L   ,     230,   1


*GET,Line_ID3,LINE,0,NUM,MAXD
CSYS,11


!!!!!!!!!!!!!!!!!!!!!!!!!!!!!!!!!!!!!!!!!!!!!!!!!!!!!!!!!!!!!!!!!!!!!!!!!!!!!!!!!!!!!!!!!!!!
!!!!!!!!!!!!!!!!!!!!!!!!!!!!!!!!!!!!!!!!!!!!!!!!!!!!!!!!!!!!!!!!!!!!!!!!!!!!!!!!!!!!!!!!!!!!
```

```
TYPE,1
SECNUM,1
REAL,1
LSEL,S,LINE,,Line_ID1+1 ,Line_ID2
LESIZE,ALL, , ,n_elements

LMESH,ALL

TYPE,2
SECNUM,1
REAL,1
LSEL,S,LINE,,Line_ID2+1 ,Line_ID3
LESIZE,ALL, , ,1
LMESH,ALL


/SOL
/ESHAPE,1
NLGEOM,1
OUTRES,ALL,ALL
SOLCONTROL,ON,ON
AUTOTS,ON
NEQIT,10
NSUBST,substeps ,,substeps

!!!!!!!!!!!!!!!!!!!!!!!!!!!!!!!!!!!!!!!!!!!!!!!!!!!!!!!!!!!!!!!!!!!!!!!
!!!!!!!!!!!!!!!First OneDOF Motion Output Is Free!!!!!!!!!!!!!!!!!!
!!!!!!!!!!!!!!!!!!!!!!!!!!!!!!!!!!!!!!!!!!!!!!!!!!!!!!!!!!!!!!!!!!!!!!!!

TIME,1

dk  ,    3 ,  all
dk  ,    5 ,  all
dk  ,    12  ,  all
dk  ,    24  ,  all

dk  ,    203 ,  all
dk  ,    205 ,  all
dk  ,    212 ,  all
dk  ,    224 ,  all
!dk,1,uy, -0.25e-3     !preloading
DK,2,ux, 0

!fk, 26, Fy, 0.00852
!fk, 226, Fy, 0.00852
SOLVE

TIME,2
DK,2,ux, 2.7e-3

!dk,2,ux,0

!dk,25,all              !hook tests
!dk,26,ux, -0.21465e-3
!fk,90, FY, -0.03

!dk, 26, uy, -0.26e-3
!dk, 226, uy, -0.26e-3
SOLVE


Time,3
DK,2,ux,-2.7e-3
solve
!!!!!!!!!!!!!!!!!!!!!!!!!!!!!!!!!!!!!!!!!!!!!!!!!!!!!!!!!!!!!!!!!!!!!!!

/POST1
/RGB,INDEX, 100, 100, 100, 0
/RGB,INDEX, 80, 80, 80, 13
/RGB,INDEX, 60, 60, 60, 14
/RGB,INDEX, 0, 0, 0,15
/ESHAPE,1
PLDISP,0

! to read stiffnesses, timehist > click plus sign > add dof > choose displacement > choose a node > ok > in the timehist first pop-up click the graph button.


!read keypoint to nodes
!klist              !keypoints to nodes uitlezen
!nlist              !all desiplacements from nodes


!/DSCALE Sets the displacement multiplier for displacement displays
!/post26
!LINES,2000  !perhaps use this earlier
!NSOL,2,2,U,X, UX_2,
!STORE,MERGE
!PRVAR,2,

!stress plot
/EFACET,1
PLNSOL, S,EQV, 0,1.0
/DIST,1,1.08222638492,1
/REP,FAST
/REPLOT,RESIZE

/POST26

ID_Node = 2
TIMERANGE,0,3        !Set the timerange over which you want to save data
RFORCE,2,ID_Node,F,X,FX    !Get reaction force data on nodenumber ID_Node
NSOL,3,ID_Node,U,X,UX        !Get displacement data on node number ID_Node
XVAR,3
PLVAR,2


*CREATE,scratch,gui    !Write data to file
  *DEL,VAR_export
  *DIM,VAR_export,TABLE,302,4            !Set dimension of table (each dimension is always 1 bigger, so this is a 20x3 table)
   VGET,VAR_export(1,0),1
   VGET,VAR_export(1,1),2
   VGET,VAR_export(1,2),3

/OUTPUT,'MEMS65_FXUXKP2_Unpreloaded','txt','C:\Users\Marije\Dropbox\02 Universiteit\Graduation Project\Thesis - Small beam preload\4 Modeling\Final Force displacement analysys'        !change to your own file name/location

*VWRITE,VAR_export(1,0),VAR_export(1,1),VAR_export(1,2)
  %G, %G, %G
  /OUTPUT,TERM
  *END
  /INPUT,scratch,gui
```

6.3 MEMS model for Modal analysis

```
FINISH
/CLEAR
/OUTPUT


pi = 3.14159265359

!!!!!!!!!!!!!!!!!!!!!!!!!!!!!!!!!!!!!!!!!!!!!!!!!!!!!!!!!!!!!!!!!!!!!!!!!!!
x1 = 0
y1 = 0
LOCAL, 11, 0, x1, y1, 0, 0, 0, 0

scale = 1
!!!!!!!!!!!!!!!!!!!!!!!!!!!!!!!!!!!!!!!!!!!!!!!!!!!!!!!!!!!!!!!!!!!!!!!!!!!
nModes = 25

L codes equal to MEMS stiffness code


!!!!!!!!!!!!!!!!!!!!!!!!!!!!!!!!!!!!!!!!!!!!!!!!!!!!!!!!!!!!!!!!!!!!!!!!!!!

n_elements = 20
substeps = 150

/PREP7
ET,1,BEAM188
ET,2,MPC184
ET,3,BEAM188

ET,5, MASS21
   !freq anal.
!KEYOPT,5,1,1
!KEYOPT,5,2,0
!KEYOPT,5,3,0
KEYOPT,2,1,1



/ESHAPE,1

SECTYPE,1,BEAM,MESH,MEMS
SECOFFSET,CENT,,,
SECREAD,'MEMS_BeamCross_Marije_24um','SECT','C:\Users
\Marije\Dropbox\02                    Universiteit\Graduation
Project\Thesis - Small beam preload\4 Modeling',MESH


MPTEMP,,,,,,,,
MPTEMP,1,0
MPDATA,EX,1,,169e9
MPDATA,EY,1,,169e9
MPDATA,EZ,1,,130e9
MPDATA,PRXY,1,,0.064
MPDATA,PRYZ,1,,0.36
MPDATA,PRXZ,1,,0.28
MPDATA,GXY,1,,50.9e9
MPDATA,GYZ,1,,79.6e9
MPDATA,GXZ,1,,79.6e9
MP,DENS,1,2330
MP,Mu,1,0.14



! point masses

R,  510,  0.00827e-3,      0.008274e-3,  0.008274e-3,
  0.68765e-9,   0.01896e-9,   0.70623e-9
R,  520,  0.08186e-3,      0.08186e-3,   0.08186e-3,
  9.44159e-9, 1.78360e-9,   11.22142e-9
R,  530,  0.10108e-3,      0.10108e-3,   0.10108e-3,
  4.86946e-9,   10.23225e-9,  15.09707e-9
R,  541,  0.00406e-3,      0.00406e-3,   0.00406e-3,
  0.42839e-9,   0.31507e-9,   0.74327e-9
R,  542,  0.00406e-3,      0.00406e-3,   0.00406e-3,
  0.42839e-9,   0.31507e-9,   0.74327e-9
R,  551,  0.00018e-3,      0.00018e-3,   0.00018e-3,
  0.00575e-9,   0.00026e-9,   0.00600e-9
R,  552,  0.00018e-3,      0.00018e-3,   0.00018e-3,
  0.00575e-9,   0.00026e-9,   0.00600e-9
R,  561,  0.000737e-3,     0.000737e-3,  0.000737e-3,
  0.14788e-9,   0.14402e-9,   0.29157e-9
R,  562,  0.000737e-3,     0.000737e-3,  0.000737e-3,
  0.14788e-9,   0.14402e-9,   0.29157e-9
R,  571,  0.00165e-3,      0.00165e-3,   0.00165e-3,
  0.02051e-9,   0.30262e-9,   0.32305e-9
R,  572,  0.00165e-3,      0.00165e-3,   0.00165e-3,
  0.02630e-9,   0.14946e-9,   0.17569e-9
R,  573,  0.00165e-3,      0.00165e-3,   0.00165e-3,
  0.02630e-9,   0.14946e-9,   0.17569e-9
R,  574,  0.00165e-3,      0.00165e-3,   0.00165e-3,
  0.02051e-9,   0.30262e-9,   0.32305e-9



!!!!!!!!!!!!!!!!!!!!!!!!!!!! Keypoints   !!!!!!!!!!!!!!!!!!!!!!!!!!!!

Keypoint codes equal to MEMS stiffness code

!!! keypoints for masses

k, 510,     0              ,  9.1070/1000,                0
          !preloadblock
k, 520,     -0.0797/1000   ,  -10.6588/1000,
  0         !central/main shuttle
k, 530,     0              ,  -3.6264/1000,                0
          !secondary shuttle
k, 541,     -8.7751/1000   ,  10.2541/1000,
  0         !preload secondary shuttle left
k, 542,     8.7751/1000        ,  10.2541/1000,
  0         !preload secondary shuttle right
k, 551,     -1.2007/1000   ,  5.5710/1000,
  0         !hook left
k, 552,     1.2007/1000    ,     5.5710/1000,
  0         !hook right
k, 561,     -3.8389/1000   ,  -2.9212/1000,
  0         !lever left
k, 562,     3.8389/1000    ,  -2.9212/1000,
  0         !lever left
k, 571,     -13.5360/1000  ,  -3.2723/1000,
  0         !DFF midpieces from left to right
k, 572,     -9.5120/1000   ,  -3.7703/1000,
  0         !DFF midpieces
k, 573,     9.5120/1000        ,  -3.7703/1000,
  0         !DFF midpieces
k, 574,     13.5360/1000   ,  -3.2723/1000,
  0         !DFF midpieces

!!!!!!!!! Lines !!!!!!!!!!!!!!!!!!!!!!!!!!!!!!!!

!!!!!!!!!Flexiblelines!!!!!!!
*GET,Line_ID1,LINE,0,NUM,MAXD
CSYS,11


LARC,1,2,300,Curve_Rad1
!LARC,30,31,300,Curve_Rad1
L ,  3    ,  4
L ,  5    ,  6
```

```
L , 7   , 8
L , 9   , 10
L , 11  , 12
L , 13  , 14
L , 15  , 16
L , 17  , 18
L , 19  , 20
L , 21  , 22
L , 23  , 24
L , 25, 26


LARC,201,202,300,Curve_Rad1
!LARC,230,231,300,Curve_Rad1
L , 203, 204
L , 205, 206
L , 207, 208
L , 209, 210
L , 211, 212
L , 213, 214
L , 215, 216
L , 217, 218
L , 219, 220
L , 221, 222
L , 223, 224
L , 225, 226


*GET,Line_ID2,LINE,0,NUM,MAXD


!!!!!!!!!Rigidlines!!!!!!!!!!
CSYS,11

L , 1   , 7
L , 1   , 9
L , 7   , 9
L , 1 , 510

L , 4   , 6
L , 8   , 10
L , 6   , 8
L , 4   , 10
L , 4   , 8
L , 6   , 542
L , 8   , 542

L , 11  , 13
L , 16  , 13
L , 16  , 11
L , 13 , 562
L , 16,  562

L , 14  , 17
L , 17  , 21
L , 14  , 21
L , 14, 530

L , 18, 19
L , 18  , 573
L , 19 , 573

L , 22, 23
L , 22, 574
L , 23 , 574

L , 15  , 20
L , 15 , 520

L , 20  , 2
L , 2   , 15

L , 9   , 25
L , 7   , 25

L, 26, 552

L , 226 , 290
!mirror

L , 201, 207
L , 201, 209
L , 207, 209
L , 201 , 510

L , 204, 206
L , 208, 210
L , 206, 208
L , 204, 210
L , 204, 208
L , 206  , 541
L , 208, 541

L , 211, 213
L , 216, 213
L , 216, 211
L , 213  , 561
L , 216  , 561

L , 214, 217
L , 217, 221
L , 214, 221
L , 214  , 530

L , 218, 219
L , 218, 572
L , 219  , 572

L , 222, 223
L , 222  , 571
L , 223  , 571

L , 215, 220
L , 215  , 520

L , 220, 202
L , 202, 215

L , 209, 225
L , 207, 225

L , 26 , 90
L, 226, 551
!cross links
L , 20  , 220
L , 21  , 221
L , 17  , 217
L , 21  , 217
L , 17  , 221
L , 25  , 225
L , 15, 215

L , 1,  201     !outer preload beams
L , 2,  202
L , 1,  207
L , 7,  201
L , 20, 202
L , 2,  220

!L  ,   202,  231        !inner preload beams connection
(down and top part)
!L  ,   31,  2
!L  ,   231,  31
!L  ,   202,  31
!L  ,   231,  2

!L  ,   201,  230
!L  ,   30,  1
```

```
!L   ,     230,   30
!L   ,     201,   30
!L   ,     230,   1


! lines for frequency analysis keypoints 500 series


*GET,Line_ID3,LINE,0,NUM,MAXD


!!!!!!!!!!!!!!!!!!!!!!!!!!!!!!!!!!!!!!!!!!!!!!!!!!!!!!!!!!!!!!!!!!!!!!!!!!!!!!!!!!!!!!!!!!
!!!!!!!!!!!!!!!!!!!!!!!!!!!!!!!!!!!!!!!!!!!!!!!!!!!!!!!!!!!!!!!!!!!!!!!!!!!!!!!!!!!!!!!!!!

!  flexures type 1
TYPE,1
SECNUM,1
Mat,1
LSEL,S,LINE,,Line_ID1+1 ,Line_ID2
LESIZE,ALL, , ,n_elements
LMESH,ALL

!  ridig lines
TYPE,2
SECNUM,1
Mat,2
LSEL,S,LINE,,Line_ID2+1 ,Line_ID3
LESIZE,ALL, , ,1
LMESH,ALL

!  flexures type 3
TYPE,1
SECNUM,3
Mat,1
LSEL,S,LINE,,Line_ID3+1 ,Line_ID4
LESIZE,ALL, , ,1
LMESH,ALL

Type, 5
Real, 510
Kmesh, 510, 510

Type, 5
Real, 520
Kmesh, 520, 520

Type, 5
Real, 530
Kmesh, 530, 530

Type, 5
Real, 541
Kmesh, 541, 541

Type, 5
Real, 542
Kmesh, 542, 542

Type, 5
Real, 551
Kmesh, 551, 551

Type, 5
Real, 552
Kmesh, 552, 552

Type, 5
Real, 561
Kmesh, 561, 561

Type, 5
Real, 562
Kmesh, 562, 562

Type, 5
Real, 571
Kmesh, 571, 571

Type, 5
Real, 572
Kmesh, 572, 572

Type, 5
Real, 573
Kmesh, 573, 573

Type, 5
Real, 574
Kmesh, 574, 574




!!!!!!!!!!!!!!!!!!!!!!!!!!!!!!!!!!!!!!!!!!!!!!!!!!!!!!!!!!!!!!!!!!!!!
!!!!!!!!!!!!!!First OneDOF Motion Output Is Free!!!!!!!!!!!!!!!!!
!!!!!!!!!!!!!!!!!!!!!!!!!!!!!!!!!!!!!!!!!!!!!!!!!!!!!!!!!!!!!!!!!!!!!

!TIME,1

dk  ,     3 ,  all
dk  ,     5 ,  all
dk  ,     12  ,  all
dk  ,     24  ,  all

dk  ,     203 ,  all
dk  ,     205 ,  all
dk  ,     212 ,  all
dk  ,     224 ,  all

!dk,1,uy, -0.25e-3*scale          !preloading
!dk,2, all



!!!!!!!!!!!!!!!!!!!!!!!! static
/SOL
antype,0
/ESHAPE,1
OUTRES,ALL,ALL
SOLCONTROL,ON,ON
AUTOTS,ON

NLGEOM,1

AUTOTS,ON
!NEQIT,10
NSUB,substeps,substeps,substeps
save
solve
finish


!!!! modal analysis
!!!!!!!!!! Step 2: modal analysis !!!!!!!!!!!!
/solu                          ! re-enter solution so we can do a new analysis
antype,,restart,1,substeps,perturb       ! specify restart option for linear perturbation
! from last substep in this case
perturb,modal                ! specify modal as next analysis
solve,elform                 ! calculate element formulation with solve command
modopt,subsp,nModes                  ! specify modal options for solution
mxpand,nModes,,,YES               ! specify number of modes for results calc
solve
```

```
!!!!!!!!!!!!!!!!!!!!!!!!!!!!!!!!!!!!!!!!!!!!!!!!!!!!!!!!!!!!!!!!!!!!!!!


!!!!!!!!!!! Postprocessing for frequency
/post1                    ! enter general postprocessor
INRES,ALL                 ! make sure we read in all results from file
FILE,'Opti','rstp'        ! specify special results file for modal results
! rsts file: modal analysis with sets being modes
! rst file: the static prestress results with sets being substeps
SET,LIST                  ! List solutions


!!!!!!!!!!!  Save mode shapes

/RGB,INDEX, 100, 100, 100, 0
/RGB,INDEX, 80, 80, 80, 13
/RGB,INDEX, 60, 60, 60, 14
/RGB,INDEX, 0, 0, 0,15



i_=nModes
*DO,i_,1,25,1

SET,,, ,,, ,i_ ! Select nth mode shape (set)

!PLDISP,0          ! 0 only deformed, 1 def + undeformed

PLNS,EPTO,EQV       ! nodal Von Misses strain

/ESHAPE,0.15          ! SCALE=1 (use real constants and section defenitions)
/GFILE, 2400
/SHOW,PNG
/VIEW,1,0,0,1        ! Window number, XV, YV, ZV

!/REP,FAST
/REPLOT

!ANMODE,10,0.15, ,0          ! Animate mode shape, ANMODE, NFRAM, DELAY, NCYCL, KACCEL

!/image,save,strcat('Mode',chrval(i_)),png
i_=i_+1
/SHOW,CLOSE
*ENDDO


!!!!!!!!!!!!!!!!!!! View mode shapes directly

SET,,, ,,, ,13   ! Select nth mode shape (set)

!PLDISP,0          ! 0 only deformed, 1 def + undeformed

PLNS,EPTO,EQV       ! nodal Von Misses strain

/ESHAPE,0.05          ! SCALE=1 (use real constants and section defenitions)

!/VIEW,1,1,1.3,3          ! Window number, XV, YV, ZV

/VIEW,1,0,0,1        ! Window number, XV, YV, ZV
!/VIEW,1,0,0,3          ! Window number, XV, YV, ZV



!/REP,FAST
/REPLOT

ANMODE,10,0.10, ,0    ! Animate mode shape, ANMODE, NFRAM, DELAY, NCYCL, KACCEL
```

6.4 Prototype model for stiffness calculation

```
FINISH
/CLEAR
/OUTPUT


pi = 3.14159265359
scale = 6
!!!!!!!!!!!!!!!!!!!!!!!!!!!!!!!!!!!!!!!!!!!!!!!!!!!!!!!!!!!!!!!!!!!!!!!!!!!!!!!!
x1 = 0
y1 = 0
LOCAL, 11, 0, x1, y1, 0, 0, 0, 0

!!!!!!!!!!!!!!!!!!!!!!!!!!!!!!!!!!!!!!!!!!!!!!!!!!!!!!!!!!!!!!!!!!!!!!!!!!!!!!!!


L12 = 16.5e-3        !length preload beam
L34 = 7e-3              !length smalldff
L1112 = 6e-3            !length lever

!L1720 = 12.5e-3              !length total beam big dff
L1819 = 4.5e-3            !length ridig part big dff

L1720 = (6.5e-3+L1819)
L2526 = 2.9e-3          !length hooks
L2690 = 0.25e-3            !hook width
L1113 = 6.2e-3          !length arms lever
L2024 = 4e-3         !length between big dff arms one side
L220 = 8.5e-3              !length between center en inner big
dff
L35 =  1e-3             ! length between beams small dff
Loff = 1e-6          !offset for big dff
Curve_Rad1 = 1000e-3

LBuck=2
!!!!! Calculation for arce center1 !!!!!!
CX1 = -Curve_Rad1

!      material
E1 = 183e9
v1 = 0.3
rho1 = 7930       ! 7990 = stainless steel, originally 2320
Mu1 = 0.14



!!!!!!!!!!!!!!!!!!!!!!!!!!!!!!!!!!!!!!!!!!!!!!!!!!!!!!!!!!!!!!!!!!!!!!!!!!!!!!!!

n_elements = 20
substeps = 100             !was 100

/PREP7
ET,1,BEAM188
ET,2,MPC184
ET,3,BEAM188
KEYOPT,2,1,1


/ESHAPE,1

SECTYPE,1,BEAM,MESH,MEMS
SECOFFSET,CENT,,,
SECREAD,'MEMS_BeamCross_Marije_150umSteel','SECT','C:\
Users\Marije\Dropbox\02              Universiteit\Graduation
Project\Thesis - Small beam preload\4 Modeling',MESH

! Material properties 1
MP,EX,1,E1      ! Young's modulus
MP,PRXY,1,v1     ! Poisson's ratio
MP,DENS,1,rho1     ! Density
MP,Mu,1,Mu1


SECTYPE,3,BEAM,MESH,MEMS
SECOFFSET,CENT,,,
SECREAD,'MEMS_BeamCross_Marije_100umSteel','SECT','C:\
Users\Marije\Dropbox\02              Universiteit\Graduation
Project\Thesis - Small beam preload\4 Modeling',MESH



!!!!!!!!!!!!!!!!!!!!!!!!! Keypoints   !!!!!!!!!!!!!!!!!!!!!!!!

CSYS,11


k    ,     1 ,  3.08e-3          ,  49.50e-3      ,              0
k    ,     2 ,  3.08e-3          ,  -49.50e-3     ,              0
k    ,     3 ,  30.97e-3           ,  79.39e-3    ,              0
k    ,     4 ,  72.97e-3           ,  79.39e-3    ,              0
k    ,     5 ,  30.97e-3           ,  73.39e-3    ,              0
k    ,     6 ,  72.97e-3           ,  73.39e-3    ,              0
k    ,     7 ,  30.97e-3           ,  63.39e-3    ,              0
k    ,     8 ,  72.97e-3           ,  63.39e-3    ,              0
k    ,     9 ,  30.97e-3           ,  57.39e-3    ,              0
k    ,    10  ,  72.97e-3           ,57.39e-3     ,              0
k    ,    11  ,  30.77e-3           ,5.89e-3      ,              0
k    ,    12  ,  66.77e-3           ,5.89e-3      ,              0
k    ,    13  ,  30.77e-3           ,-31.31e-3    ,              0
k    ,    14  ,  66.77e-3           ,-31.31e-3    ,              0
k    ,    15  ,  30.77e-3           ,-68.51e-3    ,              0
k    ,    16  ,  66.77e-3           ,-68.51e-3    ,              0
k    ,    17  ,  91.90e-3           ,-9.77e-3     ,              0
k    ,    18  ,  91.91e-3           ,-29.27e-3    ,              0
k    ,    19  ,  91.90e-3           ,-56.27e-3    ,              0
k    ,    20  ,  91.90e-3           ,-75.77e-3    ,              0
k    ,    21  ,  140.00e-3   ,  -9.77e-3         ,              0
k    ,    22  ,  140.00e-3   ,  -29.27e-3        ,              0
k    ,    23  ,  140.00e-3   ,  -56.27e-3        ,              0
k    ,    24  ,  140.00e-3   ,  -75.77e-3        ,              0
k    ,    25  ,  16.57e-3           ,55.47e-3     ,              0
k    ,    26  ,  16.57e-3           ,38.06e-3     ,              0

!mirror
k    ,    201 ,  -3.08e-3      ,  49.50e-3      ,              0
k    ,    202 ,  -3.08e-3      ,  -49.50e-3     ,              0
k    ,    203 ,  -30.97e-3   ,  79.39e-3        ,              0
k    ,    204 ,  -72.97e-3     ,  79.39e-3      ,              0
k    ,    205 ,  -30.97e-3   ,  73.39e-3        ,              0
k    ,    206 ,  -72.97e-3     ,  73.39e-3      ,              0
k    ,    207 ,  -30.97e-3   ,  63.39e-3        ,              0
k    ,    208 ,  -72.97e-3     ,  63.39e-3      ,              0
k    ,    209 ,  -30.97e-3   ,  57.39e-3        ,              0
k    ,    210 ,  -72.97e-3     ,  57.39e-3      ,              0
k    ,    211 ,  -30.77e-3   ,  5.89e-3         ,              0
k    ,    212 ,  -66.77e-3   ,  5.89e-3         ,              0
k    ,    213 ,  -30.77e-3   ,  -31.31e-3       ,              0
k    ,    214 ,  -66.77e-3   ,  -31.31e-3       ,              0
k    ,    215 ,  -30.77e-3   ,  -68.51e-3       ,              0
k    ,    216 ,  -66.77e-3   ,  -68.51e-3       ,              0
k    ,    217 ,  -91.90e-3   ,  -9.77e-3        ,              0
k    ,    218 ,  -91.91e-3   ,  -29.27e-3       ,              0
k    ,    219 ,  -91.90e-3   ,  -56.27e-3       ,              0
k    ,    220 ,  -91.90e-3   ,  -75.77e-3       ,              0
k    ,    221 ,  -140.00e-3  ,  -9.77e-3        ,              0
```

```
k   ,   222 ,  -140.00e-3  ,  -29.27e-3   ,        0
k   ,   223 ,  -140.00e-3  ,  -56.27e-3   ,        0
k   ,   224 ,  -140.00e-3  ,  -75.77e-3   ,        0
k   ,   225 ,  -16.57e-3   ,  55.47e-3    ,        0
k   ,   226 ,  -16.57e-3   ,  38.06e-3    ,        0
k   ,   300 ,  -(Curve_Rad1)*scale,     0,         0


!!!!!!!!! Lines !!!!!!!!!!!!!!!!!!!!!!!!!!!!!!


!!!!!!!!!Flexures type 1   !!!!!!
*GET,Line_ID1,LINE,0,NUM,MAXD
CSYS,11


LARC,1,2,300,Curve_Rad1
!LARC,30,31,300,Curve_Rad1
L   ,   3 ,  4
L   ,   5 ,  6
L   ,   7 ,  8
L   ,   9 ,  10
L   ,   11  ,  12
L   ,   13  ,  14
L   ,   15  ,  16



L   ,   25,  26

LARC,201,202,300,Curve_Rad1
!LARC,230,231,300,Curve_Rad1
L   ,   203 ,  204
L   ,   205 ,  206
L   ,   207 ,  208
L   ,   209 ,  210
L   ,   211 ,  212
L   ,   213 ,  214
L   ,   215 ,  216



L   ,   225 ,  226




*GET,Line_ID2,LINE,0,NUM,MAXD


!!!!!!!!!Rigidlines!!!!!!!!!
CSYS,11

L   ,   1 ,  7
L   ,   1 ,  9
L   ,   7 ,  9

L   ,   4 ,  6
L   ,   8 ,  10
L   ,   6 ,  8
L   ,   4 ,  10
L   ,   4 ,  8

L   ,   11  ,  13
L   ,   16  ,  13
L   ,   16  ,  11

L   ,   14  ,  17
L   ,   17  ,  21
L   ,   14  ,  21

L   ,   18,  19
L   ,   22,  23

L   ,   15  ,  20
L   ,   20  ,  2
L   ,   2 ,  15

L   ,   9 ,  25
L   ,   7 ,  25

!L , 226 , 290
!mirror

L   ,   201 ,  207
L   ,   201 ,  209
L   ,   207 ,  209

L   ,   204 ,  206
L   ,   208 ,  210
L   ,   206 ,  208
L   ,   204 ,  210
L   ,   204 ,  208

L   ,   211 ,  213
L   ,   216 ,  213
L   ,   216 ,  211

L   ,   214 ,  217
L   ,   217 ,  221
L   ,   214 ,  221

L   ,   218,   219
L   ,   222,   223

L   ,   215 ,  220
L   ,   220 ,  202
L   ,   202 ,  215

L   ,   209 ,  225
L   ,   207 ,  225

!L , 26 , 90
!cross links
L   ,   20  ,  220
L   ,   21  ,  221
L   ,   17  ,  217
L   ,   21  ,  217
L   ,   17  ,  221
L   ,   25  ,  225
L   ,   15,  215

L   ,   1,    201        !outer preload beams
L   ,   2,    202
L   ,   1,    207
L   ,   7,    201
L   ,   20,  202
L   ,   2,    220


!!!!!!!!!Flexures type 3   !!!!!!
*GET,Line_ID3,LINE,0,NUM,MAXD
CSYS,11

L   ,   17  ,  18
L   ,   19  ,  20
L   ,   21  ,  22
L   ,   23  ,  24

L   ,   217 ,  218
L   ,   219 ,  220
L   ,   221 ,  222
L   ,   223 ,  224

*GET,Line_ID4,LINE,0,NUM,MAXD
!!!!!!!!!!!!!!!!!!!!!!!!!!!!!!!!!!!!!!!!!!!!!!!!!!!!!!!!!!!!!!!!!!!!!!!!!!!!!!!!
    Meshing
```

```
!!!!!!!!!!!!!!!!!!!!!!!!!!!!!!!!!!!!!!!!!!!!!!!!!!!!!!!!!!!!!!!!!!!!!!!!!!!!!!!!!!!!!!!
!!!!!!!!!!!

!   flexures type 1
TYPE,1
SECNUM,1
Mat,1
LSEL,S,LINE,,Line_ID1+1 ,Line_ID2
LESIZE,ALL, , ,n_elements
LMESH,ALL

!   ridig lines
TYPE,2
SECNUM,1
Mat,1
LSEL,S,LINE,,Line_ID2+1 ,Line_ID3
LESIZE,ALL, , ,1
LMESH,ALL

!   flexures type 3
TYPE,1
SECNUM,3
Mat,1
LSEL,S,LINE,,Line_ID3+1 ,Line_ID4
LESIZE,ALL, , ,1
LMESH,ALL


!!!!!!!!!!!!!!!!!!!!!!!
/SOL
/ESHAPE,1
NLGEOM,1
OUTRES,ALL,ALL
SOLCONTROL,ON,ON
AUTOTS,ON
NEQIT,10
NSUBST,substeps ,,substeps

!!!!!!!!!!!!!!!!!!!!!!!!!!!!!!!!!!!!!!!!!!!!!!!!!!!!!!!!!!!!!!!!!!!!
!!!!!!!!!!!!!!!First OneDOF Motion Output Is Free!!!!!!!!!!!!!!!!!
!!!!!!!!!!!!!!!!!!!!!!!!!!!!!!!!!!!!!!!!!!!!!!!!!!!!!!!!!!!!!!!!!!!!

TIME,1

dk  ,     3 ,  all
dk  ,     5 ,  all
dk  ,     12  ,  all
dk  ,     24  ,  all

dk  ,     203 ,  all
dk  ,     205 ,  all
dk  ,     212 ,  all
dk  ,     224 ,  all

!dk,1,uy, -0.25e-3*scale        !preloading
SOLVE

Time,2
DK,2,ux, 2.7e-3*scale
SOLVE

Time, 3
DK,2,ux, -2.7e-3*scale
SOLVe

!!!!!!!!!!!!!!!!!!!!!!!!!!!!!!!!!!!!!!!!!!!!!!!!!!!!!!!!!!!!!!!!!!!!
/POST1
/RGB,INDEX, 100, 100, 100, 0
/RGB,INDEX, 80, 80, 80, 13
/RGB,INDEX, 60, 60, 60, 14
/RGB,INDEX, 0, 0, 0,15
/ESHAPE,1
PLDISP,0

! to read stiffnesses, timehist > click plus sign > add dof > choose displacement > choose a node > ok > in the timehist first pop-up click the graph button.


!read keypoint to nodes
!klist          !keypoints to nodes uitlezen
!nlist          !all desiplacements from nodes


!/DSCALE Sets the displacement multiplier for displacement displays
!/post26
!LINES,2000   !perhaps use this earlier
!NSOL,2,2,U,X, UX_2,
!STORE,MERGE
!PRVAR,2,

!stress plot
/EFACET,1
PLNSOL, S,EQV, 0,1.0
/DIST,1,1.08222638492,1
/REP,FAST
/REPLOT,RESIZE


/POST26

ID_Node = 2
TIMERANGE,0,3        !Set the timerange over which you want to save data
RFORCE,2,ID_Node,F,X,FX    !Get reaction force data on nodenumber ID_Node
NSOL,3,ID_Node,U,X,UX      !Get displacement data on node number ID_Node
XVAR,3
PLVAR,2


*CREATE,scratch,gui   !Write data to file
  *DEL,VAR_export
  *DIM,VAR_export,TABLE,302,4          !Set dimension of table (each dimension is always 1 bigger, so this is a 20x3 table)
   VGET,VAR_export(1,0),1
   VGET,VAR_export(1,1),2
   VGET,VAR_export(1,2),3

/OUTPUT,'Prototype4_FXUXKP2_Unpreloaded','txt','C:\Users\Marije\Dropbox\02 Universiteit\Graduation Project\Thesis - Small beam preload\4 Modeling\Final Force displacement analysys'        !change to your own file name/location

*VWRITE,VAR_export(1,0),VAR_export(1,1),VAR_export(1,2)
  %G, %G, %G
  /OUTPUT,TERM
  *END
  /INPUT,scratch,gui
```

6.5 Prototype model for Modal analysis

```
FINISH
/CLEAR
/OUTPUT


pi = 3.14159265359
scale = 6
!!!!!!!!!!!!!!!!!!!!!!!!!!!!!!!!!!!!!!!!!!!!!!!!!!!!!!!!!!!!!!!!!!!!!!!!!!!
x1 = 0
y1 = 0
LOCAL, 11, 0, x1, y1, 0, 0, 0, 0

!!!!!!!!!!!!!!!!!!!!!!!!!!!!!!!!!!!!!!!!!!!!!!!!!!!!!!!!!!!!!!!!!!!!!!!!!!!
nModes = 10

L codes equal to Prototype stiffness code

!     material
E1 = 183e9
v1 = 0.3
rho1 = 7930       ! 7990 = stainless steel, originally 2320
Mu1 = 0.14

E2 = 0
v2 = 0
rho2 = 0      ! 7990 = stainless steel, originally 2320
Mu2 = 0


!!!!!!!!!!!!!!!!!!!!!!!!!!!!!!!!!!!!!!!!!!!!!!!!!!!!!!!!!!!!!!!!!!!!!!!!!!!
n_elements = 20
substeps = 150            !was 100

/PREP7
ET,1,BEAM188
ET,2,MPC184
ET,3,BEAM188

ET,5, MASS21
      !freq anal.
KEYOPT,2,1,1


/ESHAPE,1

SECTYPE,1,BEAM,MESH,MEMS
SECOFFSET,CENT,,,
SECREAD,'MEMS_BeamCross_Marije_150umSteel','SECT','C:\
Users\Marije\Dropbox\02                Universiteit\Graduation
Project\Thesis - Small beam preload\4 Modeling',MESH

! Material properties 1
MP,EX,1,E1     ! Young's modulus
MP,PRXY,1,v1    ! Poisson's ratio
MP,DENS,1,rho1    ! Density
MP,Mu,1,Mu1

! Material properties 1
MP,EX,2,E2     ! Young's modulus
MP,PRXY,2,v2    ! Poisson's ratio
MP,DENS,2,rho2    ! Density
MP,Mu,2,Mu2

SECTYPE,3,BEAM,MESH,MEMS
SECOFFSET,CENT,,,
SECREAD,'MEMS_BeamCross_Marije_100umSteel','SECT','C:\
Users\Marije\Dropbox\02                Universiteit\Graduation
Project\Thesis - Small beam preload\4 Modeling',MESH

! point masses
R,   510, 7.32e-3      , 7.32e-3    , 7.32e-3                ,
155.45e-9    , 2227.93e-9      , 2305.33e-9
R,   520, 52.74e-3 , 52.74e-3 , 52.74e-3     ,          9231.24e-9
          , 122089.71e-9     , 130758.38e-9
R,   530, 52.54e-3 , 52.54e-3 , 52.54e-3     ,      113150.83e-9
     , 480215.55e-9   , 592805.93e-9
R,   541, 2.13e-3      , 2.13e-3   , 2.13e-3                ,
151.66e-9    , 22.66e-9       , 151.64e-9
R,   542, 2.13e-3      , 2.13e-3   , 2.13e-3                ,
151.66e-9    , 22.66e-9       , 151.64e-9
R,   551, 0.41e-3    , 0.41e-3      , 0.41e-3                ,  5.47e-
9            , 3.30e-9           , 4.39e-9
R,   552, 0.41e-3    , 0.41e-3      , 0.41e-3                ,  5.47e-
9            , 3.30e-9           , 4.39e-9
R,   561, 5.59e-3    , 5.59e-3      , 5.59e-3                ,
2750.88e-9  , 1384.75e-9    , 4076.06e-9
R,   562, 5.59e-3    , 5.59e-3      , 5.59e-3                ,
2750.88e-9  , 1384.75e-9    , 4076.06e-9
R,   571, 1.58e-3      , 1.58e-3    , 1.58e-3                ,
103.60e-9    , 13.54e-9       , 100.27e-9
R,   572, 1.58e-3      , 1.58e-3    , 1.58e-3                ,
103.60e-9    , 13.54e-9       , 100.27e-9
R,   573, 1.58e-3    , 1.58e-3      , 1.58e-3                ,
103.60e-9    , 13.54e-9       , 100.27e-9
R,   574, 1.58e-3    , 1.58e-3      , 1.58e-3                ,
103.60e-9    , 13.54e-9       , 100.27e-9

!!!!!!!!!!!!!!!!!!!!!!!!!! Keypoints   !!!!!!!!!!!!!!!!!!!!!!!!!!

Keypoint codes equal to prototype stiffness code

!!! keypoints for masses

k, 510,     0,              60.04/1000,              0
        !preloadblock
k, 520,     0,              -87.15/1000,             0
        !central/main shuttle
k, 530,     0,              -68.95/1000,             0
        !secondary shuttle
k, 541,     -78.99/1000,    68.39/1000,              0
        !preload secondary shuttle left
k, 542,     76.99/1000,           68.39/1000,
     0      !preload secondary shuttle right
k, 551,     -15.43/1000,    33.80/1000,              0
        !hook left
k, 552,     15.43/1000,           33.80/1000,
     0      !hook right
k, 561,     -42.03/1000,    -36.47/1000,
     0      !lever left
k, 562,     42.03/1000,           -36.47/1000,
     0      !lever left
k, 571,     -140/1000,      -42.77/1000,
     0      !DFF midpieces from left to right
k, 572,     -91.90/1000,    -42.77/1000,
     0      !DFF midpieces
k, 573,     91.90/1000,           -42.77/1000,
     0      !DFF midpieces
k, 574,     140/1000,       -42.77/1000,
     0      !DFF midpieces

!!!!!!!!! Lines !!!!!!!!!!!!!!!!!!!!!!!!!!!!!!!


!!!!!!!!!Flexures type 1   !!!!!!!
*GET,Line_ID1,LINE,0,NUM,MAXD
CSYS,11


LARC,1,2,300,Curve_Rad1
```

```
L   ,   3 , 4
L   ,   5 , 6
L   ,   7 , 8
L   ,   9 , 10
L   ,   11 , 12
L   ,   13 , 14
L   ,   15 , 16
L   ,   25, 26

LARC,201,202,300,Curve_Rad1
L   ,   203, 204
L   ,   205, 206
L   ,   207, 208
L   ,   209, 210
L   ,   211, 212
L   ,   213, 214
L   ,   215, 216
L   ,   225, 226


*GET,Line_ID2,LINE,0,NUM,MAXD
!!!!!!!!!Rigidlines!!!!!!!!!!
CSYS,11

L   ,   1 , 7           !preloadblock
L   ,   1 , 9
L   ,   7 , 9
L   ,   9 , 25
L   ,   7 , 25
L ,  1 ,  510



L   ,   4 , 6
L   ,   8 , 10
L   ,   6 , 8
L   ,   4 , 10
L   ,   4 , 8
L ,  6   , 542
L , 8    , 542

L   ,   11 , 13
L   ,   16 , 13
L   ,   16 , 11
L , 13 , 562
L ,  16,   562

L   ,   14 , 17
L   ,   17 , 21
L   ,   14 , 21
L ,  14,  530

L   ,   18 , 19
L   ,   18 , 573
L   ,   19 , 573

L   ,   22 , 23
L   ,   22, 574
L   ,   23 , 574

L   ,   15 , 20
L   ,   15 , 520

L   ,   20 , 2
L   ,   2 , 15

L, 26, 552



!mirror

L   ,   201,  207
L   ,   201,  209
L   ,   207,  209
L ,  201 ,  510

L   ,   204,  206
L   ,   208,  210
L   ,   206,  208
L   ,   204,  210
L   ,   204,  208
L ,  206  , 541
L ,  208,  541

L   ,   211,  213
L   ,   216,  213
L   ,   216,  211
L ,  213   , 561
L ,  216  , 561

L   ,   214,  217
L   ,   217,  221
L   ,   214,  221
L ,  214   , 530

L   ,   218,  219
L   ,   218,  572
L   ,   219   , 572

L   ,   222,  223
L   ,   222   , 571
L   ,   223   , 571

L   ,   215,  220
L   ,   215   , 520

L   ,   220,  202
L   ,   202,  215

L   ,   209,  225
L   ,   207,  225

L, 226, 551
!cross links
L   ,   20  , 220
L   ,   21  , 221
L   ,   17  , 217
L   ,   21  , 217
L   ,   17  , 221
L   ,   25  , 225
L   ,   15, 215

L   ,   1,   201      !outer preload beams
L   ,   2,   202
L   ,   1,   207
L   ,   7,   201
L   , 20,   202
L   ,   2,   220

! lines for frequency analysis keypoints 500 series



!!!!!!!!!Flexures type 3   !!!!!!!
*GET,Line_ID3,LINE,0,NUM,MAXD
CSYS,11

L   ,   17  , 18
L   ,   19  , 20
L   ,   21  , 22
L   ,   23  , 24

L   ,   217,  218
L   ,   219,  220
L   ,   221,  222
L   ,   223,  224
```

```
*GET,Line_ID4,LINE,0,NUM,MAXD
!!!!!!!!!!!!!!!!!!!!!!!!!!!!!!!!!!!!!!!!!!!!!!!!!!!!!!!!!!!!!!!!!!!!!!!!!!!!
      Meshing
      !!!!!!!!!!!!!!!!!!!!!!!!!!!!!!!!!!!!!!!!!!!!!!!!!!!!!!!!!!!!!!!!!!!!!!!!!!!!
!!!!!!!!!!!

!     flexures type 1
TYPE,1
SECNUM,1
Mat,1
LSEL,S,LINE,,Line_ID1+1 ,Line_ID2
LESIZE,ALL, , ,n_elements
LMESH,ALL

!     ridig lines
TYPE,2
SECNUM,1
Mat,2
LSEL,S,LINE,,Line_ID2+1 ,Line_ID3
LESIZE,ALL, , ,1
LMESH,ALL

!     flexures type 3
TYPE,1
SECNUM,3
Mat,1
LSEL,S,LINE,,Line_ID3+1 ,Line_ID4
LESIZE,ALL, , ,1
LMESH,ALL

Type, 5
Real, 510
Kmesh, 510, 510

Type, 5
Real, 520
Kmesh, 520, 520

Type, 5
Real, 530
Kmesh, 530, 530

Type, 5
Real, 541
Kmesh, 541, 541

Type, 5
Real, 542
Kmesh, 542, 542

Type, 5
Real, 551
Kmesh, 551, 551

Type, 5
Real, 552
Kmesh, 552, 552

Type, 5
Real, 561
Kmesh, 561, 561

Type, 5
Real, 562
Kmesh, 562, 562

Type, 5
Real, 571
Kmesh, 571, 571

Type, 5
Real, 572
Kmesh, 572, 572

Type, 5
Real, 573
Kmesh, 573, 573

Type, 5
Real, 574
Kmesh, 574, 574



!!!!!!!!!!!!!!!!!!!!!!!!!!!!!!!!!!!!!!!!!!!!!!!!!!!!!!!!!!!!!!!!!!!!!!!!!!!!
!!!!!!!!!!!!!!!First OneDOF Motion Output Is Free!!!!!!!!!!!!!!!!!!
!!!!!!!!!!!!!!!!!!!!!!!!!!!!!!!!!!!!!!!!!!!!!!!!!!!!!!!!!!!!!!!!!!!!!!!!!!!!

!TIME,1

dk  ,    3 ,  all
dk  ,    5 ,  all
dk  ,    12  ,  all
dk  ,    24  ,  all

dk  ,    203 ,  all
dk  ,    205 ,  all
dk  ,    212 ,  all
dk  ,    224 ,  all

!dk,1,uy, -0.25e-3*scale        !preloading
!dk,2, all



!!!!!!!!!!!!!!!!!!!!!!!! static
/SOL
antype,0
/ESHAPE,1
OUTRES,ALL,ALL
SOLCONTROL,ON,ON
AUTOTS,ON

NLGEOM,1

AUTOTS,ON
!NEQIT,10
NSUB,substeps,substeps,substeps
save
solve
finish


!!!! modal analysis
!!!!!!!!! Step 2: modal analysis !!!!!!!!!!!!
/solu                    ! re-enter solution so we can do a new
analysis
antype,,restart,1,substeps,perturb     ! specify restart option
for linear perturbation
! from last substep in this case
perturb,modal            ! specify modal as next analysis
solve,elform             ! calculate element formulation with
solve command
modopt,subsp,nModes              ! specify modal options for
solution
mxpand,nModes,,,YES          ! specify number of modes for
results calc
solve
!!!!!!!!!!!!!!!!!!!!!!!!!!!!!!!!!!!!!!!!!!!!!!!!!!!!!!!!!!!!!!!!!!!!!!!!!!!!


!!!!!!!!!!! Postprocessing for frequency
/post1                   ! enter general postprocessor
INRES,ALL                ! make sure we read in all results
from file
```

```
FILE,'Prototype4','rstp'      ! specify special results file for modal results
! rsts file: modal analysis with sets being modes
! rst file: the static prestress results with sets being substeps
SET,LIST              ! List solutions


!!!!!!!!!!  Save mode shapes

/RGB,INDEX, 100, 100, 100, 0
/RGB,INDEX, 80, 80, 80, 13
/RGB,INDEX, 60, 60, 60, 14
/RGB,INDEX, 0, 0, 0,15



i_=1
*DO,i_,1,10,1
!i_1=2 !hoort hier eigenlijk niet
SET,,, ,,, ,i_ ! Select nth mode shape (set)

!PLDISP,0         ! 0 only deformed, 1 def + undeformed

PLNS,EPTO,EQV       ! nodal Von Misses strain

/ESHAPE,1          ! SCALE=1 (use real constants and section defenitions)
/GFILE, 2400
/SHOW,PNG

/VIEW,1,0,0,1       ! Window number, XV, YV, ZV

!/REP,FAST
/REPLOT

!ANMODE,10,0.15, ,0          ! Animate mode shape, ANMODE, NFRAM, DELAY, NCYCL, KACCEL

/image,save,strcat('Mode',chrval(i_)),png
i_=i_+1
/SHOW,CLOSE
*ENDDO


!!!!!!!!!!!!!!!!!! View mode shapes directly

SET,,, ,,, ,2 ! Select nth mode shape (set)

!PLDISP,0         ! 0 only deformed, 1 def + undeformed

PLNS,EPTO,EQV       ! nodal Von Misses strain

/ESHAPE,1          ! SCALE=1 (use real constants and section defenitions)

!/VIEW,1,1,1.3,3         ! Window number, XV, YV, ZV

!/VIEW,1,0,0,1        ! Window number, XV, YV, ZV
/VIEW,1,0,0,3       ! Window number, XV, YV, ZV



!/REP,FAST
/REPLOT

ANMODE,10,0.10, ,0   ! Animate mode shape, ANMODE, NFRAM, DELAY, NCYCL, KACCEL
```

7 Modelling stresses

7.1 MEMS, after preloading

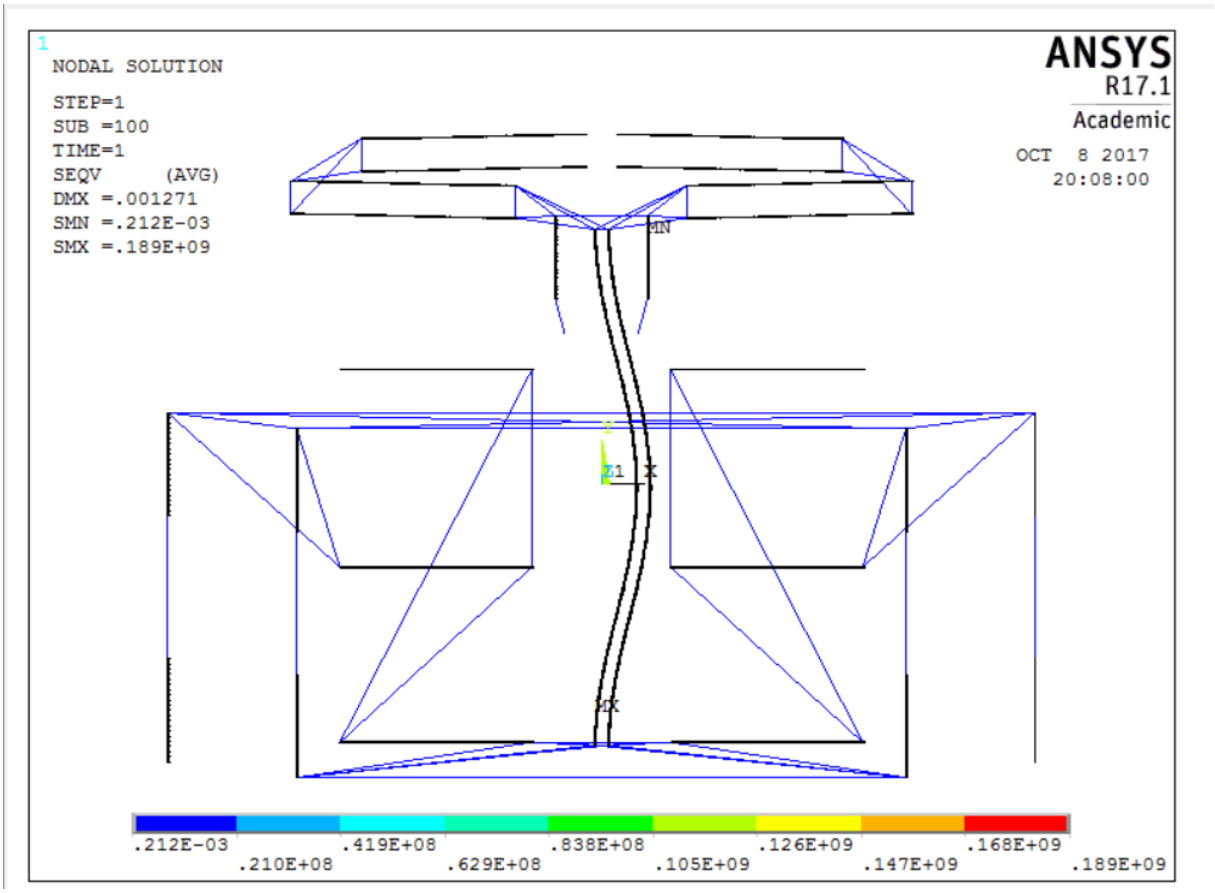

Figure 54 Deformation configuration after preloading MEMS

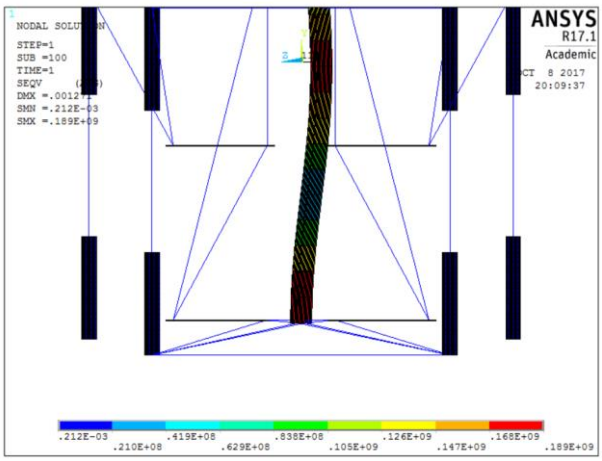

Figure 55 Stresses in flexures zoom-in bottow part

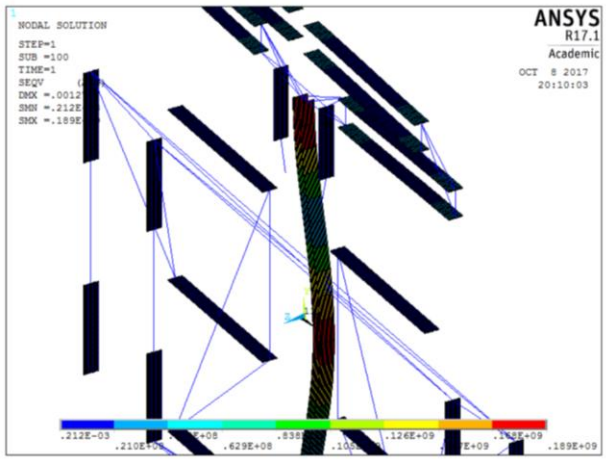

Figure 56 Stress in flexure soom in top-part

7.2 MEMS, at extreme MS displacement

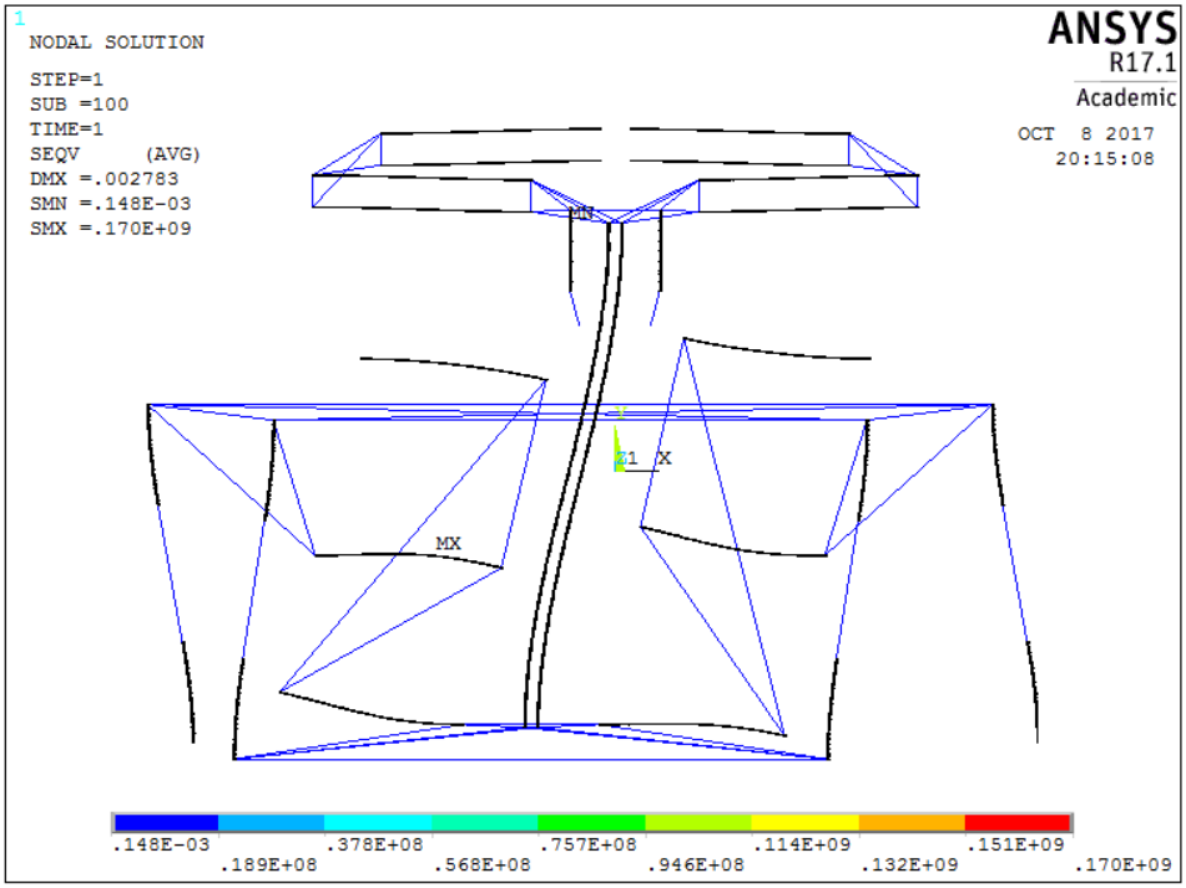

Figure 57 Deformation configuration at extreme MS displacement MEMS

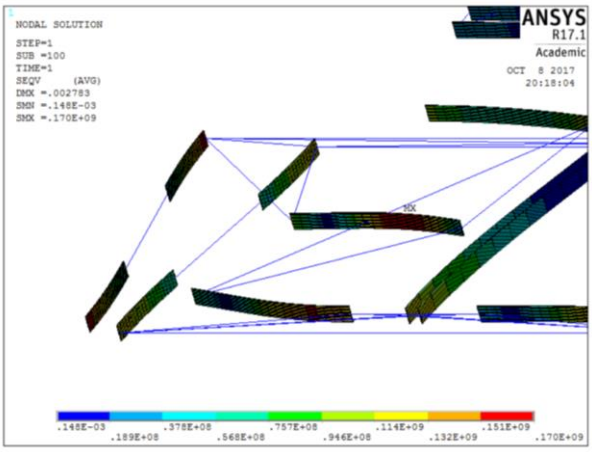

Figure 58 Stresses in flexures zoom-in bottow part left

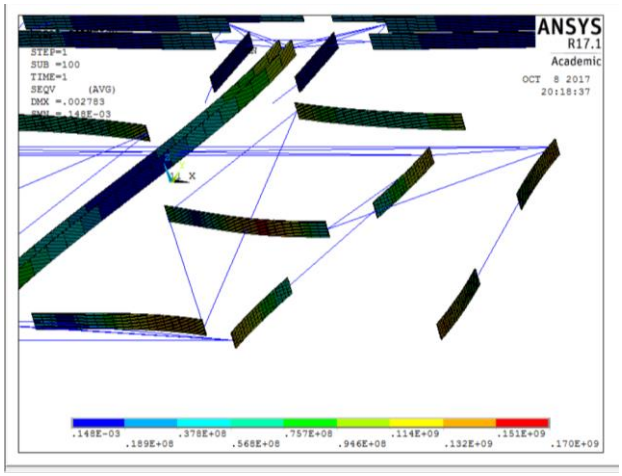

Figure 59 Stress in flexure soom in down-part right

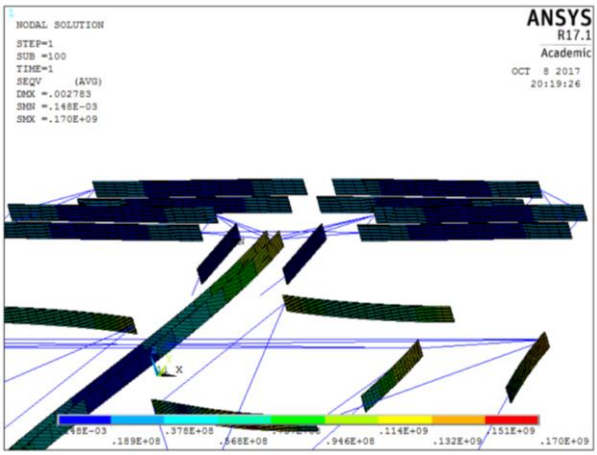

Figure 60 Stress in flexure zoom in top-part

7.3 Prototype, after prelaoding

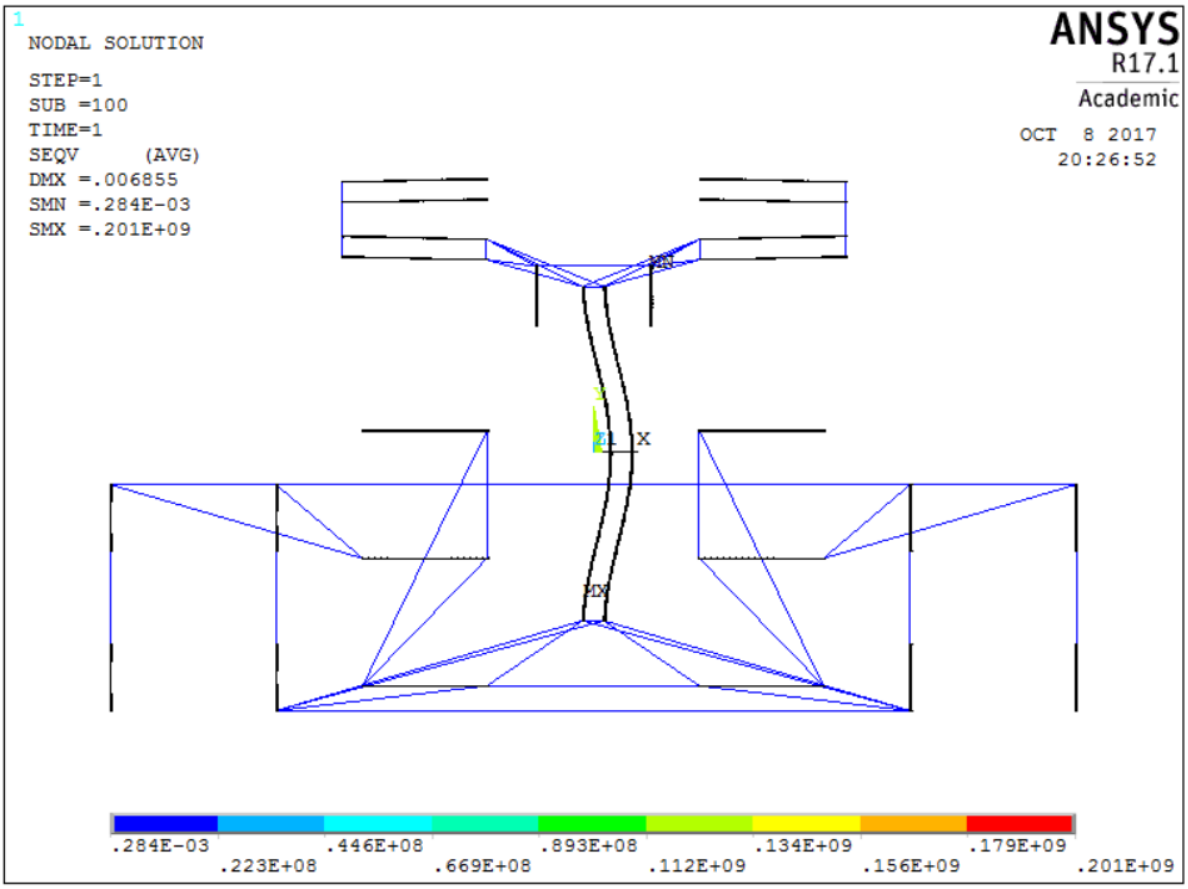

Figure 61 Deformation configuration after preloading Prototype

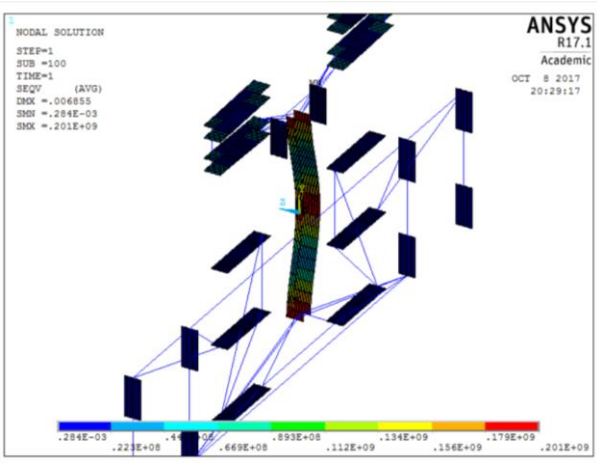

Figure 62 Stresses in flexures zoom-in bottow part

7.4 Prototype, at extreme MS displacment

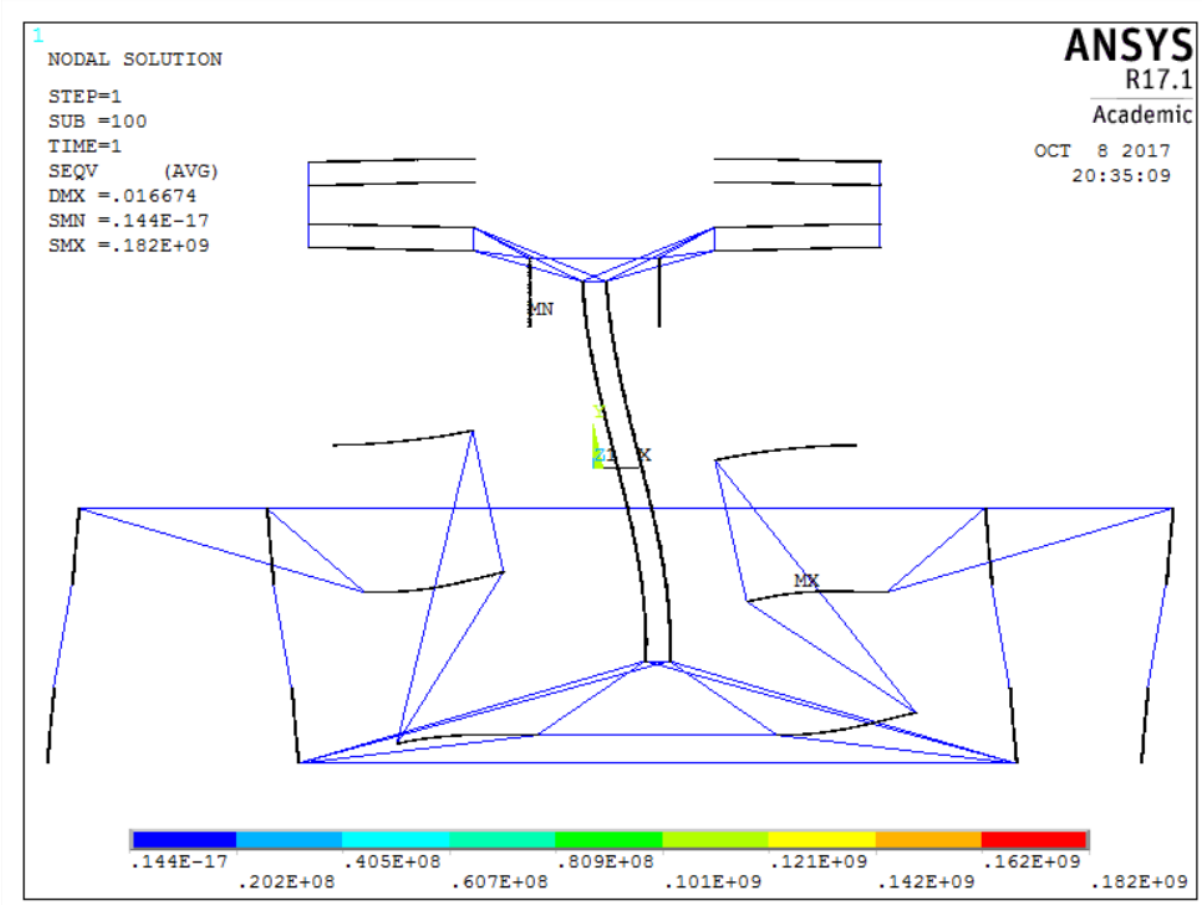

Figure 63 Deformation configuration at extreme MS displacement Prototype

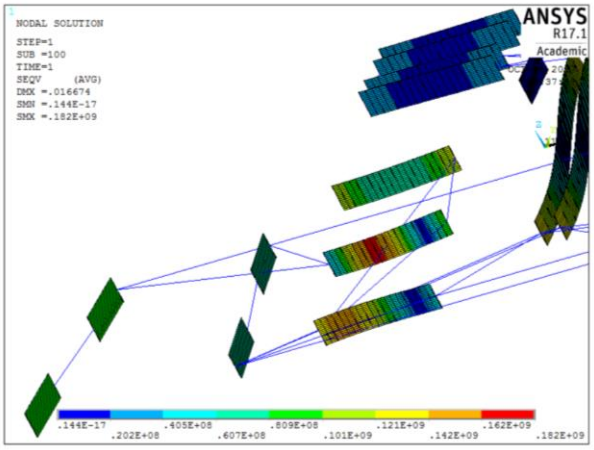

Figure 64 Stresses in flexures zoom-in bottow part left

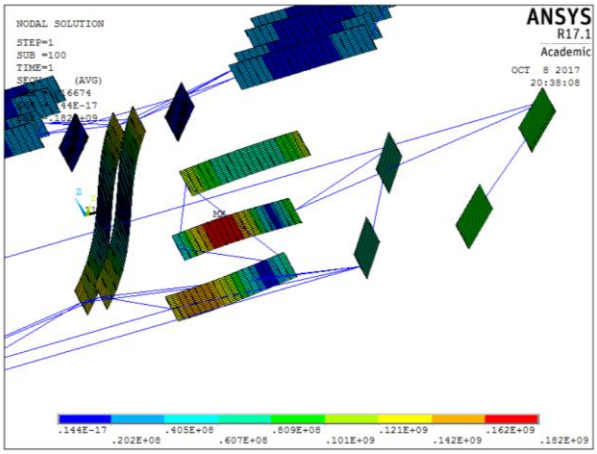

Figure 65 Stress in flexure soom in down-part right

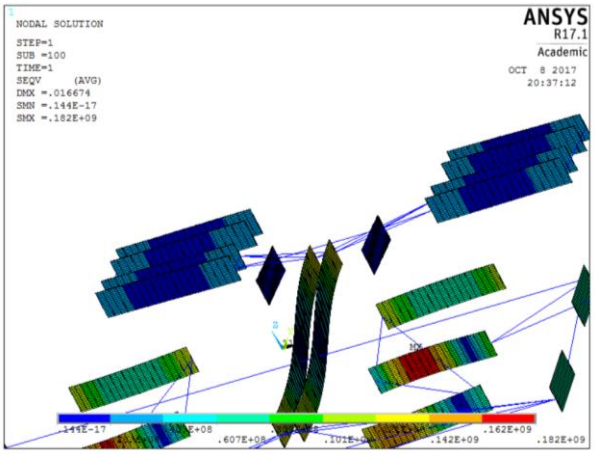

Figure 66 Stress in flexure zoom in top-part

7.5 Comsol modelling of hooks stresses

7.5.1 Tip displacement MEMS model

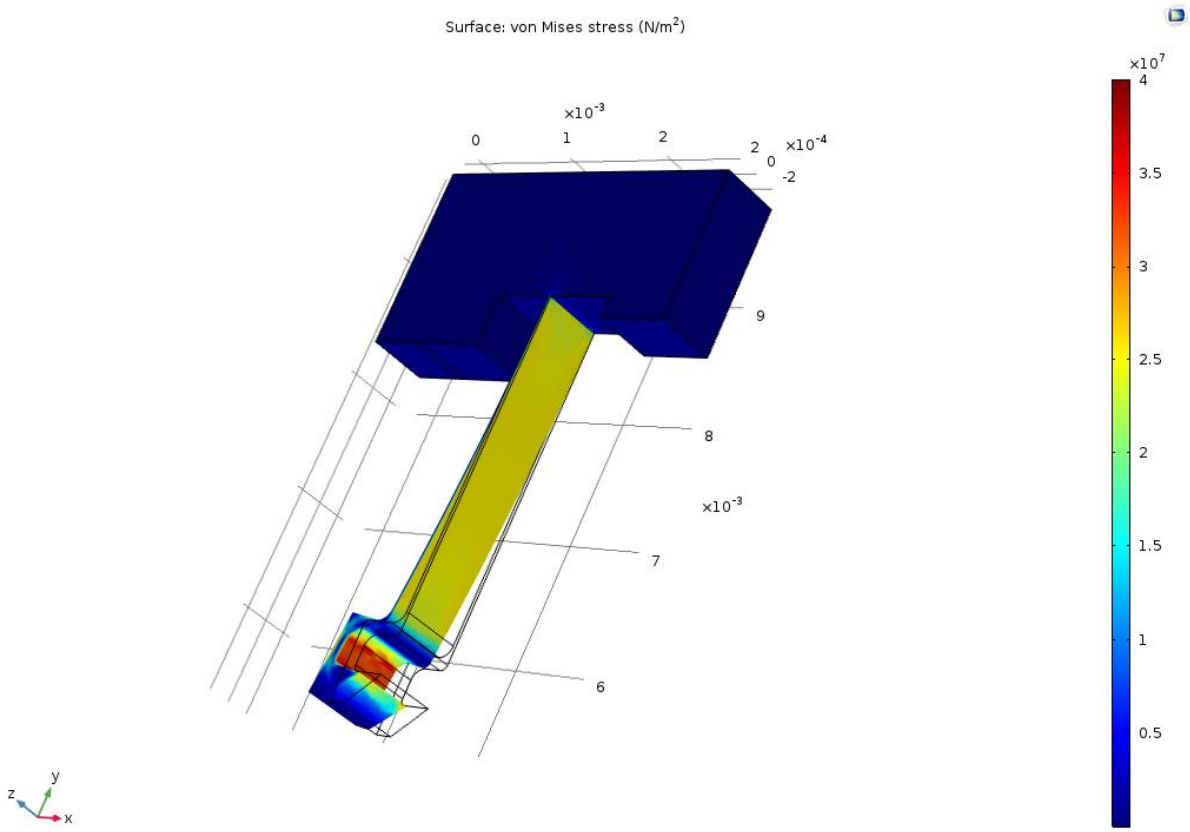

Figure 67 Tip displacement MEMS model

7.5.2 Tip load MEMS model

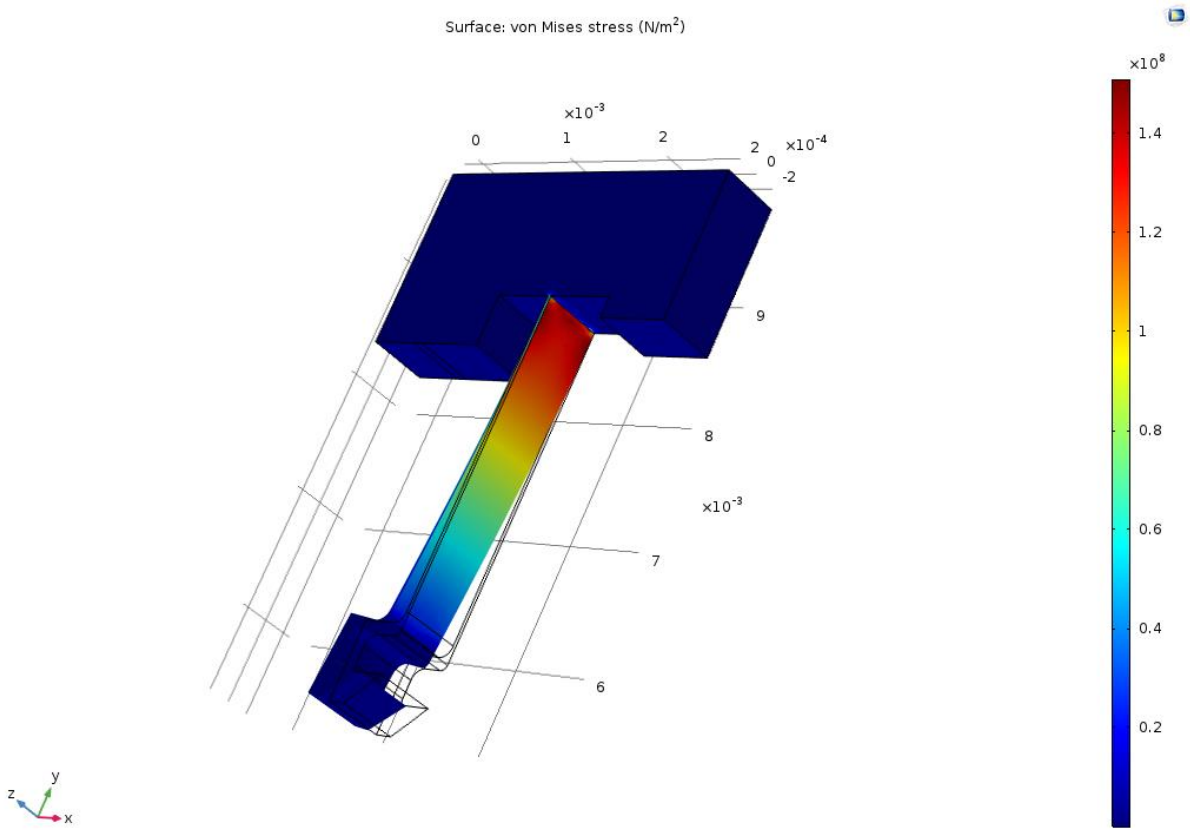

Figure 68 Tip load MEMS model

7.5.3 Tip load Prototype model

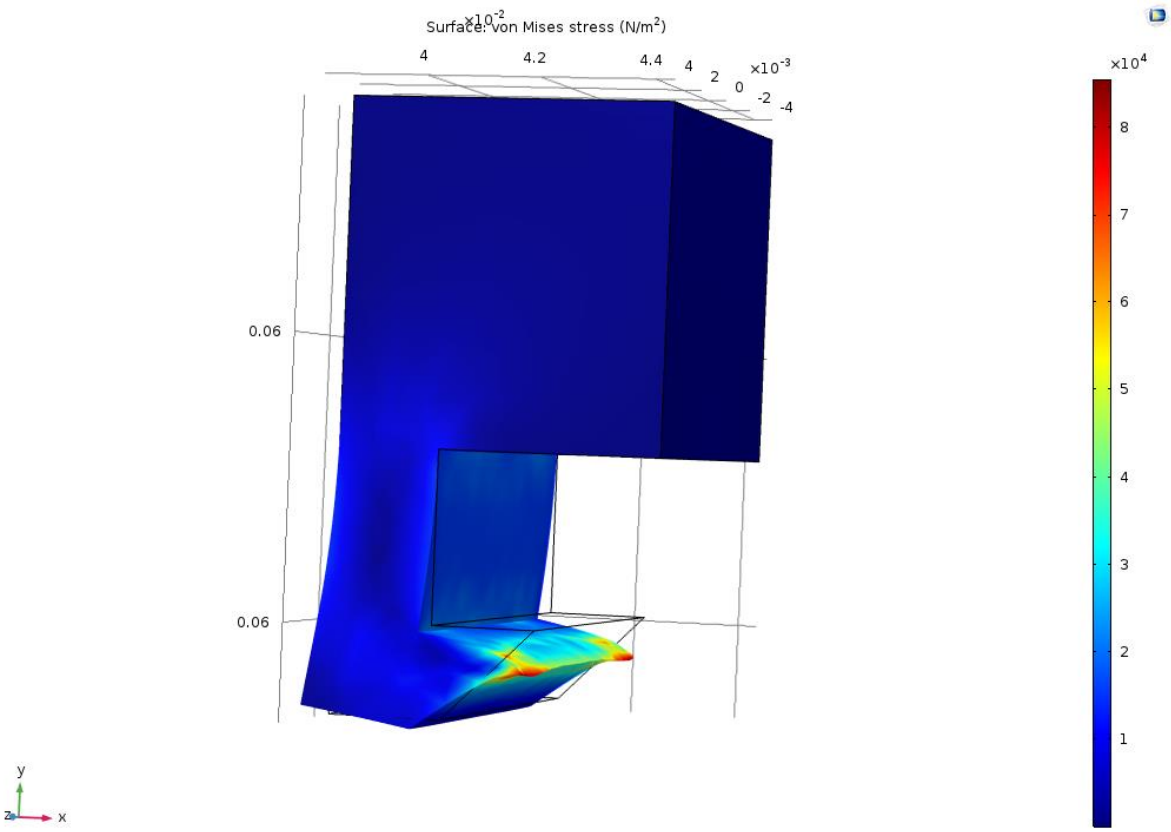

Figure 69 8.5.3 Tip load Prototype model

8 Eigenmodes

8.1 Models for MEMS

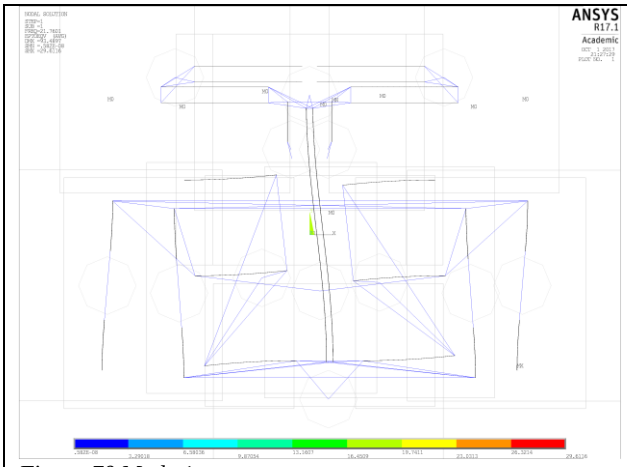

Figure 70 Mode 1

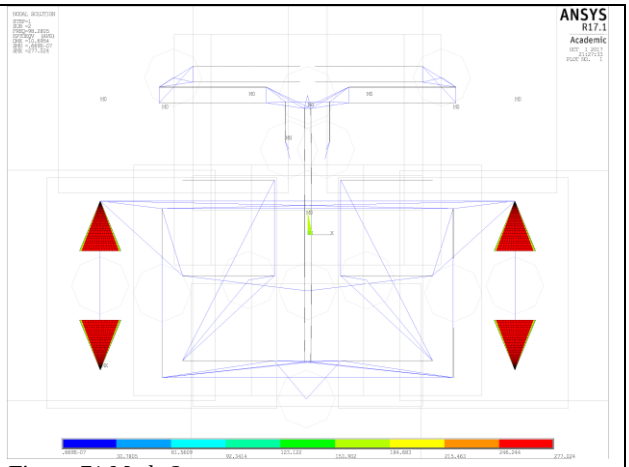

Figure 71 Mode 2

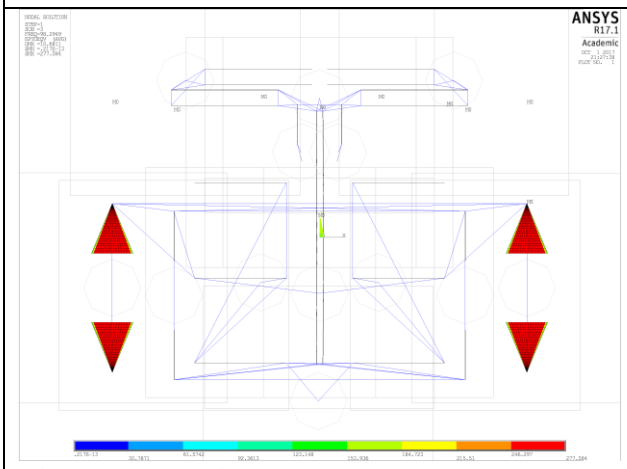

Figure 72 Mode 3

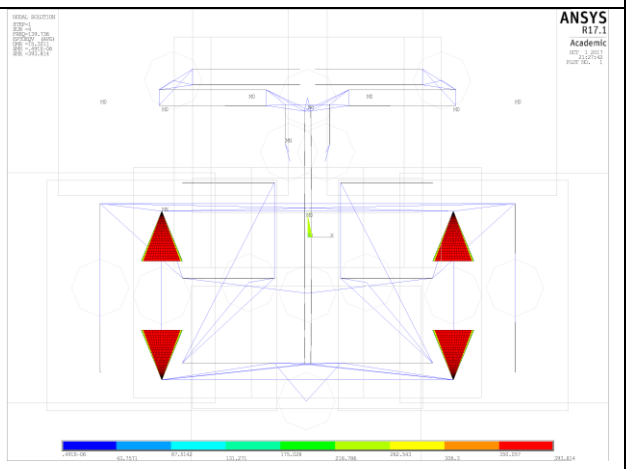

Figure 73 Mode 4

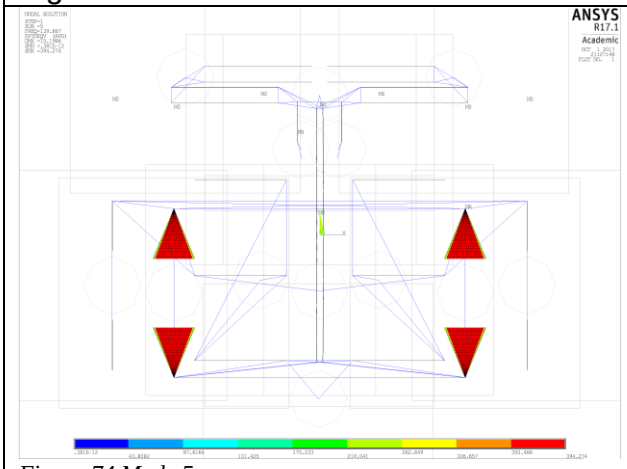

Figure 74 Mode 5

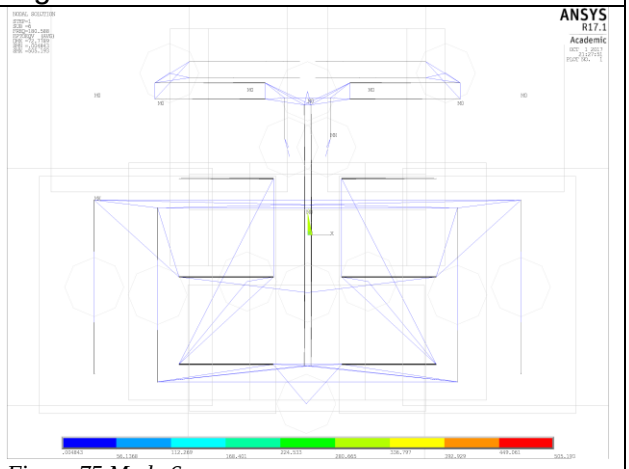

Figure 75 Mode 6

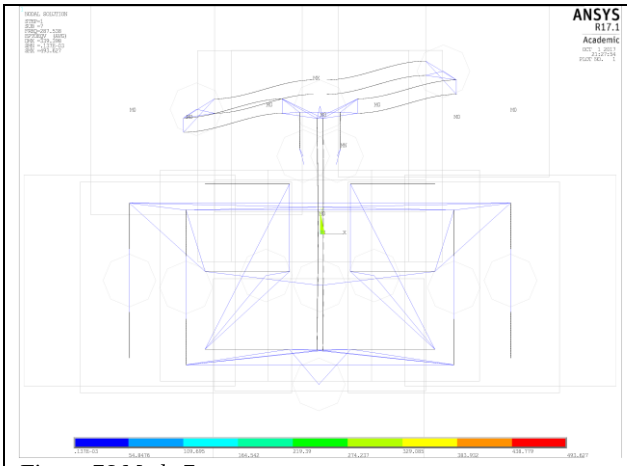

Figure 76 Mode 7

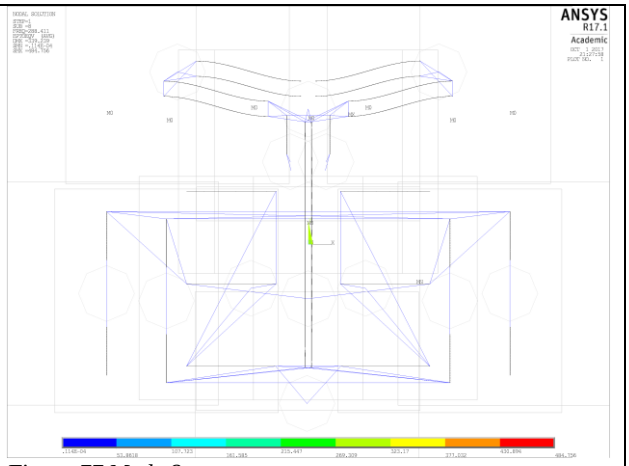

Figure 77 Mode 8

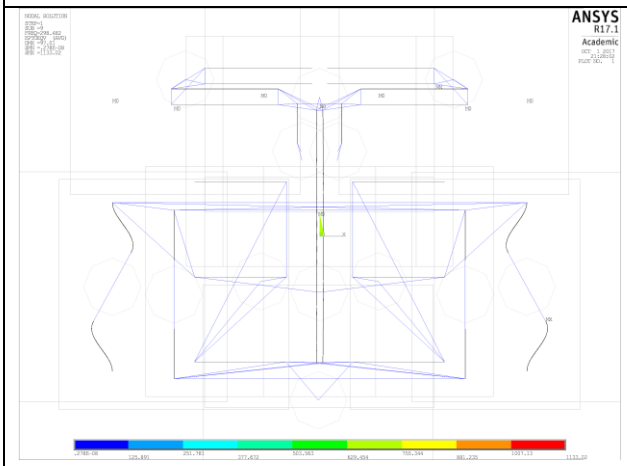

Figure 78 Mode 9

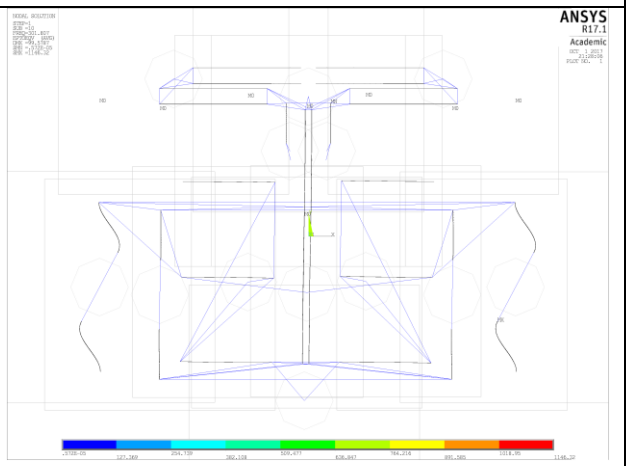

Figure 79 Mode 10

8.2 Modes for prototype

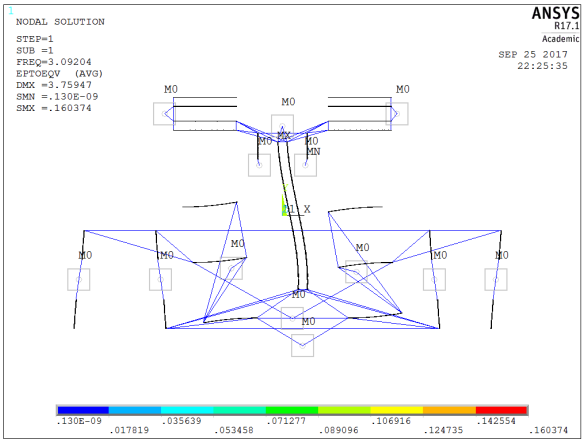

Figure 80 Mode 1

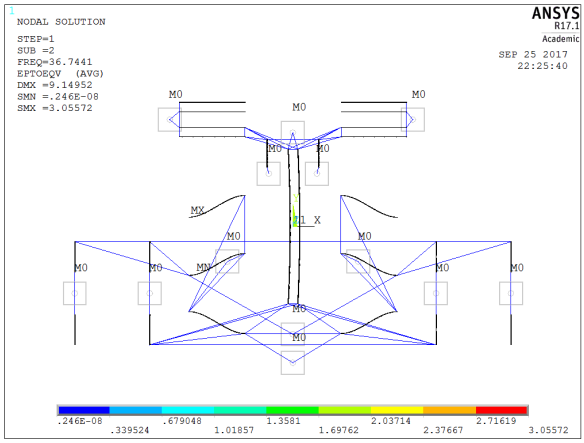

Figure 81 Mode 2

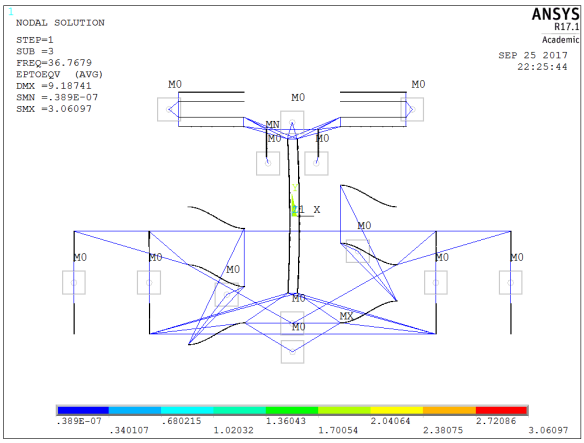

Figure 82 Mode 3

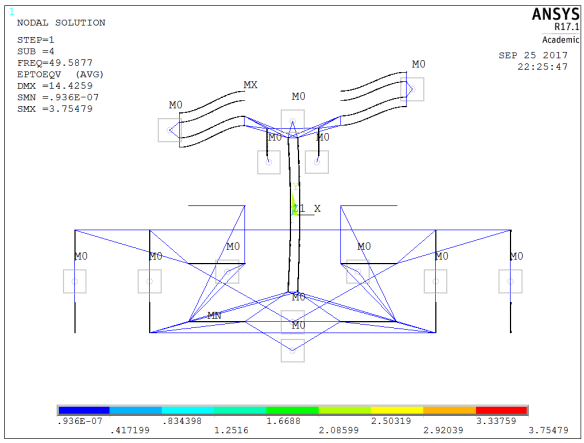

Figure 83 Mode 4

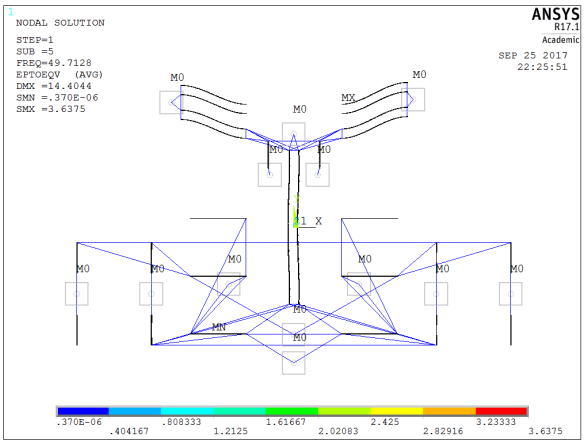

Figure 84 Mode 5

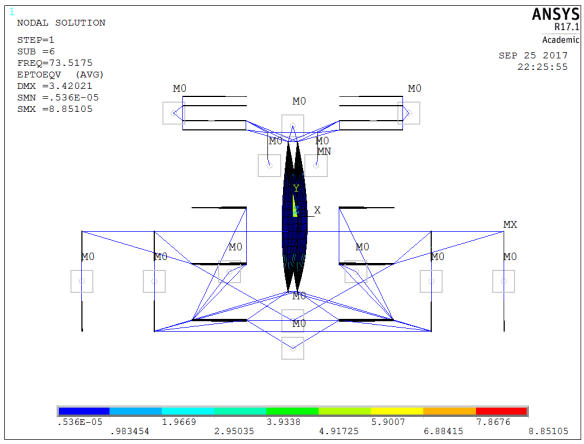

Figure 85 Mode 6

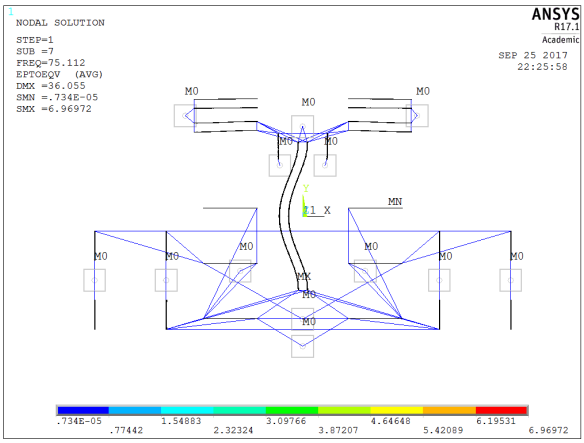

Figure 86 Mode 7

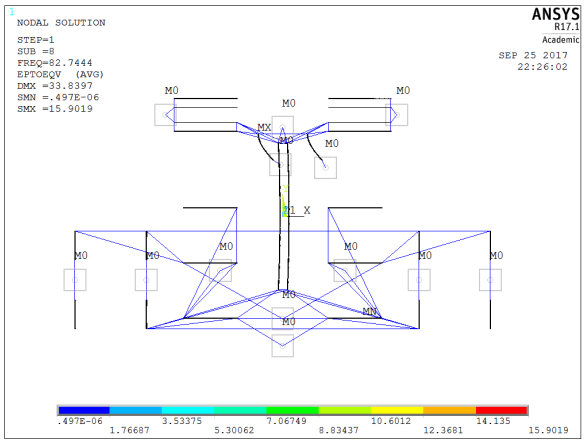

Figure 87 Mode 8

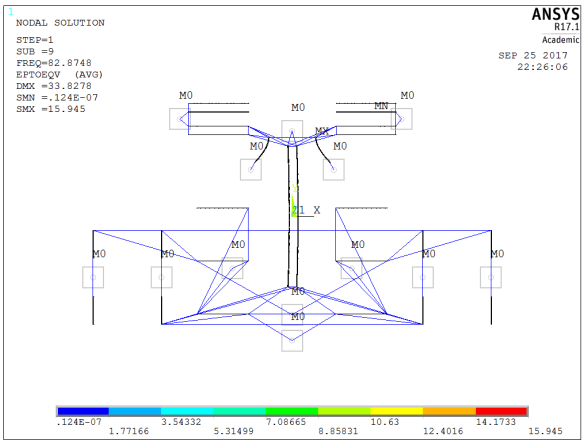

Figure 88 Mode 9

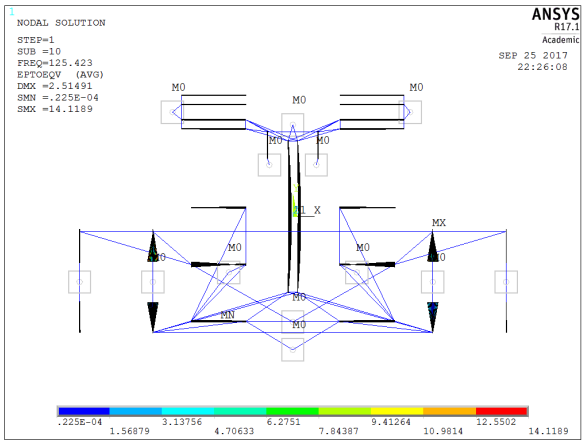

Figure 89 Mode 10

9 Bibliography

1. Hao, G., et al., *Conceptual design of compliant translational joints for high-precision applications.* Frontiers of Mechanical Engineering, 2014. **9**(4): p. 331-343.
2. Panas, R.M., *Eliminating underconstraint in double parallelogram flexure mechanisms.* Journal of Mechanical Design, 2015. **137**(9): p. 092301.
3. James D. Ervin, D.M., Gregory F. Ervin, Sridhar Kota, Joel A. Hetrick, *Surface Vibration Using compliant Mechanical Amplifier*. 2010: United State.
4. Mu, X.J., et al., *MEMS Electrostatic Double T-Shaped Spring Mechanism for Circumferential Scanning.* Journal of Microelectromechanical Systems, 2013. **22**(5): p. 1147-1157.
5. Choi, K.B., J.J. Lee, and S. Hata, *A piezo-driven compliant stage with double mechanical amplification mechanisms arranged in parallel.* Sensors and Actuators a-Physical, 2010. **161**(1-2): p. 173-181.
6. Hetrick, J. and S. Kota, *An energy formulation for parametric size and shape optimization of compliant mechanisms.* Journal of Mechanical Design, 1999. **121**(2): p. 229-234.
7. Hetrick, J.A., *AN ENERGY EFFICIENCY APPROACH FOR UNIFIED TOPOLOGICAL AND DIMENSIONAL SYNTHESIS OF COMPLIANT MECHANISMS*, in *Mechanical Engineering*. 1999, University of Michigan: USA. p. 172.
8. J, M.H., *Motion amplication switch means*. 1964, Texas Instruments Inc: United State.
9. Mattson, C.A., L.L. Howell, and S.P. Magleby, *Development of commercially viable compliant mechanisms using the pseudo-rigid-body model: case studies of parallel mechanisms.* Journal of Intelligent Material Systems and Structures, 2004. **15**(3): p. 195-202.
10. Haruhiko Harry Asada, D.M.N., *Phased array buckling actuator*. 2013, Massachusetts Institute Of Technology: United State.
11. Krishnan, G., C. Kim, and S. Kota, *LOAD-TRANSMITTER CONSTRAINT SETS: PART I-AN EFFECTIVE TOOL FOR VISUALIZING LOAD FLOW IN COMPLIANT MECHANISMS AND STRUCTURES.* Ann Arbor, 2010. **1001**: p. 48109.
12. Grossard, M., et al., *Gramian-based optimal design of a dynamic stroke amplifier compliant micro-mechanism*. 2007 Ieee/Rsj International Conference on Intelligent Robots and Systems, Vols 1-9. 2007, New York: Ieee. 4013-4018.
13. Brouwer, D., et al., *Sub-nanometer stable precision MEMS clamping mechanism maintaining clamp force unpowered for TEM application.* Journal of Micromechanics and Microengineering, 2006. **16**(6): p. S7.
14. Martin, T., et al., *Silicon linkage with novel compliant mechanism for piezoelectric actuation of an intraocular implant.* Sensors and Actuators a-Physical, 2012. **188**: p. 335-341.
15. Dinesh, M. and G. Ananthasuresh, *Micro-mechanical stages with enhanced range.* International Journal of Advances in Engineering Sciences and Applied Mathematics, 2010. **2**(1-2): p. 35-43.

16. Kim, C. and S. Kota. *Design of a novel compliant transmission for secondary microactuators in disk drives*. in *ASME International Design Engineering Technical Conferences, Montreal, CA*. 2002.
17. Grossard, M., et al., *Mechanical and Control-Oriented Design of a Monolithic Piezoelectric Microgripper Using a New Topological Optimization Method.* Ieee-Asme Transactions on Mechatronics, 2009. **14**(1): p. 32-45.
18. Bolsman, C.T., J.F.L. Goosen, and F. van Keulen, *Design Overview of a Resonant Wing Actuation Mechanism for Application in Flapping Wing MAVs.* International Journal of Micro Air Vehicles, 2009. **1**(4): p. 263-272.
19. Li, Y.M., et al., *Design, Modeling, Control and Experiment for a 2-DOF Compliant Micro-Motion Stage.* International Journal of Precision Engineering and Manufacturing, 2014. **15**(4): p. 735-744.
20. Mohaupt, U.H., *Mechanical displacement amplifier and thermostat embodying same*. 1987, Canadian Industrial Innovation Centre: United State.
21. Li, Z. and S. Kota. *Dynamic analysis of compliant mechanisms*. in *ASME 2002 International Design Engineering Technical Conferences and Computers and Information in Engineering Conference*. 2002. American Society of Mechanical Engineers.
22. Frecker, M. and S. Canfield, *Optimal design and experimental validation of compliant mechanical amplifiers for piezoceramic stack actuators.* Journal of Intelligent Material Systems and Structures, 2000. **11**(5): p. 360-369.
23. Yilin, L. and Q. Xu. *Design of a novel integrated micromanipulator for cell gripping and injection*. in *Nano/Micro Engineered and Molecular Systems (NEMS), 2015 IEEE 10th International Conference on*. 2015.
24. Li, Y. and Q. Xu, *Design and analysis of a totally decoupled flexure-based XY parallel micromanipulator.* IEEE Transactions on Robotics, 2009. **25**(3): p. 645-657.
25. Jiang, C.D., et al., *Topology Optimization and Control of Rotating Compliant Mechanism*. Ccdc 2009: 21st Chinese Control and Decision Conference, Vols 1-6, Proceedings. 2009, New York: Ieee. 1347-1350.
26. Hetrick, J. and S. Kota. *Size and Shape Optimization of Compliant Mechanisms: An Efficiency Formulation (DETC/MECH-5943)*. in *ASME Design Engr. Technical Conf*. 1998.
27. Chu, L.L., J.A. Hetrick, and Y.B. Gianchandani, *High amplification compliant microtransmissions for rectilinear electrothermal actuators.* Sensors and Actuators a-Physical, 2002. **97-8**: p. 776-783.
28. Yang, X.F., W. Li, and Y.Q. Wang, *Analysis the Displacement Amplification of Compliant Parallel Four-Bar Using Piezo Actuator*, in *Mechanical Engineering and Green Manufacturing Ii, Pts 1 and 2*, S. Zhong and X. Qu, Editors. 2012, Trans Tech Publications Ltd: Stafa-Zurich. p. 201-205.
29. Yogesh B. Gianchandani, J.A.H., Larry Li-Yang Chu, *Micromechanical actuation apparatus*. 2003, Wisconsin Alumni Research Foundation: United State.
30. Huang, S.c. and G.j. Lan. *Design and Fabrication of Micro-Compliant Amplifier with Topology Optimal Compliant Mechanism Integrated with a Piezoelectric Microactuator*. in *2005 Conference on High Density Microsystem Design and Packaging and Component Failure Analysis*. 2005.
31. Kim, C.J., S. Kota, and Y.M. Moon, *An instant center approach toward the conceptual design of compliant mechanisms.* Journal of Mechanical Design, 2006. **128**(3): p. 542-550.

32. Xu, Q.S., Y.M. Li, and Ieee, *Design of a New Decoupled XYZ Compliant Parallel Micropositioning Stage with Compact Structure*. 2009 Ieee International Conference on Robotics and Biomimetics. 2009, New York: Ieee. 901-906.
33. Howell, L.L., A. Midha, and T. Norton, *Evaluation of equivalent spring stiffness for use in a pseudo-rigid-body model of large-deflection compliant mechanisms.* Journal of Mechanical Design, 1996. **118**(1): p. 126-131.
34. Sridhar Kota, M.S.R., Joel A. Hetrick, *Compliant displacement-multiplying apparatus for microelectromechanical systems*. 2001, Sridhar Kota, M. Steven Rodgers, Joel A. Hetrick: United State.
35. Saxena, A., *Topology design of large displacement compliant mechanisms with multiple materials and multiple output ports.* Structural and Multidisciplinary Optimization, 2005. **30**(6): p. 477-490.
36. Tang, H. and Y.M. Li, *Design, Analysis, and Test of a Novel 2-DOF Nanopositioning System Driven by Dual Mode.* Ieee Transactions on Robotics, 2013. **29**(3): p. 650-662.
37. Henein, S., *Short Communication: Flexure delicacies.* Mechanical Sciences, 2012. **3**(1): p. 1-4.
38. Samuel Lee Miller, M.S.R., Stephen Matthew Barnes, Jeffry Joseph Sniegowski, Paul Jackson McWhorter, Less «, *Microelectromechanical system with non-collinear force compensation*. 2006, Memx, Inc.: United State.
39. Saxena, A. and G. Ananthasuresh, *Topology synthesis of compliant mechanisms for nonlinear force-deflection and curved path specifications.* Journal of mechanical Design, 2001. **123**(1): p. 33-42.
40. Tang, H. and Y. Li, *Development and Active Disturbance Rejection Control of a Compliant Micro-/Nanopositioning Piezostage With Dual Mode.* IEEE Transactions on Industrial Electronics, 2014. **61**(3): p. 1475-1492.
41. Hara, A. and K. Sugimoto, *Synthesis of parallel micromanipulators.* Journal of mechanisms, transmissions, and automation in design, 1989. **111**(1): p. 34-39.
42. Li, J., et al. *A self-limited large-displacement-ratio micromechanical amplifier*. in *The 13th International Conference on Solid-State Sensors, Actuators and Microsystems, 2005. Digest of Technical Papers. TRANSDUCERS '05.* 2005.
43. Tan, U.X., et al., *Design and Development of a 3-Axis MRI-compatible Force Sensor.* 2010 Ieee International Conference on Robotics and Automation (Icra), 2010: p. 2586-2591.
44. Choi, K.-B., et al., *A compliant parallel mechanism with flexure-based joint chains for two translations.* International Journal of Precision Engineering and Manufacturing, 2012. **13**(9): p. 1625-1632.
45. Joel Hetrick, S.K., *Displacement amplification structure and device*. 2003, The Regents Of The University Of Michigan: United State.
46. Liu, A.Q., et al., *Self-latched micromachined mechanism with large displacement ratio.* Journal of Microelectromechanical Systems, 2006. **15**(6): p. 1576-1585.

VB (1)
24-2